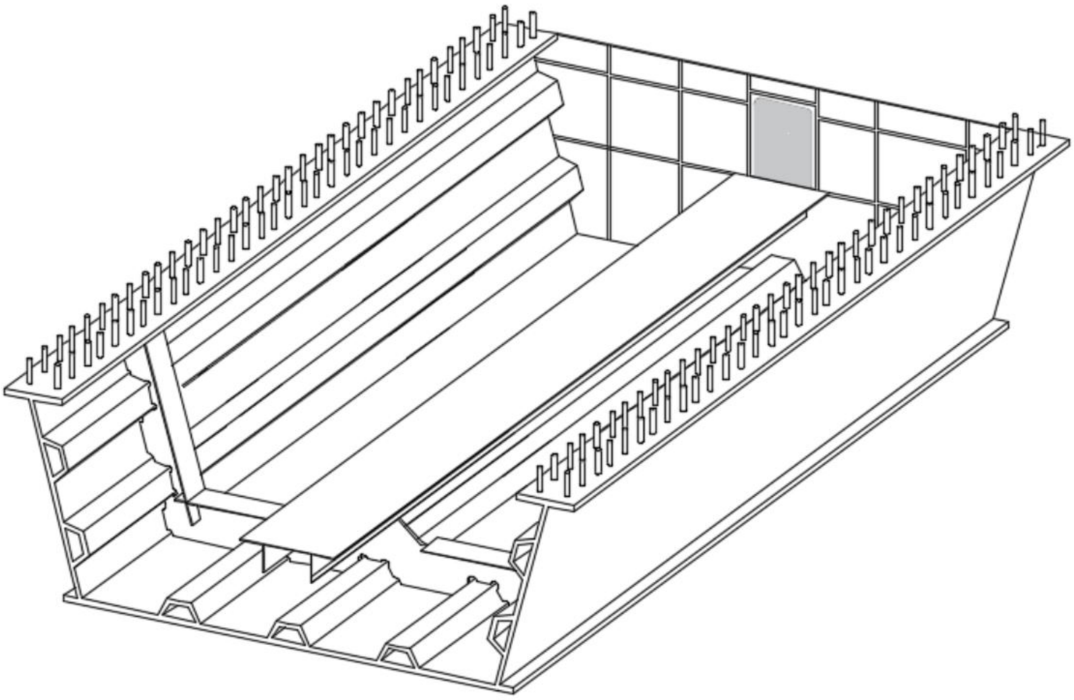

Stainless-Steel in Hisings-Bridge as An Alternative for Carbon Steel

Buckling Capacity and LCCA of Trapezoidal Box Girders Made of Stainless-Steel in Composite Concrete-Steel Bridges

Master's thesis in Master Program Structural engineering and building technology

MOHAMMAD ALSHIHABI
NIKOLAOS MADENTZOGLOU

Department of Architecture and Civil Engineering

CHALMERS UNIVERSITY OF TECHNOLOGY
Gothenburg, Sweden 2021
www.chalmers.se

MASTER'S THESIS 2021

Stainless-Steel in Hisings-Bridge as An Alternative for Carbon Steel

Buckling Capacity and LCCA of Trapezoidal Box Girders Made of Stainless-Steel in Composite Concrete-Steel Bridges

MOHAMMAD ALSHIHABI

NIKOLAOS MADENTZOGLOU

Department of Architecture and Civil Engineering
Division of Structural Engineering
Lightweight Structures
CHALMERS UNIVERSITY OF TECHNOLOGY
Gothenburg, Sweden 2021

Stainless-Steel in Hisings-Bridge as an Alternative for Carbon Steel
Buckling Capacity and LCCA of Trapezoidal Box Girders Made of Stainless-Steel in Composite Concrete-Steel Bridges

MOHAMMAD ALSHIHABI

NIKOLAOS MADENTZOGLOU

Supervision Team: Jonas Zachrisson, Filip Nilenius, and Thomas Darholm/ COWI
Examiner: Professor Mozhdeh Amani, Department of Architecture and Civil Engineering

Master's Thesis 2021
Department of Architecture and Civil Engineering
Division of Structural Engineering
Lightweight Structures
Chalmers University of Technology
SE-412 96 Gothenburg
Telephone +46 31 772 1000

Cover: Trapezoidal open box girder used in steel-concrete composite bridges.

Typeset in LaTeX
Printed by Chalmers Reproservice
Department of Architecture and Civil Engineering
Gothenburg, Sweden 2021

Stainless-Steel in Hisings-Bridge as an Alternative for Carbon Steel
Buckling Capacity and LCCA of Trapezoidal Box Girders Made of Stainless-Steel in Composite Concrete-Steel Bridges
Mohammad Alshihabi
Nikolaos Madentzoglou
Department of Architecture and Civil Engineering
Division of Structural Engineering and Building Technology
Lightweight Structures
Chalmers University of Technology

Abstract

In addition to its comparatively low price, conventional carbon steel provides the bridge industry with several advantages such as high strength, lightweight, and recyclability, making it a preferable material in bridge engineering. On the other hand, carbon steel is highly susceptible to corrosion, which requires higher maintenance costs during its life cycle.

Recently, the usage of stainless steel in the bridge industry became an issue for research, its higher corrosion resistance reduces maintenance costs during the bridge life cycle. On the contrary, investment costs increase remarkably due to the expensive alloying components used in stainless steel.

Therefore, the bridge department at COWI wanted to investigate the efficiency of using Stainless steel in Hisings-bridge using life cycle cost analysis. Buckling capacities using duplex stainless-steel grade 1.4662 are calculated for the original cross-section and an optimized cross-section. The results are compared afterward using life cycle cost analysis. The investigation shows that saving in the material can be achieved using higher-strength stainless steel with an optimized cross-section. Life cycle cost analysis shows that profitability depends on stainless steel prices and the post-weld treatment cost.

Keywords: Composite bridges, Trapezoidal open box girders, Hisings-bridge, LCCA study, Duplex stainless steel, Buckling capacity.

Acknowledgements

This master thesis was conducted with collaboration between the bridge department at COWI and the structural engineering division at Chalmers University of Technology, Department of Architecture and Civil Engineering. The work was carried out between January 2021 to June 2021. We would like to express our gratitude to our supervisors Jonas Zachrisson, Filip Nilenius, and Thomas Darholm at COWI for their time and dedication throughout this work. Special thanks to the lightweight research group at Chalmers University and our examiner Mozhdeh Amani and Mohammad Al-Emrani for their constant support during the whole thesis.

Mohammad, and Nikolaos
Gothenburg, 06/2021

Contents

List of Figures

List of Tables

Glossary

Roman upper-case letters:

$A_{c,eff}$	Effective area in a stiffened plate
A_n	Accident frequency during normal conditions in accident/vehicle-km.
A_r	Accident frequency during road work in accident/vehicle-km.
$A_{st,1,eff}$	Effective section of the stiffener with adjacent panels.
C_{acc}	Cost of an accident for the society in SEK.
C_t	Total cost of a certain LCM performed at a time t.
E_{cm}	Elastic modulus of concrete.
E_{s1}	Secant modulus of elasticity in the tensioned flange.
E_{s2}	Secant modulus of elasticity in the compressed flange.
I_{sl}	Sum of the second moment of area of the individual longitudinal stiffeners.
L_t	Affected roadway length in m.
N_t	Total amount of days that are needed to carry out a certain LCM.
O_p	Average operating cost in SEK/h for a passenger car.
O_t	Average operating cost in SEK/h for a heavy vehicle, including transported goods.
$P_{Rd,1}$	Shear resistance of a stud in a case of base failure.
$P_{Rd,2}$	Shear resistance of a stud in a case of concrete crashing.
$P_{Rd,SLS}$	Shear resistance of studs in the serviceability limit state.
$P_{Rd,ULS}$	Shear resistance of studs in the ultimate limit state.
$V_{bw,Rd}$	Shear buckling resistance (web contribution).
A_c	Gross area of the plate with stiffeners except for edge panels.
$A_{sl,1}$	Sectional area of the stiffener with adjacent panels (Gross section).
B_{bott}	Bottom width of stiffener.
B_{top}	Top width of a stiffener.
$I_{sl,1}$	Out of plate Second moment of area for the stiffener and adjacent panels.
M_{el}	Moment capacity with elastic stress distribution.
M_pl	Plastic moment capacity.
N_{cr}	Elastic critical force.
T_{ED}	Service temperature.
T	Expected travel delay time in case of a roadway work measured in h.
$T1$	Stiffener number 1

$T2$	Stiffener number 2.
$T3$	Stiffener number 3.
E	Modulus of elasticity.
G	Shear modulus.
H	Height of a stiffener.
K	Compression modulus.
L	Life span of the infrastructure.

Roman lower-case letters:

h_{sc}	Height of the stud.
h_w	Height of a web
k_σ	Buckling factor
b_{eff}	Effective width from shear lag
f_{ck}	Characteristic compressive strength for concrete
k_t	Shear buckling coefficient
p_L	Nominal interest rate for extended loans.
p_c	Factor accounting for a positive or negative effect in the structure.
p_i	Interest rate from inflation.
r_t	Percentage of heavy vehicles out of the ADTt.
w_p	Hourly time value for a passenger car in SEK/h.
w_t	Hourly time value for a heavy vehicle measured in SEK/h.
a	Transverse stiffener spacing
$a0$	Thermal expansion
b	Plate width
$b0$	Transversal spacing between shear connectors.
d	Diameter of shear stud
f_u	Tensile strength
fy	Yield strength of steel type.
g	Specific weight
t	Plate Thickness
t_w	Thickness of the web
p	Interest rate

Greek letters:

$\sigma_{cr,st}$	Critical stress in column type buckling
χ_w	Shear buckling reduction factor
λ_0	Non-dimensional slenderness
ρ_c	Reduction factor resulting from the interaction between plate and column type buckling
ρ_{loc}	Reduction factor for each subpanel
$\sigma_{cr,p}$	Critical stress in plate type buckling
$\sigma_{x,Ed}$	Applied normal stresses
$\sigma_{x,Rd}$	Direct stress capacity
$\sigma_{y,Ed}$	Applied stresses in the transversal direction
$\sigma_{y,Rd}$	Transversal stress capacity
τ_{Ed}	Applied shear stresses
τ_{Rd}	Shear capacity
τ_{cr}	Critical shear stress
χ_c	Reduction factor, column type buckling
λ	Slenderness parameter
ρ	Density
α	Imperfection factor
ϵ	Material factor
χ	Reduction factor for the relevant buckling mode
ϕ	Global initial sway imperfection

Acronyms:

ADT_t	Average daily traffic at a time t measured in vehicles/day.
FEA	Finite Element Analysis
INV	Investment
Kg	Kilograms
LCC	Life Cycle Cost
$LCCA$	Life Cycle Cost Analysis
LCM	Life Cycle Measures
$MSEK$	Million Swedish Krona (Currency)
NPV	Net Present Value
SEK	Swedish Krona (Currency)
SS	Stainless Steel
TDC	Traffic Delay Cost
$TRVK$	Trafikverket (Swedish Transport Administration Authority)
VOC	Vehicle Operation Costs

1 Introduction

Hisings-bridge is a new steel-concrete composite bridge constructed at the center of Gothenburg city, connecting the two sides of the Göta river. The new bridge consists of two side spans and one vertical lift span in the middle. With a length of 216m, the northern side span connects the river's north bank with the vertical lift span. While the southern span provides the connection with the south bank of the river with a length of 172m. The lift span is 48m in width, and the overall bridge width is around 440 meters. Hisings-bridge is designed to carry two roadways for private vehicles, one way for public transport: trams and busses, two walking ways, and a balcony on one side of the bridge. (Figure 1.1). The bridge's structural system contains three open box girders of carbon steel with a trapezoidal cross-section. The box girders support a concrete slab deck to form continuous beams. On the southern, four columns are used as supports for each girder. On the northern side, five supports are used, with a maximum span of 72 meters (Figure 3.2). Open-box girders are usually used for continuous bridges with a span length larger than 50 meters (Vayas and Iliopoulos, 2014). Through decades conventional carbon steel has been used in bridge Engineering, recently the use of stainless steel instead of carbon steel became a perceived issue. The investment cost of carbon steel bridges is cheap compared to stainless steel. At the same time, carbon steel is highly affected by corrosion and requires higher maintenance costs during its service life. On the contrary, stainless steel is not susceptible to corrosion and does not require surface treatment and maintenance as much as carbon steel. In this master thesis, the northern part of the new Hisings-bridge will be re-designed using higher strength stainless steel. And the results are compared with the original design using life cycle cost analysis.

1.1 Aims

This master thesis aims to study the applicability of using high-strength duplex stainless steel as an alternative structural material for carbon steel in Hisings-bridge. Changing the structural steel affects buckling capacity and flexural rigidity for the section. Only buckling capacities are considered in this thesis for the original cross-section and an optimized one. All of the alternatives are compared afterward with the original design using life cycle cost analysis.

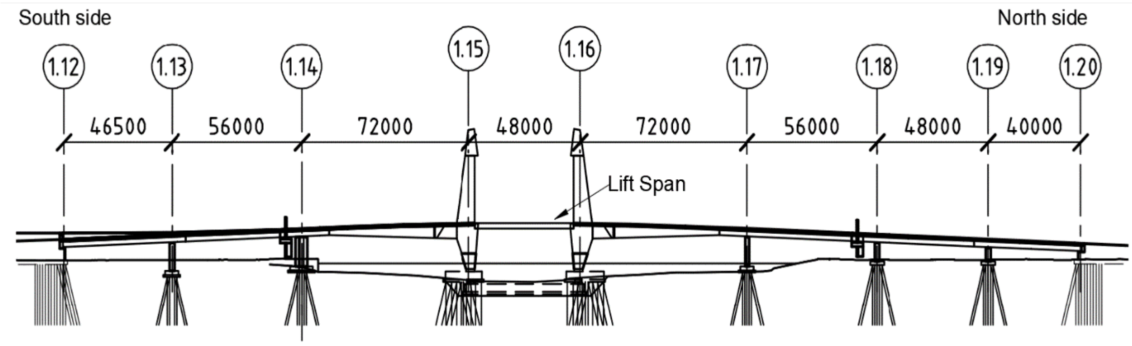

Figure 1.1: Hisings-Bridge (Longitudinal cross section)

1.2 Objectives

More researches are being conducted recently on stainless steel as a structural material in composite bridges. This work is a step forward to study the possibility of using stainless steel in open box girders.

1.3 Limitations

1. All of the calculations and design procedures are done according to the Eurocode and the Swedish Transport Administration regulations.
2. The bridge's lifting and southern sides are excluded from this study, and only the northern side is investigated (Figure 3.2).
3. Support sections and the hunched region are not included in the calculations. i.e., only span sections between the supports are considered (Figure 3.20).
4. The reinforced concrete deck is excluded from the study.
5. The bridge must be aesthetically looking like the original bridge, and no changes in the initial concept are adopted.
6. The reduced stress method is not used, and only results from the reduced section method are compared when calculating buckling capacities.

1.4 Methodology

Several stages were carried out in sequence, starting with a literature review about composite bridges with trapezoidal box girders, then reviewing the design calculations of the structural steel in Hisings-bridge. After that, the analysis stage was done by replacing carbon steel with stainless steel and optimizing the cross-sectional area with the new material. Finally, a life cycle cost analysis is carried out to compare the original design with other solutions.

1.4.1 Literature review

This part covers the following topics:

1. The theoretical background of composite bridges with more focus on trapezoidal box girders.
2. Stainless steel properties and classification.
3. The application of carbon steel and stainless steel in box girders according to Eurocode.

1.4.2 Hisings-bridge

This part presents the used steel grades, geometry, and cross-sections of Hisings-bridge. Moreover, the overall design philosophy and calculations concerning buckling capacities for different parts of the box girder are also included.

1.4.3 Case Study

The stainless steel grade is determined according to the corrosivity class of the region. Next, buckling capacities are calculated for the original cross-section but with the chosen stainless steel grade. Finally, an optimized cross-section is introduced to achieve similar buckling capacities as in the original design.

1.4.4 Life cycle cost analysis

After determining the reduced cross-sectional area for the box girder using stainless steel, the original design and the new suggestion are compared. This comparison is conducted in two levels. First, when using duplex stainless steel everywhere in the box girder. Second, using duplex stainless steel in the plates which are in contact with the outside environment and lean duplex stainless steel in the inside members (stiffeners and cross frames).

2

Literature Review

This is a preparation chapter before starting with the analysis part. It covers all of the used theories in the calculations. Start by describing the concept of composite bridges and how steel and concrete interact and explain trapezoidal open box girders. Stainless steel grades and properties are also included. Next, the design procedures used in the Eurocode for carbon steel and stainless steel are briefly explained. Finally, the reader can find helpful information about life cycle cost analysis and its applications in bridge engineering.

2.1 Steel-Concrete composite bridges

Bridges, in general, consists of superstructure, substructure, and foundations. In this work, the phrase composite bridge is referring to the superstructure part of the bridge. The basic concept of composite bridges was found to combine the advantages of steel as a material capable of withstanding tensile stresses and concrete for compression. Composite bridges consist of a reinforced concrete slab resting on a series of steel girders. Composite bridges are suitable for short, medium, and long spans. Moreover, one of the most beneficial aspects of this type of bridge is reducing the superstructure's self-weight significantly. The cross-section of a composite bridge in (Figure 2.1) shows a group of steel girders (two or more) connecting to a reinforced concrete slab deck by shear studs. In positive bending moments, the reinforced slab works under compression as a part of the steel girder's upper flange. In negative moments, the concrete slab is considered fully cracked. The interaction between the slab deck and the structural steel can be achieved by shear connectors (shear studs) which are welded directly to the top flange of the steel girder (Vayas and Iliopoulos, 2014). The concrete slab has several functions in this concept. It transfers loads from the road transversally to the steel girders and longitudinally to the piers as a part of the composite beam. Moreover, the concrete deck has a diaphragm action in transferring lateral loads such as wind load, breaking, accelerating, and seismic loads. To achieve the aforementioned functionalities, a concrete slab should have sufficient stiffness. This can be ensured by an adequate slab thickness, normally between 25 to 30 cm (Vayas and Iliopoulos, 2014). As mentioned before, the slab deck at sagging bending regions acts as a part of the upper flange of the steel girder. This leads to the slab effective width definition, a deck width with a combined action with the structural steel. Therefore, it is beneficial to choose a spacing between girders equal to the slab effective width to guarantee that all slab cross-sections are included in the combined action. The concrete slab deck can be

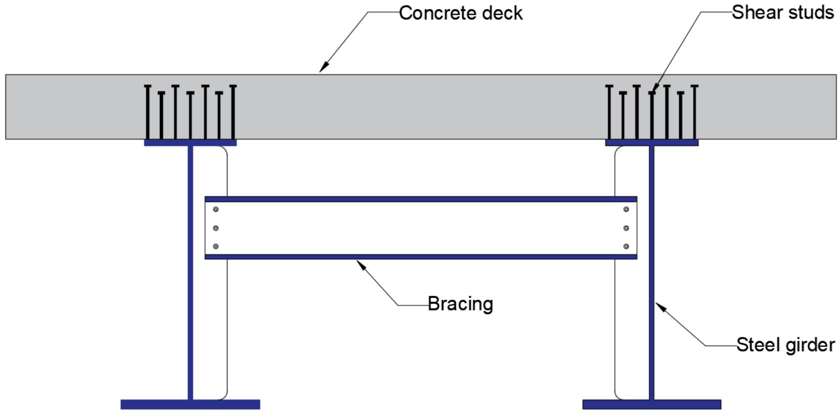

Figure 2.1: A cross-section in a double I-girders composite bridge

cast in situ, semi-precast, or fully pre-cast slab. In some cases, it can be a composite slab with steel sheeting. Composite bridges can be classified according to the form and shape of structural steel:

- Double girder bridges or ladder deck bridges (Figure 2.1).
- Closed-box girder bridges (Figure 2.2).
- Open-box girder bridges (Figure 2.3).

Structural steel in composite bridges can even have several shapes like trusses, pipes, or filler beam bridges (Vayas and Iliopoulos, 2014).

2.1.1 Box Girders

Box girders in composite bridges have widely been used for their superiority over other types of plate girders. Standard plate girders are not economically practical for spans larger than 60 m, while box girders can significantly reduce the material consumption in these cases (Vayas and Iliopoulos, 2014). From a structural point of view, box girder has a higher torsional stiffness, making it very effective in horizontally curved roads or highway conjunctions, or even for straight bridges with a cantilever where very high torsion stresses are induced. Torsional rigidity in box girders can be 100 to 1000 times larger than I girders.

2.1.2 Trapezoidal Open Box girder

A typical cross-section for a trapezoidal box girder is shown in (Figure 2.3). In addition to the economic advantages of these types of bridges, trapezoidal girders have some aesthetical benefits. Cross bracing and stiffeners are hidden inside the box, but the outer shape is still smooth and elegant. As illustrated in (Figure 2.3), an open trapezoidal box girder consists of a bottom flange stiffened with longitudinal stiffeners, two inclined webs, and two upper flanges. In addition, an internal bracing system is provided each 4-7m (Vayas and Iliopoulos, 2014) to improve the torsional rigidity of the section. This system consists of T transverse stiffeners, diagonals, and ties. In some cases, it is sufficient to use only transverse stiffeners. However, if more

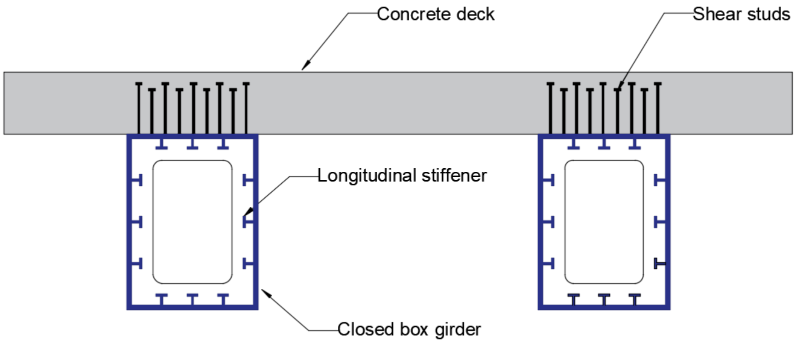

Figure 2.2: A cross-section in a composite bridge with closed box girders

torsional rigidity is required, diagonals and ties can be added. Longitudinal stiffeners are also added to avoid local buckling of the plate, especially at the support when the bottom flange is exposed to high compressive stresses. Longitudinal stiffeners can have opened or closed sections. A highly stiff diaphragm is provided at the end of the box girder, above piers instead of transverse stiffeners. This diaphragm is mounted to ensure a safe transfer of the high reactions from the superstructure to the substructure. A maintenance hole is needed for inspection and maintenance (Vayas and Iliopoulos, 2014).

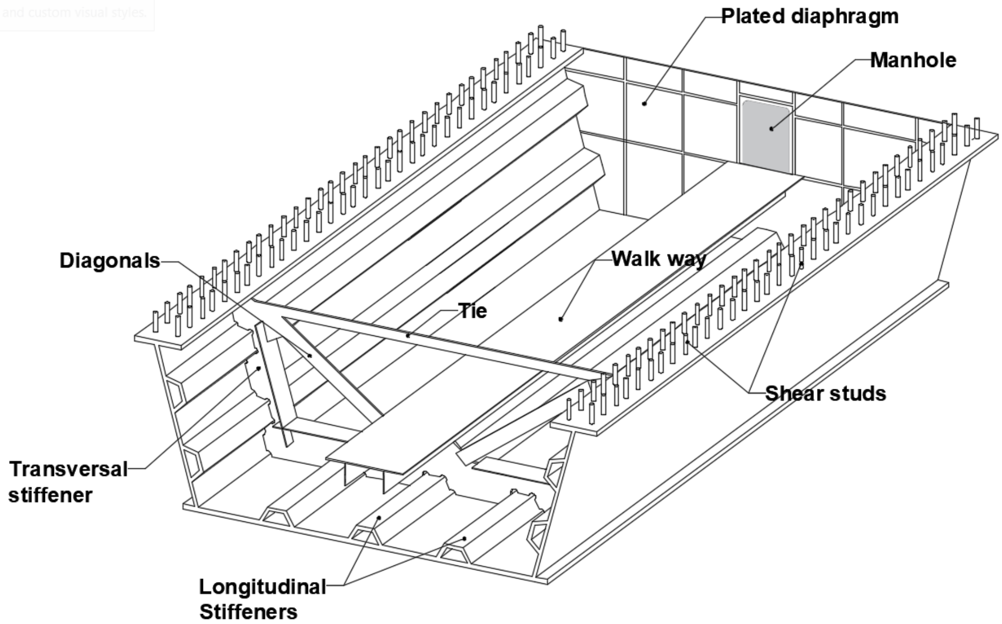

Figure 2.3: Trapezoidal open box girder

2.1.3 Interaction between steel and concrete via shear studs

Shear connectors or shear studs in composite bridges ensure the combined action between steel and concrete. For example, if the concrete slab is resting on the steel girder without any bond between them, the slab will bend in the longitudinal direction around its own neutral axis, and the steel girder will act the same. In this case, lower fibers of the slab deck are tensioned, i.e., will elongate, while the adjacent steel fibers are compressed, i.e., will shorten. As a result, a deferential displacement takes place, and no combined action occurs. On the other hand, if shear connectors restrain this displacement, the combined behavior is ensured, and one neutral axis for the whole system is existed (Vayas and Iliopoulos, 2014). Hence, shear connectors are generally subjected to horizontal shear stresses in the longitudinal direction. These stresses are induced by the vertical shear forces in the composite system. When the concrete slab bends transversally, additional moments are transferred to the girder's web through shear studs. These moments induce tension and compression stresses in the studs in addition to shear stresses. If the studs are buttwelded to the upper flange, tension stresses can be ignored, and the studs can be designed for shear only (Vayas and Iliopoulos, 2014). In a particular case in box girders, shear studs are subjected to shear stresses in the perpendicular direction also. These stresses are induced by the torsional forces in the box girder. More shear connectors can be provided in the bottom flange of a continuous box girder above the internal supports when the box is filled with concrete to resist compression stresses with the lower flange. Design procedure and requirements can be found in EN 1994-2 for the round-headed studs (Vayas and Iliopoulos, 2014).

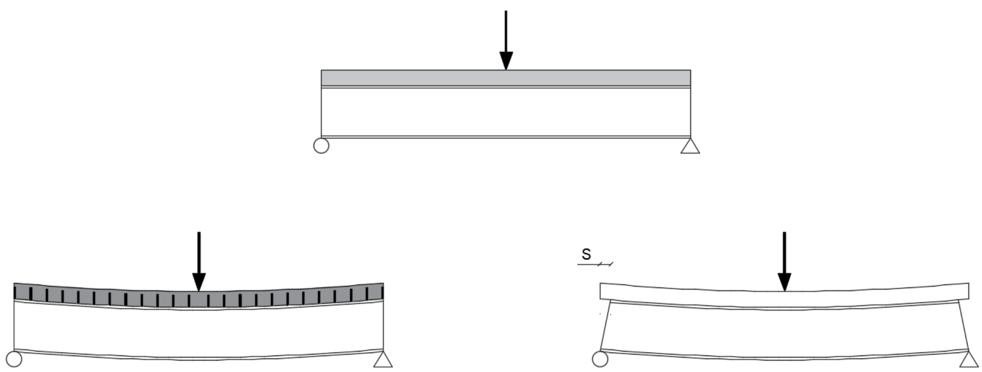

Figure 2.4: Shear stud's mechanism. (left) When there are shear connectors between steel and concrete. (right) when there is no connection between steel and concrete.

2.2 Stainless steel

Stainless steel is the name given to a family of corrosion-resistant steels containing a minimum of 10,5% chromium. A wide variety of stainless steel exists, with different properties regarding the levels of corrosion resistance and strengths. These properties are governed by the alloying elements' additions, which affect the mechanical properties and the ability to resist different corrosive environments. Therefore, the selection of the stainless-steel category must be relevant to the application environment, so unnecessary high alloying and cost can be avoided. A transparent and tightly adherent layer of chromium-rich oxide forms spontaneously on the surface of stainless steel due to a combination of chromium content above 10,5%, a clean surface, and exposure to air or any oxidizing (SS-EN 1993-1-4:2006/A1:2017). This layer is self-healing in the presence of oxygen if scratching or cutting damages the film. The film is thin, about 5x10-6mm, but it is both stable and nonporous, assuming that the corrosion resistance is sufficient for the service environment; it will not interact with the surroundings. This layer is called the passive film, and its stability depends on the surface treatment, the composition of stainless steel, and the environment's corrosiveness. With the increase in the chromium content, the constancy of the passive film increases and is further improved by alloying additions of molybdenum and nitrogen.

2.2.1 Stainless steel types

Stainless steel is classified into the following five primary groups, with each group providing unique properties and a range of different corrosion resistance levels (SS-EN 1993-1-4:2006/ A1:2017).

- Austenitic stainless steel.
- Ferritic stainless steel.
- Duplex stainless steel.
- Martensitic stainless steel.
- Precipitation hardening stainless steel.

2.2.1.1 Austenitic stainless steel

Austenitic stainless steel is widely used in building and construction. The most commonly used austenitic stainless steels are 17 to 18% chromium and 8 to 11% nickel additions. Austenitic stainless steel has corrosion resistance and high ductility, so consequently is easily cold formed and readily weldable. This occurs due to the facecantered cubic atomic structure of austenitic stainless steel. Compared to carbon steels, they also have significantly better toughness over a wide range of temperatures (SS-EN 1993-1-4:2006/A1:2017). A method to strengthen them is by cold working, but not heat treatment. Improvements in the corrosion performance can be made through increasing chromium content and additions of molybdenum and nitrogen.

2.2.1.2 Ferritic stainless steel

Ferritic stainless steel, which is most commonly used, has a chromium content between 10.5 and 18% (SS-EN 1993-1-4:2006/A1:2017). Similar to carbon steel, they contain minimal or no nickel additions, their atomic structure is body-centered. Both forming and machining properties of ferritic grades are similar to S355 structural carbon steel. Compared to the austenitic grades of equivalent corrosion resistance, they cost less, and the price is more stable. Furthermore, they have smaller ductility and weldability. They can be strengthened by cold working but to a less extent than the austenitic grades. In parallel, their strength cannot be strength by heat treatment. Application environments for ferritic grades are interior and mild exterior atmospheric conditions. A way to increase the corrosion performance is with the addition of molybdenum, and they demonstrate an excellent resistance to stress corrosion cracking. Ferritic grades can be used as an alternative solution when galvanized steel is used, and they are commonly used in thicknesses of 4 mm and below.

2.2.1.3 Duplex (austenitic-ferritic) stainless steels

Duplex stainless steels typically contain 20 to 26% chromium, 1 to 8% nickel, 0.05 to 5% molybdenum and 0.05 to 0.3% nitrogen (Design manual for structural stainless steel). Their atomic structure is a mixture between austenite and ferritic. Consequently, they sometimes are called austenitic-ferritic steels. With a less amount of nickel-concentration than austenitic grades, Duplex price shows less variability. Duplex grades are ideal for weight-sensitive structures such as bridges or offshore topsides because they have twice strength in the annealed (soft) condition as the austenitic grades, allowing section size reduction. They are suitable for a broad range of corrosive environments. However, duplex steel grades have good ductility because of their high strength. The formability of those grades is restricted in contrast with the austenitic alloys. Duplex stainless steel can also be strengthened by cold working but not heat treatment. Proprieties of good weldability and resistance to stress cracking are observed. Duplex grades can be seen as extending of ferritic stainless-steel grades, but they are most commonly used in higher thicknesses than the ferritic grades.

2.2.1.4 Martensitic stainless steel

Martensitic stainless-steel grades have higher carbon content so that they can be strengthened by heat treatment. Their atomic structures are body-centered cubic, similar to ferritic stainless and structural carbon steels. They are produced in hardened and tempered conditions, resulting in higher strength and moderate corrosion resistance due to the higher carbon content. As a result, martensitic stainless-steel grades have good wear and abrasion resistance. However, they are less ductile and notch sensitive than ferritic, austenitic, and duplex stainless steel. Welding in martensitic stainless-steel grades requires preheating and post-weld treatment, which limits the applicability in welded components. They are used in cutlery applications, surgical instruments, industrial knives, wear, and turbine blades.

2.3 Design procedure

This chapter includes an illustration of the used methods in the design stage. Some of these assumptions and regulations are extracted from the Eurocode and some of them from national standards. Exact chapters from the Eurocode and national

Table 2.1: Hot-rolled Steel grades and strengths according to thickness changing (EN 10025, 2004).

Steel Grade	Yield strength fy (MPa)			Tensile strength fu (MPa)
	$16 < t \leq 40$	$40 < t \leq 63$	$63 < t \leq 80$	$3 < t \leq 100$
S355JR, J0, J2, K2	*345*	*335*	*325*	*470-630*
S355N, NL	*345*	*335*	*325*	*470-630*
S355M, ML	*345*	*335*	*325*	*440-600*

annex will be referred to in the coming sub-chapters.

2.3.1 Material

Carbon steel and stainless steel have different material grades and properties, and each one of these two categories has different grades when used in plate girders or shear connectors. In this chapter, each material is explained and classified according to Eurocode.

2.3.1.1 Carbon steel

Carbon steel in composite bridges can be found as plate girders or as shear connectors. Accordingly, different standards are used to determine the properties of carbon steel.

Carbon steel in girders
Structural steel properties and grades are defined in EN10025 part 1-6, CEN (European Committee for standardization). Each steel grade is characterized by a letter S followed by the yield strength of steel (for thicknesses smaller than 16mm) and a symbol or two to define the impact energy from the Charpy test. S355 steel grade has good mechanical properties comparing to its manufacturing cost. That's why it is widely used in steel-concrete composite bridges. The values of yield strength in EN10025 are the minimum strengths that the manufacturer can warrant, and this allows to reduce the safety factors in the design process (Vayas and Iliopoulos, 2014)
As mentioned before, steel yield strength varies according to thickness. When thicknesses are smaller than 16 mm, yield strength is equal to the defined steel grade. For thicknesses higher than 16mm, yield strength and tensile strength is determined according to the (EN 10025:2004) (Table 2.1).
Steel thicknesses in bridges can increase significantly. Large thicknesses improve the section behavior in resisting local buckling without welding any additional stiffeners. This will reduce the residual stresses coming from welding and the labor cost for the welding process. At the same time, increasing the plate thickness will decrease the steel strength (Table 2.2). (Vayas and Iliopoulos, 2014).

Fracture toughness
Brittle fracture of steel is determined by material toughness, which can be measured by the V-notched Charpy test. The temperature has a vital effect on structural steel

toughness and response. The impact energy-temperature curve can describe this effect (SS-EN 1993-1-10) (Figure 2.5).

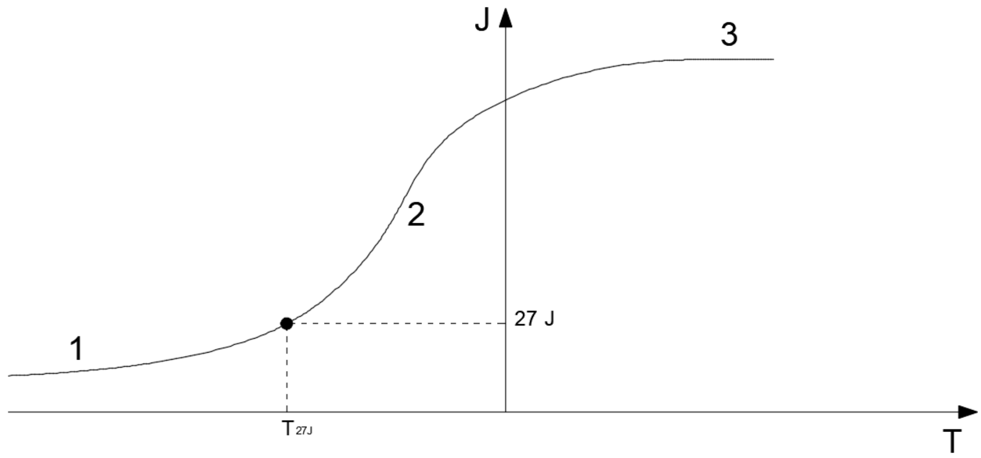

Figure 2.5: Relation between impact energy and temperature.

Three regions can be noticed in this curve: 1. Lower shelf region, 2. Transition shelf region, 3. Upper shelf region. The third region shows elastic-plastic behavior with a ductile response, while the first region indicates a brittle failure. The region in between is called the transition region in which steel changes its behavior from brittle to ductile. EN 1993-1-10 provides a simplified method to determine elements thicknesses with respect to three parameters (Table 2.2):

- Service temperature (τ_{ED}): calculated as the average temperature during the last half a century.
- Stress (σ_{ED}): calculated from the accidental load combination, and can be assumed as 0,5*fy at the preliminary stage design.
- Steel subgrade (Impact energy from Charpy test).

Maximum plate thickness can then be determined from the following table (SS-EN 1993-1-10).Moreover, Structural steel has some other properties: Specific weight g=78.5 kN/m3, Modulus of elasticity E=210 GPa, Poisson ratio $\nu = 0.3$, shear modulus G=91 GPa, and coefficient of thermal expansion a=10*10-6.

Shear Studs

Shear studs made of stainless steel are classified according to EN ISO 3506, using the letter “A” for austenitic, “F” for ferritic, “C” for martensitic, and “D” for duplex. After this letter, a number is provided to describe the corrosion resistance. These numbers are (1, 2, 3, 4, 5, 6, or 8). Increasing the number reflects a higher corrosion resistance and more durable shear studs. Choosing the corrosion resistance or the bolt class should be based on the grade of the plates being connected to, and both of them need to have similar corrosion resistance. (Table 2.5) shows stud’s classification according to the chosen stainless-steel grade.

- Shear at the base of the stud (shaft toe):

$$P_{Rd,1} = (0.8 * f_u * (\pi * d^2/4))/\gamma_v \tag{2.1}$$

Table 2.2: Maximum permissible values of element thickness t in mm (SS-EN 1993-1-10)

Steel Grade	Sub Grade	KV		Reference Temperature						
				10	*0*	*-10*	*-20*	*-30*	*-40*	*-50*
		T	*J*							
S355	*JR*	*20*	*27*	*40*	*35*	*25*	*20*	*15*	*15*	*10*
	J0	*0*	*27*	*60*	*50*	*40*	*35*	*25*	*20*	*15*
	J2	*-20*	*27*	*90*	*75*	*60*	*50*	*40*	*35*	*25*
	K2,M,N	*-20*	*40*	*110*	*90*	*75*	*60*	*50*	*40*	*35*
	ML,NL	*-50*	*27*	*155*	*130*	*110*	*90*	*75*	*60*	*50*

- Concrete crushing:

$$P_{Rd,2} = (0.29 * \alpha * d^2 * \sqrt{(f_{ck} * E_{cm})})/\gamma_v \tag{2.2}$$

- At ULS

$$P_{Rd,ULS} = min(P_{Rd,1}, P_{Rd,2} \tag{2.3}$$

- At SLS

$$P_{Rd,SLS} = 0.75 * P_{Rd,ULS} \tag{2.4}$$

Where:

$$\alpha = 0.2 * (h_{sc}/d + 1) : 3 \leq (h_{sc}/d) \leq 4 \tag{2.5}$$

$$\alpha = 1 : h_{sc}/d > 4 \tag{2.6}$$

$$\gamma_\nu = 1.25 \tag{2.7}$$

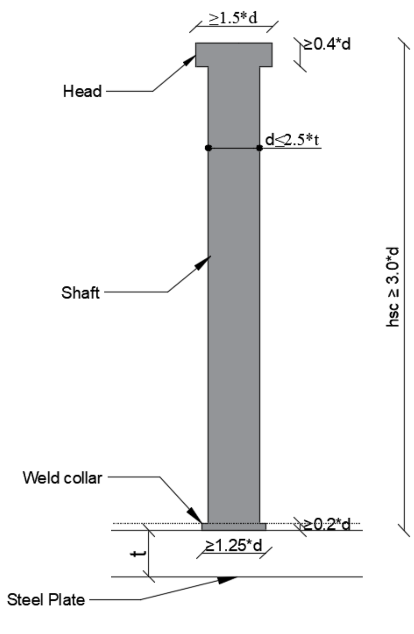

Figure 2.6: Shear stud type SD. Size and dimension.

2.3.1.2 Stainless steel

Similar to carbon steel, stainless steel has several grades and types. However, it can be classified according to the functionality into two primary subtitles; stainless steel in girders and in shear connectors. **Stainless steel in girders** EN 1993-1-4 and other design manuals apply to the austenitic, duplex, and ferritic stainless steels. Structural stainless steel is classified according to its chemical compositions. (Table 2.3) shows different duplex stainless steel grades with their composition (SS EN 1993-1-4:2006/ A1:2017).

Table 2.3: Content of alloying element for different stainless-steel grades.

<table>
<tr><td rowspan="2"></td><td rowspan="2">Grade</td><td colspan="5">Content of alloying element weight (%)</td></tr>
<tr><td>C</td><td>Cr</td><td>Ni</td><td>Mo</td><td>Others</td></tr>
<tr><td rowspan="3">Duplex</td><td rowspan="2">1.4162</td><td rowspan="2">0,04</td><td rowspan="2">21,0-22,0</td><td rowspan="2">1,35-1,7</td><td rowspan="2">0,1-0,8</td><td>N: 0,2-0,25</td></tr>
<tr><td>Cu: 0,1-0,8</td></tr>
<tr><td>1.4462</td><td>0,03</td><td>21,0-23,0</td><td>4,5-6,5</td><td>2,5-3,5</td><td>N: 0,1-0,22</td></tr>
</table>

According to (SS-EN 10088-1), the choice of stainless-steel grade can be determined according to the corrosivity class of a specific bridge. These grades can be used without any surface treatment or corrosion protection, according to (Table 2.4):

Table 2.4: Stainless steel grade corresponding to the corrosivity class.

Corrosivity class	Stainless steel grade
C5-M	1.4462, 1.4529, 1.4539, 1.4410, and 1.4547
C4	1.4162, 1.4362, 14401, 1.4404, and 1.4571

Fracture toughness
Stainless steel shows sufficient fracture toughness down to temperature -40°C. However, with reducing the temperature, authentic stainless-steel toughness decreases proportionally, and no transition region from ductile to brittle is noticed. A transition region is detected in duplex and ferritic stainless steel, but both show an adequate toughness down to service temperature -40°C (A1:2017).

Galvanic corrosion
When two different types of metallic materials have an electrical connection throughout an electrically conducting medium (as seawater), an electrical current is initiated from the metal representing the anode to the other representing the cathode through the conducting medium (electrolyte). This reaction is a corrosion reaction, and it results by corroding the less noble metal, which is the anode. When stainless steel is present with carbon steel in a galvanic cell, stainless steel forms the cathode, and it does not suffer any corrosion, while mean carbon steel became the less noble metal and is corroded. When different stainless steel types are present, galvanic corrosion is hardly initiated unless severe conditions similar to the laboratory conditions exist. Galvanic corrosion between different metal types can be prevented by interrupting the electrical path in the direct metal connection or in the electrolyte bridging. For

example, insulating washers can be used between two dissimilar metals in direct contact while coating the more noble metal to break the electrolyte bridging.

Modulus of elasticity

Carbon steel and stainless steel have different mechanical properties. These differences can be noticed in the stress-strain curve for each of them. In carbon steel, the relation between stress and strain remains linear elastic until yielding and a plateau afterward before the final failure. The behavior of the stress-strain curve for stainless steel is different; it has a smoother transition between the linear elastic stage and the plateau, and no well-defined peak value is observed (Figure 2.7) (SS-EN 1993-1-4:2006/A1:2017).

Modulus of elasticity is considered to be 200GPa in the structural design for all types of stainless steel. For calculating deformations (no plastic hinges), a secant modulus of elasticity is calculated according to the following (SS-EN 1993-1-4:2006/A1:2017).

$$E_s = (E_{s1} + E_{s2})/2 \tag{2.8}$$

$$E_{s,i} = E/(1 + 0.002 * [E/\sigma_{i,Ed,ser}] * [\sigma_{i,Ed,ser}/f_y]^n) \tag{2.9}$$

Where:

E_{s1}	Secant modulus of elasticity in the tensioned flange
E_{s2}	Secant modulus of elasticity in the compressed flange
i	1,2
$\sigma_{i,Ed,ser}$	Serviceability design stress
E	Modulus of elasticity 200GPa
n	Ramberg Osgood parameter. n=8 for Duplex stainless steel

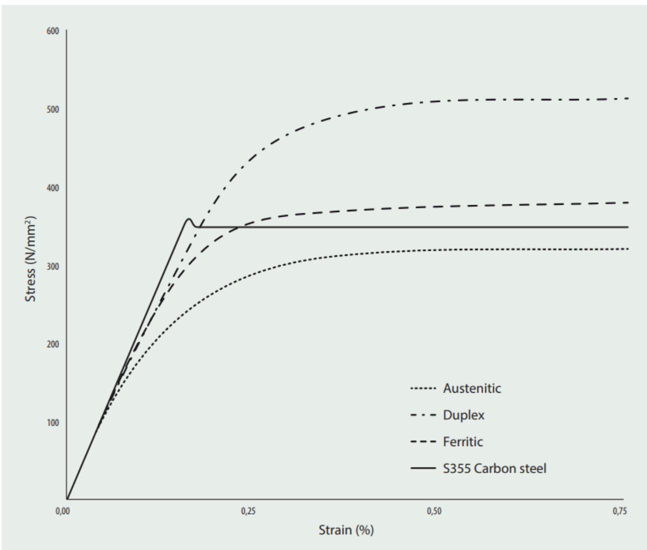

Figure 2.7: Stress-strain curve for different types of stainless steel compared to carbon steel (S355) (A1:2017, Figure 2.1).

The characteristic yield strength f_y and the ultimate strength f_u is obtained from (Table 2.5) (SS-EN 1993-1-4:2006/A1:2017).

Table 2.5: Yield strength and tensile strength of different stainless-steel products (SS-EN 1993-1-4:2006/ A1:2017).

Grade	Product form							
	Cold-rolled strip		Hot-rolled strip		Hot rolled plate		Bars, rods & sections	
	Nominal thickness t							
	$t \leq 8mm$		$t \leq 13,5mm$		$t \leq 75mm$		$t, or\phi \leq 250mm$	
	f_y	f_u	f_y	f_u	f_y	f_u	f_y	f_u
1.4162	530	700	480	680	450	650	450	650
1.4462	500	700	460	700	460	640	450	650

Shear Studs

Shear studs made of stainless steel are classified according to EN ISO 3506, using the letter “A” for austenitic, “F” for ferritic, “C” for martensitic, and “D” for duplex. After this letter, a number is provided to describe the corrosion resistance. These numbers are (1, 2, 3, 4, 5, 6, or 8). Increasing the number reflects a higher corrosion resistance and more durable shear studs. Choosing the corrosion resistance or the bolt class should be based on the grade of the plates being connected to, and both of them need to have similar corrosion resistance. (Table 2.6) shows stud’s classification according to the chosen stainless-steel grade.

Table 2.6: Shear connectors made of Stainless steel classification. (SS EN 1993-1-4:2006/ A1:2017).

Type	Class	Stainless steel grade
Austenitic	A1	1.4570, 1.4305
	A2	1.4301, 1.4307
	A3	1.4541, 1.4550
	A4	1.4401, 1.4404
	A5	1.4571
	A8	1.4529, 1.4547
Duplex	D2	1.4482, 1.4362
	D4	1.4162, 1.4062
	D6	1.4462
	D8	1.4410, 1.4501, 1.4507

Different manufacturing processes achieve different strength levels for each class. These strength levels or property classes are (50, 70, 80, or 100). (Table 2.7) shows the tensile strength of different bolt grades with varying property classes.

Table 2.7: Yield strength and tensile strength of Stainless steel studs (SS-EN 1993-1-4:2006/ A1:2017).

Group	Grade	Property class	Yield strength (MPa)	Tensile strength (MPa)
Austenitic	A1, A2, A3, A5	50	210	500
		70	450	700
		80	600	800
	A4	50	210	500
		70	450	700
		80	600	800
		100	800	1000
	A8	70	450	700
		80	600	800
		100	800	1000
Duplex	D2, D4, D6, D9	70	450	700
		80	600	800
		100	800	1000

2.3.2 Plated structural elements

2.3.2.1 Carbon Steel

Cross-section classification
Eurocode classifies four different classes for cross-sections with respect to their slenderness:

Class 1
Also known as a compact cross-section, when the cross-section has very low slenderness. Compacted sections can form plastic hinges in undetermined structures like continuous beams. At a full moment capacity, all of the cross-sections is plasticized (Mpl) is reached.

Class 2
The cross-section is again compact but doesn't have enough rotational capacity to form plastic hinges as in Class 1.

Class 3
Semi-compact section, with a risk for local buckling, moment capacity for the section is calculated for a linear stress distribution (Mel) with a maximum stress of f_y.

Class 4
Thin-walled section. Buckling takes place before the outer fiber is yielding. The section is designed for the effective cross-section, excluding the buckled regions. EN 1993-1-1 section 5,5 provides a procedure to determine cross-section classes. The effective cross-section for class four is determined according to EN 1993-1-5, 4.

Effective width due to shear lag
When a continuous composite beam is subjected to bending, normal stresses (compression or tension) transfer from the steel flanges into the concrete slab through shear connectors. This transformation is done in the form of shear stresses (theoretically concentrated at the flange edge). The magnitude of these shear stresses varies with the variation of the bending moment diagram in the whole beam. Consequently, the aforementioned normal stresses in the concrete flange will vary with the variation of shear stresses and will decrease gradually away from the web-flange connection point. This distortion in the concrete slab stresses is called the shear lag effect and can be found in the bottom flange of a box girder with large sections (Vayas and Iliopoulos, 2014). To overcome this phenomenon, the effective width due o shear lag is calculated according to EN1994-2 for concrete and steel flanges. For the purpose of this study, effective width in steel flanges is introduced.
Effective width due to shear lag in box girders is determined using the following formula:

$$b_{eff,i} = \beta * b_{0i} : i = 1,2 \quad (Figure 2.8) \tag{2.10}$$

Where:

b_{oi}	As shown in Figure 2.8 and Figure 2.9
β	Reduction factor according to Table 2.8 and Table 2.10
κ_i	$(\alpha_0 * \beta_{0i})/L_e$
α_{0i}	$\sqrt{(1 + (A_{sI,i}/b_{0i} * t)}$

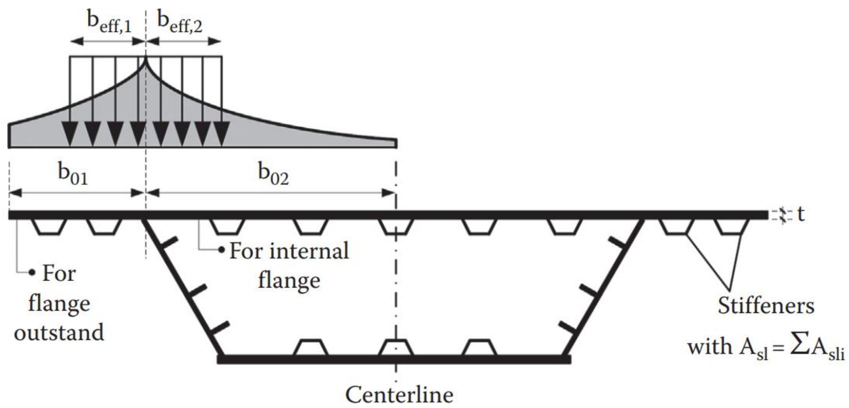

Figure 2.8: Notation for shear lag (Vayas and Iliopoulos, 2014).

Table 2.8: Effective width factor β for sagging and hoggings moments

κ	Sagging moments	Hogging moments
$\leq 0,02$	$\beta = 1$	$\beta = 1$
$0,02 < \kappa \leq 0,7$	$\beta = \beta_1 = 1/(1+6,4\kappa^2)$	$\beta = \beta_2 = 1/(1+6(\kappa - 1/2500\kappa) + 1,6\kappa^2)$
> 0.7	$\beta = \beta_1 = 1/(5,9\kappa)$	$\beta = \beta_2 = 1/(8,6\kappa)$

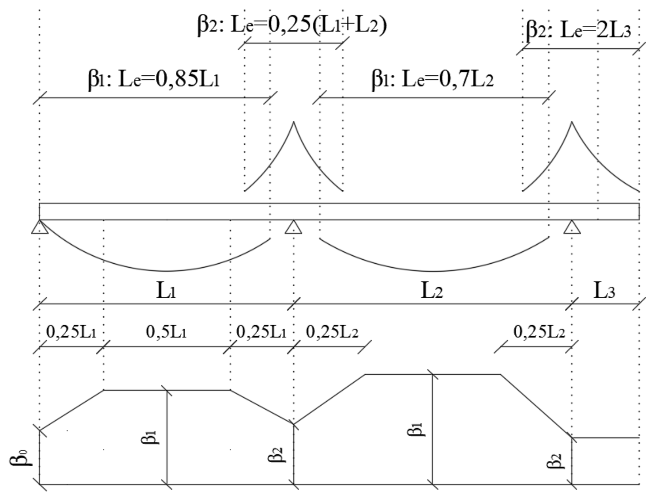

Figure 2.9: Effective width factor β

Table 2.9: Effective width factor β for cantilever and end support

Factor κ	Location	β value
All κ	End Support	$\beta_0 = (0.55 + 0.025/\kappa) * \beta_1 < \beta_1$
All κ	Cantilever	$\beta = \beta_2 atsupportandatend$

Stiffened plate buckling due to direct stresses

Effective area for plate elements with longitudinal stiffeners under compression is calculated according to (EN 1993-1-5, 4.5) using the following formula

$$A_{c,eff} = \rho_c.A_{c,eff,loc} + \sum b_{edge,eff}.t \tag{2.11}$$

$$A_{c,eff,loc} = A_{st,eff} + \sum \rho_{loc}.b_{c,loc}.t \tag{2.12}$$

Where:

$A_{c,eff,loc}$ The sum of effective cross-sections for all stiffeners and adjacent plates
ρ_{loc} Reduction factor for each subpanel

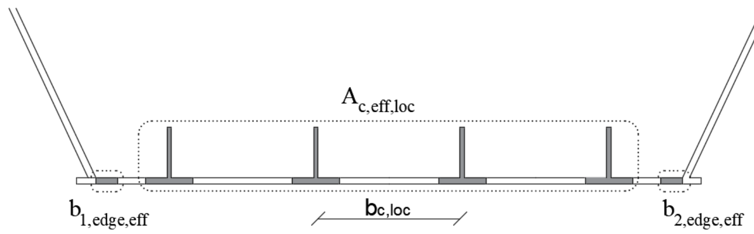

Figure 2.10: Stiffened plate under uniform compression (SS EN 1993-1-5).

Plate type behavior:

$$\lambda_p = \sqrt{\beta_{A,c}.f_y/\sigma_{cr,p}} \tag{2.13}$$

$$\beta_{A,c} = A_{c,eff,loc}/A_c \tag{2.14}$$

Where:

$\sigma_{cr,p}$ SS EN 1993-1-5 Annex A
A_c Gross area of the plate with stiffeners except for edge panels

The reduction factor for plate type behavior can be determined according to EN 1993-1-5, 4.4.

Column type buckling behavior:

$$\sigma_{cr,st} = (\pi^2.E.I_{st,1})/(A_{st,1}.a^2) \tag{2.15}$$

$$\lambda_p = \sqrt{(\beta_{A,c}.f_y)/\sigma_{cr,c}} \tag{2.16}$$

$$\beta_{A,c} = A_{st,l,eff}/A_{st1} \tag{2.17}$$

Where:

$I_{st,l}$ Out of plate Second moment of area for the stiffener and adjacent panels (gross area)
$A_{st,l}$ Sectional area of the stiffener with adjacent panels (Gross section)
$A_{st,l,eff}$ Effective section of the stiffener with adjacent panels

Interaction between plate and column buckling:

$$\rho_c = (\rho - \chi_c).\xi.(2 - \xi) + \chi_c \tag{2.18}$$

$$\xi = (\sigma_{cr,p})/(\sigma_{cr,c}) - 1 : \quad 0 \leq \xi \leq 1 \tag{2.19}$$

Shear Resistance
Shear buckling resistance is calculated according to EN 1993-1-5 5.2 for carbon steel. Buckling reduction needs to be checked for the following limits:
For unstiffened web:

$$(h_w/t) > (72/\eta).\epsilon \tag{2.20}$$

For Stiffened web:

$$(h_w/t) > (31/\eta).\epsilon.\sqrt{\kappa_t} \tag{2.21}$$

$$\epsilon = \sqrt{235/f_y} \tag{2.22}$$

Where:

h_w Height of the web

t_w Thickness of the web

η 1,2

κ_t Shear buckling coefficient:

$$5,34 + 4,00.(h_w/a)^2 + \kappa_{sl} \qquad a/h_w \geq 1 \tag{2.23}$$

$$4,00 + 5,34.(h_w/a)^2 + \kappa_{sl} \qquad a/h_w < 1 \tag{2.24}$$

$$\kappa_{sl} = 9.(h_w/a)^2 + \sqrt[4]{(I_{sl}/(t^3.h_w))^3} \qquad \leq (2.1/t)\sqrt[3]{I_{sl}/h_w} \tag{2.25}$$

a Transverse stiffener spacing

I_{sl} Sum of the second moment of area of the individual longitudinal stiffeners

Shear buckling resistance (web contribution):

$$V_{bw,RD} = (\chi_w.f_{yw}.h_w.t)/(\sqrt{3}\gamma_{M1}) \tag{2.26}$$

$$\lambda_w = 0.76\sqrt{f_{yw}/\tau_{cr}} \tag{2.27}$$

$$\tau_{cr} = \kappa_t.\sigma_E \tag{2.28}$$

$$\sigma_E = (\pi^2.E.t^2)/(12.b^2.(1 - \nu^2)) \tag{2.29}$$

Where:

χ_w Shear buckling reduction factor Table2.10

$\tau_c r$ Critical shear stress

Table 2.10: Shear buckling reduction factor (SS EN 1993-1-5).

	Rigid end post	Non-rigid end post
$\lambda_w < 0,83/\eta$	η	η
$0,83/\eta \leq \lambda_w < 1,08$	$0,83/\lambda_w$	$0,83/\lambda_w$
$\lambda_w \geq 1,08$	$1,37/(0,7+\lambda_w)$	$0,83/\lambda_w$

2.3.2.2 Stainless steel

Thin-walled elements made of stainless steel are designed according to SS-EN 1993-1-4 and A1:2017.

Cross-section classification

Similarly, to carbon steel, stainless steel members can be classified into four classes as defined in section 2.3.2.1. Cross-section class limits are shown in Figure 2.11.

Effective width due to shear lag

The shear lag effect for stainless steel structural members can be taken according to SS-EN 1993-1-5 for carbon steel. See section 2.3.2.1 of this report for more information. **Plate buckling due to direct stresses** Reduced cross-section area according to SS-EN 1993-1-5, 4 can be used in plate members made of stainless steel. The reduction factor ρ for plate type buckling is calculated according to A1:2017, 5.4.1: Internal cross-section elements:

$$\rho = (0,772/\lambda_P) - (0,079/\lambda_P^2) \leq 1 \tag{2.30}$$

$$\lambda = (b/t)/(28,4.\epsilon.\sqrt{\kappa_\sigma}) \tag{2.31}$$

$$\epsilon = [(235/f_y).(E/210000)]^{0,25} \tag{2.32}$$

Where:

t plate thickness

b Plate width

λ_P Plate slenderness

ϵ Material factor

κ Buckling factor (Figure 2.12)

Internal compression parts

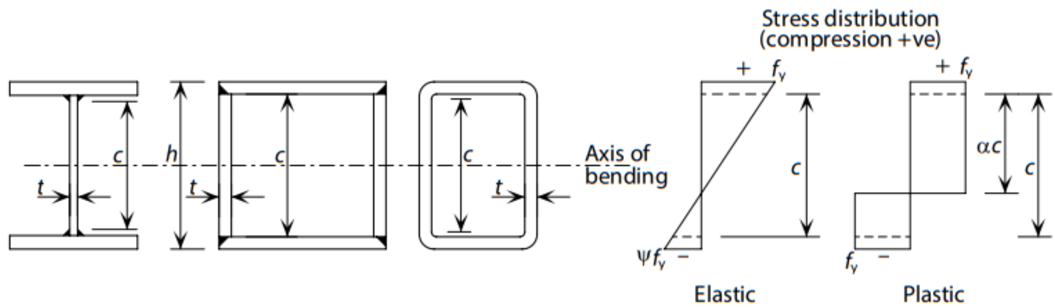

Class	Part subject to bending	Part subject to compression	Part subject to bending and axial force
1	$c/t \leq 72{,}0\varepsilon$	$c/t \leq 33{,}0\varepsilon$	When $\alpha > 0{,}5$: $c/t \leq 396{,}0\varepsilon/(13\alpha - 1)$ When $\alpha \leq 0{,}5$: $c/t \leq 36{,}0\varepsilon/\alpha$
2	$c/t \leq 76{,}0\varepsilon$	$c/t \leq 35{,}0\varepsilon$	When $\alpha > 0{,}5$: $c/t \leq 420{,}0\varepsilon/(13\alpha - 1)$ When $\alpha \leq 0{,}5$: $c/t \leq 38{,}0\varepsilon/\alpha$
3	$c/t \leq 90{,}0\varepsilon$	$c/t \leq 37{,}0\varepsilon$	$c/t \leq 18{,}5\varepsilon\sqrt{k_\sigma}$ For k_σ see 5.4.1

$$\varepsilon = \left[\frac{235}{f_y}\frac{E}{210\,000}\right]^{0,5}$$

Grade	1.4301	1.4401	1.4462
f_y (N/mm²)	210	220	460
ε	1,03	1,01	0,698

Notes:
For hollow sections, c may be taken as $(h - 3t)$ or $(b - 3t)$
$E = 200 \times 10^3$ N/mm²

$\alpha = \frac{1}{2}\left(1 + \frac{N_{Ed}}{f_y\, c \sum t_w}\right)$ for sections which are symmetrical about the major axis

Figure 2.11: Cross-section classification (A1:2017).

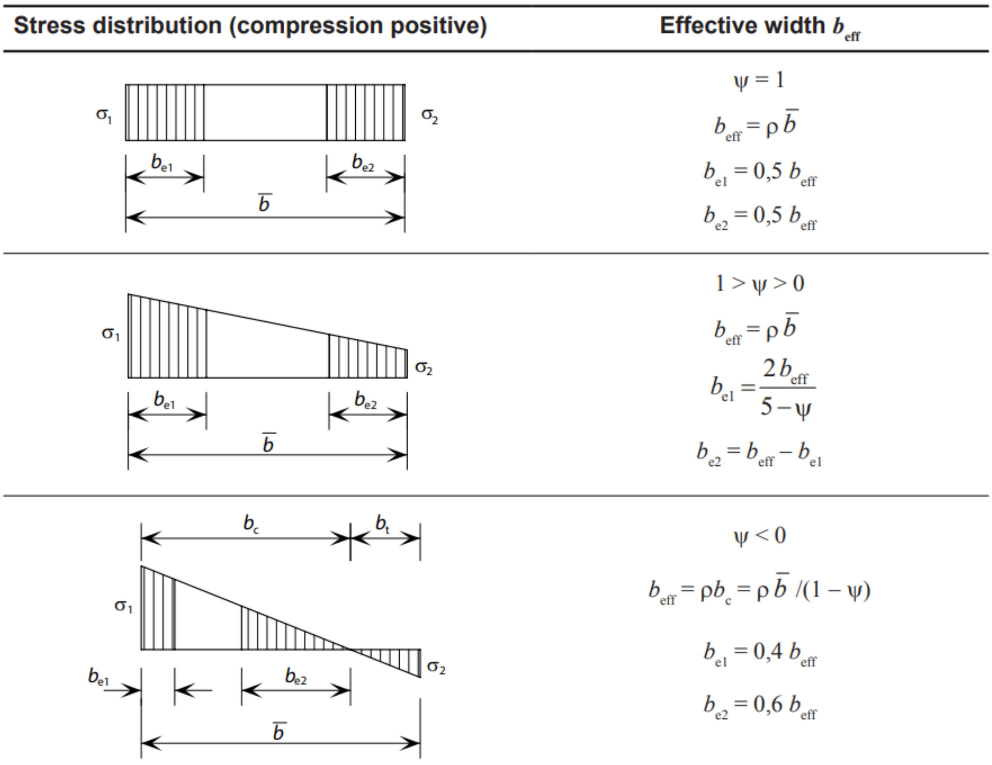

$\psi = \sigma_2 / \sigma_1$	1	$1 > \psi > 0$	0	$0 > \psi > -1$	-1	$-1 > \psi \geq -3$
Buckling factor k_σ	4,0	$8{,}2 / (1{,}05 + \psi)$	7,81	$7{,}81 - 6{,}29\psi + 9{,}78\psi^2$	23,9	$5{,}98\ (1 - \psi)^2$

Figure 2.12: The effective width of internal compression elements (A1:2017).

The reduction factor χ_c for column type buckling is determined according to A1:2017, 6.3.3.

$$\chi = 1/(\phi + [\phi^2 - \lambda^2]) \leq 1 \tag{2.33}$$

$$\phi = 0.5(1 + \alpha.(\lambda - \lambda_0) + \lambda^2) \tag{2.34}$$

$$\lambda = \sqrt{(A_{eff}.f_y)/N_{cr}} \tag{2.35}$$

Where:

N_{cr} Elastic critical force
α Imperfection factor (Figure 2.13)
λ_0 Non-dimensional slenderness (Figure2.13)

Type of member	Axis of buckling	Austenitic and duplex		Ferritic	
		α	$\bar{\lambda}_0$	α	$\bar{\lambda}_0$
Cold formed angles and channels	Any	0,76	0,2	0,76	0,2
Cold formed lipped channels	Any	0,49	0,2	0,49	0,2
Cold formed RHS	Any	0,49	0,3	0,49	0,2
Cold formed CHS/ EHS	Any	0,49	0,2	0,49	0,2
Hot finished RHS	Any	0,49	0,2	0,34	0,2
Hot finished CHS/EHS	Any	0,49	0,2	0,34	0,2
Welded or hot rolled open sections	Major	0,49	0,2	0,49	0,2
	Minor	0,76	0,2	0,76	0,2

Figure 2.13: Imperfection factor α and non-dimensional slenderness λ_0 (A1:2017).

Shear buckling resistance
Shear buckling resistance is calculated according to A1:2017, buckling reduction is calculated in the following limits:

For unstiffened web:

$$(h_w/t) > (56,2/\eta).\epsilon \tag{2.36}$$

Shear buckling resistance (web contribution):

$$V_{bw,RD} = (\chi_w.f_{yw}.h_w.t)/(\sqrt{3}.\gamma_{M1}) \tag{2.37}$$

Where:

$$\lambda_w = h_w/(37,4.t_w.\epsilon.\sqrt{\kappa_t}) \tag{2.38}$$
$$\kappa_t = 5,34 + 4,00.(h_w/a)^2 + \kappa_{sl} \qquad a/h_w \geq 1 \tag{2.39}$$
$$\kappa_t = 4,00 + 5,34.(h_w/a)^2 + \kappa_{sl} \qquad a/h_w < 1 \tag{2.40}$$
$$\kappa_{sl} = 9.(h_w/a)^2 + \sqrt[4]{(I_{sl}/(t^3.h_w))^3} \qquad \leq (2.1/t)\sqrt[3]{I_{sl}/h_w} \tag{2.41}$$

h_w	Web depth
t_w	Plate thickness
f_{yw}	Yield strength
η	1.2 according to SS-EN 1993-1-4
γ_{M1}	1.1 according to A1:2017
χ_w	Shear buckling reduction factor (Table 2.11)
λ_w	Non- dimensional slenderness
κ_t	minimum shear buckling coefficient
a	Transverse stiffener spacing
I_{sl}	Sum of the second moment of area of the individual longitudinal stiffeners

Table 2.11: Shear buckling reduction factor $_w(A1:2017)$.

	Rigid end post	Non-rigid end post
$\lambda \leq 0,65/\eta$	η	η
$0,65/\eta \ < \lambda_w < 0,65$	$0,65/\lambda_w$	$0,65/\lambda_w$
$0,65 \geq \lambda_w$	$1,56/(0,91+\lambda_w)$	$1,19/(0,54+\lambda_w)$

2.4 Life Cycle Cost Analysis

LCC analysis is used for cost estimation under a specific period, taking into account relevant economic factors. Economic factors can contain initial construction and maintenance costs under a time period. When conducting an LCC analysis, the goal is defined as the optimal creation of a product with the minimum investment cost by considering the function purpose. It is widely used in bridge management systems because it defines the selection of an optimal life cycle strategy, taking into account the structure's life span. The definition of LCC and LCCA according to (ISO15686-5,2008) is: Life-cycle Cost (LCC) is the cost of an asset or its parts while fulfilling its performance requirements. Life-cycle Cost Analysis (LCCA) is a methodology for the systematic evaluation of the life-cycle cost over a specified period as defined in the agreed scope. The contributors of LCC analysis can be divided into the following parts:

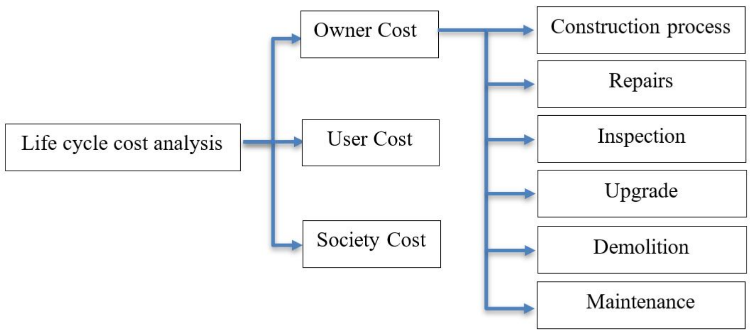

Figure 2.14: Life Cycle Cost Analysis.

According to (Veganzones, Sundquist, Pettersson, Karoumi, 2015), other aspects need to be considered for a holistic approach. Failure cost and Aesthetical Cultural cost are such. Even though the features above have significant importance for Hisings-bridge, it has been decided not to include them as a widely acceptable calculation method cannot be found. In order to formulate the fundamental equation of LCC analysis, owner, user, and society costs are used.

$$LCC = LCC_{owner} + LCC_{user} + LCC_{society} \tag{2.42}$$

The future costs along the life span of the structure are discounted by using the discount rate. The value of the discount rate is usually accounted as the actual interest rate. The real interest rate is calculated from the nominal interest rate from long loans, inflation, and possible positive or negative effects on the structure.

$$P = (P_L - P_i - P_c)/(1 + P_i) \tag{2.43}$$

Where:

P_L Nominal interest rate for extended loans

P_i inflation

P_c Factor accounting for a positive or negative effect in the structure

Inflation usually accounts for society, obtained from the net price index (José Javier Veganzones Muñoz, 2016). According to Trafikverket, the discount rate for social projects is 3.5% (Traffikverket, 2020, Kapitel 19 ASEK guidelines). According to the costs in the construction sector grow more rapidly than those in society (Figure 2.15).

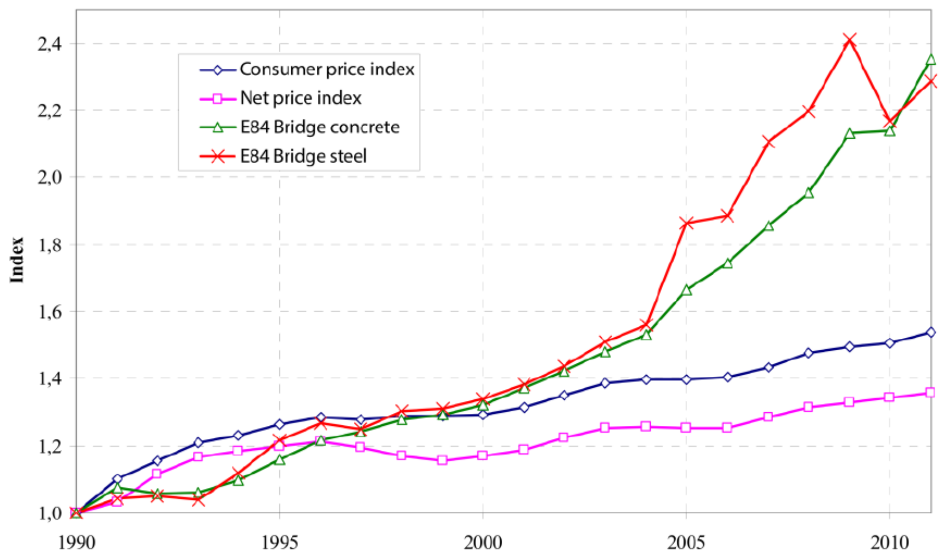

Figure 2.15: Comparison of the evolution costs according to E84 for steel and concrete structures, the consumer price index, and the following price index (Sundquist, 2014).

Consequently, higher inflation and lower real interest rate are expected over time. It is common practice in LCCA to perform sensitivity analysis with different discount costs. Different discount rates between 2 and 7% are investigated on how they influence the parameters in the LCC analysis. This is a typical interval for industrialized countries (Salokangas, 2009; Christensen, 2011).

Owner cost

The influence on infrastructure users during the construction works and LCM are referred to as user costs. The user cost is calculated as the summation of traffic delay cost (TDC) and vehicle operations costs (VOC). An example of TDC is when a road is repaired. Transported goods can delay because the transporter must drive slowly due to the reparations along the road. During a road or bridge construction, the users must find alternative routes till the project. This induces tire damages, extra fuel costs, and earlier engine maintenance from using an alternative way that affects the user's economy. Those types of expenses are VOC (José Javier Veganzones Muñoz, Lars Pettersson, Håkan Sundquist Raid Karoumi, 2016).

$$VOC = \sum_{t=0}^{L} T.ADT_t.N_t.(r_i.w_t + (1 - r_i).w_p).(1/(1 + P)^t) \tag{2.44}$$

$$TDC = \sum_{t=0}^{L} T.ADT_t.N_t.(r_i.O_t + (1 - r_i).O_p).(1/(1 + P)^t) \tag{2.45}$$

Where:

T	Expected travel delay time in case of a roadway work measured in h
ADT_i	average daily traffic at a time t measured in vehicles/day
N_t	Total amount of days that are needed to carry out a certain LCM
r_t	Percentage of heavy vehicles out of the ADTt
w_t	Hourly time value for a heavy vehicle measured in SEK/h
w_p	Hourly time value for a passenger car in SEK/h
O_t	average operating cost in SEK/h for a heavy vehicle, including transported goods
O_p	Average operating cost in SEK/h for a passenger car

Society costs

Society costs append to accidents, environmental impact, non-renewable materials, and other related issues (José Javier Veganzones Muñoz, Lars Pettersson, Håkan Sundquist Raid Karoumi, 2016).

$$LCC_{society} = ACC = \sum_{t=0}^{L} L_t.ADT_t.N_t.C_{acc}.(A_r - A_n).(1/(1 + p)^t) \tag{2.46}$$

L_t	Affected roadway length in m
ADT_i	Cost of an accident for the society in SEK
N_t	Accident frequency during road work in accident/vehicle-km
r_t	accident frequency during normal conditions in accident/vehicle-km

3
Hisings-Bridge

Through the center of Gothenburg city, Göta älv river drains lake Vänern into the sea. The two parts of the town are connected by an old bridge called Göta älv-bridge, constructed in 1937. Göta älv-bridge has already exceeded its designed service life, and the demolishing work of it will start after the opening day of the new Hisings-bridge. Despite the aesthetic advantages of the new bridge for Gothenburg city, it will facilitate the transportation of trams, public vehicles, bicycles, and pedestrians. A vertical lifting span will ensure ships' movement along the river at the middle of the bridge. Figure 3.1 shows a plan view for different fields on the bridge.

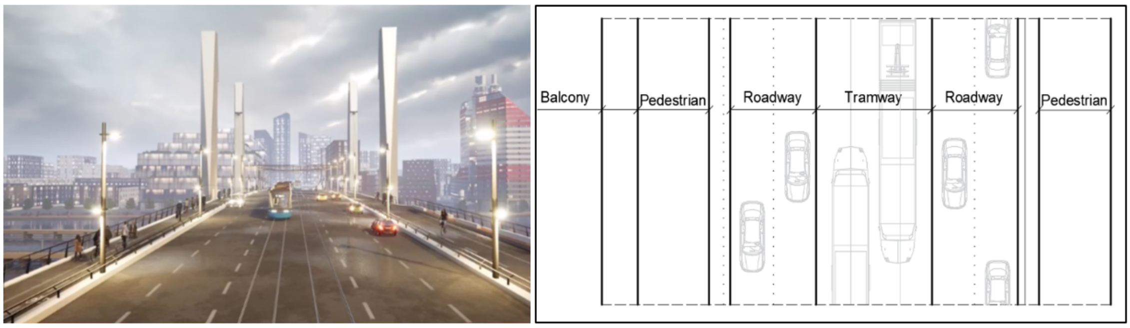

Figure 3.1: An architectural view for Hisings-bridge to the left and a plan view to the right.

As shown in Figure 3.2, the lifting span with 48m length and 32m width is resting on four pylons between axis 1.15 and 1.16. The height of the towers is 56m. The bridge's total length is about 440m crossing the river from south to north. Figure 3.2 shows different parts of the bridge with spacing between supports. In this work, the superstructure between axis 1.17 and 1.20 is investigated. This chapter is an overview for the original design of Hisings-bridge, it starts by a description for the geometry, cross sections, and material, followed by a brief explanation for loading, analysis stage and results.

3.1 Northern Side Span

The superstructure of the side bridges is a steel-concrete composite bridge consisting of three parallel box girders connected to a concrete slab through shear studs Figure 3.3. A set of three circular concrete columns supports the bridge at each axis. Crossbeams are provided at each support to connect the three boxes and to ensure

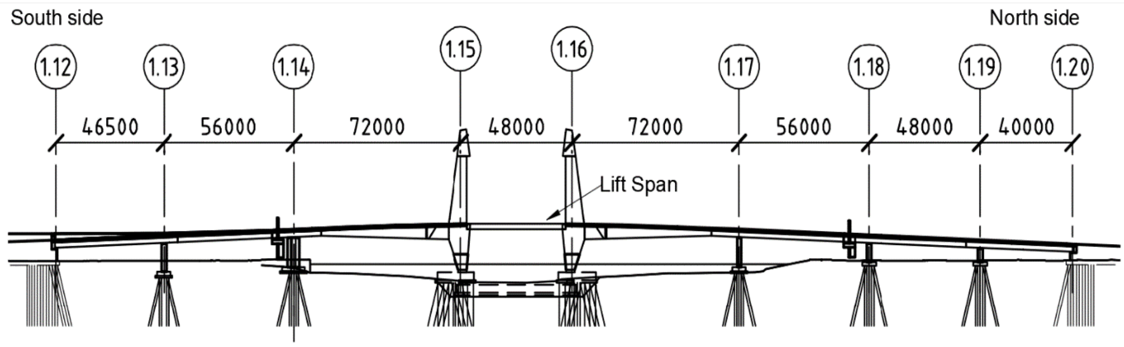

Figure 3.2: Side elevation for Hisings-bridge showing two side spans and one lifting span at the middle

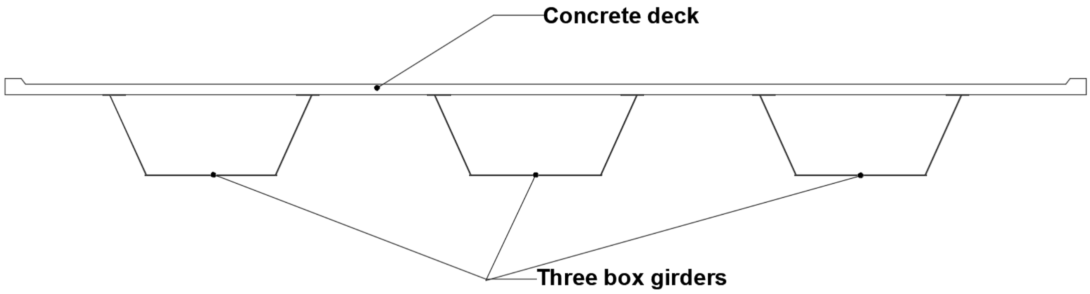

Figure 3.3: Cross-section in the bridge northern side span.

safe lifting in a case of bearing changing. The northern side span extends from axis 1.16 to axis 1.20. Height and stiffness of the box girders decrease from axis 1.16 towards axis 1.17. after that, it continues with the same height but with varying plate thicknesses until the end of the side span, i.e., until axis 1.20. Box girders have different cross-sections at piers and in the span. Support sections are not redesigned in chapter 4 (Redesign using stainless steel), but they are considered with the same section in stainless steel during the life cycle cost analysis. More details and drawings are provided about the cross-sections at the span and at the support in the coming chapters. Appendix A includes a side elevation for the northern bridge with more details about the cross-section and plate thicknesses.

3.1.1 Material

3.1.1.1 Structural steel

The structural steel used in the box girders in Hisings-bridge is S355, with a unit weight of 78.5kN/m3; this unit weight includes painting weight, welding. . . . etc. Ductility class is determined for a service temperature of -40°C. Moreover, structural steel should meet the minimum requirements shown in Table 3.1 (TRVFS 2011).

Table 3.1: Additional Requirements (TRVFS 2011)

Nominal Thickness t (mm)	T_{27j} °C	Steel Type
$t \leq 30$	*-20*	-
$30 < t \leq 80$	*-20*	*Fine Grain Steel*
t > 80	*-40*	*Fine Grain Steel*

For architectural aspects, the minimum thickness of the external plates needs to be at least 16 mm. This condition ensures a smooth appearance for the outer surfaces after welding the inner stiffeners and is based on the designer's previous experience. However, this condition is not considered when redesigning with stainless steel as long as all other thickness requirements are respected. Moreover, architectural demands vary from one project to another, and the purpose of this work is to reduce the material consumption when using stainless steel. Table 3.2 includes all of the used steel properties in the analysis of Hisings-bridge side spans.

Table 3.2: S355, structural steel properties in Hisings-bridge.

Young modulus E	*210000*	*MPa*
Poisson ratio ν	*0.30*	-
Shear modulus G	*80769*	*MPa*
Compression modulus K	*17500*	*MPa*
Weight γ	*78.5*	*kN/m3*
Density ρ	*7850*	*Kg/m3*
Elongation coefficient α	*1.00E-05*	*1/K*

3.1.1.2 Shear connectors (Studs)

The used shear studs in Hisings-bridge are SD1 with yield strength f_{yk} = 350 MPa, and ultimate tensile strength $f_{uk} = 450MPa$. Automatically welded according to (SS-EN ISO 14555).

3.1.2 Cross section

Each box girder of the northern side between axis 1.17 and axis 1.20 has two different cross-sections, support section, and span section. Plate thicknesses of each of the crosssections mentioned earlier vary along the bridge. For more details, see Appendix A.

3.1.2.1 Span cross section

The Span section has a trapezoidal shape, with two stiffeners located in the web and three stiffeners in the bottom flange. Three types of hollow stiffeners with trapezoidal cross-sections exist; T1, T2, and T3 (Figure 3.4). These stiffeners have three different thicknesses, 6, 8, and 10 mm, in various positions. More details about thicknesses can be found in Appendix A. Figure 3.5 illustrates the span cross-section shape and dimensions.

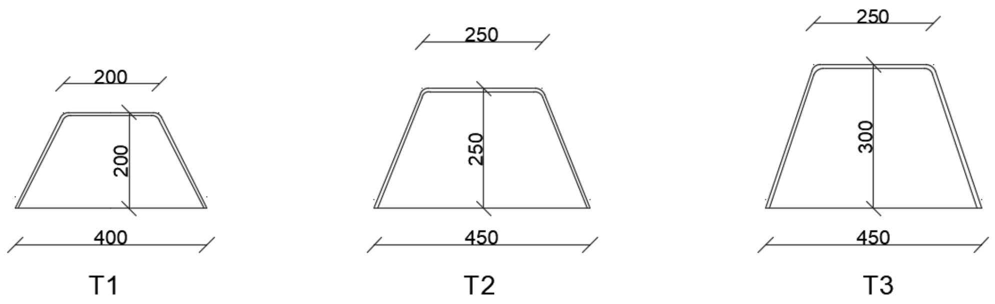

Figure 3.4: Hollow stiffeners dimensions.

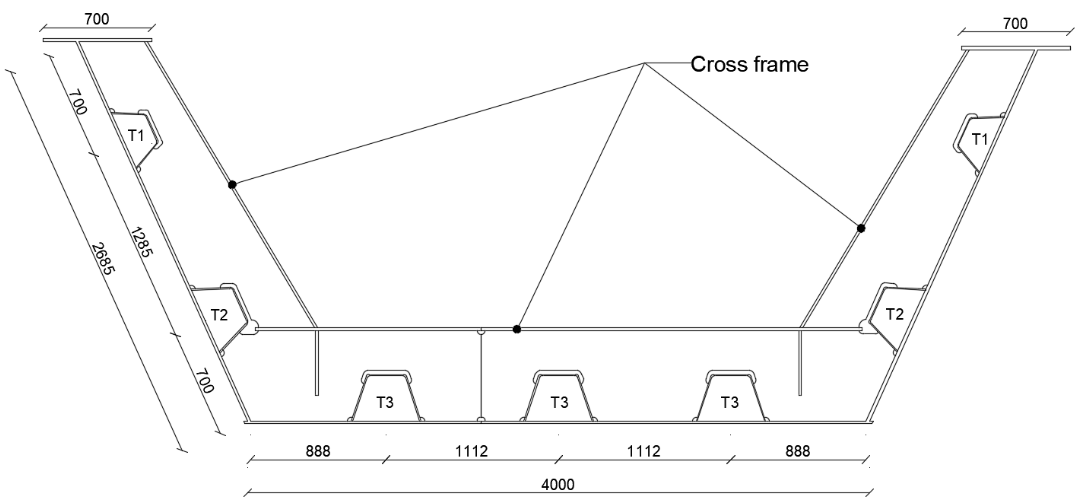

Figure 3.5: Span cross-section in a northern box girder (mm).

3.1.2.2 Support cross section

As mentioned in section 1.3, support sections are excluded from the stainless steel redesigning part, but it is included in the life cycle cost analysis using similar cross-sections. Cross-sections above the supports have a different geometry from span sections. It includes more stiffeners and two plated diaphragms. Support sections occupied 8m from the bridge length at each axis. Figure 3.6 shows support cross-section. Two plated diaphragms are provided Above each pier, a set of stiffeners are added to ensure a safe transition of reactions from the boxes to the piers. More stiffeners are provided at four corners to transfer temporary reactions from the bridge to the lifting jack when bearing changing.

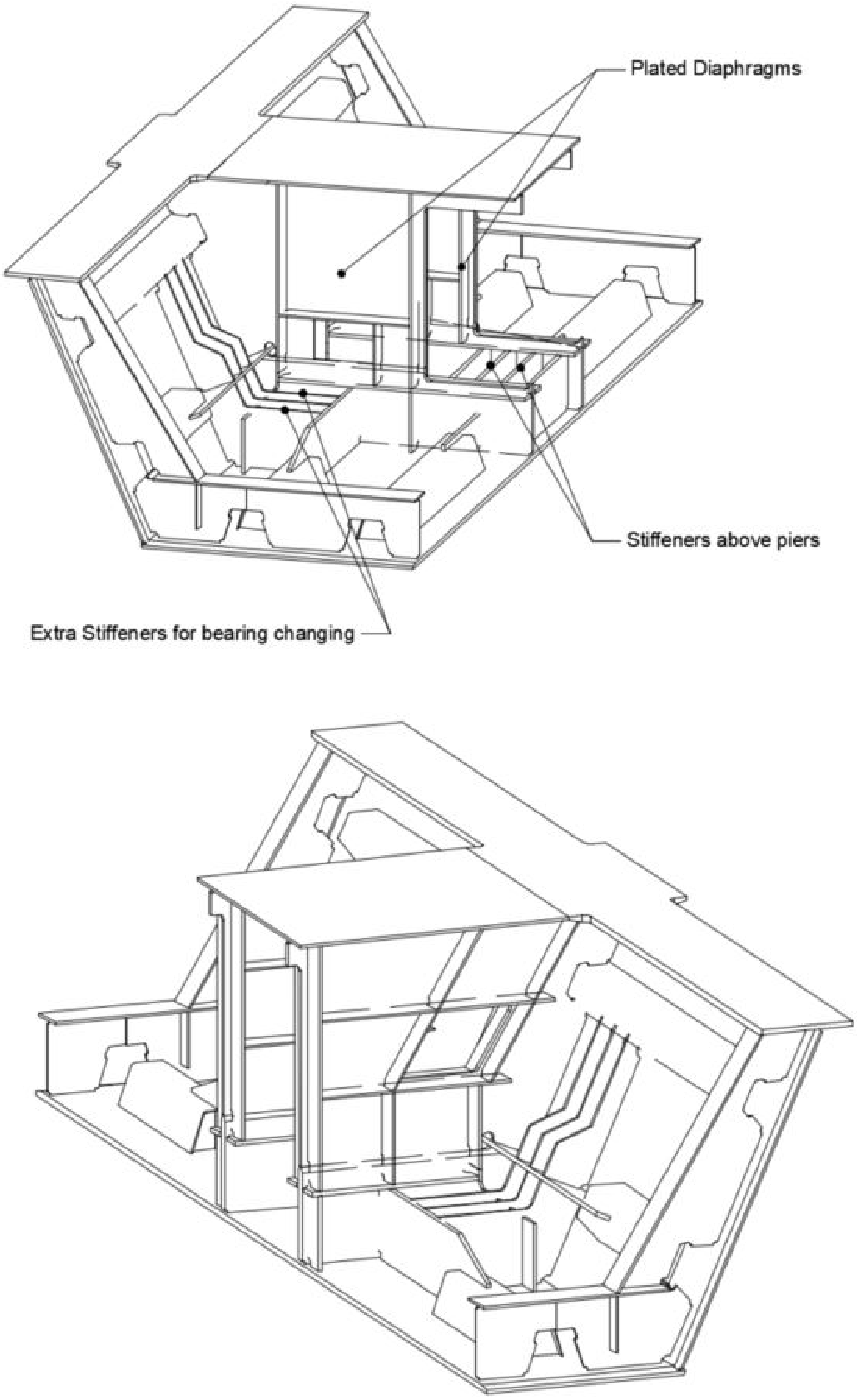

Figure 3.6: Support cross-section in a northern box girder (Stålöverbyggnad Norra Sidan, Östra Balken, 625/10-59161 A, Provided by COWI).

3.1.2.3 Cross frames

Cross frames are located every 4m along the bridge. Typically, they are used to increase the torsional capacity for the whole section and provide transversal support for the longitudinal stiffeners in the webs and the bottom flange. They provide lateral support for top flanges to avoid global torsional buckling for the whole box under construction. Cross frames have a T section with two different dimensions in the bottom flange and in webs, as shown in Figure 3.7.

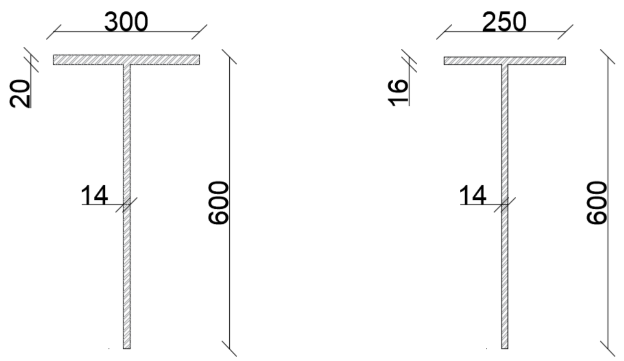

Figure 3.7: Cross frames sections. (left) at bottom flange. (right) at the webs.

3.2 Global design and stress distribution

In the original design, the whole bridge was modeled in Sofistik, as shown in Figure 3.8. The concrete deck and the box girders (top flanges, bottom plates, and webs) are modeled as shell elements, whereas longitudinal stiffeners and transversal stiffeners are generated as beam elements. Appendix A Shows the implemented varying thicknesses along the bridge. Thickness changing is taking place towards the inner side of the box girders, and the outer surfaces share the same line along the bridge. After the analysis, all of the results are stresses; these stresses were used later for buckling verifications.

3.2.1 Loading

In order to better understand the problem, loadings from the original design are presented here briefly. Nine main load categories were taken into account during the original design phase of Hisings-bridge. In this work, no details about the load combination are provided as the final results are used directly in the analysis.

Construction loads
The weight of the scaffolding was hand calculated and then applied to the model. The load was used based on the construction sequences that were followed. This was done to simulate any frozen in stresses coming from the concrete. Crane loading was not applied in the global loading. It was considered only in the local design, as the crane placing is predefined and more specific; it is considered acting directly on the cross frames of the design.

Permanent Loads

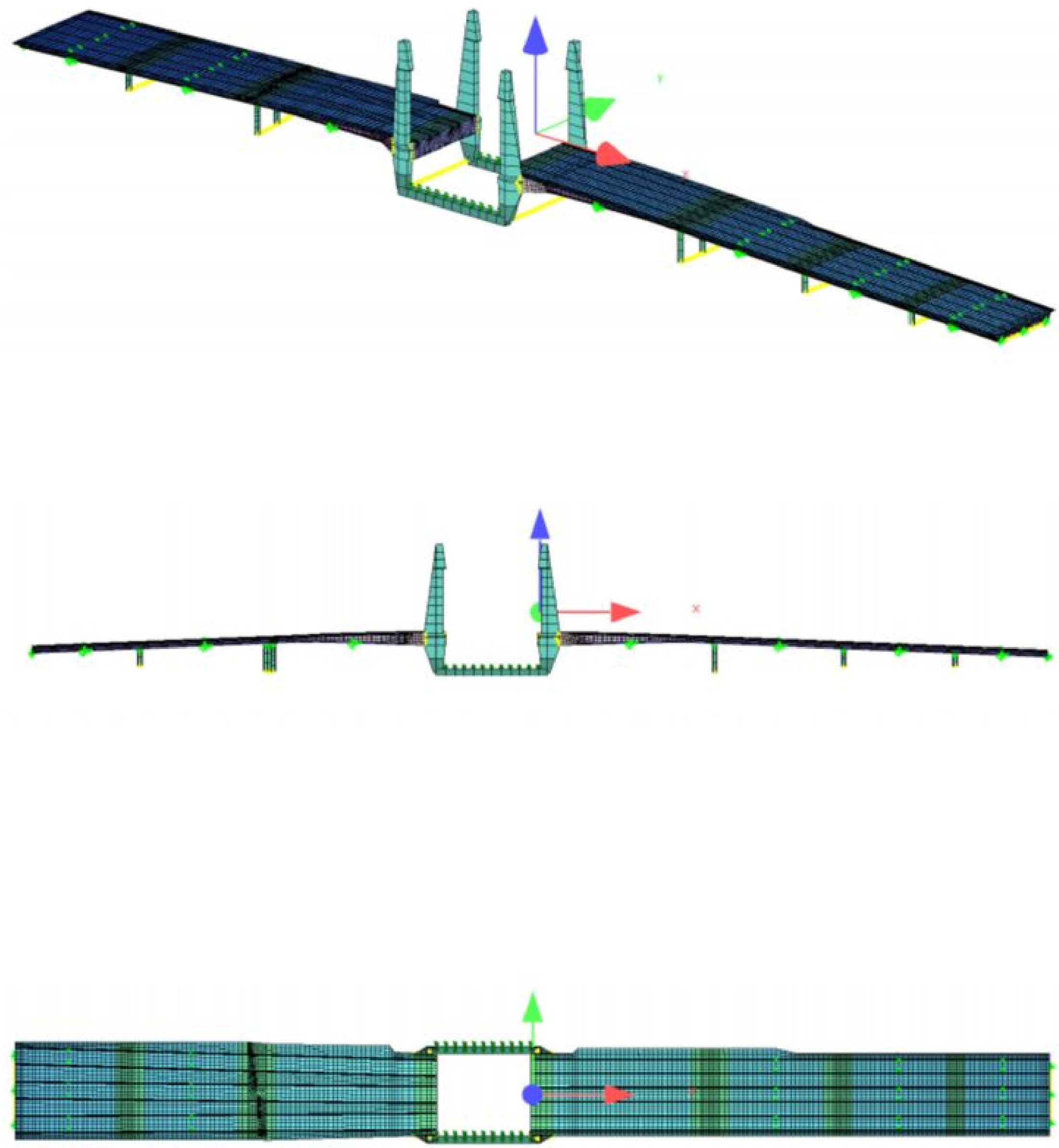

Figure 3.8: Hisings-bridge modelled originally in Sofistik

Permanent loads were calculated regarding the construction sequence and activated step by step in the model. Creep and shrinkage are considered during those construction sequences, until the time of traffic loading and until the expected lifetime of 120 years. The self-weight of structural steel was assumed to be 77 kN/m3. To consider thickness tolerances, welds, painting, etc., the final load is 78.5 kN/m3. Reinforced concrete self-weight was assumed 25.2 kN/m3. All the permanent loads, as well as creep and shrinkage, were automatically calculated in SOFISTIK.

Temperature loads
Temperature loads are extracted from the national annex (TRVFS 2011:12). (SS-EN 1991-1-5 Cl. 6.1.2) has two methods regarding the temperature gradient. In this project, both can be applied. The first method is chosen to be used. The ambient temperature gradient is set to $T_0 = 10°C$. From National annex the temperature for Gothenburg is $T_{max} = 35°C$ and $T_{min} = -29°C$. According to Figure 6.1 of the national annex and type 2 (composite cross-section) the design temperatures are $T_{E.max} = 39°C$ and $T_{E.min} = -24°C$. The uniform temperature change was taken into account for the whole model and the design of bearings and expansion joints according to the relevant chapters of NA and Eurocodes. Differential horizontal and horizontal temperature change was applied in the model relevant to EN 1991-1-5:2003 Cl. 6.1. The interaction of global and local temperature according to EN 1991-1-5:2003 Cl. 6.1.5.

Wind Loads
Wind load was applied on deck, pylons, piers, and lifting span. Interaction between the wind loads and the effect of the different lifting span positions was also considered. For the calculation of wind load for each case, a 10min- mean essential wind speed of vb= 25 m/s for a 50-year-return period at an elevation of 10m above ground is given for Göteborg from (TRVFS 2011:12 Table 4). Different terrain types are used for the wind calculation in each direction due to the other surroundings.

Live loads
Different types of Live loads which were taken into account are presented in (Table 3.3) below. The Live loads are based on the national Annex (TRVS 2011:12) and (Teknisk Handbook for Göteborgs TH 2014:1).

Table 3.3: Different load categories.

Loading Category	*Loading Sub Categories*
Road traffic – Vertical Loads	*Load Model LM1 Load Model LM2* *Load Model LM3*
Road traffic – Horizontal Loads	-
Pedestrian / Cycle Lanes	*Regular Vertical loads* *Regular Horizontal loads* *Special Vehicle Vertical Loads* *Special Vehicle Horizontal Loads*
Railway traffic Vertical Loads	*Rail load SPV1* *Rail load SPV2* *New tram load* *Single boogie load* *Rail working train* *UDL for road assignment* *Axle loads for road assignment*
Railway traffic Horizontal Loads	-

LM1 is related to the traffic vehicle loads used for the design of the traffic lanes. LM2 is not considered in the global analysis; it is considered only for local design. LM3 is related to special vehicles defined by the owner.
Two types of special vehicles are considered in this bridge. First, special civil vehicles, according to (TRVK , 2013), with a dynamic increase of 20% to all point loads of the model. Second, military vehicles, according to (TRVK, 2013).
The horizontal loads are referred to as braking and accelerating force created by the vehicles, taking into account the relevant eccentricity from the center of mass of the vehicles as the load is applied on the bridge deck. Although these horizontal forces of braking and acceleration do not exceed the horizontal forces induced by bearing friction, they are never considered leading.
The regular vertical loads for pedestrian/cycle lanes are 5 kN/m2 for pedestrian cycle lanes and balconies. Normal horizontal loads are considered to be acting simultaneously with the vertical loads. EN 1991-2 Cl. 5.4 (2) states that the horizontal loads are considered as 10% of the vertical loads. For the special vehicles, a rescue vehicle is considered acting on the pedestrian/vehicle lane.

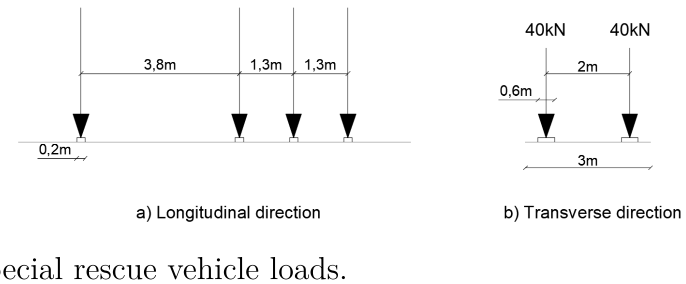

Figure 3.9: Special rescue vehicle loads.

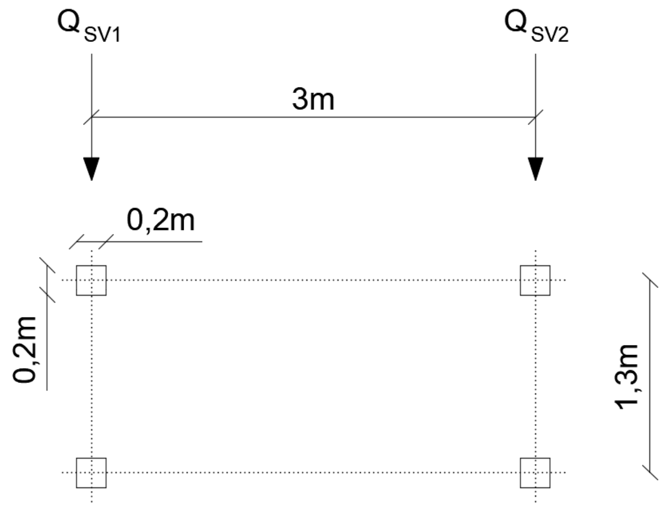

Figure 3.10: Garbage vehicle loads.

As the edge beam can be demounted, this load is considered to act directly on the road slab. Another type of special vehicle which is considered is the garbage collecting vehicle acting only on the balconies with loading equal to $Q_{sv1} = 2 * 40kN and Q_{sv2} = 2 * 20kN$. The model is according to EN 1991-2 Cl. 5.6.2, and a combination where both types of vehicles to be present is not considered. The special vehicle's horizontal loads are, according to TRVK Brücke 11, as a percentage of 60% of the horizontal vehicle loads.

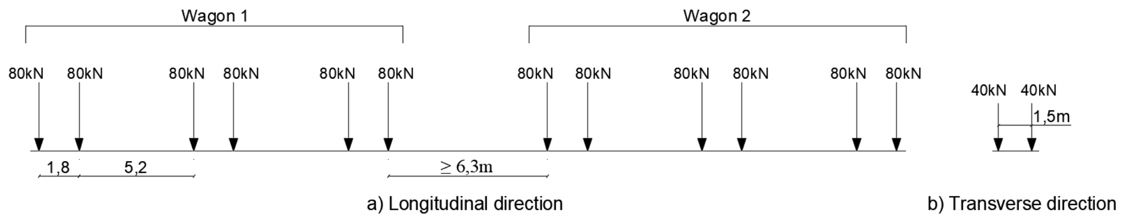

Figure 3.11: Tram load.

All the train loads are multiplied by 1.33, which is the dynamic amplification factor. This model considers either 1 or 2 wagons with a minimum distance of 26.3 m between the trains when there is no traffic jam. However, when a traffic jam exists, this distance becomes a minimum of 6.3 m. In the traffic jam case, the load is not amplified as the wagons make no move.
SPV2 is similar to SPV1 model. The values of each point load equal to 100 instead of 80 kN, and the distances between the axis become 1.7, 7.7, and 8.4. The values are multiplied with a classification factor of =1.33 and a dynamic amplification factor of ϕ_2.
The new tram load is similar to loading model SPV2 but with different values for point loads and distances. As stated in C-2019-01-22 p. C.5-53.2, the new load model for the tram is therefore not governing and not integrated into this model. According to)Broar för spårbunden trafik- 2HA1.3(one single boogie-load (one pair

of axles) is placed on the bridge with a 1.5 as an alternative factor to the beforementioned tram point loads.
The working train is taken into account with a length of 30 m and load density of 46.55 kN/m. No other train traffic is assumed on the same track as the working train. For each other track, SPV1 can be considered. The working train is applied as two lines load equal 23.28 kN/m. For determination of the worst placement, the loads are moved each 10 m.
The railway part of the bridge is also used for bus traffic, so the LM1 model must be applied in the relevant areas to determine UDL load for road assignment. The axle load is applied in the areas of tram traffic. Three different lanes are possible, and the loading is done in loops over the entire bridge length every 5 m, which is sufficient for the analysis of internal global forces (C-2019-01-22 p. C.5-58.1).
For horizontal loads in railway traffic (TH 2014:1, 2HA1.6) is applied. In track 1, 30% of the vertical component of either SV1 or SV2 is required. While in track 2, 15% of the vertical components. But here, the loads are defined with 30% for each track separately. The reduction to 15% for the second track is not considered, as these loads do not have any significant impact.

Bearing friction
Bearing friction is taken into account from SS-EN 1337-1 Cl. 6.2 and EN 1993-2 Annex A.3.6. In Sweden, pot bearing with PTFE sliding surface is quite common. The effective bearing friction depends on the contact pressure of the PTFE sliding. It is assumed Chrome/PTFE friction.

Settlements
A preliminary piles design shows considerable negative skin friction for the piles. That means with time, the soil is settling and results in additional loadings on the piles. According to the design document, the following settlements are assumed.

- Abutments 1.12 and 1.20: 50 mm
- Piers 1.13, 1.18, 1.19: 150 mm
- Standard piers: 50 mm
- Pylon axes 1.15 and 1.16: 50 mm assumed

The larger settlements on piers 1.13, 1.18, and 1.19 are assumed because the foundation's piles are not resting on a rock, but clayey soil, and the loads are transferred to the ground by friction, so larger settlements are expected.

Ice and Flooding
Ice and flooding are considered lateral and longitudinal loads acting on the 1.15, 1.16, and 1.17 (Table 3.4).

Table 3.4: Ice and flooding loading.

Pylon 1:15	*I lateral= 1080 kN*	*I long=540 kN*
Pylon 1:16	*I lateral= 1200 kN*	*I long=600 kN*
Pylon 1:17	*I lateral= 1000 kN*	*I long=500 kN*

Bearing replacement The bearing code SS-EN 1337-1 Cl. 5.1 not refers to Annex

A of SS-EN 1993-2 for the loadings to be considered for the transient situation of bearing replacement. SS-EN 1993-2 A.4.2.3.2 (informative [TRVK 2011: Kap 19 §20] states that bearing replacement might be considered a transient situation with reduced traffic and refers to EN 1991-2 for transient design situations traffic and Cl. A.4.2.7 for combinations. Transient traffic is defined in SS-EN 1991-2 Cl. 4.5.2, which would allow the tandem load to be reduced to 80%. No further reduction is allowed [TRVK Bro11 Cl. B.4.3] (C-2019-01-22 p. C.9.1).
All the different load replacements from various load subcategories are superimposed and extracted as load envelopes with max and min values. All subcategories are combined with the relevant factors. The combinations are done in SOFISTIK, and the maximum and minimum resultants for each load combination are extracted.

3.2.2 Results

As all the relevant loadings are performed, and load combinations are automatically generated, the relevant results can be extracted from SOFISTIK. These results can be either forces or stresses depending on the element type which was used in the model.
In this master thesis, only the following components are examined:

- Top flanges
- Web
- Bottom flange

Maximum and minimum values for each part are extracted in the ultimate limit state. For the top flange, stresses from the construction stage are checked because the top flange is checked for the risk of buckling in the construction stages.

3.2.2.1 Top flange longitudinal stresses

The stresses in the top flange are shown along the bridge axis at the connection between the flange and the web (Figure 3.12).

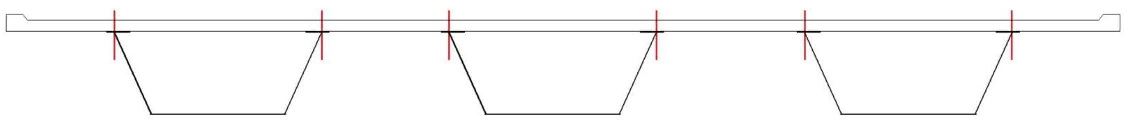

Figure 3.12: Sections where the top flange stresses are documented.

In Figure 3.13, the stress diagram for ULS of the north side is presented. Top view for the top flanges is shown. Stresses are presented every 40 m starting from support 1.16. The relevant scale of the results, the number of the load case for the relevant results, and the units are presented on the right side of the figure. Different colors are used for different thicknesses of the top flange. Dimensions existing on the bottom and right side refer to the dimensions of the bridge. Red is referring to the minimum values (compression), and blue to the maximum values (tension). Two stresses diagram are presented. On the top, the combination for the maximum

stresses, and at the bottom the combination for the minimum values. The spikes in the values are expected due to the change in the thickness of the top flange; similarly, this will be observed where the thickness of the part changes.
A maximum or minimum value is extracted from stress diagrams (Figure 3.13) for each position of the relevant checks to be performed. However, in this thesis, those stress results are converted to excel figures to ease the redesign's check process (Figure 3.14).
One theoretical flange is created per box girder with the maximum or minimum values per position. The combination where the maximum values (blue lines) come up in most parts is named tension and with minimum values (red, yellow, and green lines) is a compression (Figure 3.14).
In Figure 3.14 the stress values though the total length of the bridge are presented. In total, 6 cases exist. Two cases per box, one compressive and one tensile case.

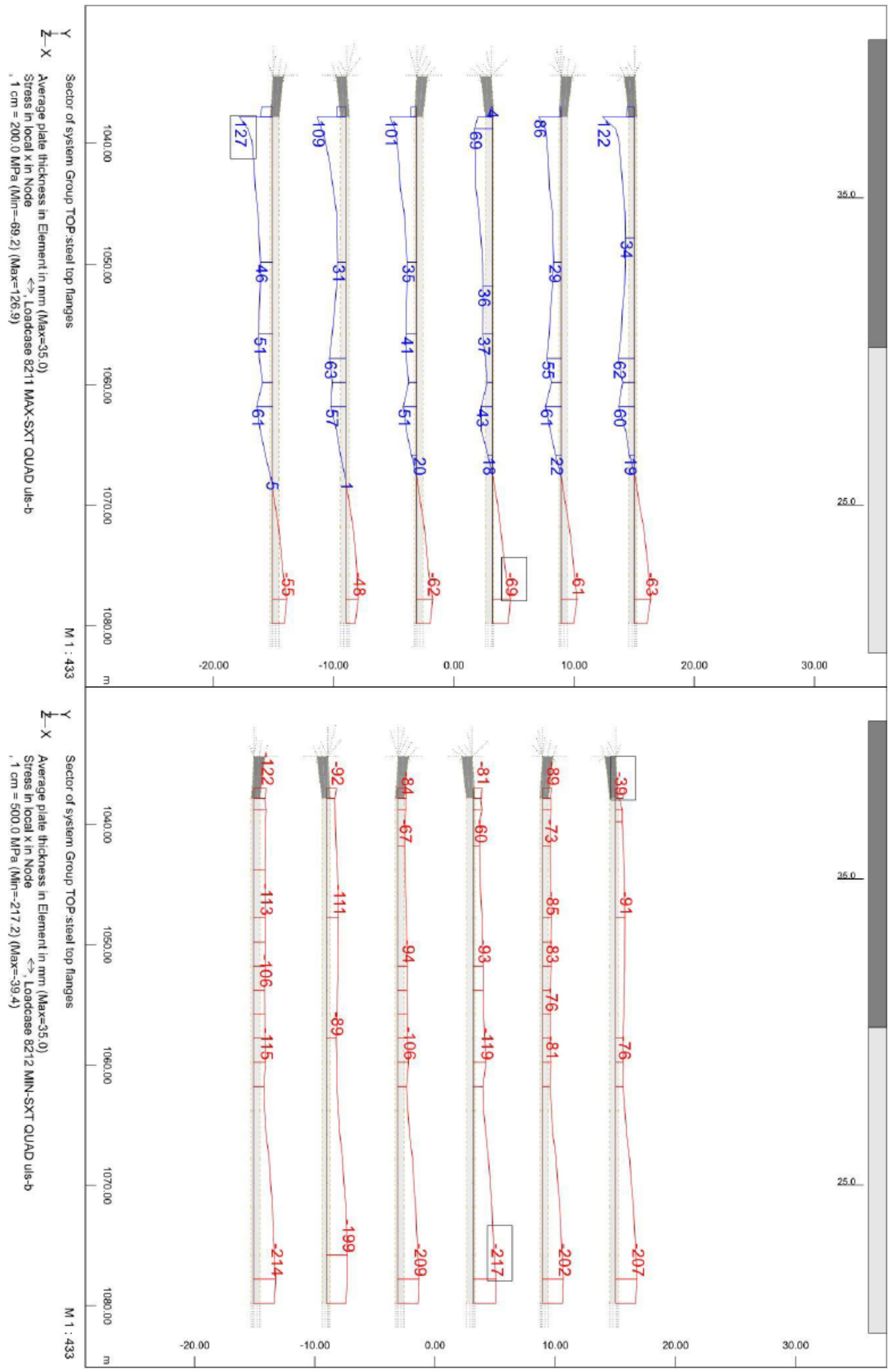

Figure 3.13: Extracted stresses of the top flange for 40 m length (SOFISTIK).

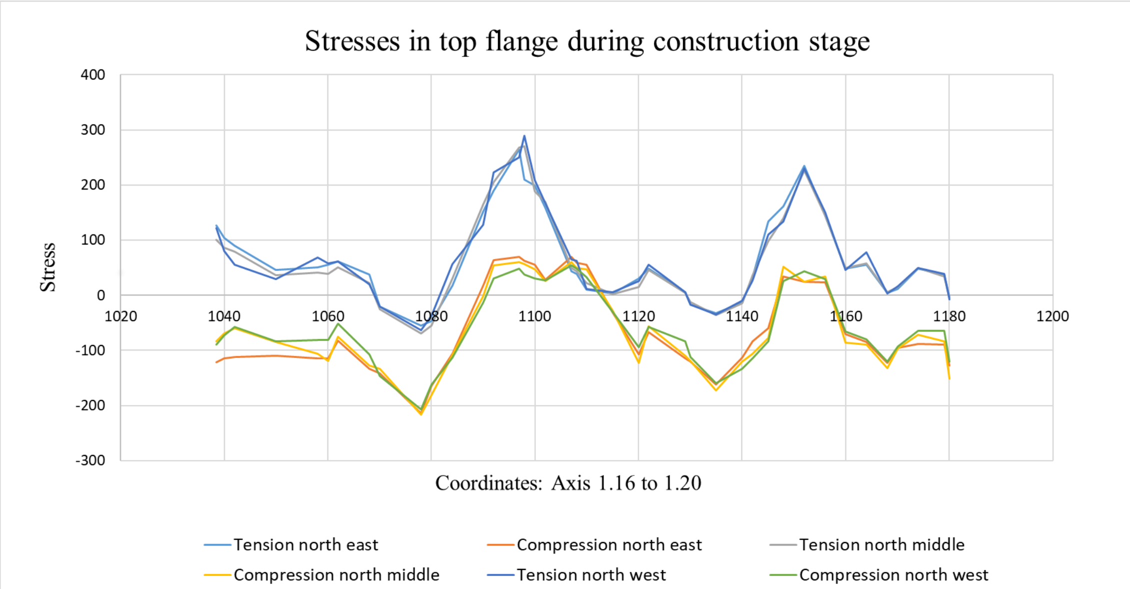

Figure 3.14: Extracted stresses of the top flange for 40 m length (SOFISTIK).

3.2.2.2 Web longitudinal stresses

The results for the web are separated in:

- Top fields
- Middle field
- Bottom field

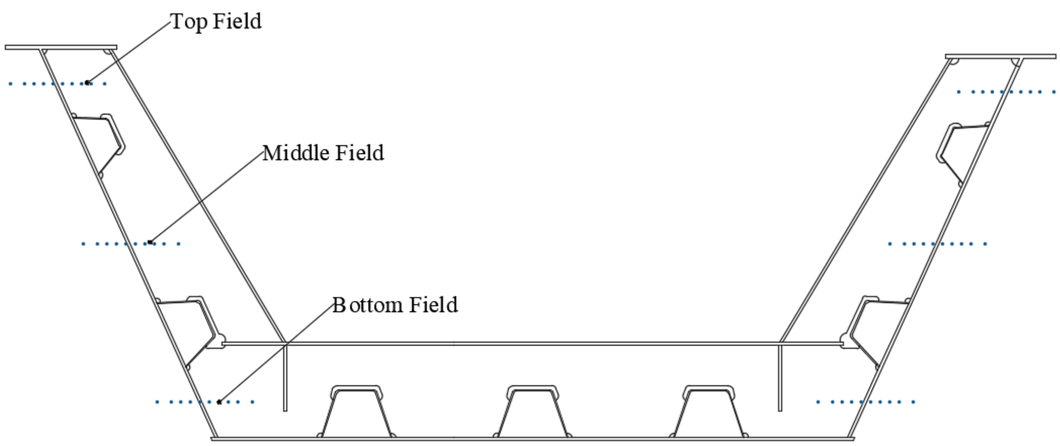

Figure 3.15: Sections where the stresses of the top, middle, and bottom fields of the webs are extracted (at the middle of each subpanel).

Following the same procedure as the top flange, the relevant graphs are created. The diagram is not made for the center field, as we are only interested in the top and bottom field as the highest stress values are expected. The stress values will be compared with the resistance of the different subparts of the web.

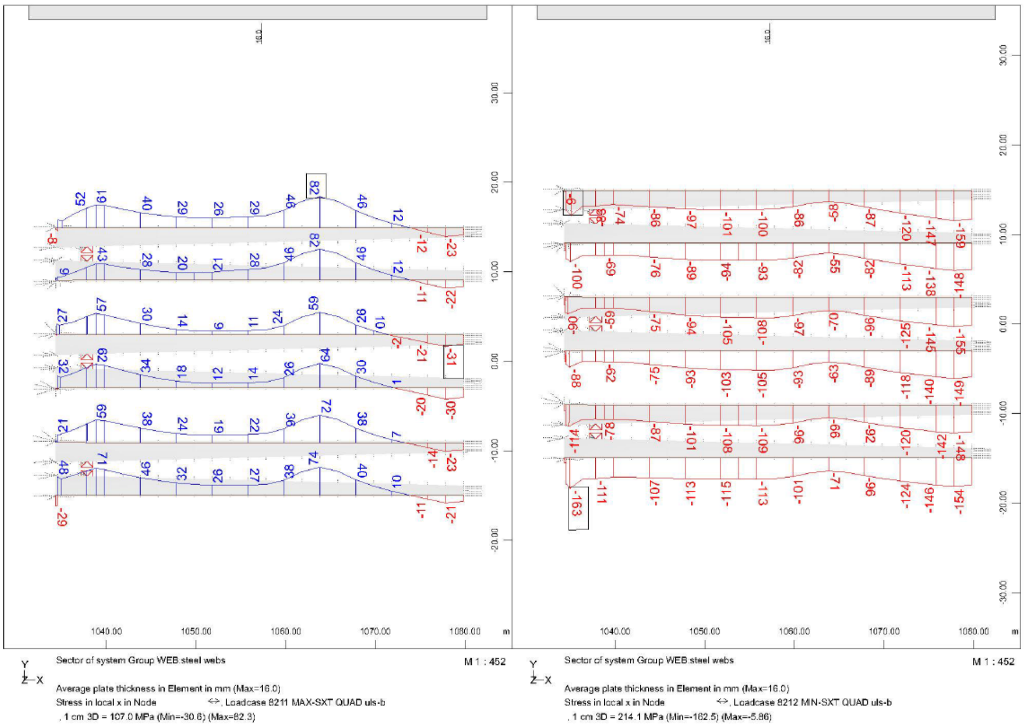

Figure 3.16: Extracted stresses of the web's top field for 40 m length (SOFISTIK).

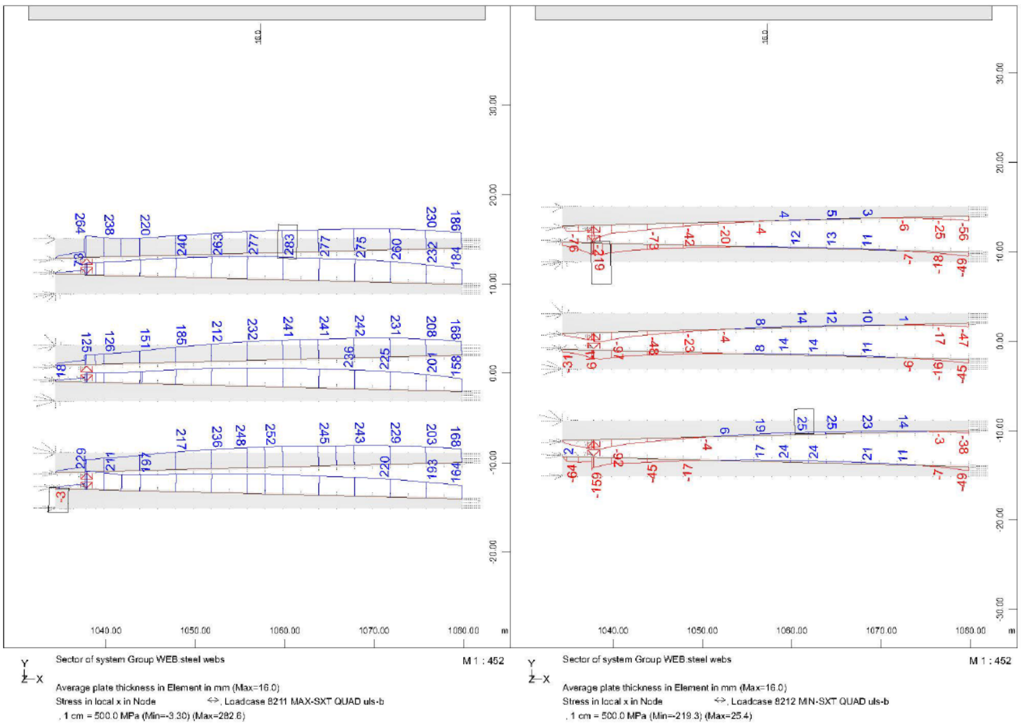

Figure 3.17: Extracted stresses of the web's bottom field for 40 m length (SOFISTIK).

3.2.2.3 Bottom flange longitudinal stresses

Figure 3.18 shows the position where the bottom flange's stresses are extracted.

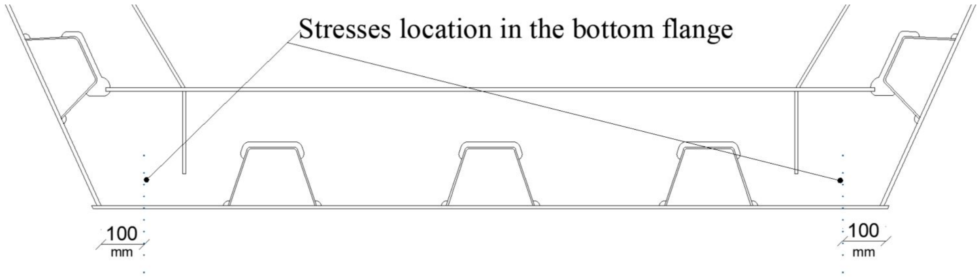

Figure 3.18: Sections where the stresses for the bottom flange are extracted.

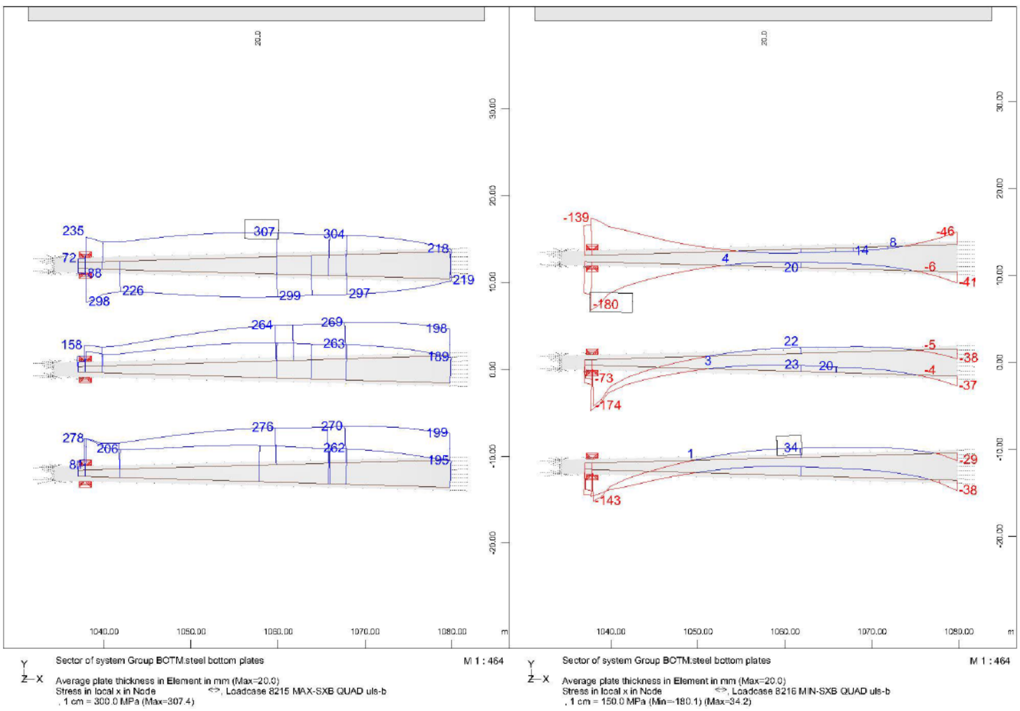

Figure 3.19: Extracted stresses of the bottom flange for 40 m length (SOFISTIK).

3.3 Local Buckling

The stresses and deformations resulting from the global model are used in the design of the steel box girder. Each part of the box girder (Bottom flange, webs, and top flanges) is designed to resist the stresses gained from the global shell model. This chapter calculates buckling capacity for each subpart of the box and compares it with the resultant stresses. Local buckling is a crucial phenomenon in plated members, and in most cases, it governs the design of a plate girder.
As mentioned earlier, the northern side is located between axis 1.16 and 1.20. the box height is changing between 1.16 and 1.17. Then the box section continues with the same size but with different plate thicknesses until it reaches its end at axis 1.20. Sections at piers have other details and were treated separately by FEM analysis; thus, they are excluded from this work. Figure 3.20 shows the northern side of the bridge with the excluded regions from this study. The used coordinates are also visible to be used in the results and the comparison in a coming chapter.
In the original design sheet, buckling checks for each subpart were done according to (SS-EN 1993-1-5). In this step, buckling capacities were calculated for direct, transverse, and shear stresses with respect to interaction between different stresses. This check was re-calculated using the reduced stress method according to (SS-EN 1993-1-5, 10) and compared with the results from the reduced area method. In this work, only the reduced area method is demonstrated.

3.3.1 Hollow Stiffeners

As mentioned above, three types of hollow stiffeners are existed, T1, T2, and T3. These stiffeners are used to stiffen the webs and the bottom flange. The buckling capacity of each stiffener is calculated according to EN 1993-1-5, 4.4 for unstiffened internal compression elements (Figure 3.21). Each stiffener can withstand direct stress equal to $\sigma Rd, loc$ as shown in Table 3.5.

Table 3.5: Buckling strength of the hollow stiffeners. S355.

Type	T	B_{bott}	B_{top}	H	R	C_{top}	$\lambda_P(/)$	$\rho(/)$	C_{web}	$\lambda_P(/)$	$\rho(/)$	$\sigma_{Rd,loc}$
T1	*6*	*400*	*200*	*200*	*20*	*160*	*0.577*	*1*	*199*	*0.716*	*0.97*	*343*
	8	*400*	*200*	*200*	*20*	*160*	*0.433*	*1*	*199*	*0.537*	*1*	*355*
T2	*6*	*450*	*250*	*250*	*20*	*210*	*0.757*	*0.94*	*244*	*0.881*	*0.85*	*302*
	8	*450*	*250*	*250*	*20*	*210*	*0.568*	*1*	*244*	*0.661*	*1*	*355*
	10	*450*	*250*	*250*	*20*	*210*	*0.454*	*1*	*244*	*0.529*	*1*	*355*
T3	*6*	*450*	*250*	*300*	*20*	*210*	*0.757*	*0.94*	*291*	*1.050*	*0.75*	*267*
	8	*450*	*250*	*300*	*20*	*210*	*0.568*	*1*	*291*	*0.788*	*0.91*	*325*
	10	*450*	*250*	*300*	*20*	*210*	*0.454*	*1*	*291*	*0.630*	*1*	*355*
	12	*450*	*250*	*300*	*20*	*210*	*0.379*	*1*	*291*	*0.525*	*1*	*355*

3.3.2 Bottom flange

Buckling capacity for the bottom flange is calculated in two steps; first, for single panels between and inside the stiffeners. Then, for the global buckling of the whole

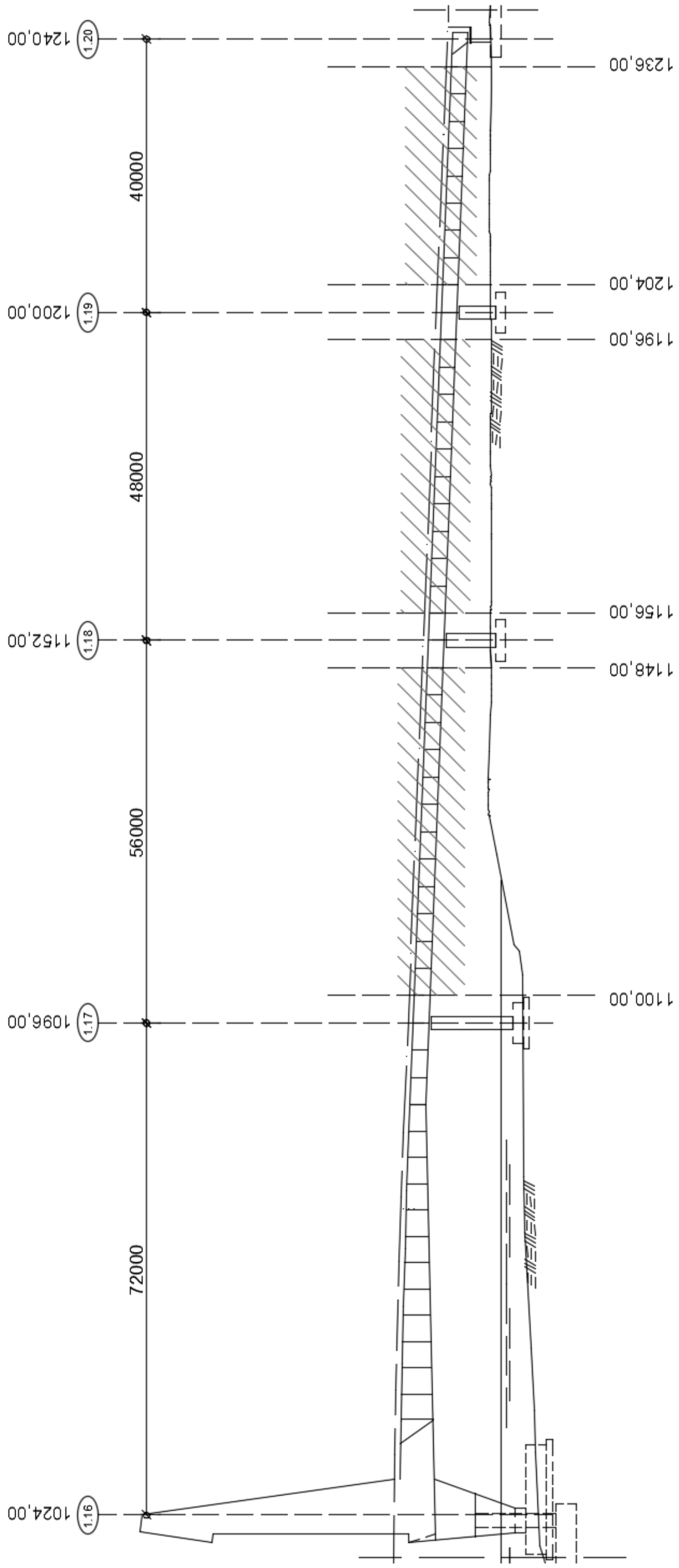

Figure 3.20: Northern side of Hisings-bridge with coordinates. The inclined hatches show the included regions in this work.

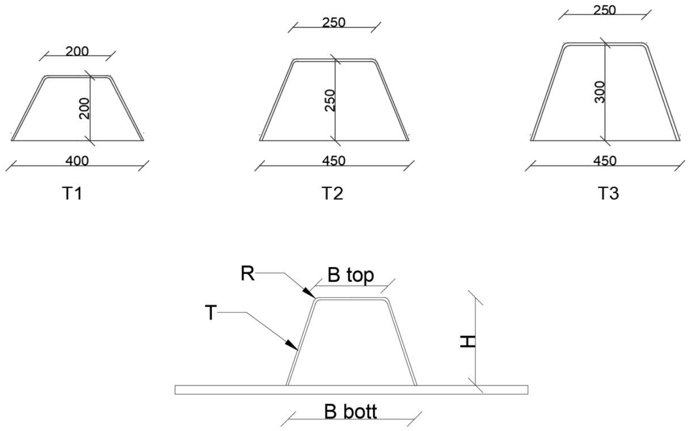

Figure 3.21: Hollow stiffeners dimensions

stiffened plate between two adjacent transverse stiffeners (4m).

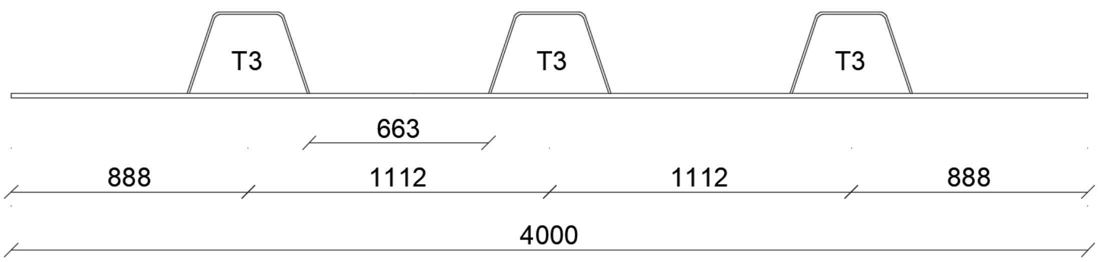

Figure 3.22: Bottom flange dimensions at the northern side of Hisings-bridge.

3.3.2.1 Local single panel buckling

Buckling capacity for the local single panel is calculated according to (SS-EN 1993-1-5, 4.4). The bottom flange is subjected to longitudinal stresses and some shear stresses at the single outer panels towards the webs. The resultant shear stresses from global analysis do not exceed 50 MPa. In order to avoid interaction between direct and shear stresses, the shear capacity for single panels needs to be larger than 100 MPa according to (SS-EN 1993-1-5, 7.1 (1)). Single panel's buckling capacities for the northern side with varying plate thickness from 12mm to 80 mm are shown in (Table 3.6). Every single panel is subjected to direct stress equal to its buckling capacity $\sigma_{Rd,local}$, and shear stress of 50 MPa; we can see that η_3 in all cases is less than 0.5, there is no need for interaction check for the single panels.

Table 3.6: Buckling strength of the single panels in bottom flanges.

$t(mm)$	$f_{yk}(MPa)$	$B(mm)$	$\sigma_{Rd,loc}(MPa)$	$\tau_{Rd,loc}(MPa)$	$\sigma_{Ed,loc}(MPa)$	$\eta_3(-)$
16	*355*	*663*	*299*	*246*	*299*	*0.203*
20	*345*	*663*	*333*	*239*	*333*	*0.209*
25	*345*	*663*	*345*	*239*	*345*	*0.209*
35	*345*	*663*	*345*	*239*	*345*	*0.209*
40	*345*	*663*	*345*	*239*	*345*	*0.209*
45	*335*	*663*	*335*	*232*	*335*	*0.215*

3.3.2.2 Global buckling of the bottom flange

Assuming that no local buckling occurs at each panel of the bottom flange, including the hollow stiffeners, global stability is verified according to (SS-EN 1993-1-5, 4.5). The reduced section is calculated according to shear lag (SS-EN 1993-1-5, 3.3). Table 3.7 shows the final details for varying plate thicknesses.

Table 3.7: Global buckling strength of bottom flange.

$t(mm)$	$f_{yk}(MPa)$	$\sigma_{Rd,global}(MPa)$
16	*355*	*299*
20	*345*	*289*
25	*345*	*281*
35	*345*	*267*
40	*345*	*261*
45	*335*	*250*

3.3.3 Webs

Webs are stiffened with two hollow stiffeners, T1 at the top and T2 down. Their axis is placed 700mm from each end. Figure 3.23 shows web cross-section with stiffeners and dimensions. In the coming analysis, the web is divided into three parts; top field located between the upper edge of the web to the axis of stiffener T1, middle field between the axis of T1 and T2, and bottom field between the bottom edge of the web the axis of T2. Three thicknesses were used in webs along the bridge; 16, 20, and 25 mm.

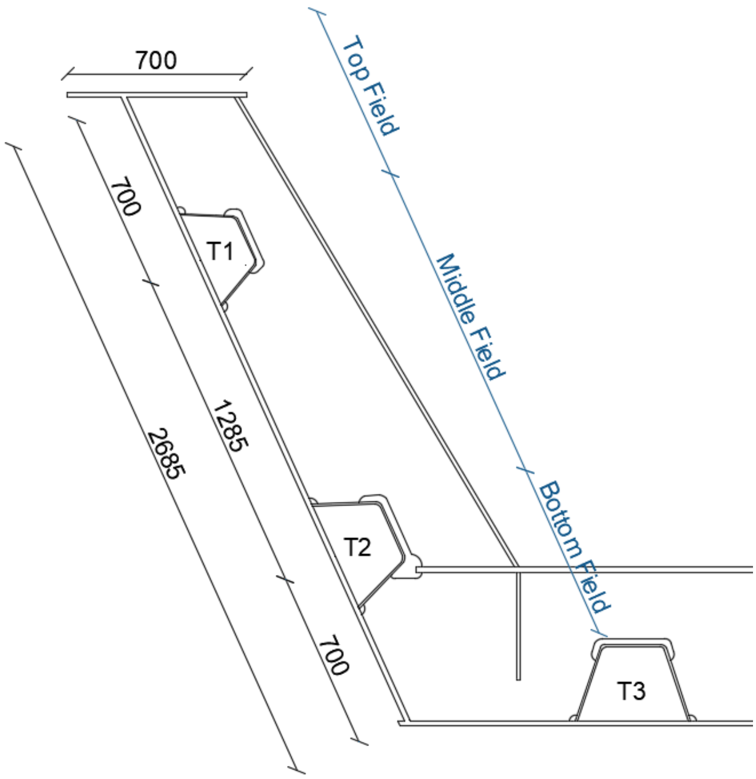

Figure 3.23: Web cross-section.

Buckling capacities for the web are determined using the same procedure followed for bottom flange, starting by single panel buckling followed by global buckling analysis.

3.3.3.1 Local single panel buckling

Shear stresses on the webs are higher than those on the bottom flange. In addition, the top panel is subjected to some vertical stresses. According to the results from the global analysis maximum, vertical stresses are about $-40MPa$. Buckling resistance due to transversal stresses is calculated according to (SS-EN 1993-1-5, 6). Web resistance for transversal stresses when having a web thickness of 16mm is $\sigma_{y,Rd} = 90MPa$ Applying interaction equation in (SS-EN 1993-1-5, eq 7.2), and assuming that the panels are fully used in the longitudinal direction, i.e., $\sigma_{x,Ed} = \sigma_{x,Rd}$, we have:

$$(\sigma_{y,Ed}/\sigma_{y,Rd}) + 0.8 * (\sigma_{x,Ed}/\sigma_{x,Rd}) = 0.44 + 0.8 = 1.24 < 1.4 \tag{3.1}$$

$$\Longrightarrow \text{No interaction is needed}$$

After checking for transversal stresses, calculating web panels resistance for longitudinal stresses is done according to (SS-EN 1993-1-5, 4.4), considering three different thicknesses 16, 20, and 25.
In order not to have interaction between longitudinal and shear stresses, shear resistance is designed to be twice the maximum shear stresses resulting from the global analysis, which was 113 MPa. In some points in the hunched area, shear stresses

Table 3.8: Single panel strengths to normal and shear stresses.

	Thickness(mm)	$\sigma_{x,Rd}(MPa)$	$\tau_{Rd}(MPa)$
Top Panel	*16*	*354*	*246*
	20	*345*	*239*
	25	*345*	*239*
Middle panel (compression)	*16*	*247*	*226*
	20	*286*	*239*
	25	*329*	*239*
Middle panel (bending)	*16*	*355*	*226*
	20	*345*	*239*
	25	*345*	*239*

Table 3.9: Shear buckling global capacity of the web.

Plate thickness(mm)	$\tau_{Rd}(MPa)$
16	*246*
20	*282*
25	*317*

were found larger than 113MPa, the reduced stress method is used to check these points, but this is not covered in this work. (Table 3.8) Summarize the resistances for each of the single panels.
The top and bottom panels have the exact dimensions; this means that they have the same resistances. Middle panel resistance is calculated assuming two different scenarios; first when it is totally under compression, and second when the panel is subjected to pure bending, i.e., compression at the top and tension at the bottom or vice-versa.
Table 3.8 shows that the minimum shear resistance at the top panel is 239 MPa, and at the middle panel is 226; this means that no interaction is needed as long as shear stresses do not exceed 113MPa, which is a high value.

3.3.3.2 Global buckling check of the web

Global buckling check for the whole web is done in two steps; the first one by calculating buckling shear resistances and ensuring that these resistances are larger or equal to the shear resistances for every single panel. The critical shear stresses for the web are calculated using software called EBplate. The second step is done by calculating the longitudinal stress resistance in two representative load scenarios considered the most extreme situations. Webs at the northern side have the geometry and dimensions illustrated in the following figure.
Comparing results from Table 3.8 and Table 3.9 shows that shear capacity from the global buckling analysis is higher than those from single local panels. This means that no interaction will be necessary as long as shear stresses from the global FEM analysis do not exceed $113MPa$ (Section 3.3.3.1). Therefore, only longitudinal stress stability needs to be verified as no interaction between different stress components occurs.

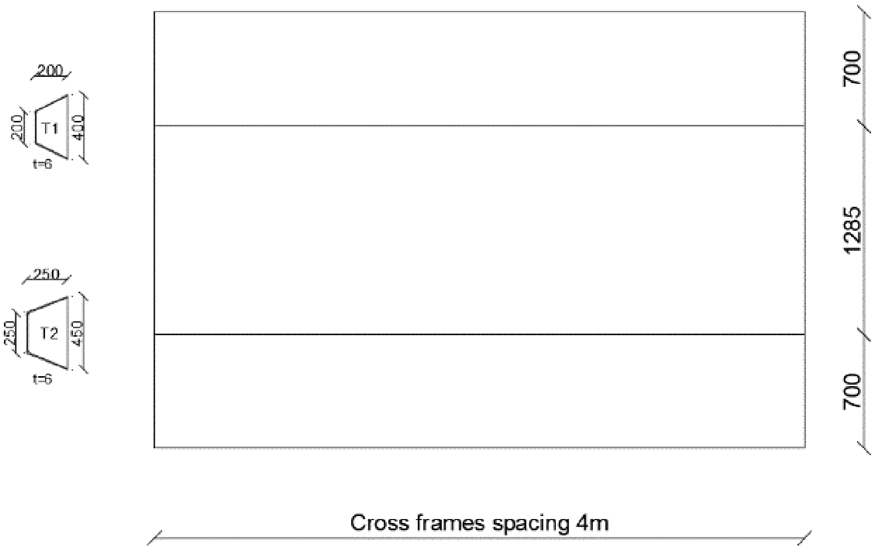

Figure 3.24: Stiffener's location in the web.n

The resulted longitudinal stresses in webs from the global FEM analysis show that webs are subjected in most cases to tension at one edge and compression at the other. In most critical cases, webs have compression at one edge and zero stress at the another. Thus, buckling capacities in webs can be calculated under two representative loading shapes. Both of them have a triangular shape with a maximum value equal to $300MPa$. Figure 3.25.
From single panel buckling the maximum allowed stress on the middle panel is 242 MPa.In most cases web will have compression at one side and tension at another, and in critical cases web will have compression at one side and zero tension at the other side. This compression stress is chosen to be 300 MPa in order not to exceed the maximum allowed stress in a single panel.

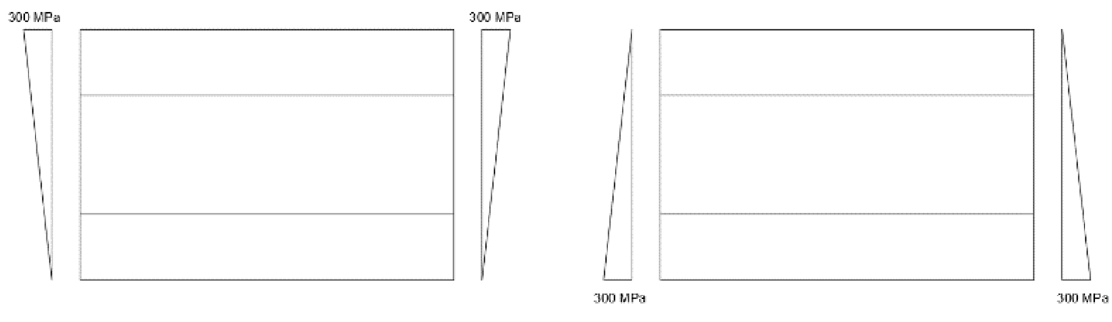

Figure 3.25: The introduced load cases to the webs.

For plate type buckling, critical stresses in the upper mentioned load cases are calculated using software EBplate by introducing three plate thicknesses each time (16, 20, 25) mm. Column type buckling behavior was determined using (SS-EN 1993-1-5, 4.5.3). The final results for buckling capacities in webs are shown in Table 3.10.

Table 3.10: Web capacities in top and bottom fields.

Web thickness(mm)	$\sigma_{Rd,top}(MPa)$	$\sigma_{Rd,bott}(MPa)$
16	*-285*	*0*
20	*-310*	*0*
25	*-341*	*0*
16	*0*	*-291*
20	*0*	*-296*
25	*0*	*-312*

3.3.4 Top flanges

After the concrete deck is casted and hardened, top flanges will not have any stability problems as they are connected and stiffened by the concrete deck. During construction, top flanges stability needs to be verified. This verification is done locally for a single flange buckling and globally for the stability of the whole box girder section.

3.3.4.1 Local stability of top flange.

Every 4m, a cross-frame is added to stiffen the box girder. These cross-frames are considered as a support for top flanges. Additionally, top flanges are connected to the web at a point 200mm from the edge of the top flange (Figure 3.26). As a result, each top flange during construction forms a plate supported at three edges, one from the web and two supports from two adjacent cross frames (Figure 3.27).

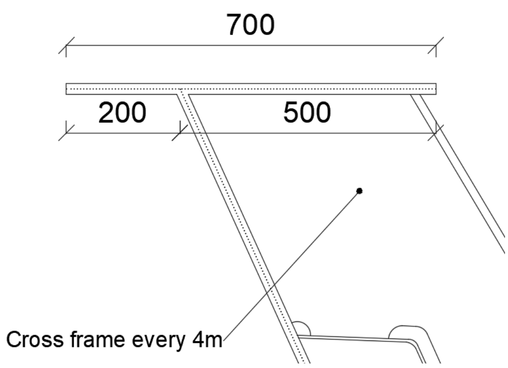

Figure 3.26: Top flange dimensions.

Table 3.11: Top flange buckling capacities

$Thickness(mm)$	$\sigma_{Rd,local}(MPa)$	$Thickness(mm)$	$\sigma_{Rd,local}(MPa)$
20	*134*	*32*	*343*
22	*162*	*35*	*411*
24	*193*	*38*	*484*
25	*210*	*40*	*536*
26	*227*	*42*	*591*
28	*263*	*45*	*679*
30	*302*	*50*	*838*

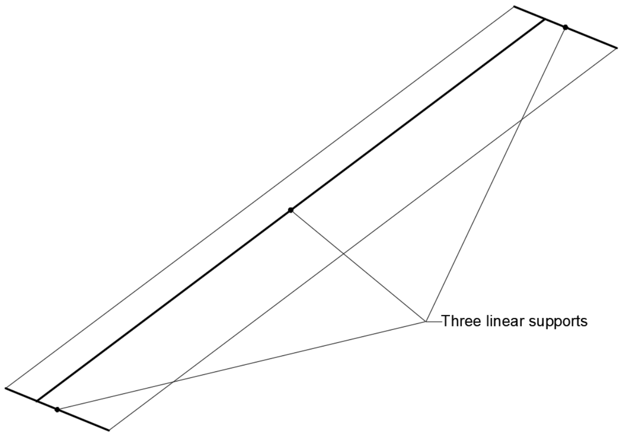

Figure 3.27: Boundary conditions in top flanges.

According to (SS-EN 1993-1-5 table 4.2), the buckling coefficient $k_\sigma = 0,43$. In (Al-Emrani and Åkesson, 2020) buckling coefficient for plates with axial compression with three supports is 0.425. In the original design of Hisings-bridge, a higher value of the buckling coefficient is calculated (Alf, 1974):

$$K_\sigma = [1/(a+b)^2] + 0.425 = [1/(4000+500)^2] + 0.425 = 0.441 \tag{3.2}$$

Table 3.11 shows the final results for the local stability of top flanges during construction.

3.3.4.2 Global stability of top flanges

In global buckling during the construction phase it is assumed that the whole box girder is susceptible to overlapping due to buckling initiated by top flanges. Two bars with 25mm diameter are placed near top flanges at the location of the cross frames to increase the stability during concrete casting. These provided ties have a thread that can adjust the box through prior casting (Figure 3.28). The box girder cross frames together with the provided ties form a 2D closed frame. The stiffness of this frame contributes in the global stability of top flanges.

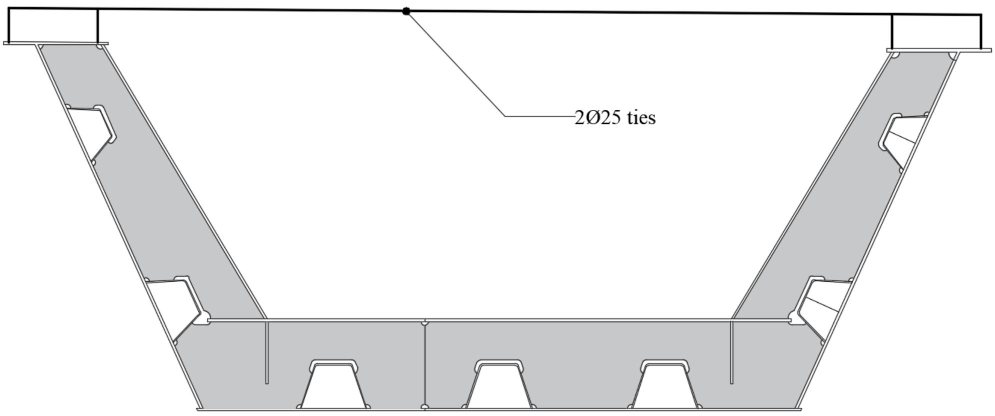

Figure 3.28: Box girder cross frame with ties.

To calculate the stiffness of the closed frame, the effective width of this frame needs to be evaluated. The effective width of the frame includes some regions of the webs and bottom flange. This width is 1000mm calculated using the shear lag effect according to)SS-EN 1993-1-5, 3.2.1(. At the top of the frame, the effective width is considered to be 300mm, as the load from the framework is locally concentrated. Figure 3.29 shows the frame with different cross-sections.

This 2D frame with the geometry described in Figure 3.29 is simulated using (Software ESK1 for plane frames) with boundary conditions as described in Figure 3.30. After that, a horizontal point load of 1000kN is applied three times. The first time, at node 1 in the x-direction. The second time at node 9 in the same direction, and the third time at both nodes (Figure 3.30). The resultant horizontal displacements at nodes 1 and 9 from each load case are then used to calculate the frame's stiffness, as shown in (Table 3.12).

Table 3.12: Resulted displacements and stiffness in the 2D analysis.

LC	Displacement		Stiffness	
	Node 1 (cm)	*Node 9 (cm)*	*Node 1 (kN/cm)*	*Node 9 (kN/cm)*
1	*1.37*	*0.60*	*728*	*1679*
2	*0.60*	*1.67*	*1680*	*598*
3	*2.29*	*2.27*	*441*	*441*

Thus, the stiffness of the cross frame is 441kN/cm. The frame stiffness c is considered as a spring stiffness in the system shown in Figure 3.31. Spring stiffness is used in determining the maximum compression stress that top flanges can withstand (Petersen, 1982).

Maximum compressive stress from global and local buckling analysis during construction is shown in (Table 3.13).

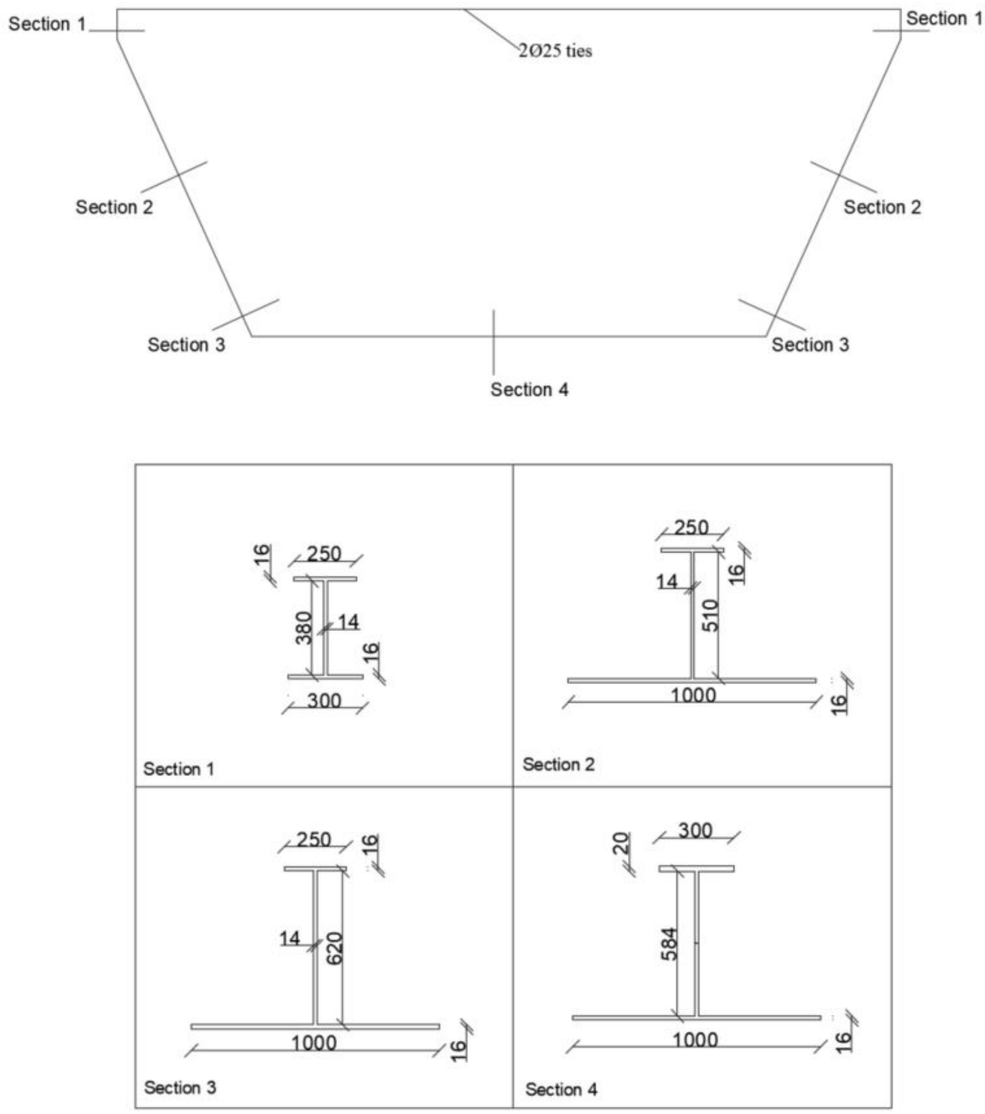

Figure 3.29: Different sections of the 2D frame.

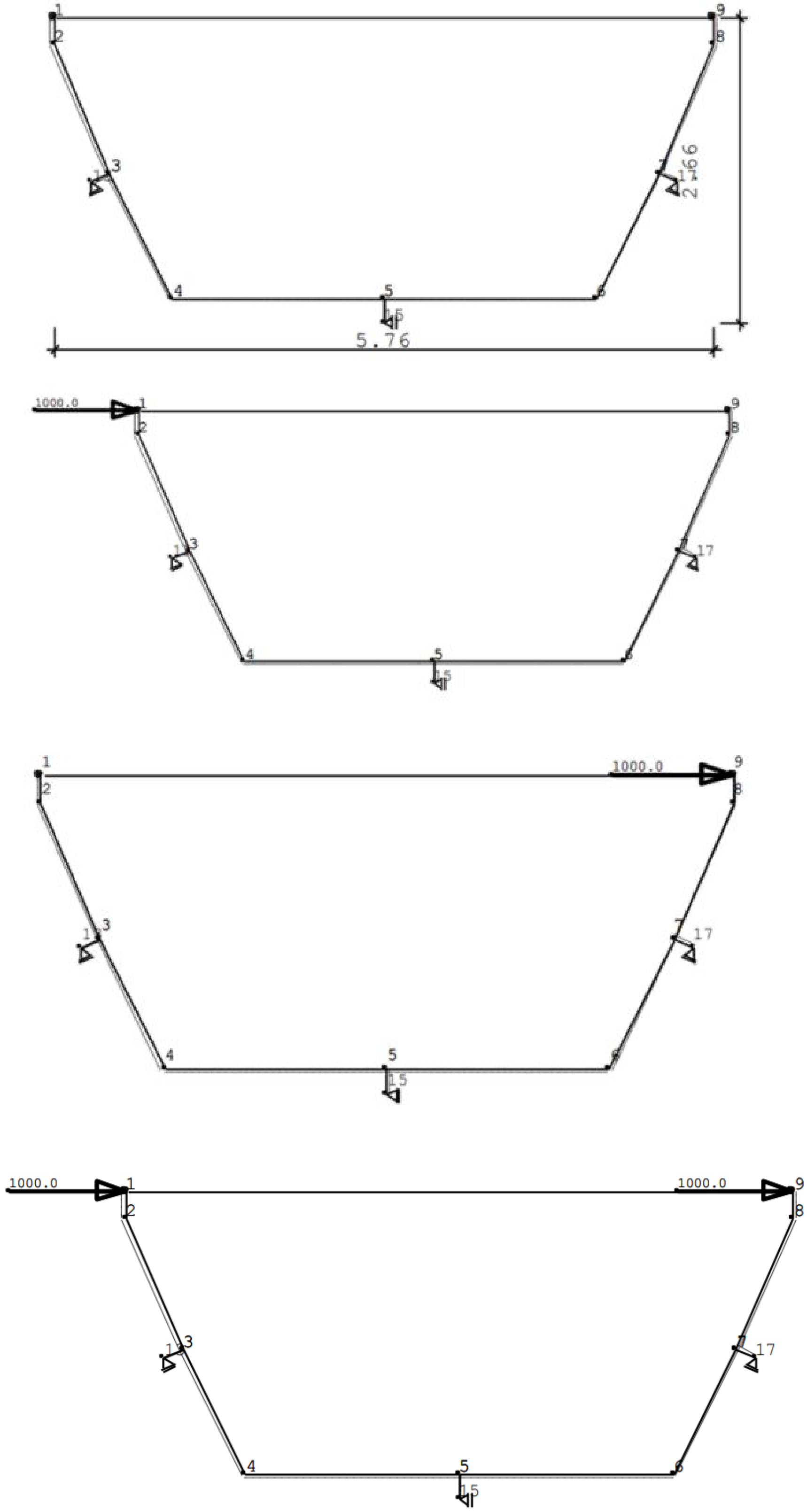

Figure 3.30: Boundary conditions and load cases on the 2D frame.

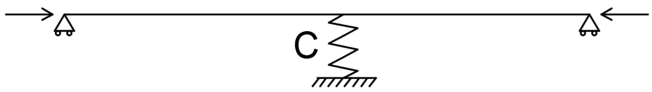

Figure 3.31: The cross-frame stiffness equalized as a spring stiffness (Petersen, 1982).

Table 3.13: Buckling capacity of top flanges from global and local design.

$Platethickness(mm)$	$\sigma_{Rd,Global}(MPa)$	$\sigma_{Rd,Local}(MPa)$	$\sigma_{Rd,governing}(MPa)$
20	*336*	*134*	*134*
25	*334*	*209*	*209*
30	*333*	*302*	*302*
35	*332*	*411*	*332*
50	*321*	*838*	*321*

4

Re-design with stainless steel

In this chapter, the structural steel in Hisings-bridge is replaced by duplex stainless steel. Buckling verifications are done according to (SS-EN 1993-1-4, A1: 2017). Starting by choosing the suitable grade of stainless steel according to the environmental effects in the location of Hisings-bridge. Then Buckling capacities for the same cross-section in the original design are recalculated for chosen stainless steel grade. Finally, a new cross-section is introduced with a possibility for material saving.

4.1 Material

4.1.1 Structural stainless steel

The stainless steel grade is chosen according to the corrosivity class of the area. Hisings-bridge has a C5-M corrosivity class. According to (SS-EN 10088-1), duplex stainless-steel grade 1.4462 can be used. Duplex stainless steel has an adequate fracture toughness down to -40°C, which is the service temperature of Hisings-bridge. Hence no thickness limitations need to be considered.

4.2 Local buckling check

In this chapter, buckling capacities using duplex stainless-steel grade 1.4662 are calculated for the original cross-section and an optimized cross-section.

4.2.1 Original cross-section

In the original design of Hisings-bridge, the span section at the northern side has the section shown in Figure 4.1.

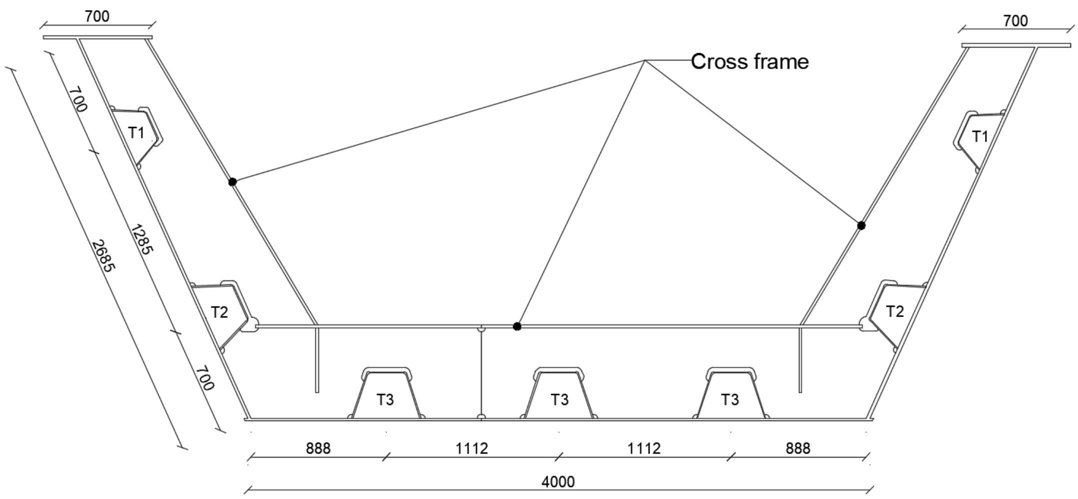

Figure 4.1: Cross-section of the box girder in the original design.

4.2.1.1 Hollow stiffeners

As mentioned before in section 3.3.1, three types of hollow stiffeners are available. Stiffener T1 has two different thicknesses 6, and 8mm. Stiffener T2 has four thicknesses 6, 7, 8, and 10mm. While T3 has 6, 8, 10, and 12mm. Buckling capacities for the hollow stiffeners are calculated using duplex stainless steel 1.4462 according to (A1:2017 and SS-EN 1993-1-4). Detailed calculations are shown in (Appendix A) (Table 4.1) includes final results for buckling capacities in hollow stiffeners.

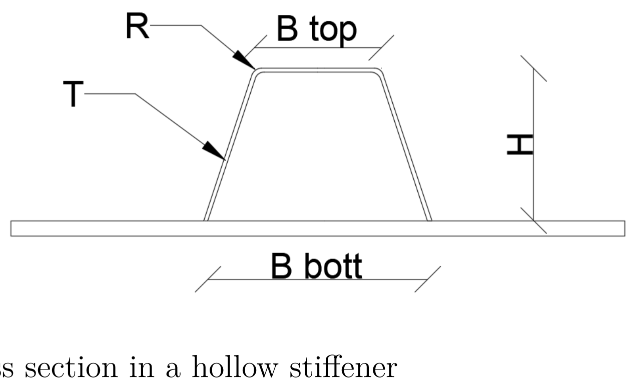

Figure 4.2: Cross section in a hollow stiffener

Table 4.1: Buckling capacity of the hollow stiffeners using stainless steel 1.4462.

Type	T	B_{bott}	B_{top}	H	R	C_{top}	$\lambda_{p.top}$	ρ	C_{web}	λ_p	ρ	$\sigma_{Rd,loc}$
T1	*6*	*400*	*200*	*200*	*20*	*160*	*0.673*	*0.87*	*199*	*0.837*	*0.744*	*342*
	8	*400*	*200*	*200*	*20*	*160*	*0.505*	*1*	*199*	*0.628*	*0.912*	*419*
T2	*6*	*450*	*250*	*250*	*20*	*210*	*0.883*	*0.71*	*244*	*1.026*	*0.633*	*291*
	7	*450*	*250*	*250*	*20*	*210*	*0.757*	*0.80*	*244*	*0.88*	*0.716*	*329*
	8	*450*	*250*	*250*	*20*	*210*	*0.663*	*0.88*	*244*	*0.77*	*0.792*	*364*
	10	*450*	*250*	*250*	*20*	*210*	*0.53*	*1*	*244*	*0.616*	*0.924*	*425*
T3	*6*	*450*	*250*	*300*	*20*	*210*	*0.883*	*0.71*	*291*	*1.224*	*0.547*	*251*
	8	*450*	*250*	*300*	*20*	*210*	*0.663*	*0.88*	*291*	*0.918*	*0.693*	*318*
	10	*450*	*250*	*300*	*20*	*210*	*0.53*	*1*	*291*	*0.734*	*0.819*	*377*
	12	*450*	*250*	*300*	*20*	*210*	*0.442*	*1*	*291*	*0.612*	*0.928*	*427*

4.2.1.2 Bottom flange

Following the same procedures in chapter 3.3.2, but concerning (SS-EN 1993-1-4 and A1:2017) for stainless steel applications.

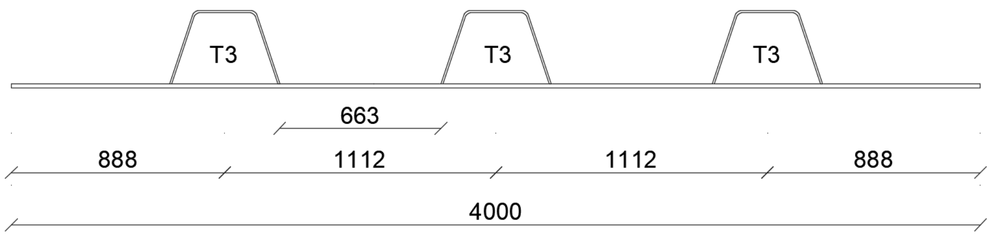

Figure 4.3: Cross-section in bottom flange/ original design.

A comparison between S355 and 1.4462 when using the same cross-section is shown in chapter 5.

Local single panel buckling.

As described earlier in chapter 3.3.2.1, maximum shear stresses from the global analysis do not exceed 50MPa. To avoid interaction between different stress components. Shear capacity in every single panel needs to be larger than twice the applied shear stress. Table 4.2 shows the final results for single panel buckling in the bottom flange. For detailed calculations, see (APPENDIX A).

In (Table 4.2) it is shown that $\eta_3 < 0.5$ assuming that the applied direct stress is equal to buckling capacity in the same direction, and thus no interaction between shear and normal stresses is needed.

Table 4.2: Buckling capacity of single panels in the bottom flange.

t(mm)	$f_{yk}(MPa)$	$B(mm)$	$\sigma_{Rd,loc}(MPa)$	$\tau_{Rd,loc}(MPa)$	$\sigma_{Ed,loc}(MPa)$	$\eta_3(/)$
16	*460*	*663*	*287*	*255*	*287*	*0.20*
20	*460*	*663*	*342*	*302*	*342*	*0.17*
25	*460*	*663*	*402*	*319*	*402*	*0.16*
35	*460*	*663*	*460*	*319*	*460*	*0.16*
40	*460*	*663*	*460*	*319*	*460*	*0.16*
45	*460*	*663*	*460*	*319*	*460*	*0.16*

Global stability of bottom flange
The global stability for the bottom flange is calculated similarly to chapter 3.3.2 of this report concerning the regulations in (SS-EN 1993-1-4 and A1:2017). The final results for buckling capacity are shown in (Table 4.3). Detailed calculations in (APPENDIX A).

Table 4.3: Buckling capacity of bottom flange/ Global buckling.

t(mm)	$f_yk(MPa)$	$\sigma_{Rd,global}(MPa)$
16	*460*	*374*
20	*460*	*365*
25	*460*	*354*
35	*460*	*336*
40	*460*	*327*
45	*460*	*320*

4.2.1.3 Webs

A cross-section for the web with dimensions is shown in Figure 3.23. Depending on the same geometry but with different materials, web buckling capacity is calculated according to (SS-EN 1993-1-4 and A1:2017). As mentioned previously in section 3.3.3, the web is divided into three fields; upper field, middle field, and bottom field, Three different thicknesses along the bridge are used 16, 20, 25 mm.

Local single panel buckling
As mentioned before in chapter 3.3.3.1, webs are subjected to longitudinal stresses, shear stresses, and transversal stresses. Maximum transversal stresses were found to be $-40MPa$. Buckling resistance due to transversal stresses is calculated according to (A1:2017, 6.4.4). in the middle panel, which has a maximum height of 880mm.

$\sigma_{y,Rd} = 95MPa$ For detailed calculations, see APPENDIX C.

assuming that the panels are fully used in the longitudinal direction, i.e.:

$\sigma_{x,Ed} = \sigma_{x,Rd}$, we have:

$$(\sigma_{y,Ed}/\sigma_{y,Rd}) + 0.8 * (\sigma_{x,Ed}/\sigma_{x,Rd}) = 0.44 + 0.8 * 1 = 1.218 < 1.4 \tag{4.1}$$

Shear buckling capacity and direct stress capacity in each sing panel of the web are shown in (Table 4.4). The minimum shear resistance is 231Mpa, and no interaction between different stress components as long as the applied shear stresses from the global analysis do not exceed $113MPa$.

Table 4.4: Buckling capacity of the web panels.

	$T(mm)$	$\sigma_{x,Rd}(MPa)$	$\tau_{Rd}(MPa)$
Top Panel	*16*	*392*	*318*
	20	*460*	*318*
	25	*460*	*318*
Middle panel (compression)	*16*	*242*	*231*
	20	*296*	*257*
	25	*360*	*307*
Middle panel (bending)	*16*	*460*	*231*
	20	*460*	*257*
	25	*460*	*307*

Global Buckling of the web

Start by calculating buckling shear resistance for the whole web with stiffeners in the distance equal to 4m between cross frames. Then finding buckling capacity in the longitudinal direction in two different load shapes as shown in Figure 3.25. Shear buckling capacity for the whole web is shown in Table 4.5. Detailed calculations are shown in APPENDIX C.

Table 4.5: Global shear buckling capacity of the web.

Plate thickness(mm)	$\tau_{Rd}(MPa)$
16	*246*
20	*260*
25	*285*

All of the upper shear buckling resistances have a value higher or equal to $(2 * \tau_{Ed})$ and no interaction between shear and longitudinal stress is needed. To calculate the capacity under normal stresses, the similar stress distribution is considered, as shown in Figure 3.25. For plate type buckling, critical stresses were calculated using software (EBplate) by introducing three plate thicknesses each time (16, 20, 25) mm. The final results for buckling capacities in webs are shown in (Table 4.6) For detailed calculations, see APPENDIX C.

Table 4.6: Buckling capacity of the web under normal stresses, global analysis.

Web thickness(mm)	$\sigma_{Rd,top}(MPa)$	$\sigma_{Rd,bott}(MPa)$
16	*-312*	*0*
20	*-339*	*0*
25	*-380*	*0*
16	*0*	*-351*
20	*0*	*-363*
25	*0*	*-383*

4.2.1.4 Top flanges

Top flanges buckling capacity is calculated to determine whether using stainless steel will reduce the stability during construction. After the concrete deck is totally hardened, there will be no risk for buckling in top flanges.

Local stability

Considering the same boundary conditions in 3.3.4.1, and similar value for buckling coefficient $k_\sigma = 0.441$, the following results are obtained.

Table 4.7: Local buckling stability of top flanges.

Thickness(mm)	$\sigma_{Rd,local}$(MPa)	Thickness(mm)	$\sigma_{Rd,local}$(MPa)
20	*65*	*32*	*166*
22	*79*	*35*	*199*
24	*94*	*38*	*235*
25	*102*	*40*	*260*
26	*110*	*42*	*287*
28	*127*	*45*	*329*
30	*146*	*50*	*406*

Global stability of top flanges

It is explained in chapter 3.3.4.2 that the cross frame stiffness contributes to the global stability of top flanges. This stiffness is calculated in the original design using software ESK1. In this chapter, the frame stiffness is re-calculated using the same procedure in (3.3.4.2) but with an E-modulus of 200GPa. This time the 2D frame is analyzed using a demonstration version of the software (RISA 2D). Boundary conditions are similar to what is used in chapter 3.3.4.2. Figure 4.4 show the frame modeled in RISA with boundary conditions and applied horizontal loads.

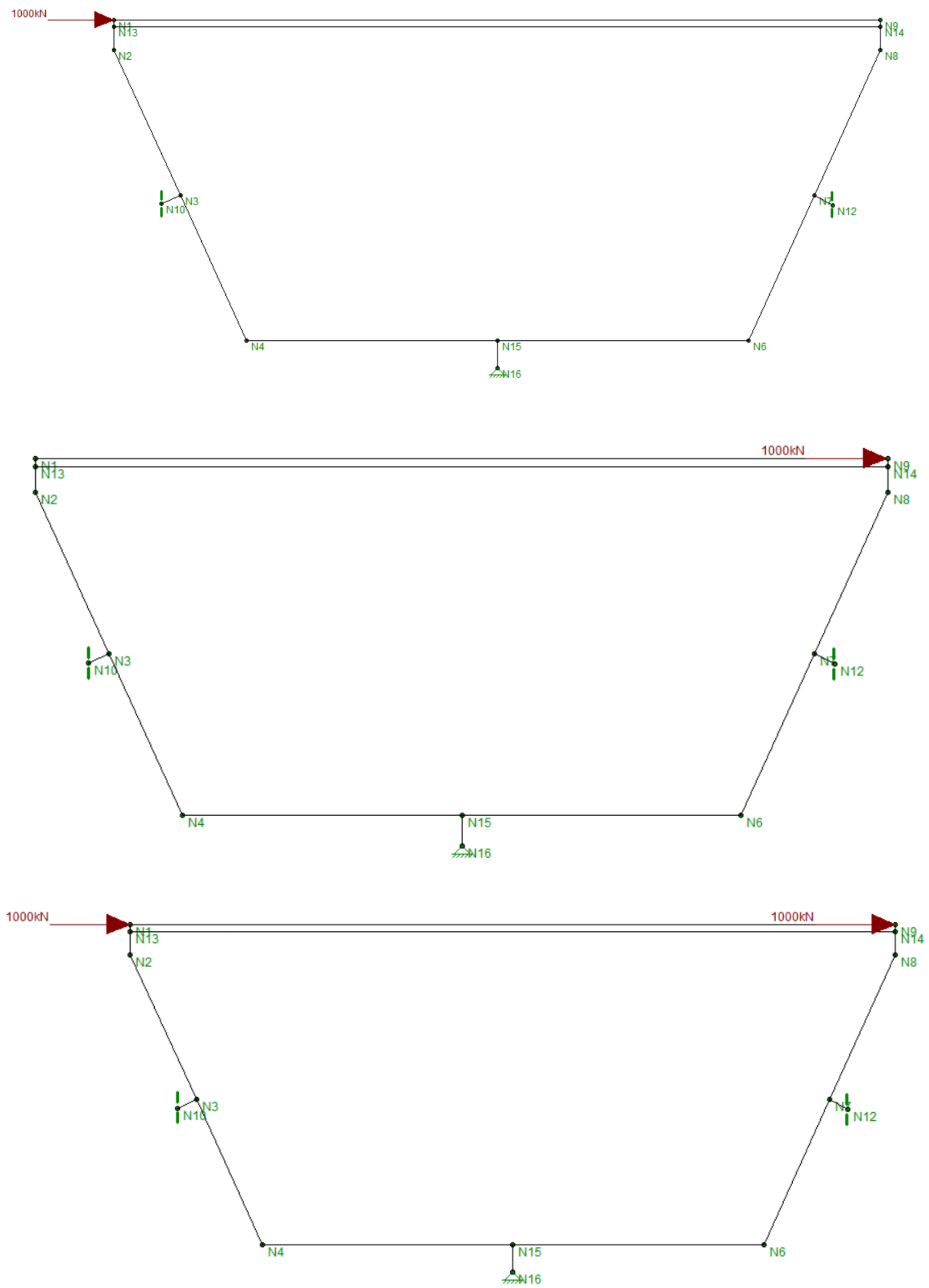

Figure 4.4: Boundary conditions and load cases on the 2D frame.

Displacement results and cross frame stiffness from the upper three load cases are summarized in (Table 4.8).

Table 4.8: Displacements and stiffness from the 2D analysis.

LC	Displacement		Stiffness	
	Node 1 (cm)	*Node 9 (cm)*	*Node 1 (kN/cm)*	*Node 9 (kN/cm)*
1	*1.93*	*0.69*	*518.78*	*1455.82*
2	*0.69*	*1.87*	*1455.82*	*534.67*
3	*2.62*	*2.56*	*382.47*	*391.05*

As a result, cross-frame stiffness is considered to be 382.5 kN/cm. Final results for top flanges compressive stresses from local and global stability are shown in (Table 4.9).

Table 4.9: Global and local buckling capacities of the top flange.

Plate thickness (mm)	$\sigma_{Rd,Global}$(MPa)	$\sigma_{Rd,Local}$(MPa)	$\sigma_{Rd,governing}$(MPa)
20	*460*	*65*	*65*
25	*460*	*102*	*102*
30	*460*	*146*	*146*
35	*460*	*199*	*199*
50	*460*	*406*	*406*

4.2.2 New Geometry

From previous results, it is visible that with same geometry buckling capacities are not increasing when using a higher yield strength stainless steel and as a consequence material saving cannot be achieved. This is due to the fact that stainless steel is more susceptible to buckling than conventional carbon steel. Plated stainless steel needs to be designed in an efficient way in order to get the benefit of the higher yield strength.
In order to increase the capacity of the bottom flange, the geometry is edited by using four stiffeners, type T2 with 7mm thickness instead of three type T3 with 8mm, and the lower plate is reduced by 4mm along the bridge.
The web section is also altered slightly by:

- Increasing stiffener T2 thickness to 7mm can improve the buckling capacity of the bottom field of the web.
- Shifting each axis of stiffeners T1 and T2 towards the center of the web by 8 cm to improve the shear buckling capacity of the single middle panel.
- As a result of the upper two steps, web plate thickness can be reduced by 3mm everywhere along the bridge.

As a result, a total saving in the cross-section along the bridge span is achieved:

$$A_{red} = A_{red,flange} + A_{red,flange} = 154.4cm^2 + 72.65cm^2 = 227.05cm^2 \tag{4.2}$$

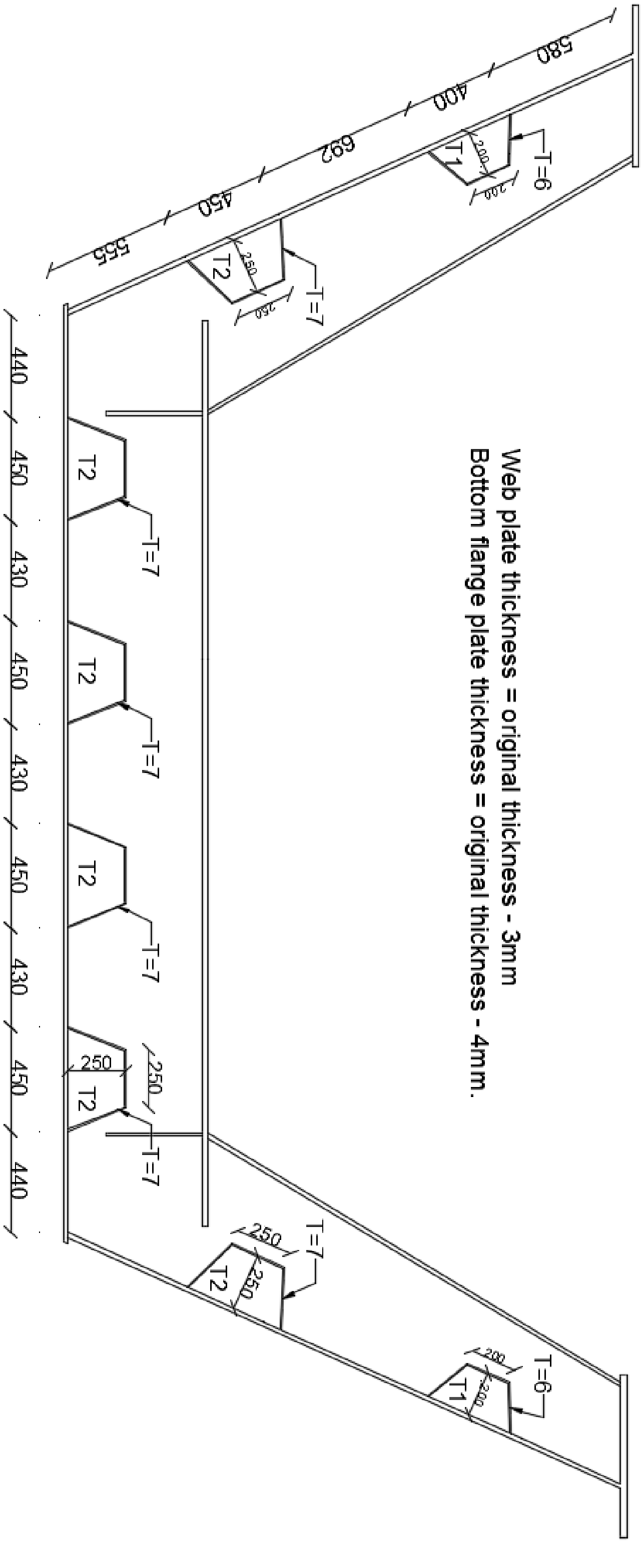

Figure 4.5: Cross-section of the box girder, new geometry.

4.2.2.1 Hollow stiffeners

Hollow stiffeners buckling capacity is similar to chapter 4.2.1.1. As no change in the stiffener's dimensions was done, and similar thicknesses to those presented are used.

4.2.2.2 Bottom flanges

A new cross-section for the bottom flange is shown in Figure 4.6.

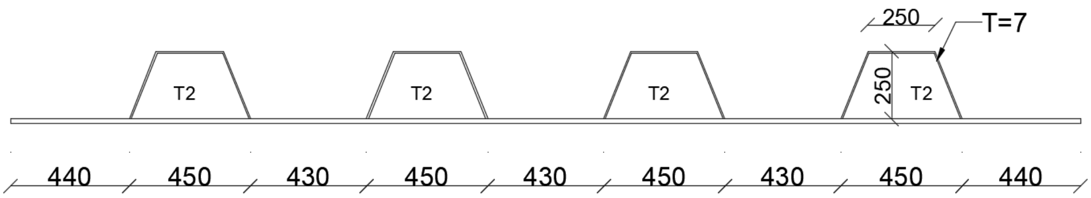

Figure 4.6: Cross-section in bottom flange/ new section.

Local single panel buckling
Using this cross-section with four stiffeners instead of three reduces the length of single panels that improve buckling performance. (Table 4.10) shows the resultant strengths for single local panels buckling.

Table 4.10: Buckling capacity of single panels in the bottom flange.

t (mm)	$f_{yk}(MPa)$	B (mm)	$\sigma_{Rd,loc}(MPa)$	$\tau_{Rd,loc}(MPa)$	$\sigma_{Ed,loc}(MPa)$	η_3 (/)
12	*460*	*440*	*317*	*279*	*317*	*0.18*
16	*460*	*440*	*392*	*319*	*392*	*0.16*
21	*460*	*440*	*460*	*319*	*460*	*0.16*
31	*460*	*440*	*460*	*319*	*460*	*0.16*
36	*460*	*440*	*460*	*319*	*460*	*0.16*
41	*460*	*440*	*460*	*319*	*460*	*0.16*

Global buckling of the bottom flange
According to A1:2017, the final results for buckling capacities are shown in (Table 4.11) from the global analysis of the bottom flange.

Table 4.11: Buckling capacity of bottom flange/ Global buckling.

t (mm)	$f_{yk}(MPa)$	$\sigma_{Rd,global}(MPa)$
12	*460*	*369*
16	*460*	*330*
21	*460*	*315*
31	*460*	*319*
36	*460*	*322*
41	*460*	*324*

4.2.2.3 Webs

Single panel buckling

Table 4.12: Buckling capacity of the single web panels.

	Thickness (mm)	$\sigma_{x,Rd}$ (MPa)	$\tau_{Rd}(MPa)$
Top Panel	*13*	*287*	*252*
	17	*363*	*307*
	21	*451*	*318*
Middle panel (compression)	*13*	*242*	*231*
	17	*308*	*261*
	22	*385*	*318*
Middle panel (bending)	*13*	*460*	*231*
	17	*460*	*261*
	22	*460*	*318*

Global buckling
Shear buckling capacity of the whole web is shown in (Table 4.13)

Table 4.13: Global shear buckling capacity of the web.

Plate thickness (mm)	τ_{Rd}(MPa)
13	*248*
17	*265*
22	*297*

Buckling capacity for normal stresses is shown in (Table 4.14).

Table 4.14: Buckling capacity of the web under normal stresses, global analysis.

Web thickness (mm)	$\sigma_{Rd,top}(MPa)$	$\sigma_{Rd,bott}(MPa)$
13	*-312*	*0*
17	*-328*	*0*
21	*-366*	*0*
13	*0*	*-358*
17	*0*	*-370*
21	*0*	*-385*

4.3 Comparison

In this chapter, a comparison between carbon steel and stainless steel is made concerning buckling strengths. Starting by comparing buckling strengths for the original cross-section but with two different materials, i.e., carbon steel S355 and stainless steel 1.4462. Afterward, a comparison between the original cross-section with S355 carbon steel and the reduced cross-section with 1.4462 stainless steel.

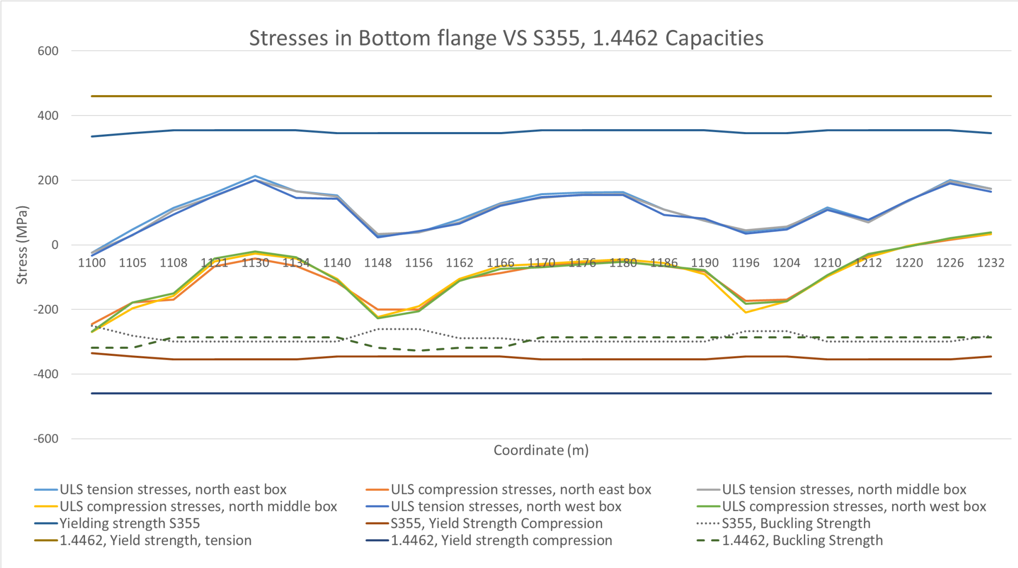

Figure 4.7: Applied stresses Vs. Buckling capacities of the bottom flange with different material/ Original cross-section.

4.3.1 Original cross-section

Buckling capacity for the original cross-section is calculated using duplex stainless steel 1.4462. The final results are compared with the resultant stresses from global analysis in the ultimate limit state and plotted in the same chart.

4.3.1.1 Bottom flange

The Y-axis in Figure 4.7 represents the stresses and x-axis, starting from axis 1.17 to axis 1.20 and without the support sections. The wavy two groups of lines represent the applied stresses in the ultimate limit state.
The green dashed line represents the buckling capacity of the bottom flange with similar cross-sections and similar plate thicknesses. The dotted line is buckling capacity using S355 carbon steel. The higher yield strength of stainless steel is not contributing to improving the buckling capacity of the bottom flange. This is due to the higher susceptibility of stainless steel to buckling compared with carbon steel. Depending on this chart, material saving cannot be achieved unless the cross-section is optimized.

4.3.1.2 Webs

As described earlier, web buckling is calculated for the top field and bottom field separately. **Bottom field**
Buckling capacities of the web bottom field are almost the same for the two materials. Material saving cannot be achieved unless the cross-section is optimized.
Top field
The web's top field Buckling capacities using duplex stainless steel are higher than S355 carbon steel (Figure 4.9), but the section still needs to be optimized due to the low buckling capacity in the bottom field.

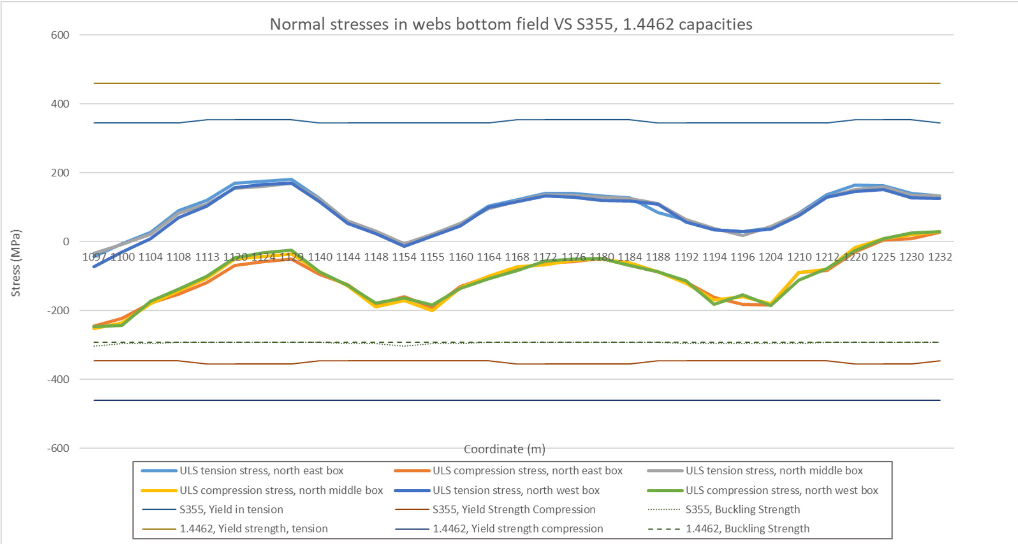

Figure 4.8: Applied normal stresses Vs. Buckling capacities of the web's bottom field using different material/ Original cross-section.

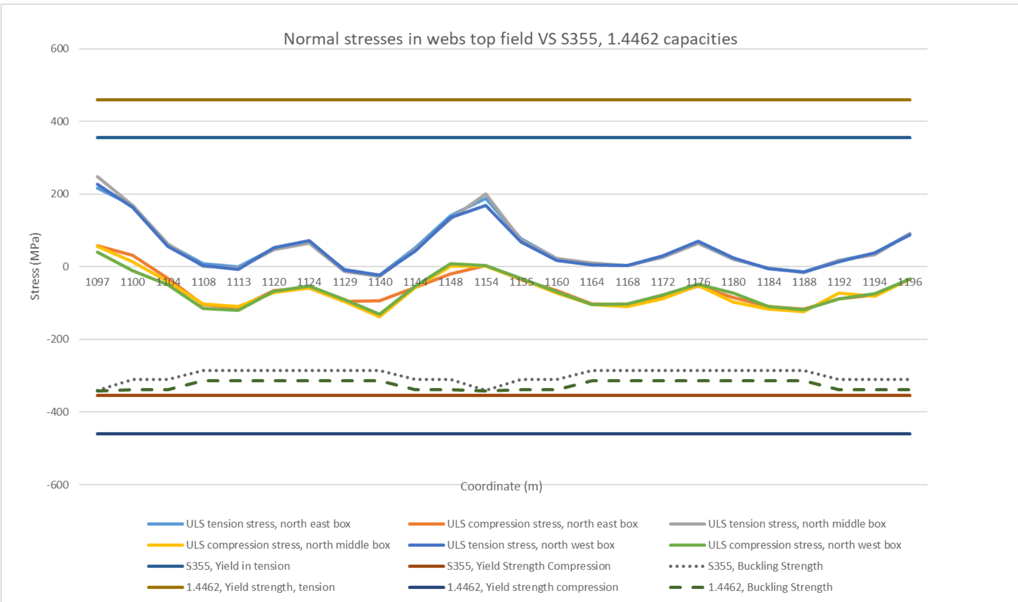

Figure 4.9: Applied normal stresses Vs. Buckling capacities of the web's top field using different material/ Original cross-section.

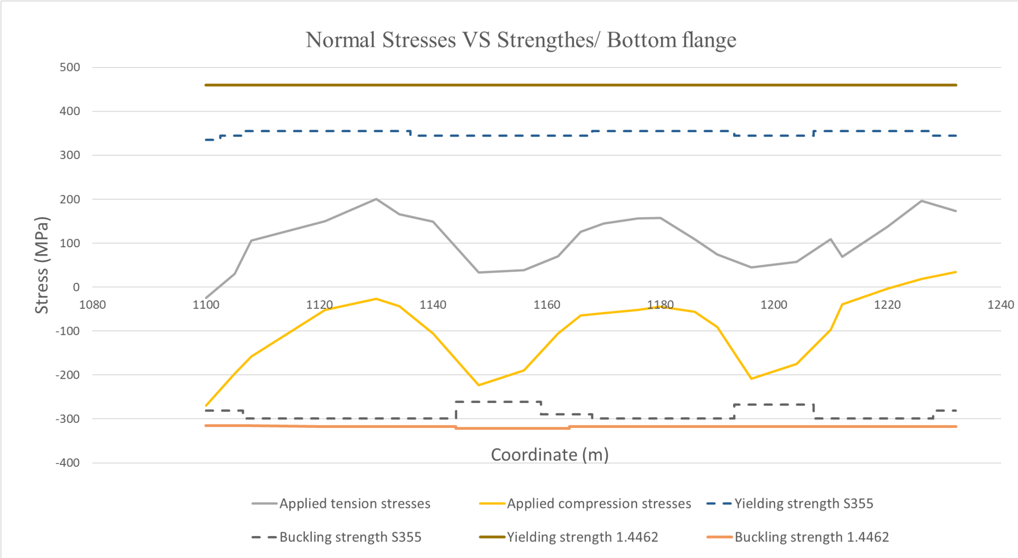

Figure 4.10: Applied stresses Vs. Buckling capacities of the bottom flange with different material/ New cross-section.

4.3.2 Optimized cross-section

After changing the cross-section and reducing plate thicknesses as described in the previous figure, new buckling capacities for each part are calculated and compared.

4.3.2.1 Bottom flange

In Figure 4.10, the dashed black line represents the buckling capacity of the original cross-section using S355 carbon steel. The orange straight line represents the buckling capacity of the optimized section with duplex stainless steel 1.4462.
Compared to each other, the optimized cross-section has a slightly higher buckling capacity. This is achieved by reducing the width of the single panels, and higher buckling coefficients are obtained.

4.3.2.2 Webs

Bottom field

After optimizing the cross-section, the buckling capacity of the web's bottom field becomes equal to the original design using carbon steel S355 (Figure 4.11).

Top field

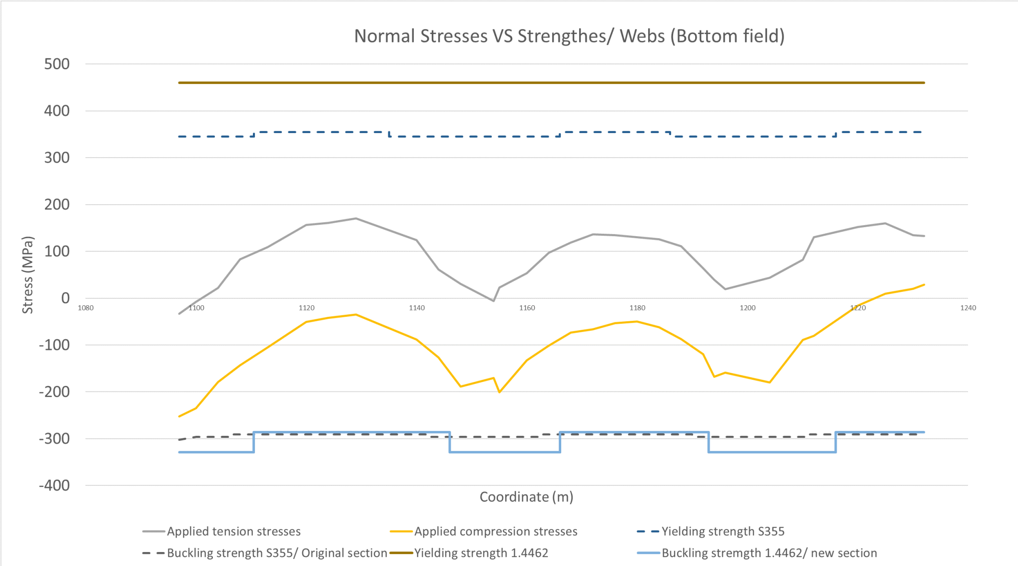

Figure 4.11: Applied normal stresses Vs. Buckling capacities of the web's bottom field using different material/ New cross-section.

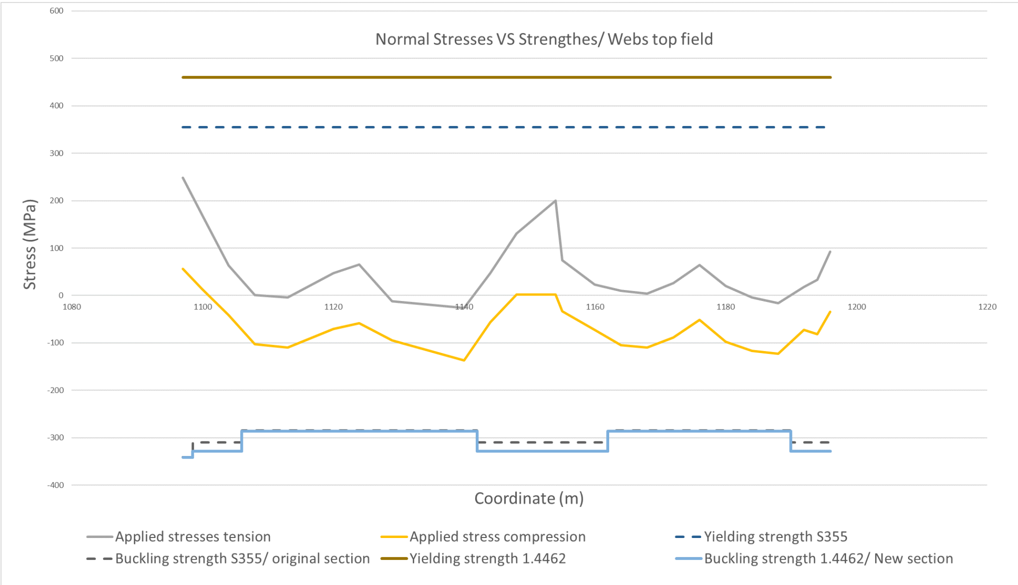

Figure 4.12: Applied normal stresses Vs. Buckling capacities of the web's top field using different material/ New cross-section.

In Figures 4.11, and 4.12, the buckling capacity of the original cross-section and the optimized one with stainless steel are close to each other. This shows the significance of using stainless steel in an optimized way to increase material savings and benefit from the higher yield strength of duplex stainless steel.

4.3.3 Weight Comparison

By optimizing the cross section, the total weight is reduced as shown in Figure 4.13.

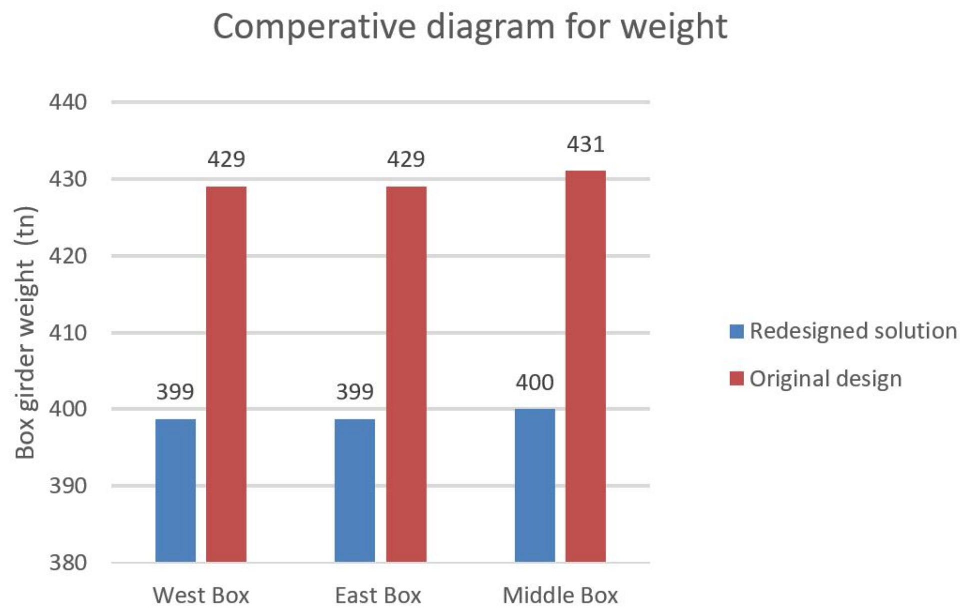

Figure 4.13: Comparative diagram for weight between the original design and the redesigned solution.

As it is observed from the figure above, the new solution with stainless steel presents a reduction of around 8% in the total weight per box. The highest weight reduction is observed in the east box and the smallest in the east box. This happens because the three boxes do not have the same cross-section. In Table 4.15 the reduction percentage will be presented per box.

Table 4.15: Weight reduction percentage per box due to weight optimization.

Box	Reduction
West	*8%*
East	*8%*
Middle	*8%*

5

Life Cycle Cost Analysis

Bridges are structures with a long life cycle. For a bridge to remain functional through the life cycle, maintenance needs to be conducted for all structural parts. Therefore, when designing a bridge, the emphasis is given to the bridge's initial investment cost by taking into consideration the functional demands. Naturally, this factor leads to solutions with lower investment costs. However, the lower investment cost does not guarantee a low maintenance cost of the structure during its service life. So actually, it is pretty common that lower initial investment costs can lead to a higher total cost through the structure's service life. In order to evaluate different solutions, LCCA is used.

LCCA takes into account all the relevant economic factors, both in terms of initial capital costs and future operational and maintenance costs, over a specific time period (Sundquist and Karoumi, 2016).

The material cost of stainless steel is relatively high due to alloying, nevertheless it can lead to solutions with a lower total price through the life cycle. This is achieved through the low maintenance costs, as the stainless steel does not need to be repainted. As the goal of the thesis is to redesign the main box girders in stainless steel, it is interesting to investigate the new proposal regarding the life cycle cost and compare it with the original design.

5.1 Assumptions

Only the INV cost, according to chapter 2.3, will be taken into account for the LCCA. According to the design document, the lifecycle class of the bridge is L100 due to its high importance. So, according to EN 1992-2, the lifecycle of the bridge is 120 years. The discount rate is taken as 3.5% according to TRVK for this year.

To calculate the INV cost, prices for the different types of steel are required. The base price range of the raw carbon steel material is between 15-20 SEK/kg. Therefore, the authors assumed15 SEK/kg for the original design of the bridge.

Regarding prices for stainless steel grade 1.4162 and 1.4462, the price of stainless-steel products, in general, is not stable over time, as the cost of the alloying is constantly shifting. Therefore, to calculate the base price of stainless steel, the base price and the cost of alloying are summed per type of stainless steel. Alloying prices for the specific type of stainless steel were extracted from the Outokumpu website and used for this study.

Table 5.1: Table of alloy surcharges for May 2021 (Provided by Outokumpu).

Alloy Surcharges in May for Flat products		
EN	*Outokumpu*	*SEK/kg*
1.4162	*Forta LDX 2101*	*12*
1.4462	*Forta DX 2205*	*23*

For stainless steel material prices, Outokumpu requested not to put the exact value in SEK/kg that was provided, as the data can be used from their competitors. Initial painting cost was extracted from (Wahlsten, Heshmati, Al-Emrani, Åke, 2018). Regarding the post-weld treatment cost of stainless steel, two methods exist. The first is called pickling. More specific is a process where the stainless steel section is sprayed with chemicals and then is water washed. This process removes the damaged material from the welds. As a consequence, the protective layer of stainless steel can be reformed. However, if not the whole area of the stainless steel section is sprayed, this can lead to the different coloring of surfaces, which is not appealing. The second method is experimental yet and involves the use of a laser. The laser removes the damaged material from the weld again. In this project, the first method will be used; after a recommendation from Outukumpu, there is uncertainty regarding the efficiency of the second method.
The major and minor inspection costs and the time intervals between inspections were extracted from a price list for the life cycle plan. The same applies to the cost of repainting outside the box girder. The cost of repainting inside the box girder was assumed to be the same. All the relevant costs which were taken into account are presented in the table below.

Table 5.2: Values of different costs for determination of INV cost.

Investment Costs		
Item	*Unit*	*SEK/Unit*
Steel S355J2	*kg*	*15*
Stainless steel Duplex 1.4462	*kg*	*Base price + Alloy surcharge*
Stainless steel Lean Duplex 1.4162	*kg*	*Base price + Alloy surcharge*
Initial Painting	*m2*	*1900*
Post weld treatment (Pickling)	*m2*	*340*
Welding of box girder (S355)	*kg*	*18*
Welding of box girder (SS)	*kg*	*22*
Montage	*kg*	*16*
Project administration	*kg*	*6*

Table 5.3: Values of different costs and interval year for determination of LCM costs.

Life cycle plan			
Description	*Interval year*	*Unit*	*SEK/Unit*
Minor inspection of the box girders	*1*	-	*20 000*
Major inspection of the whole bridge	*6*	-	*65 000*
External re-painting of the box girders	*25*	*m2*	*1900*
Internal re-painting of the box girders	*50*	*m2*	*1900*

5.2 Calculation schedule

To perform the LCCA and the weight calculations for the box girders, an excel file was created. In total, three alternatives will be compared with the original design.

1. Use of 1.4462 stainless steel with the exact dimensions as the original design.
2. Use of 1.4462 stainless steel with the redesign.
3. Use of 1.4162 lean duplex and 1.4462 stainless steel with the redesign.

First, the calculations for stiffeners are created. In order to get the weight for each stiffener, the length and the area of each stiffener are required. Below, the area calculator is presented for the original design.

Table 5.4: Table for area calculation for each stiffener type.

Stiffener type	T1	T2	T3	T4	Unit
Bs outside	*400*	*450*	*450*	*450*	*mm*
bs outside	*200*	*250*	*250*	*250*	*mm*
Hs outside	*200*	*250*	*300*	*300*	*mm*
ts	*6*	*6*	*8*	*10*	*mm*
A outside	*60 000*	*87 500*	*105 000*	*105 000*	*mm2*
Bs inside	*387*	*437*	*433*	*429*	*mm*
bs inside	*192*	*242*	*240*	*238*	*mm*
Hs inside	*194*	*244*	*292*	*290*	*mm*
A inside	*56 163*	*82 838*	*98 258*	*96 715*	*mm2*
Astiffener	*3837*	*4662*	*6742*	*8285*	*mm2*

In (Table 5.4) the required input data are only the outer dimensions. The inner dimensions are dependent on the external dimension, thicknesses, and the radius of the stiffeners. Then the inner and outer areas of the stiffeners are calculated as a trapezoidal area with dimensions as the one presented in Figure 5.1. Next, the inner and outer are subtracted to calculate the area of the stiffener. It is chosen to calculate the areas in that manner because later, the outer area of the stiffeners is removed from each cross frame plate.

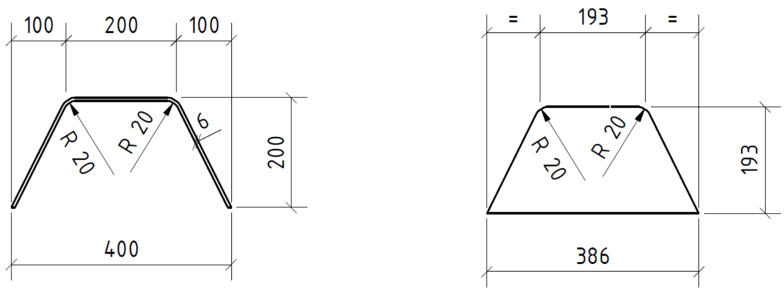

Figure 5.1: Internal and external dimensions for stiffener T1.

Following the original drawings, the material tables are created in excel (Table 5.5).

Table 5.5: Materials list for the production of part N1V-101 of the original design. (dimension in mm, area in mm^2, and weight in Kg).

N1V-101							
Position		*Profile*	*Width*	*Thick*	*Length*	*Weight*	*Area*
N1V-1001	*1*	*Top falnge*	*700*	*25*	*7607*	*1025*	*11 030 150*
N1V-1002	*1*	*Cross-frame Web*	*584*	*14*	*1612*	*86*	*1 927 952*
N1V-1004	*1*	*Cross-frame Web*	*550*	*14*	*2188*	*115*	*2 468 064*
N1V-1006	*1*	*Cross-frame Web*	*584*	*18*	*1068*	*80*	*1 285 872*
N1V-1009	*1*	*Bottom Flange*	*2532*	*16*	*7607*	*2373*	*38 765 272*
N1V-1011	*1*	*Web*	*2569*	*16*	*7699*	*2437*	*39 803 830*
N1V-1013	*1*	*Cross-frame Plate*	*250*	*16*	*2036*	*63*	*1 083 152*
N1V-1014	*2*	*Cross-frame Plate*	*116*	*16*	*420*	*12*	*221 760*
N1V-1016	*1*	*Cross-frame Flange*	*300*	*20*	*2464*	*114*	*1 576 960*
N1V-1019	*1*	*End Plate*	*194*	*6*	*387*	*3*	*154 800*
N1V-1020	*1*	*End Plate*	*244*	*6*	*437*	*5*	*218 500*
N1V-1021	*2*	*End Plate*	*292*	*6*	*433*	*12*	*516 136*
N1V-1015	*1*	*Stiffener*	*T1*		*7306*	*262*	*1 827 039*
N1V-1018	*1*	*Stiffener*	*T2*		*7306*	*216*	*1 461 647*
N1V-1022	*2*	*Stiffener*	*T3*		*7306*	*759*	*3 654 265*
Total						*7560*	*105 995 399*

All the plates are assumed to have a rectangular cross-section, the three dimensions are multiplied, and the part's weight is calculated. To the components marked with blue, the formula changes as the outer area of the stiffeners are subtracted from the cross frames.
The original painting area of each part is calculated as it will be later required for in LCC. Each plate is painted in the dimension width x length from both sides. The calculation is are different for the bottom flange and web, as from the calculated area the outer width of the stiffener multiplied by the length is subtracted. The stiffeners are painted only on the outer sides.

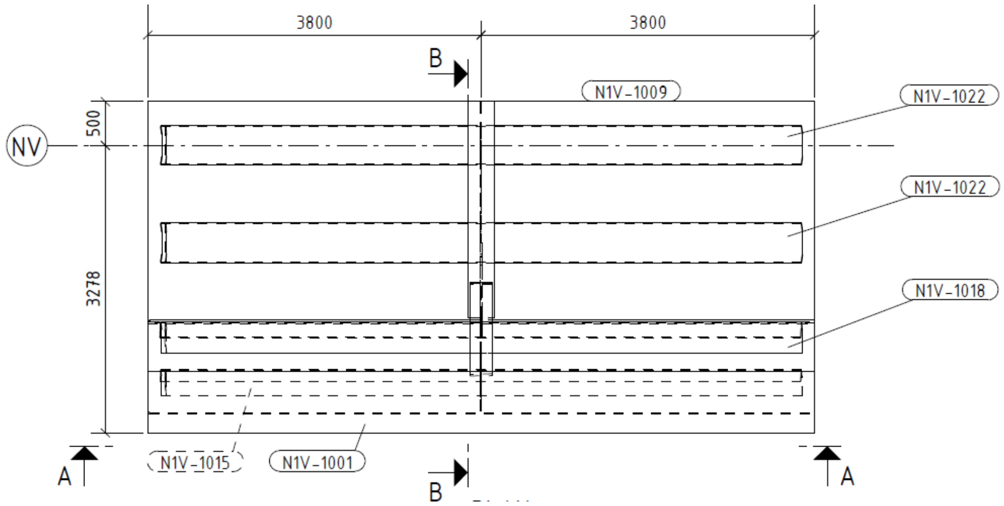

Figure 5.2: Plan view of part N1V-101 (Provided by COWI).

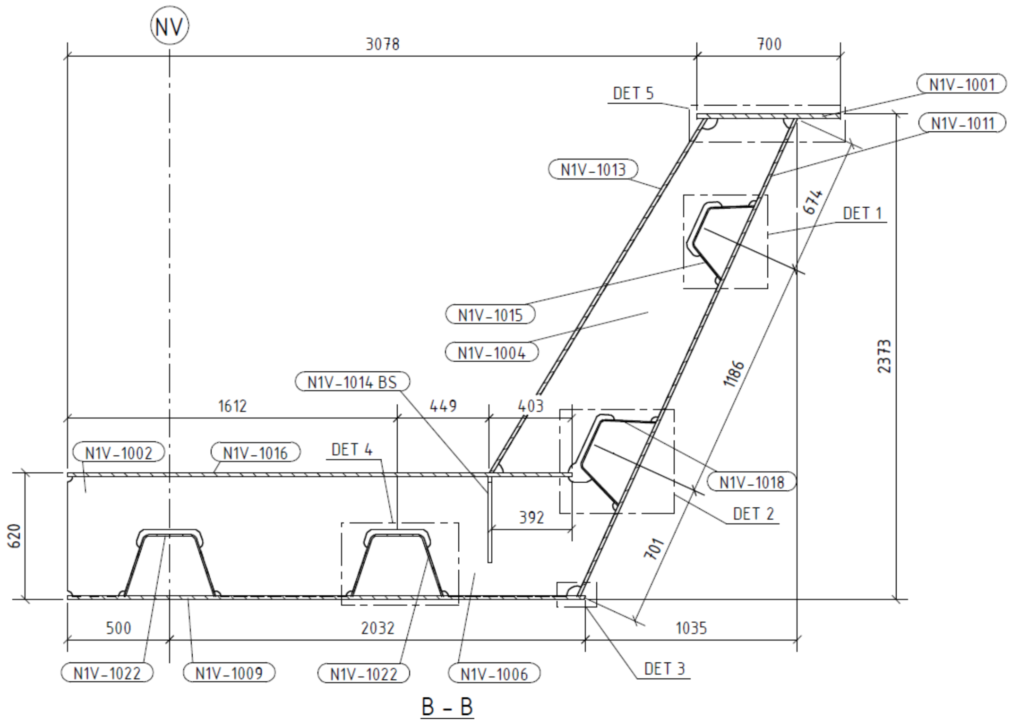

Figure 5.3: B-B section of the part N1V-101(Provided by COWI).

The total weight and painted area are calculated by summing the relevant subparts. The weight as the value of the original design is also presented. The error is relatively small, so a compromise is made. This is happening due to the weight calculation of the stiffener, as the shape is not precisely trapezoidal. Some slight differences can also exist between the calculated weights of the different parts.
In order to be sure that the total error is relatively small, the summation of all the weights is compared with the extracted weight from the original drawings. As it is observed, the error is 0.1%, so it is acceptable. For later use, the weight of the parts

in stainless steel 1.4462 and 1.4162 are separated, and the calculated error in the redesign will represent the weight reduction of the design.

Table 5.6: Information for the West box required for calculations in the LCCA.

West Box		
Total weight	*428 606*	*kg*
Original section	*429 020*	*kg*
Calculator Error	*-0,1%*	*-*
Painted Area In+ out	*5186*	*m2*
Weight 1.4462	*291 161*	*kg*
Weight 14162	*137 445*	*kg*
Studied length	*166,1*	*m*

The external painted area needs to be calculated because the relevant area needs to be multiplied with the relevant cost for the LCC analysis. The dimensions of flange and webs are documented and multiplied in order to get the painted area for each part. All the areas are added to get the final value.
It is decided to gather the relevant cost in three categories; material, Production, and Surface treatment cost.

Table 5.8: Cost sub-categories in carbon steel solution.

Material Cost	Production Cost	Surface treatment
Carbon steel S355	*Welding of box girder*	*Initial paiting*
	Montage	
	Project administration	

Table 5.9: Cost sub-categories in stainless steel solutions.

Material Cost	Production Cost	Surface treatment
Stainless steel 1.4462, and 1.4162	*Welding of box girder*	*Pickling*
	Montage	
	Project administration	

As all the input data are set up, the LCCA can be conducted. First, for each year of the lifespan of the building, the relevant cost is taken into account. For example, in the year 0, only the INV cost is taken into account, and the following year's only maintenance costs are taken into account. The next step is to calculate the NPV using Excel's build in function, declaring only the range of the cells that contains years and the applicable discount rate.

Table 5.7: Calculation of outside painting area for West box. length in mm, and area in mm^2

West Box					
Section Name	*Length*	H_{web}	L_{web}	$W_{bottomplate}$	*Area*
N1V-101	*7600*	*2373*	*2578*	*2532*	*38 835 493*
N1V-102	*7600*	*2232*	*2425*	*1532*	*30 071 348*
N1V-501	*8200*	*2232*	*2425*	*1532*	*32 445 402*
N1V-502	*8200*	*2373*	*2578*	*2532*	*41 901 452*
N2V-101	*12 000*	*2373*	*2578*	*1532*	*49 319 198*
N2V-102	*8000*	*2373*	*2578*	*2532*	*40 879 465*
N2V-103	*12 000*	*2332*	*2533*	*1532*	*48 784 708*
N2V-104	*8000*	*2332*	*2533*	*1532*	*32 523 139*
N3V-101	*8000*	*2332*	*2533*	*1532*	*32 523 139*
N3V-102	*8000*	*2372*	*2577*	*2532*	*40 870 774*
N3V-103	*7600*	*2332*	*2533*	*1532*	*30 896 982*
N3V-104	*7600*	*2373*	*2578*	*2532*	*38 835 492*
N3V-501	*8400*	*2373*	*2578*	*2532*	*42 923 438*
N3V-502	*8400*	*2332*	*2533*	*1532*	*34 149 296*
N4V-101	*16 000*	*2373*	*2578*	*2532*	*81 758 930*
N4V-102	*8000*	*2373*	*2578*	*2534*	*40 895 465*
N4V-103	*16 000*	*2332*	*2533*	*1532*	*65 046 278*
N4V-104	*8000*	*2332*	*2533*	*1534*	*32 539 139*
N5V-101	*8000*	*2373*	*2578*	*2534*	*40 895 465*
N5V-102	*11 600*	*2373*	*2578*	*2532*	*59 275 224*
N5V-103	*11 600*	*2332*	*2533*	*1532*	*47 158 551*
N5V-104	*8000*	*2332*	*2533*	*1534*	*32 539 139*
N5V-501	*8400*	*2373*	*2578*	*2534*	*42 940 238*
N5V-502	*8400*	*2332*	*2533*	*1532*	*34 149 296*
N6V-101	*8000*	*2373*	*2578*	*2532*	*40 879 465*
N6V-102	*8000*	*2332*	*2533*	*1532*	*32 523 139*
N6V-103	*12 000*	*2373*	*2578*	*2532*	*61 3191 98*
N6V-104	*12 000*	*2332*	*2533*	*1532*	*48 784 708*
N6V-105	*8000*	*2332*	*2533*	*1536*	*32 555 139*
N6V-106	*8000*	*2373*	*2578*	*2536*	*40 911 465*
N7V-101	*7800*	*2373*	*2578*	*2535*	*39 880 878*
N7V-102	*7800*	*2332*	*2533*	*1536*	*31 741 260*
N7V-103	*9100*	*2858*	*3105*	*2425*	*50 321 343*
N7V-104	*6050*	*2206*	*2397*	*709*	*18 788 341*
N7V-501	*8400*	*2373*	*2578*	*2675*	*44 124 638*
N7V-502	*8400*	*2332*	*2533*	*1545*	*34 258 496*
Total Area					*1 488 245 134*

5.3 Comparison

LCCA results are presented in Figure 5.4 and 5.5 for each solution.

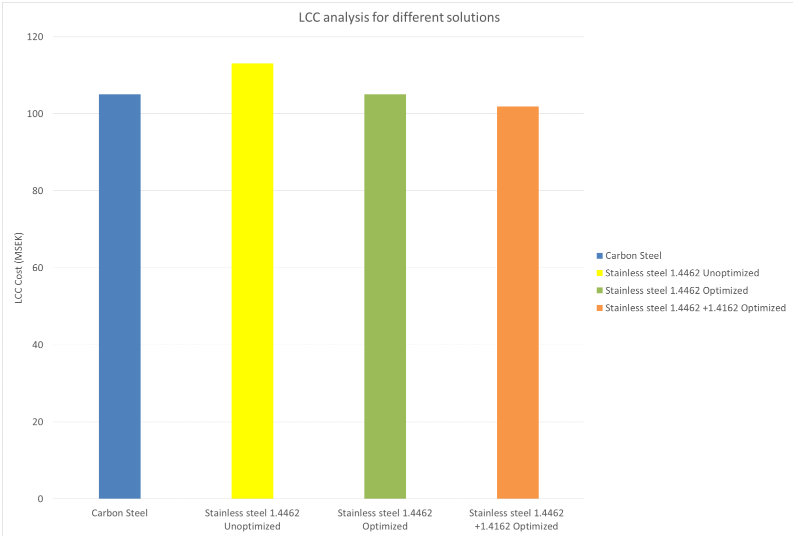

Figure 5.4: Results for the LCC cost per solution.

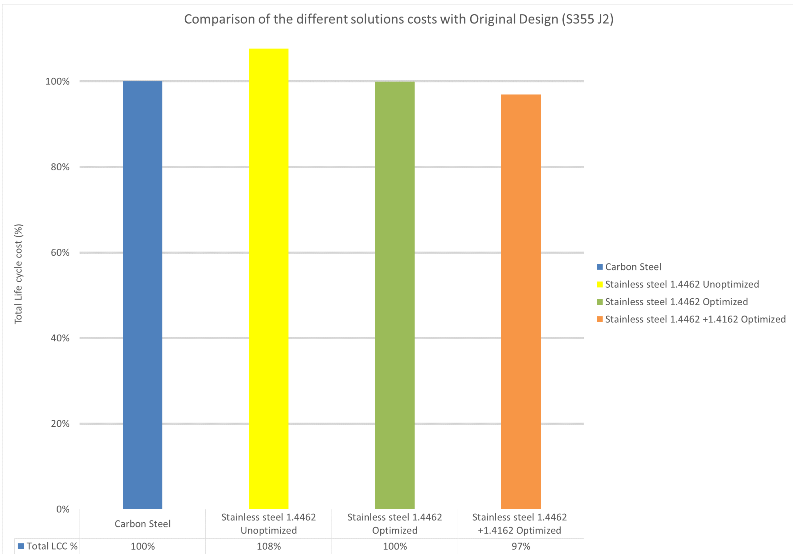

Figure 5.5: Comparison of the total LCC savings per solution compared to the original design.

Comparing the original design (Blue) with unoptimized 1.4462 stainless steel (Yellow), it is observed that the yellow solution is 8% more expressive than the original solution. This is expected as the material cost for the stainless-steel solution is very high. In order to achieve savings, the cross-section needs to be optimized and the high resistance of stainless steel to be highly utilized.
Comparing the original design (Blue) with optimized 1.4462 stainless steel (green), small cost savings are observed. However, as those are too low, the total lifecycle

cost is assumed to be the same as the original solution. Consequently, to achieve profitability, it is required either to optimize the cross-section either as in this problem by using different grades of stainless steel for the various components in the box sections.
Comparing the original design (Blue) with the optimized cross-section and combination of 1.4462 and 1.4162 (Orange), 3% cost savings are observed. The savings in this solution are higher compared to the previous solution. This occurs due to the cross-section optimization and the use of different stainless-steel grades for the various components.

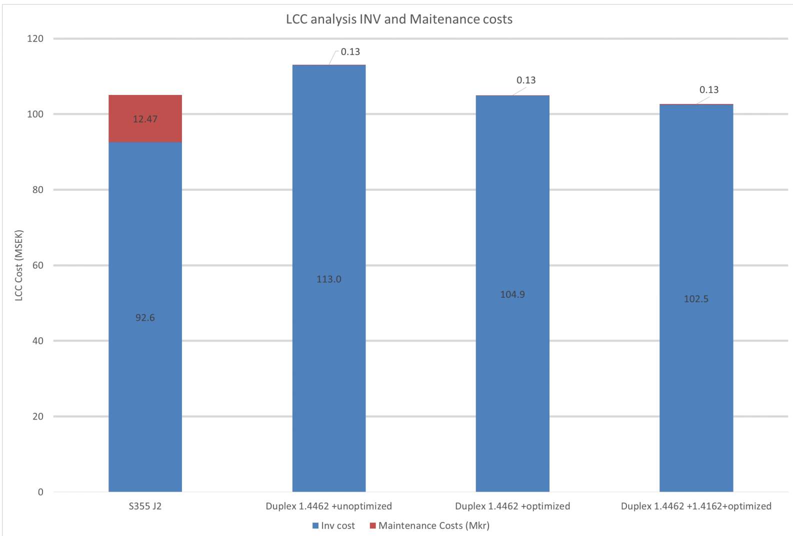

Figure 5.6: Comparison of investment and maintenance costs for each solution.

From the comparison, maintenance costs are a significant part of the original solution. Maintenance costs are almost negligible in the stainless-steel solutions as only the inspection costs are considered. Regarding the initial investment cost, as it is expected, it is higher in all-stainless-steel solutions. In the optimized solution with 1.4462 and 1.4162, the original investment cost is not so high compared to the other solutions. This cost can be lower with further cross-section optimization than the initial investment cost in the original S355 solution.

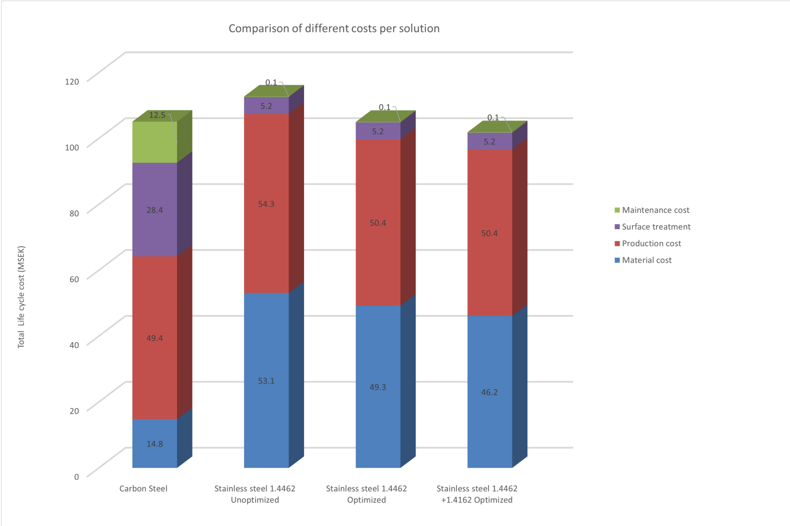

Figure 5.7: Influence of different costs per solution.

Material cost of stainless steel has a significant influence on the total LCCA cost. Consequently, the base material cost of stainless steel and the price surcharge of stainless-steel products influence the total cost. Therefore, different types of stainless steel can be used in box girder projects to achieve higher cost savings.

In all stainless-steel solutions, post-weld treatment has a significant influence on the total LCC cost. Thus when stainless steel solutions are investigated in LCCA, post-weld treatment needs to be taken into account.

Comparing the influence of surface treatment cost in the total LCCA, it is observed that it is a significant part of the total cost in the carbon steel solution. This occurs because it refers to the original painting of the cross-section. On the other hand, the surface treatment of stainless steel refers to pickling, which has a lower cost than the original painting of the cross-section. However, lower-cost can be achieved for the post-weld treatment cost of stainless steel with an experimental method. In this experimental method, a laser is used to treat the weld to remove the damaged layer of stainless steel. Compared to the traditional pickling method where the whole box girder is sprayed with chemicals and then washed, this method is more environmentally friendly as no chemicals are disposed.

Following, the results of the sensitivity analysis for different discount rates are presented.

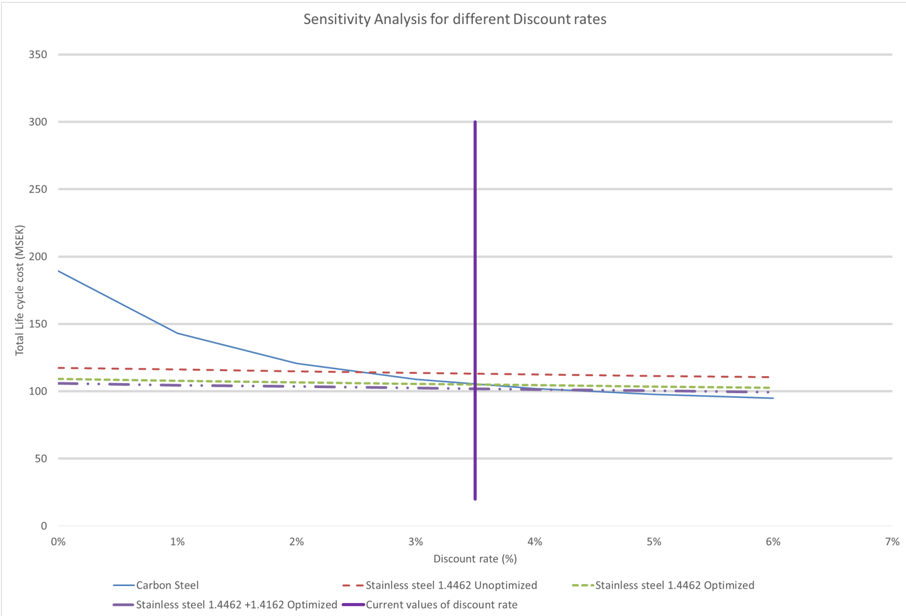

Figure 5.8: Sensitivity analysis for different discount rates.

Here it is clear that the discount rate has significant importance in the value of total LCCA. For a discount rate of 0%, the cost of the original solution is extremely high. This occurs because the NPV formula is equivalent to adding all the costs for 120 years.
Comparing the carbon steel solution (the blue line) with the red solution, profitability cannot be achieved for higher than 2.5% discount rates. The first solution has an 8% higher total LCCA cost than the carbon steel design, so it is expected to be very sensitive regarding the discount rate.
The green solution is not profitable for discount rates of more than 3.5%. This occurs because the savings margin is small.
Finally, regarding the optimized solution with 1.4162 and 1.4462 with stainless steel (Purple); The purple solution has savings of 3%, so it stops being profitable for discount rates higher than 4.5%. The sensitivity of each solution to the different values of discount rates depends on the savings margins. It can be concluded that the highest the value of cost savings, the less sensitive the solution is on different discount rates.
The importance of section optimization is highlighted as better section optimizations lead to larger material savings and, consequently, solutions with the lower influence of different discount rates.

6
Discussion and Conclusion

This master thesis begins with a revision for the design procedures of steel-concrete composite bridges with more focus on trapezoidal open box girders. Next, the different types of stainless steel used in the bridge industry are presented and how the design manuals treat stainless steel differently. Finally, the literature review chapter closes with LCCA methodology, which is used in chapter 5. These were done with scope to get familiar with the design methodology of composite bridges and identify the relevant stainless steel types that are applicable as a structural material.

The design methodology of the new Hisings Bridge was studied and presented briefly, with more focus on the calculations of buckling capacities in the box girder. These calculations will serve as a basis for the stainless-steel design with respect to (A1:2017, design manual for structural stainless steel). In general, stainless-steel design and conventional steel design are not so different, except for the limits of cross-section classification, material parameters, and some other requirements for shear buckling resistance.

In the redesign using stainless steel, by assuming the same cross-section with 1.4462 stainless steel, the high yield strength of 460 MPa could not be utilized. This occurs as the buckling capacity of the bottom flange and the webs did not increase compared to the original design with S355 carbon steel. In order to benefit from the high yield strength, it was concluded that the cross-section needs to be modified. Consequently, more slender sections can be used, and savings are attainable.

Critical points in the cross-section altering were the following:

- Bottom flange, single panel buckling was governing.
- Webs, shear buckling interaction limits were governing the design.
- Web lowe stiffener, the 6mm thickness had a low buckling capacity, governing the bottom field of the web.

New geometry for the cross-section was introduced, and new capacities for all of the relevant parts were calculated. Buckling capacities in the new geometry with the same plate thickness were higher than the original cross-section. Thus, the plate thicknesses of the members were reduced until a close buckling capacity to the original design was achieved. In this way, material savings are achieved.

Local buckling in the top flanges was the governing capacity when 1.4462 is used.

However, the capacity of the top flange in 1.4462 is lower than the original capacity in S355. Nevertheless, the actions are smaller than the 1.4462 capacity during the construction stages before the concrete deck is hardened. Consequently, no stability problems are expected in the top flanges in stainless steel.

Shear connectors capacity in the original design was calculated in three failure modes; the first one regarding a failure in the stud base itself, the second one considering a failure in the mature concrete around the stud, third one considering failure in the premature concrete (before full hardening). The governing capacity was the third failure mode which is related directly to the concrete maturity. That's why no reduction in shear connectors was possible using stainless steel 1.4462.

The applied stresses (Actions) used in this thesis work were obtained using the original cross-section from the original finite element analysis with SOFISTIK. Changing the geometry of the cross-section and plate thicknesses may lead to redistribution of stress in different parts of the box girder. So, a separate analysis needs to be conducted in order to ensure that the new sections are not over or underestimated through the components of the bridge.

As the design in stainless steel is similar to the carbon steel design, one can claim that no extra computational effort is required for the implementation of stainless steel. However, except for material savings, the bridge owner is interested in cost savings regarding the original investment cost and maintenance. As it was shown before the price of stainless steel as a raw material is relatively high, so to be implemented the cross-section needs to be optimized, meaning that the weight of the cross-section needs to be reduced. So, an LCCA analysis is required to investigate the cost through the life cycle.

Life cycle cost analysis was conducted for the following alternatives

1. Original cross-section with S355 carbon steel
2. Original cross-section with 1.4462 Duplex Stainless steel
3. Reduced cross-section with 1.4462 Duplex stainless steel
4. Reduced cross-section with two different grades of stainless steel; 1.4162 lean duplex stainless steel and 1.4462 duplex stainless steel.

Only owner cost is calculated in the LCCA. More specifically, investment cost and LCM were taken into account as owner cost. In the investment cost, material, welding, initial painting, and post-weld treatment cost were considered. In LCM, only major and minor inspections and repainting of the box girders inside and outside. Finally, a sensitivity analysis to evaluate the profitability for different discount rates for each solution.

Using lean duplex stainless steel with grade 1.4162 in the inner parts of the box girder is an efficient way to reduce the investment cost without reducing the material consumption. This solution can be used in girders with an inside protected space from the outer environment like box girders. However, it needs more research to ensure that no corrosion can occur, especially in bridges with corrosivity class C5M that duplex stainless steel 1.4462 must be used.

Combining two different types of stainless steel leads to a solution with a slightly lower original investment cost. However, the savings are too small, and it can be assumed that the original investment cost is the same. More material and cost savings can be achieved by optimizing the supports sections using FEM, which were excluded from the study.

A significant factor that influences the LCCA results is the price surcharge of stainless steel. As mentioned, the price of the stainless-steel alloys varies over time, and in this thesis, it was based on the Outokumpu catalogue. Also, the base price of steel products can vary through time but not to a large extent compared to steel alloying.

The Post weld treatment cost of stainless steel is high and needs to be considered in LCC studies. Two methods exist regarding the post-weld treatment, pickling and laser treatment. The laser treatment method is cheaper than pickling, and it can lead to better results in LCCA.

7
Further studies

In this master thesis, support sections were excluded from the redesign stage with stainless steel due to the complexity of the support sections. However, it is beneficial to redesign the support sections as done in the original design using FEA. In this manner, higher material saving can be achieved as the thicknesses of the parts in the support sections are double compared to a span section. Using FEA in determining buckling coefficient may lead to a higher capacity than those obtained when applying the Eurocode methodology.

It can be beneficial to determine the exact influence of the price fluctuation in the life cycle cost analysis. However, as observed in this thesis, the discount rate has a vital effect on the life cycle cost analysis. A complete factorial design with more than two factors may lead to a better capture the interaction between the different factors in the life cycle cost analysis.

Other costs during the production stage, such as the labor cost for welding and production of the box girders, transportation cost, and demolition cost, can be taken into account in the owner cost to increase the study's accuracy. In the life cycle cost analysis, user and society expenses need to be taken into account also.

Bibliography

[1] Al-Emrani, M., Åkesson, B. (2020): Steel Structures. Course Literature. Chalmers University of Technology, Gothenburg.

[2] Vayas, I., Iliopoulos, A. (2014): Design of Steel-Concrete Composite Bridges to Eurocodes. CRC Press, Boca Raton.

[3] Petersen, C. (1982): Statik und Stabilität der Baukonstruktionen (Statics and stability of building structures. In German). Vieweg, Teubner Verlag.

[4] European Commission (2006): SS-EN 1993-1-1 Eurocode 3- Design of Steel Structure- Part 1-1: General Rules and Rules for Buildings, European Committee for Standardization CEN.

[5] European Commission (2006): SS-EN 1993-1-4 Eurocode 3- Design of Steel Structure- Part 1-4: General Rules- Supplementary Rules for Stainless Steel, European Committee for Standardization CEN.

[6] European Commission (2006): SS-EN 1993-1-5 Eurocode 3- Design of Steel Structure- Part 1-5: Plated Structural Elements, European Committee for Standardization CEN.

[7] European Commission (2005): SS-EN 1993-1-10 Eurocode 3- Design of Steel Structure- Part 1-10: Material Toughness and Through-Thickness Properties, European Committee for Standardization CEN.

[8] European Commission (2004): SS-EN 10025-1 Hot Rolled Products of Structural Steel- Part 1: General Technical Delivery Conditions, European Committee for Standardization CEN.

[9] European Commission (2004): SS-EN 10088-1 Stainless Steel- Part 1: List of Stainless Steels, European Committee for Standardization CEN.

[10] Steel Construction institute SCI (2017): Design Manual for Structural Stainless Steel, 4th edition, SCI, Berkshire.

[11] Muñoz, J., Pettersson, L., Sundquist, H., Karoumi,R. (2016): Life-cycle cost analysis as a tool in the developing process for new bridge edge beam solutions, Structure and Infrastructure Engineering.

[12] Pettersson, L., Sundquist, H. (2014): Optimala kantbalkssystem: Resultat av genomfört FUD-projekt [Optimal edge beams: results of the research, development and demonstration project] (Technical Report 2014:151), Stockholm: KTH Royal Institute of Technology.

[13] Salokangas, L. (2009). ETSI project (stage 2): Bridge life cycle optimization (Technical Report ISBN 978-952-60-5052-2), Espoo: Helsinki University of Technology.

[14] Thoft-Christensen, P. (2011): Infrastructures and life-cycle cost-benefit analysis. Structure and infrastructure engineering: Maintenance, management, life-cycle design and performance.

[15] Trafikverket [The Swedish Transport Administration] (2020): A' prislista för broåtgärder år 2020 [Price list of life-cycle measures year 2020], Stockholm: Trafikverket.

[16] Troive, S. (1998): Structural LCC design of concrete bridges (Doctoral thesis), KTH Royal Institute of Technology, Stockholm.

[17] Trafikverket [The Swedish Transport Administration] (2011): Trafikverkets bro 11 (2011) [Technical requirements and advices for bridges year 2011]. Stockholm: Trafikverket.

[18] Joakim Wahlsten, Mohsen Heshmati, Mohammad Al-Emrani, Lars-Åke Bylund (2018): SIFRA,Sustainable Infrastructure through increased use of Stainless Steel, Work package reports.

[12pt,a4paper,twoside,openany]report
moreverb textcomp lmodern helvet [T1]fontenc [english]babel [utf8]inputenc amsmath amssymb graphicx subfig listings chemfig [top=3cm, bottom=3cm, inner=3cm, outer=3cm]geometry eso-pic float parskip
[labelfont=bf, textfont=normal, justification=justified, singlelinecheck=false]caption
hyperref
titlesec
fancyhdr
[textsize=tiny]todonotes

A
Northern side bridge with coordinates and plate thicknesses

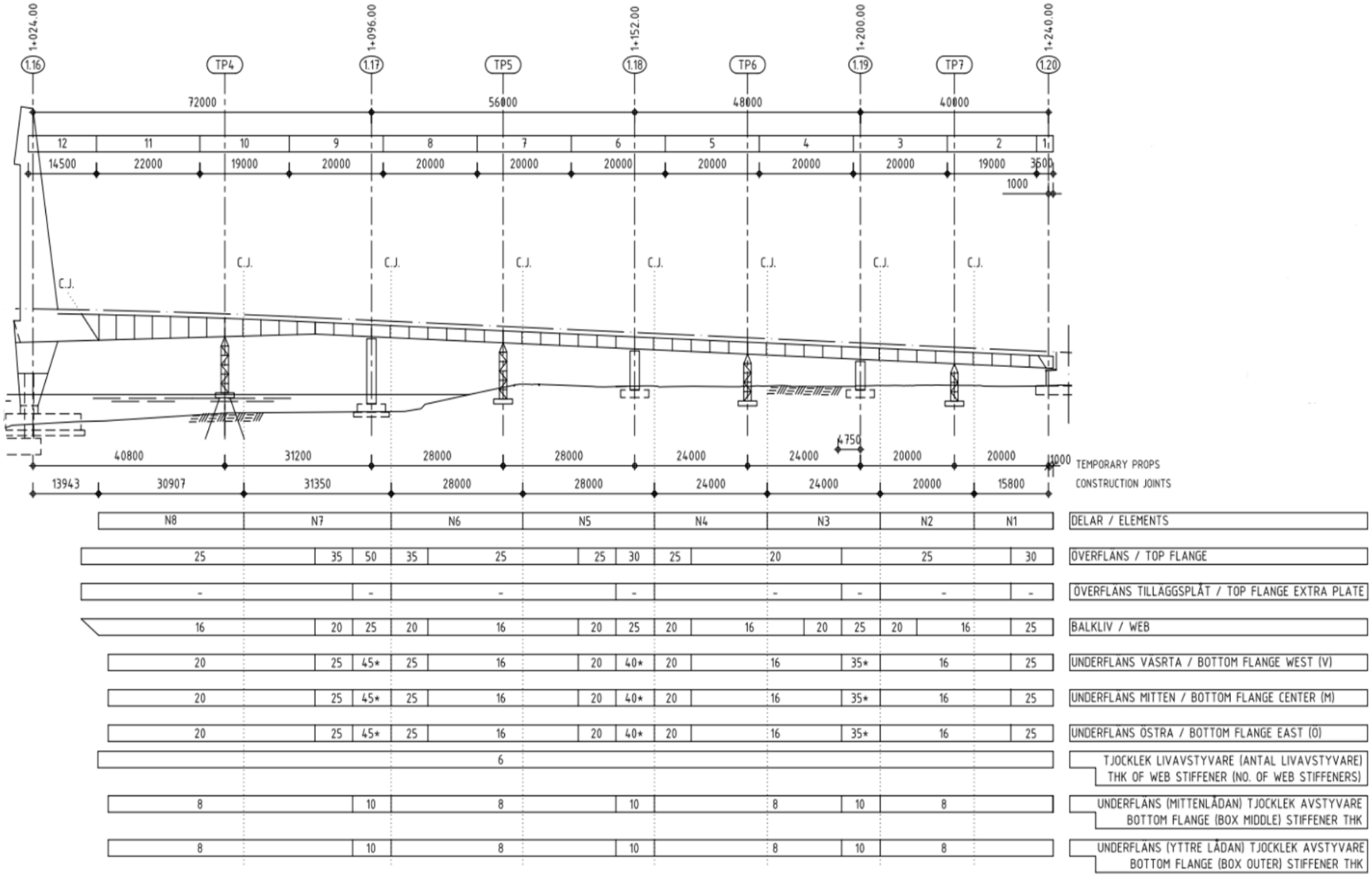

1+024.00
1+096.00
1+152.00
1+200.00
1+240.00
1.16
TP4
1.17
TP5
1.18
TP6
1.19
TP7
1.20
72000
56000
48000
40000
12
11
10
9
8
7
6
5
4
3
2
1
14500
22000
19000
20000
20000
20000
20000
20000
20000
20000
20000
19000
3600
1000
C.J.
4750
40800
31200
28000
28000
24000
24000
20000
20000
1000
TEMPORARY PROPS
13943
30907
31350
28000
28000
24000
24000
20000
15800
CONSTRUCTION JOINTS
N8
N7
N6
N5
N4
N3
N2
N1
DELAR / ELEMENTS
25
35
50
35
25
25
30
25
20
25
30
ÖVERFLÄNS / TOP FLANGE
ÖVERFLÄNS TILLÄGGSPLÅT / TOP FLANGE EXTRA PLATE
16
20
25
20
16
20
25
20
16
20
25
20
16
25
BALKLIV / WEB
20
25
45*
25
16
20
40*
20
16
35*
16
25
UNDERFLÄNS VÄSRTA / BOTTOM FLANGE WEST (V)
UNDERFLÄNS MITTEN / BOTTOM FLANGE CENTER (M)
UNDERFLÄNS ÖSTRA / BOTTOM FLANGE EAST (Ö)
6
TJOCKLEK LIVAVSTYVARE (ANTAL LIVAVSTYVARE)
THK OF WEB STIFFENER (NO. OF WEB STIFFENERS)
8
10
8
10
8
10
8
UNDERFLÄNS (MITTENLÅDAN) TJOCKLEK AVSTYVARE
BOTTOM FLANGE (BOX MIDDLE) STIFFENER THK
UNDERFLÄNS (YTTRE LÅDAN) TJOCKLEK AVSTYVARE
BOTTOM FLANGE (BOX OUTER) STIFFENER THK

B

Bottom Flange Buckling Capacity using Duplex Stainless Steel 1.4462

B- Bottom Flange Buckling Capacity using Duplex Stainless Steel 1.4462

In this calculation sheet we re-do the buckling check for bottom flange in a case of stainless steel 1.4462 instead of S355 steel, same thicknesses and stiffeners dimensions are used

Hollow Stiffeners:
The used stiffeners have the following dimensions:

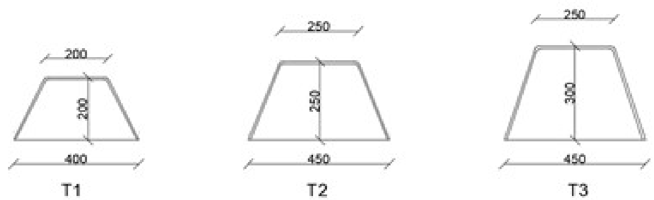

Stiffener T1:

This stiffener has two thicknesses 6, and 8 mm, dimensions as specified in the figure.

$t_1 := \begin{bmatrix} 6 \\ 8 \end{bmatrix} mm$ $\quad B_{bott1} := 400\ mm$ $\quad B_{top1} := 200\ mm$ $\quad H_1 := 200\ mm$

$R_1 := 20\ mm$ $\quad C_{top1} := 160\ mm$ $\quad C_{web1} := 199\ mm$ $\quad f_y := 460\ MPa$

$E := 200\ GPa$

According to EN- 1993-1-4 5.2.3. (1) for stainless steel, all regulations and formulas mentioned in EN 1993-1-5, 4.4 (1) to (5) for steel can be used simillarely for stainless-steel except som exceptions as shown in 5.2.3. (1).

Pure Compression $\quad \psi := 1$ $\quad K_\sigma := 4$

Each plate of the stiffener is checked seperately for buckling according to EN 1993-1-4(2)

$$\varepsilon := \sqrt{\frac{235\ MPa \cdot E}{f_y \cdot 210\ GPa}} = 0.698 \qquad \lambda_{ptop} := \frac{\dfrac{C_{top1}}{t_1}}{28.4 \cdot \varepsilon \cdot \sqrt{K_\sigma}} = \begin{bmatrix} 0.673 \\ 0.505 \end{bmatrix}$$

$i := 0..1$

$$\rho_{top_i} := \frac{0.772}{\lambda_{ptop_i}} - \frac{0.125}{\lambda_{ptop_i}^{\,2}}$$

$$\rho_{top_i} := \left\| \begin{array}{l} \text{if } \rho_{top_i} < 1 \\ \quad \| \rho_{top_i} \\ \text{else if } \rho_{top_i} \ge 1 \\ \quad \| 1 \end{array} \right. = \begin{bmatrix} 0.871 \\ 1 \end{bmatrix}$$

Cold formed or welded internal elements
EN 1993-1-4, 5.2.3 (5.1)

$$\lambda_{pweb} := \frac{\frac{C_{web1}}{t_1}}{28.4 \cdot \varepsilon \cdot \sqrt{K_\sigma}} = \begin{bmatrix} 0.837 \\ 0.628 \end{bmatrix} \qquad i := 0..1 \qquad \rho_{web_i} := \frac{0.772}{\lambda_{pweb_i}} - \frac{0.125}{\lambda_{pweb_i}^{\,2}} = \begin{bmatrix} 0.744 \\ 0.912 \end{bmatrix}$$

$$\rho_{web_i} := \left\| \begin{array}{l} \text{if } \rho_{web_i} < 1 \\ \quad \| \rho_{web_i} \\ \text{else if } \rho_{web_i} \ge 1 \\ \quad \| 1 \end{array} \right. = \begin{bmatrix} 0.744 \\ 0.912 \end{bmatrix}$$

$$\rho_{t1} := \begin{bmatrix} \left\| \begin{array}{l} \text{if } \rho_{web_0} < \rho_{top_0} \\ \quad \| \rho_{web_0} \\ \text{else} \\ \quad \| \rho_{top_0} \end{array} \right. \\ \left\| \begin{array}{l} \text{if } \rho_{web_1} < \rho_{top_1} \\ \quad \| \rho_{web_1} \\ \text{else} \\ \quad \| \rho_{top_1} \end{array} \right. \end{bmatrix} = \begin{bmatrix} 0.744 \\ 0.912 \end{bmatrix}$$

$$\sigma_{Rd.loca.1} := \rho_{t1} \cdot f_y = \begin{bmatrix} 342.161 \\ 419.747 \end{bmatrix} \mathbf{MPa}$$

$\lambda_{m1} := 1$ TSFS 2018:57. 18 KAP

Stiffener T2:

This stiffener has three thicknesses 6, 8, and 10 mm, dimensions as specified in the figure.

$t_2 := \begin{bmatrix} 6 \\ 7 \\ 8 \\ 10 \end{bmatrix} \mathbf{mm}$ $\quad B_{bott2} := 450\ \mathbf{mm}$ $\quad B_{top2} := 250\ \mathbf{mm}$ $\quad H_2 := 250\ \mathbf{mm}$

$R_2 := 20\ \mathbf{mm}$ $\quad C_{top2} := 210\ \mathbf{mm}$ $\quad C_{web2} := 244\ \mathbf{mm}$ $\quad f_y := 460\ \mathbf{MPa}$

Pure Compression $\quad \psi := 1$ $\quad K_\sigma := 4$

Each plate of the stiffener is checked seperately for buckling according to EN 1993-1-4(2)

$$\varepsilon := \sqrt{\frac{235\ MPa \cdot E}{f_y \cdot 210\ GPa}} = 0.698$$

$$\lambda_{ptop} := \frac{\frac{C_{top2}}{t_2}}{28.4 \cdot \varepsilon \cdot \sqrt{K_\sigma}} = \begin{bmatrix} 0.883 \\ 0.757 \\ 0.663 \\ 0.53 \end{bmatrix}$$

$$i := 0..3$$

$$\rho_{top_i} := \frac{0.772}{\lambda_{ptop_i}} - \frac{0.125}{\lambda_{ptop_i}^{\ 2}}$$

$$\rho_{top_i} := \begin{Vmatrix} \text{if } \rho_{top_i} < 1 \\ \quad \Vert\ \rho_{top_i} \\ \text{else if } \rho_{top_i} \geq 1 \\ \quad \Vert\ 1 \end{Vmatrix} = \begin{bmatrix} 0.714 \\ 0.802 \\ 0.88 \\ 1 \end{bmatrix}$$

Cold formed or welded internal elements EN 1993-1-4, 5.2.3 (5.1)

$$\lambda_{pweb} := \frac{\frac{C_{web2}}{t_2}}{28.4 \cdot \varepsilon \cdot \sqrt{K_\sigma}} = \begin{bmatrix} 1.026 \\ 0.88 \\ 0.77 \\ 0.616 \end{bmatrix}$$

$$i := 0..3$$

$$\rho_{web_i} := \frac{0.772}{\lambda_{pweb_i}} - \frac{0.125}{\lambda_{pweb_i}^{\ 2}} = \begin{bmatrix} 0.633 \\ 0.716 \\ 0.792 \\ 0.924 \end{bmatrix}$$

$$\rho_{web_i} := \begin{Vmatrix} \text{if } \rho_{web_i} < 1 \\ \quad \Vert\ \rho_{web_i} \\ \text{else if } \rho_{web_i} \geq 1 \\ \quad \Vert\ 1 \end{Vmatrix} = \begin{bmatrix} 0.633 \\ 0.716 \\ 0.792 \\ 0.924 \end{bmatrix}$$

$$\rho_{t2} := \begin{bmatrix} \begin{Vmatrix} \text{if } \rho_{web_0} < \rho_{top_0} \\ \quad \Vert\ \rho_{web_0} \\ \text{else} \\ \quad \Vert\ \rho_{top_0} \end{Vmatrix} \\ \begin{Vmatrix} \text{if } \rho_{web_1} < \rho_{top_1} \\ \quad \Vert\ \rho_{web_1} \\ \text{else} \\ \quad \Vert\ \rho_{top_1} \end{Vmatrix} \\ \begin{Vmatrix} \text{if } \rho_{web_2} < \rho_{top_2} \\ \quad \Vert\ \rho_{web_2} \\ \text{else} \\ \quad \Vert\ \rho_{top_2} \end{Vmatrix} \\ \begin{Vmatrix} \text{if } \rho_{web_3} < \rho_{top_3} \\ \quad \Vert\ \rho_{web_3} \\ \text{else} \\ \quad \Vert\ \rho_{top_3} \end{Vmatrix} \end{bmatrix} = \begin{bmatrix} 0.633 \\ 0.716 \\ 0.792 \\ 0.924 \end{bmatrix}$$

$$\sigma_{Rd.loca.2} := \rho_{t2} \cdot f_y = \begin{bmatrix} 291.399 \\ 329.353 \\ 364.275 \\ 425.023 \end{bmatrix} MPa$$

$\lambda_{m1} := 1$ TSFS 2018:57. 18 KAP

Stiffener T3:

This stiffener has four thicknesses 6, 8, 10, and 12 mm, dimensions as specified in the figure.

$t_3 := \begin{bmatrix} 6 \\ 8 \\ 10 \\ 12 \end{bmatrix} mm$ $\quad B_{bott3} := 450\ mm$ $\quad B_{top3} := 250\ mm$ $\quad H_3 := 300\ mm$

$R_3 := 20\ mm$ $\quad C_{top3} := 210\ mm$ $\quad C_{web3} := 291\ mm$ $\quad f_y := 460\ MPa$

Pure Compression $\quad \psi := 1$ $\quad K_\sigma := 4$

$$\lambda_{ptop} := \frac{\dfrac{C_{top3}}{t_3}}{28.4 \cdot \varepsilon \cdot \sqrt{K_\sigma}} = \begin{bmatrix} 0.883 \\ 0.663 \\ 0.53 \\ 0.442 \end{bmatrix} \qquad i := 0 .. 3$$

$$\rho_{top_i} := \frac{0.772}{\lambda_{ptop_i}} - \frac{0.125}{\lambda_{ptop_i}^{\ 2}}$$

$$\rho_{top_i} := \left\| \begin{array}{l} \text{if } \rho_{top_i} < 1 \\ \quad \left\| \rho_{top_i} \right. \\ \text{else if } \rho_{top_i} \geq 1 \\ \quad \left\| 1 \right. \end{array} \right. = \begin{bmatrix} 0.714 \\ 0.88 \\ 1 \\ 1 \end{bmatrix}$$

Cold formed or welded internal elements
EN 1993-1-4, 5.2.3 (5.1)

$$\lambda_{pweb} := \frac{\frac{C_{web3}}{t_3}}{28.4 \cdot \varepsilon \cdot \sqrt{K_\sigma}} = \begin{bmatrix} 1.224 \\ 0.918 \\ 0.734 \\ 0.612 \end{bmatrix} \qquad i := 0..3$$

$$\rho_{web_i} := \frac{0.772}{\lambda_{pweb_i}} - \frac{0.125}{\lambda_{pweb_i}^{\ 2}} = \begin{bmatrix} 0.547 \\ 0.693 \\ 0.819 \\ 0.928 \end{bmatrix}$$

$$\rho_{web_i} := \left\| \begin{array}{l} \text{if } \rho_{web_i} < 1 \\ \quad \left\| \rho_{web_i} \right. \\ \text{else if } \rho_{web_i} \geq 1 \\ \quad \left\| 1 \right. \end{array} \right. = \begin{bmatrix} 0.547 \\ 0.693 \\ 0.819 \\ 0.928 \end{bmatrix}$$

$$\rho_{t3} := \begin{bmatrix} \left\| \begin{array}{l} \text{if } \rho_{web_0} < \rho_{top_0} \\ \quad \left\| \rho_{web_0} \right. \\ \text{else} \\ \quad \left\| \rho_{top_0} \right. \end{array} \right. \\ \left\| \begin{array}{l} \text{if } \rho_{web_1} < \rho_{top_1} \\ \quad \left\| \rho_{web_1} \right. \\ \text{else} \\ \quad \left\| \rho_{top_1} \right. \end{array} \right. \\ \left\| \begin{array}{l} \text{if } \rho_{web_2} < \rho_{top_2} \\ \quad \left\| \rho_{web_2} \right. \\ \text{else} \\ \quad \left\| \rho_{top_2} \right. \end{array} \right. \\ \left\| \begin{array}{l} \text{if } \rho_{web_3} < \rho_{top_3} \\ \quad \left\| \rho_{web_3} \right. \\ \text{else} \\ \quad \left\| \rho_{top_3} \right. \end{array} \right. \end{bmatrix} = \begin{bmatrix} 0.547 \\ 0.693 \\ 0.819 \\ 0.928 \end{bmatrix}$$

$$\sigma_{Rd.loca.3} := \rho_{t3} \cdot f_y = \begin{bmatrix} 251.725 \\ 318.58 \\ 376.908 \\ 426.709 \end{bmatrix} \boldsymbol{MPa}$$

$\lambda_{m1} := 1$ TSFS 2018:57. 18 KAP

Single Panel Buckling of bottom plate/North Side b=4m

t(mm)	ƒyk(MPa	BBott (mm)	B/t	ε	Kσ	λp	ρ	ρ	σRd,local	η	(52/η)ε	ed to ch	kt	σE	tcr	λw	0.6/η	χw	tRd	σEd,local	η1	η3	Interaction
12	460	663	55.3	0.698	4	1.4	0.49	0.49	225	1.200	30	1	5.45	62	339	0.885	0.50	0.77	204	225	0.49	0.24	η3≤0.5
14	460	663	47.4	0.698	4	1.2	0.56	0.56	257	1.200	30	1	5.45	85	462	0.759	0.50	0.87	230	257	0.56	0.22	η3≤0.5
15	460	663	44.2	0.698	4	1.1	0.59	0.59	272	1.200	30	1	5.45	97	530	0.708	0.50	0.91	243	272	0.59	0.21	η3≤0.5
16	460	663	41.4	0.698	4	1.0	0.62	0.62	287	1.200	30	1	5.45	111	603	0.664	0.50	0.96	255	287	0.62	0.20	η3≤0.5
18	460	663	36.8	0.698	4	0.9	0.69	0.69	315	1.200	30	1	5.45	140	763	0.590	0.50	1.05	279	315	0.69	0.18	η3≤0.5
20	460	663	33.2	0.698	4	0.8	0.74	0.74	342	1.200	30	1	5.45	173	942	0.531	0.50	1.14	302	342	0.74	0.17	η3≤0.5
22	460	663	30.1	0.698	4	0.8	0.80	0.80	367	1.200	30	0	5.45	209	1140	0.483	0.50	1.20	319	367	0.80	0.16	η3≤0.5
24	460	663	27.6	0.698	4	0.7	0.85	0.85	391	1.200	30	0	5.45	249	1357	0.443	0.50	1.20	319	391	0.85	0.16	η3≤0.5
25	460	663	26.5	0.698	4	0.7	0.87	0.87	402	1.200	30	0	5.45	270	1472	0.425	0.50	1.20	319	402	0.87	0.16	η3≤0.5
26	460	663	25.5	0.698	4	0.6	0.90	0.90	413	1.200	30	0	5.45	292	1592	0.408	0.50	1.20	319	413	0.90	0.16	η3≤0.5
28	460	663	23.7	0.698	4	0.6	0.94	0.94	433	1.200	30	0	5.45	339	1847	0.379	0.50	1.20	319	433	0.94	0.16	η3≤0.5
30	460	663	22.1	0.698	4	0.6	0.98	0.98	452	1.200	30	0	5.45	389	2120	0.354	0.50	1.20	319	452	0.98	0.16	η3≤0.5
32	460	663	20.7	0.698	4	0.5	1.02	1.00	460	1.200	30	0	5.45	443	2412	0.332	0.50	1.20	319	460	1.00	0.16	η3≤0.5
35	460	663	18.9	0.698	4	0.5	1.07	1.00	460	1.200	30	0	5.45	529	2886	0.303	0.50	1.20	319	460	1.00	0.16	η3≤0.5
38	460	663	17.4	0.698	4	0.4	1.11	1.00	460	1.200	30	0	5.45	624	3402	0.279	0.50	1.20	319	460	1.00	0.16	η3≤0.5
40	460	663	16.6	0.698	4	0.4	1.13	1.00	460	1.200	30	0	5.45	692	3769	0.266	0.50	1.20	319	460	1.00	0.16	η3≤0.5
42	460	663	15.8	0.698	4	0.4	1.15	1.00	460	1.200	30	0	5.45	762	4155	0.253	0.50	1.20	319	460	1.00	0.16	η3≤0.5
45	460	663	14.7	0.698	4	0.4	1.17	1.00	460	1.200	30	0	5.45	875	4770	0.236	0.50	1.20	319	460	1.00	0.16	η3≤0.5
48	460	663	13.8	0.698	4	0.3	1.19	1.00	460	1.200	30	0	5.45	996	5427	0.221	0.50	1.20	319	460	1.00	0.16	η3≤0.5
50	460	663	13.3	0.698	4	0.3	1.19	1.00	460	1.200	30	0	5.45	1081	5889	0.212	0.50	1.20	319	460	1.00	0.16	η3≤0.5
55	460	663	12.1	0.698	4	0.3	1.19	1.00	460	1.200	30	0	5.45	1308	7126	0.193	0.50	1.20	319	460	1.00	0.16	η3≤0.5
60	460	663	11.1	0.698	4	0.3	1.16	1.00	460	1.200	30	0	5.45	1556	8480	0.177	0.50	1.20	319	460	1.00	0.16	η3≤0.5
63	460	663	10.5	0.698	4	0.3	1.13	1.00	460	1.200	30	0	5.45	1716	9350	0.169	0.50	1.20	319	460	1.00	0.16	η3≤0.5
65	460	663	10.2	0.698	4	0.3	1.11	1.00	460	1.200	30	0	5.45	1826	9953	0.163	0.50	1.20	319	460	1.00	0.16	η3≤0.5
70	460	663	9.5	0.698	4	0.2	1.04	1.00	460	1.200	30	0	5.45	2118	11543	0.152	0.50	1.20	319	460	1.00	0.16	η3≤0.5
80	460	663	8.3	0.698	4	0.2	0.83	0.83	384	1.200	30	0	5.45	2766	15076	0.133	0.50	1.20	319	384	0.83	0.16	η3≤0.5

Global Stability of bottom flange:

The lower flange consists of three stiffeners welded on a bottom plate. The steel panel is considered as flanges to the stiffeners, and the effective length will be calculated according to EN 1993-1-5. 4.5.

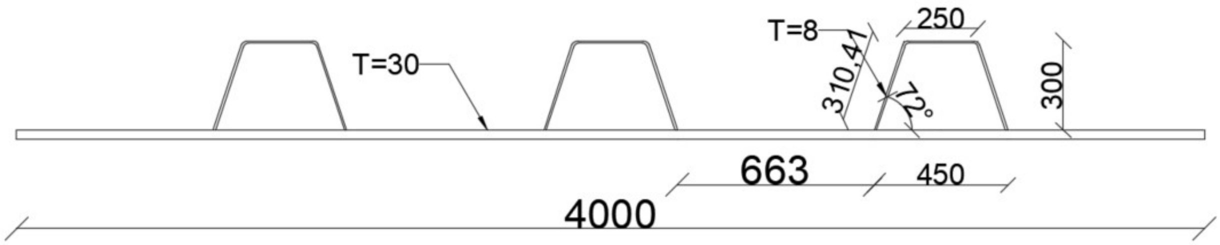

In order to find the effective width of the plate that is forming the stiffener flanges eq 3.3 EN 1993-1-5 is used. In EN 1993-1-4, 5.2.4. the effect of shear lag can be taken according to eq 3.3 EN 1993-1-5 .

$A_{eff} = A_{c.eff} \cdot \beta_{ult}$ $\qquad L_e := 0.7 \cdot 4000\ mm = 2.8\ m$

$\alpha_0 = \sqrt{\frac{A_{ceff}}{b_0 . t_f}} = 1 \qquad \alpha_0 := 1$ $\qquad$ From single plate buckling no reduction occured and $\rho = 1$

Inside stiffener $\quad b_0 := \frac{450\ mm}{2} = 225\ mm \qquad \kappa := \frac{\alpha_0 \cdot b_0}{L_e} = 0.08 \qquad \beta_{ult} := \frac{1}{1 + 6.4 \cdot \kappa^2} = 0.96$

$b_{eff} := \beta_{ult} \cdot b_0 = 216.071\ mm$

North bridge plate flange $\quad b_0 := \frac{663\ mm}{2} = 331.5\ mm \qquad \kappa := \frac{\alpha_0 \cdot b_0}{L_e} = 0.118 \qquad \beta_{ult} := \frac{1}{1 + 6.4 \cdot \kappa^2} = 0.918$

$b_{eff} := \beta_{ult} \cdot b_0 = 304.21\ mm$

Top flange $\quad b_0 := \frac{250\ mm}{2} = 125\ mm \qquad \kappa := \frac{\alpha_0 \cdot b_0}{L_e} = 0.045 \qquad \beta_{ult} := \frac{1}{1 + 6.4 \cdot \kappa^2} = 0.987$

$b_{eff} := 2 \cdot \beta_{ult} \cdot b_0 = 246.851\ mm \qquad b_{eff} := 250\ mm$

Considering Northern side only

$b_{eff} := 1040\ mm$ $f_{y.30} := 460\ MPa$ $f_{y.8} := 460\ MPa$ $t_p := 30\ mm$ $t_s := 8\ mm$

Cross section class for the plate:

$$\frac{663\ mm}{t_p} = 22.1 \qquad \varepsilon = 0.698 \qquad 30.7 \cdot \varepsilon = 21.414$$

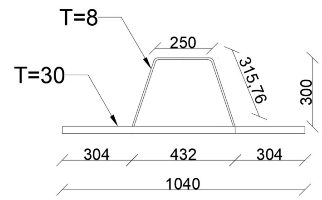

Class 4

Reduction is needed. But according to the upper calculation for single plate no reduction is needed up to $\sigma_{Rd} := 452\ MPa$

Cross section class for the stiffener:

Inclined web:

$$B := \frac{316\ mm - 5\ mm - 20\ mm}{8} = 36.375\ mm \qquad 30.7 \cdot \varepsilon = 21.414 \qquad \text{Class 4}$$

Reduction is needed. According to the upper calculation for stiffeners noreduction is needed up to $\sigma_{Rd} := 318\ MPa$

Section properties:
Stiffener only:

$t_p := 30\ mm$ $l_p := 1040\ mm$ $S_w := 316\ mm$ $Z_s := 300\ mm$
$S_t := 250\ mm$ $t_s := 8\ mm$

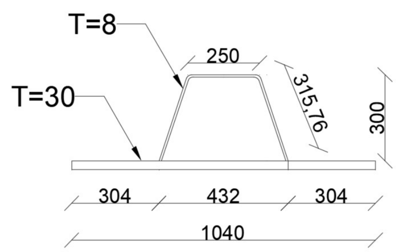

$$A_{st.0} := 2 \cdot S_w \cdot t_s + S_t \cdot t_s = \left(7.056 \cdot 10^{3}\right)\ mm^2$$

$$Z_0 := \frac{2 \cdot S_w \cdot t_s \cdot \dfrac{Z_s}{2} + S_t \cdot t_s \cdot \left(Z_s - \dfrac{t_s}{2}\right)}{A_{st.0}} = 191.383\ mm$$

$$I_{st.0} := S_t \cdot t_s \left(Z_s - \frac{t_s}{2} - Z_0\right)^2 + S_w \cdot 2 \cdot t_s \cdot \left(\frac{Z_s}{2} - Z_0\right)^2 + 2 \cdot \frac{t_s \cdot \left(Z_s\right)^3}{12} = \left(6.655 \cdot 10^{7}\right)\ mm^4$$

$$I_{st.0} = \left(6.655 \cdot 10^{-5}\right)\ m^4$$

Stiffener with the plate:

$$A_{st.1} := l_p \cdot t_p + 2 \cdot S_w \cdot t_s + S_t \cdot t_s = \left(3.826 \cdot 10^{4}\right)\ mm^2$$

$$Z_0 := \frac{l_p \cdot t_p \cdot \dfrac{t_p}{2} + 2 \cdot S_w \cdot t_s \cdot \left(\dfrac{t_s}{2} + t_p\right) + S_t \cdot t_s \cdot \left(Z_s - \dfrac{t_s}{2} + t_p\right)}{A_{st.1}} = 33.77\ mm$$

$$I_{st.1} := S_t \cdot t_s \cdot \left(Z_s + t_p - \frac{t_s}{2} - Z_0\right)^2 + 2 \cdot S_w \cdot t_s \cdot \left(\frac{Z_s}{2} + t_p - Z_0\right)^2 + l_p \cdot t_p \cdot \left(Z_0 - \frac{t_p}{2}\right)^2 + 2 \cdot \frac{t_s \cdot (Z_s)^3}{12} + \frac{l_p \cdot {t_p}^3}{12}$$

$$I_{st.1} = \left(3.282 \cdot 10^8\right)\ mm^4$$

Plate type buckling

$t := 3\ cm$ $\quad b := 400\ cm$ $\quad a := 400\ cm$ $\quad \psi := 1$ $\quad E := 200\ GPa$

$\beta := 1$ No local plate buckling is allowed

$$\sigma_E := 190000\ MPa \cdot \left(\frac{t}{b}\right)^2 = 10.688\ MPa \qquad \delta := \frac{3 \cdot A_{st.0}}{b \cdot t} = 0.176$$

$$\alpha := \frac{a}{b} = 1 \qquad I_p := \frac{b \cdot t^3}{10.92} = \left(9.89 \cdot 10^{-6}\right)\ m^4 \qquad \gamma := \frac{3 \cdot I_{st.1}}{I_p} = 99.567$$

$$\sqrt[4]{\gamma} = 3.159 \qquad \alpha < \sqrt[4]{\gamma}$$

$$K_{\sigma.p} := \frac{2 \cdot \left(\left(1+\alpha^2\right)^2 + \gamma - 1\right)}{\alpha^2\ (\psi+1)\ (1+\delta)} = 87.187 \qquad \sigma_{cr.p} := K_{\sigma.p} \cdot \sigma_E = 931.812\ MPa$$

$$\lambda_P := \sqrt{\frac{\beta \cdot f_{y.30}}{\sigma_{cr.p}}} = 0.703$$

Reduction using EN 1993-1-4, 5.2.3 $\qquad \rho := \frac{0.772}{\lambda_P} - \frac{0.125}{{\lambda_P}^2} = 0.846$

Column type buckling

$$\sigma_{cr.c} := \frac{\pi^2 \cdot E \cdot I_{st.1}}{A_{st.1} \cdot a^2} = \left(1.059 \cdot 10^3\right)\ MPa$$

$$\lambda_c := \sqrt{\frac{f_{y.30}}{\sigma_{cr.c}}} = 0.659$$

Reduction using EN 1993-1-4, 5.4.2

EN 1993-1-4 table 5.3: A1.17.2017 Table 6.1

$$\alpha := 0.49 \qquad \lambda_0 := 0.2 \qquad \phi := 0.5 \cdot \left(1 + \alpha \cdot \left(\lambda_c - \lambda_0\right) + {\lambda_c}^2\right) = 0.83$$

$$\chi_c := \frac{1}{\phi + \left(\phi^2 - {\lambda_c}^2\right)^{0.5}} = 0.75$$

$$\xi := \frac{\sigma_{cr.p}}{\sigma_{cr.c}} - 1 = -0.12$$

smaller than one, this means that the column type buckling is govering

$$\rho_c := \chi_c = 0.75 \qquad \sigma_{Rd} := \rho_c \cdot \frac{f_{y.30}}{1} = 344.89\ MPa$$

North Side Bottom flange with stiffeners t=8 mm																																
a mm	B mm	tmm	fyk	∑ Asl mm^2	Ist (mm^4)	Zstiff(m	Ast.1	Xc	Isl	Ap	Ip	δ	γ	(γ)^0.25	α	Kσ	σE	σcr,p	λp	ρp	σcr,c	λc	λ0	α	ϕ	χ	ξ	ρc	λM1	σRd, Global	σRd, local	σRd, min
4000	4000	12	460	21168	66550000	191.4	19536	40	272393926	48000	632967	0.4	1291	6	1	898	2	1536	0.5	0.99	1718	0.5	0.2	0.5	0.7	0.8	-0.1	0.8	1	383	225	225
4000	4000	14	460	21168	66550000	191.4	21616	38	281145071	56000	1005128	0.4	839	5	1	611	2	1422	0.6	0.97	1603	0.5	0.2	0.5	0.7	0.8	-0.1	0.8	1	378	257	257
4000	4000	15	460	21168	66550000	191.4	22656	37	285114002	60000	1236264	0.4	692	5	1	514	3	1372	0.6	0.96	1551	0.5	0.2	0.5	0.7	0.8	-0.1	0.8	1	376	272	272
4000	4000	16	460	21168	66550000	191.4	23696	36	288860049	64000	1500366	0.3	578	5	1	436	3	1326	0.6	0.95	1502	0.6	0.2	0.5	0.7	0.8	-0.1	0.8	1	374	287	287
4000	4000	18	460	21168	66550000	191.4	25776	35	295793117	72000	2136264	0.3	415	5	1	323	4	1244	0.6	0.93	1414	0.6	0.2	0.5	0.8	0.8	-0.1	0.8	1	369	315	315
4000	4000	20	460	21168	66550000	191.4	27856	35	302122591	80000	2930403	0.3	309	4	1	247	5	1173	0.6	0.91	1337	0.6	0.2	0.5	0.8	0.8	-0.1	0.8	1	365	342	342
4000	4000	22	460	21168	66550000	191.4	29936	34	307977229	88000	3900366	0.2	237	4	1	193	6	1111	0.6	0.90	1268	0.6	0.2	0.5	0.8	0.8	-0.1	0.8	1	361	367	361
4000	4000	24	460	21168	66550000	191.4	32016	34	313452328	96000	5063736	0.2	186	4	1	155	7	1058	0.7	0.88	1207	0.6	0.2	0.5	0.8	0.8	-0.1	0.8	1	357	391	357
4000	4000	25	460	21168	66550000	191.4	33056	34	316070772	100000	5723443	0.2	166	4	1	139	7	1033	0.7	0.88	1178	0.6	0.2	0.5	0.8	0.8	-0.1	0.8	1	354	402	354
4000	4000	26	460	21168	66550000	191.4	34096	34	318619931	104000	6438095	0.2	148	3	1	126	8	1010	0.7	0.87	1152	0.6	0.2	0.5	0.8	0.8	-0.1	0.8	1	352	413	352
4000	4000	28	460	21168	66550000	191.4	36176	34	323535513	112000	8041026	0.2	121	3	1	104	9	969	0.7	0.86	1102	0.6	0.2	0.5	0.8	0.8	-0.1	0.8	1	349	433	349
4000	4000	30	460	21168	66550000	191.4	38256	34	328242482	120000	9890110	0.2	100	3	1	87	11	932	0.7	0.85	1057	0.7	0.2	0.5	0.8	0.7	-0.1	0.7	1	345	452	345
4000	4000	32	460	21168	66550000	191.4	40336	34	332775295	128000	1.2E+07	0.2	83	3	1	74	12	899	0.7	0.84	1017	0.7	0.2	0.5	0.8	0.7	-0.1	0.7	1	341	460	341
4000	4000	35	460	21168	66550000	191.4	43456	34	339307108	140000	1.6E+07	0.2	65	3	1	59	15	857	0.7	0.82	962	0.7	0.2	0.5	0.9	0.7	-0.1	0.7	1	336	460	336
4000	4000	38	460	21168	66550000	191.4	46576	35	345581026	152000	2E+07	0.1	52	3	1	48	17	822	0.7	0.81	914	0.7	0.2	0.5	0.9	0.7	-0.1	0.7	1	331	460	331
4000	4000	40	460	21168	66550000	191.4	48656	35	349647879	160000	2.3E+07	0.1	45	3	1	42	19	801	0.8	0.80	886	0.7	0.2	0.5	0.9	0.7	-0.1	0.7	1	327	460	327
4000	4000	42	460	21168	66550000	191.4	50736	36	353637437	168000	2.7E+07	0.1	39	3	1	37	21	783	0.8	0.79	859	0.7	0.2	0.5	0.9	0.7	-0.1	0.7	1	324	460	324
4000	4000	45	460	21168	66550000	191.4	53856	37	359500016	180000	3.3E+07	0.1	32	2	1	32	24	760	0.8	0.79	823	0.7	0.2	0.5	0.9	0.7	-0.1	0.7	1	320	460	320
4000	4000	48	460	21168	66550000	191.4	56976	38	365242456	192000	4.1E+07	0.1	27	2	1	27	27	740	0.8	0.78	790	0.8	0.2	0.5	0.9	0.7	-0.1	0.7	1	315	460	315
4000	4000	50	460	21168	66550000	191.4	59056	38	369015894	200000	4.6E+07	0.1	24	2	1	25	30	730	0.8	0.77	770	0.8	0.2	0.5	0.9	0.7	-0.1	0.7	1	312	460	312
4000	4000	55	460	21168	66550000	191.4	64256	40	378298561	220000	6.1E+07	0.1	19	2	1	20	36	709	0.8	0.77	726	0.8	0.2	0.5	1.0	0.7	0.0	0.7	1	306	460	306
4000	4000	60	460	21168	66550000	191.4	69456	42	387420209	240000	7.9E+07	0.1	15	2	1	16	43	695	0.8	0.76	687	0.8	0.2	0.5	1.0	0.7	0.0	0.7	1	300	460	300
4000	4000	63	460	21168	66550000	191.4	72576	43	392838193	252000	9.2E+07	0.1	13	2	1	15	47	690	0.8	0.76	667	0.8	0.2	0.5	1.0	0.6	0.0	0.7	1	299	460	299
4000	4000	65	460	21168	66550000	191.4	74656	44	396432913	260000	1E+08	0.1	12	2	1	14	50	688	0.8	0.76	654	0.8	0.2	0.5	1.0	0.6	0.1	0.6	1	299	460	299
4000	4000	70	460	21168	66550000	191.4	79856	46	405375186	280000	1.3E+08	0.1	10	2	1	12	58	686	0.8	0.76	626	0.9	0.2	0.5	1.0	0.6	0.1	0.7	1	299	460	299
4000	4000	80	460	21168	66550000	191.4	90256	50	423158109	320000	1.9E+08	0.1	7	2	1	9	76	696	0.8	0.76	578	0.9	0.2	0.5	1.1	0.6	0.2	0.7	1	305	384	305

Comparison Between S355 and 1.4462:

In order to compare S355 and 1.4462 all stresses in ULS Bottom flange are registered in a separate excel sheet using D 5.2.6 and is compared with local, global, and stiffeners capacities. as shown in the following Excel table:

Bottom plate ULSB Longitudinal stresses																						
			Box position						S355							1.4462						
Coordinates (m)	Plates thickness	Box #	NÖ		NM		NV		yield strength		Plate Buckling strength		Stiffeners strength		Min σ	yield strength		uckling strength Plat		Stiffeners strength		Min σ
			Tension	Compress	Tension	Compress	Tension	Compress			Local	Global	8 mm	10 mm				Local	Global	T 3, 8 mm	T3, 10 mm	
1100	45&25	7&6	-25	-245	-25	-270	-33	-268	335	-335	-335	-250	-325		-250	460	-460	-402	-320	-318.6		-318.6
1105	25	6	48	-179	30	-197	31	-179	345	-345	-299	-281	-325		-281	460	-460	-402	-354	-318.6		-318.6
1108	25&16	6	114	-169	106	-158	94	-150	355	-355	-299	-299	-325		-299	460	-460	-287	-354	-318.6		-287
1121	16	6	161	-67	150	-52	151	-43	355	-355	-299	-299	-325		-299	460	-460	-287	-374	-318.6		-287
1130	16	5	213	-43	200	-27	201	-21	355	-355	-299	-299	-325		-299	460	-460	-287	-374	-318.6		-287
1134	16	5	166	-65	166	-43	145	-39	355	-355	-299	-299	-325		-299	460	-460	-287	-374	-318.6		-287
1140	16&20	5	153	-117	149	-105	143	-109	345	-345	-299	-299	-325		-299	460	-460	-287	-365	-318.6		-287
1148	20&40	5	28	-201	33	-223	23	-228	345	-345	-333	-261	-325		-261	460	-460	-342	-327	-318.6		-318.6
1156	40&20	5&4	39	-201	39	-190	43	-205	345	-345	-333	-261		-355	-261	460	-460	-342	-327		-377	-327
1162	20	4	79	-106	70	-105	65	-112	345	-345	-333	-289	-325		-289	460	-460	-342	-365	-318.6		-318.6
1166	20&16	4	128	-87	126	-65	121	-74	345	-345	-299	-289	-325		-289	460	-460	-342	-365	-318.6		-318.6
1170	16	4	157	-64	145	-59	148	-69	355	-355	-299	-299	-325		-299	460	-460	-287	-374	-318.6		-287
1176	16	4	162	-56	156	-52	154	-61	355	-355	-299	-299	-325		-299	460	-460	-287	-374	-318.6		-287
1180	16	4&3	163	-51	157	-45	154	-53	355	-355	-299	-299	-325		-299	460	-460	-287	-374	-318.6		-287
1186	16	3	109	-65	109	-56	93	-65	355	-355	-299	-299	-325		-299	460	-460	-287	-374	-318.6		-287
1190	16	3	74	-82	74	-91	81	-78	355	-355	-299	-299	-325		-299	460	-460	-287	-374	-318.6		-287
1196	16&35	3	41	-174	45	-209	35	-183	345	-345	-299	-267	-325		-267	460	-460	-287	-336	-318.6		-287
1204	35&16	3&2	54	-169	57	-175	48	-175	345	-345	-299	-267		-355	-267	460	-460	-287	-336		-377	-287
1210	16	2	116	-98	109	-97	108	-94	355	-355	-299	-299	-325		-299	460	-460	-287	-374	-318.6		-287
1212	16	2	77	-34	69	-39	77	-28	355	-355	-299	-299	-325		-299	460	-460	-287	-374	-318.6		-287
1220	16	2	136	-4	137	-3	139	-5	355	-355	-299	-299	-325		-299	460	-460	-287	-374	-318.6		-287
1226	16	1	201	15	196	19	190	20	355	-355	-299	-299	-325		-299	460	-460	-287	-374	-318.6		-287
1232	16&25	1	173	34	173	34	165	38	345	-345	-299	-281	-325		-281	460	-460	-287	-354	-318.6		-287

By plotting all of these values we get the following results:

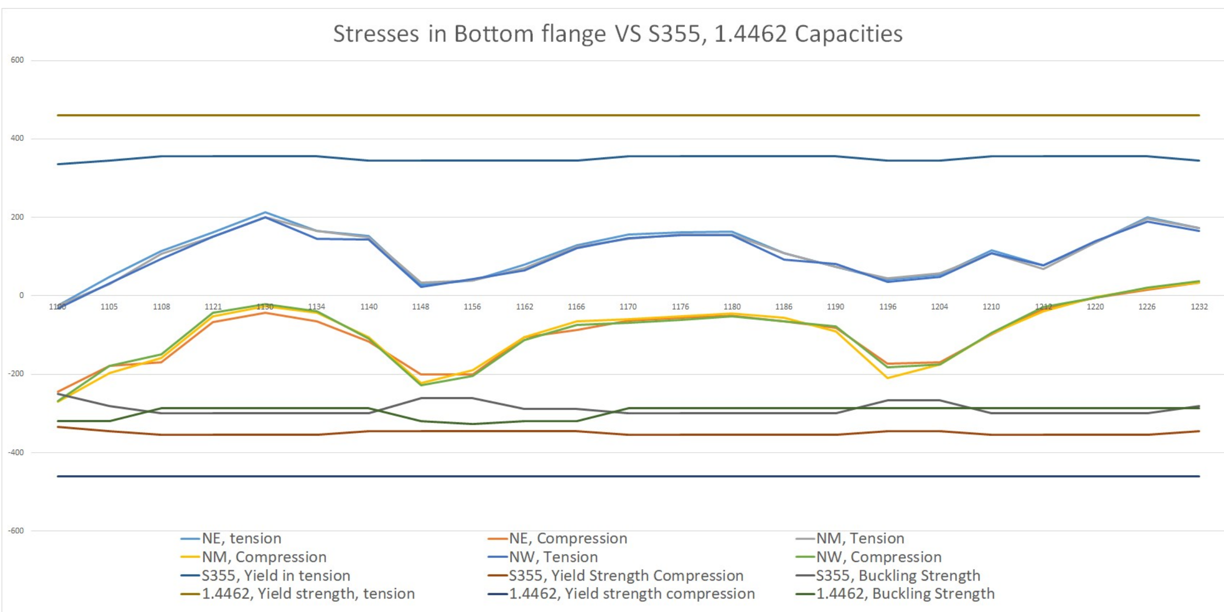

According to the previous plot, it is obvious that using 1.4462 instead of S355 in bottom flange with the same cross section will not increase the capacity of the bottom flange even though 1.4462 has higher yielding strength than S355. This is due to the fact that stainless-steel is more susceptible to buckling than conventional carbon steel.

Plated stainless-steel need to be designed and in an efficient way in order to get the benefit of the higher yield strength.

Bottom Flange, new geometry

In order to increase the capacity of the bottom flange the geometry is edited a little bit to by using 4 stiffeners type T2 with 7mm instead of three type T3 with 8mm, this change will decrease the cross sectional area of the whloe section.

$A_{old.st} := 20880\ mm^2$

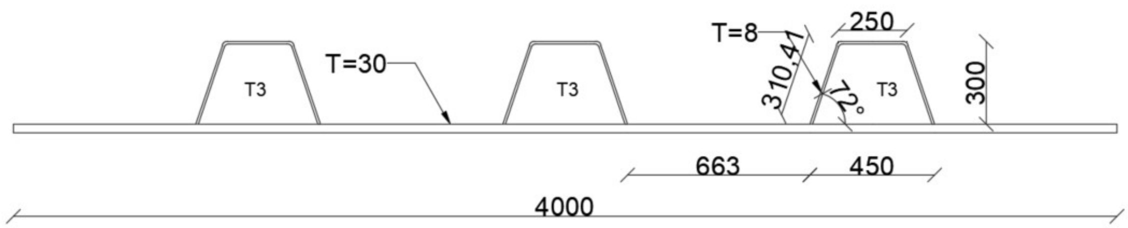

$A_{new.st} := 18624\ mm^2$

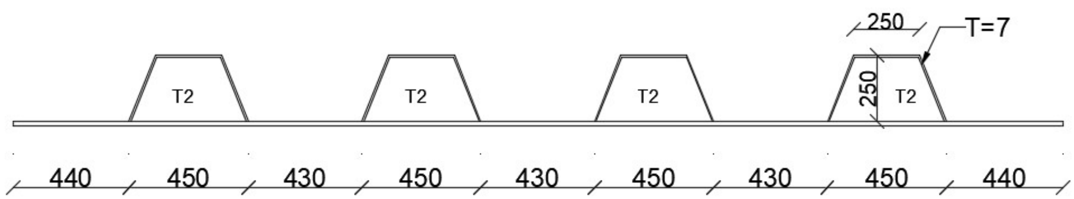

Single panel buckling:

Single Panel Buckling of bottom plate/North Side b=4m

t(mm)	fyk(MPa)	BBott (mm)	B/t	ε	Kσ	λp	ρ	ρ	σRd,local	η	(52/η)ε	Need to check	kt	σE	tcr	λw	0.6/η	χw	tRd	σEd,local	η1	η3	Interaction
12	460	440	36.7	0.698	4	0.9	0.69	0.69	317	1.200	30	1	5.39	141	762	0.591	0.50	1.05	279	317	0.69	0.18	η3≤0.5
14	460	440	31.4	0.698	4	0.8	0.77	0.77	356	1.200	30	1	5.39	192	1036	0.506	0.50	1.18	313	356	0.77	0.16	η3≤0.5
15	460	440	29.3	0.698	4	0.7	0.81	0.81	375	1.200	30	0	5.39	221	1190	0.473	0.50	1.20	319	375	0.81	0.16	η3≤0.5
16	460	440	27.5	0.698	4	0.7	0.85	0.85	392	1.200	30	0	5.39	251	1354	0.443	0.50	1.20	319	392	0.85	0.16	η3≤0.5
18	460	440	24.4	0.698	4	0.6	0.92	0.92	425	1.200	30	0	5.39	318	1713	0.394	0.50	1.20	319	425	0.92	0.16	η3≤0.5
20	460	440	22.0	0.698	4	0.6	0.98	0.98	453	1.200	30	0	5.39	393	2115	0.354	0.50	1.20	319	453	0.98	0.16	η3≤0.5
22	460	440	20.0	0.698	4	0.5	1.04	1.00	460	1.200	30	0	5.39	475	2559	0.322	0.50	1.20	319	460	1.00	0.16	η3≤0.5
24	460	440	18.3	0.698	4	0.5	1.08	1.00	460	1.200	30	0	5.39	565	3046	0.295	0.50	1.20	319	460	1.00	0.16	η3≤0.5
25	460	440	17.6	0.698	4	0.4	1.10	1.00	460	1.200	30	0	5.39	613	3305	0.284	0.50	1.20	319	460	1.00	0.16	η3≤0.5
26	460	440	16.9	0.698	4	0.4	1.12	1.00	460	1.200	30	0	5.39	663	3575	0.273	0.50	1.20	319	460	1.00	0.16	η3≤0.5
28	460	440	15.7	0.698	4	0.4	1.15	1.00	460	1.200	30	0	5.39	769	4146	0.253	0.50	1.20	319	460	1.00	0.16	η3≤0.5
30	460	440	14.7	0.698	4	0.4	1.17	1.00	460	1.200	30	0	5.39	883	4759	0.236	0.50	1.20	319	460	1.00	0.16	η3≤0.5
32	460	440	13.8	0.698	4	0.3	1.19	1.00	460	1.200	30	0	5.39	1005	5415	0.222	0.50	1.20	319	460	1.00	0.16	η3≤0.5
35	460	440	12.6	0.698	4	0.3	1.19	1.00	460	1.200	30	0	5.39	1202	6478	0.203	0.50	1.20	319	460	1.00	0.16	η3≤0.5
38	460	440	11.6	0.698	4	0.3	1.18	1.00	460	1.200	30	0	5.39	1417	7636	0.187	0.50	1.20	319	460	1.00	0.16	η3≤0.5
40	460	440	11.0	0.698	4	0.3	1.16	1.00	460	1.200	30	0	5.39	1570	8461	0.177	0.50	1.20	319	460	1.00	0.16	η3≤0.5
42	460	440	10.5	0.698	4	0.3	1.13	1.00	460	1.200	30	0	5.39	1731	9328	0.169	0.50	1.20	319	460	1.00	0.16	η3≤0.5
45	460	440	9.8	0.698	4	0.2	1.08	1.00	460	1.200	30	0	5.39	1987	10709	0.158	0.50	1.20	319	460	1.00	0.16	η3≤0.5
48	460	440	9.2	0.698	4	0.2	1.00	1.00	460	1.200	30	0	5.39	2261	12184	0.148	0.50	1.20	319	460	1.00	0.16	η3≤0.5
50	460	440	8.8	0.698	4	0.2	0.94	0.94	433	1.200	30	0	5.39	2454	13221	0.142	0.50	1.20	319	433	0.94	0.16	η3≤0.5
55	460	440	8.0	0.698	4	0.2	0.76	0.76	348	1.200	30	0	5.39	2969	15997	0.129	0.50	1.20	319	348	0.76	0.16	η3≤0.5
60	460	440	7.3	0.698	4	0.2	0.52	0.52	240	1.200	30	0	5.39	3533	19038	0.118	0.50	1.20	319	240	0.52	0.16	η3≤0.5
63	460	440	7.0	0.698	4	0.2	0.36	0.36	164	1.200	30	0	5.39	3895	20989	0.113	0.50	1.20	319	164	0.36	0.16	η3≤0.5
65	460	440	6.8	0.698	4	0.2	0.24	0.24	109	1.200	30	0	5.39	4146	22343	0.109	0.50	1.20	319	109	0.24	0.16	η3≤0.5
70	460	440	6.3	0.698	4	0.2	-0.10	-0.10	-46	1.200	30	0	5.39	4809	25912	0.101	0.50	1.20	319	-46	-0.10	0.16	η3≤0.5
80	460	440	5.5	0.698	4	0.1	-0.93	-0.93	-426	1.200	30	0	5.39	6281	33844	0.089	0.50	1.20	319	-426	-0.93	0.16	η3≤0.5

Global Stability of bottom flange:

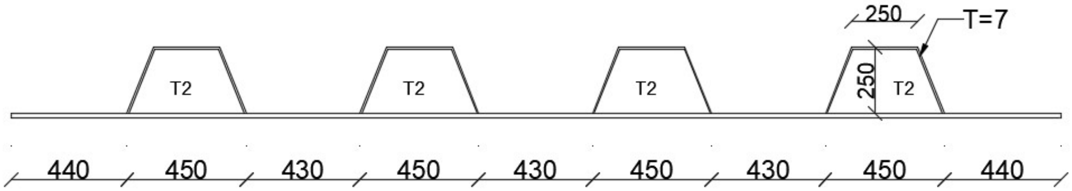

In order to find the effective width of the plate that is forming the stiffener flanges eq 3.3 EN 1993-1-5 is used. In EN 1993-1-4, 5.2.4. the effect of shear lag can be taken according to eq 3.3 EN 1993-1-5 .

$A_{eff} = A_{c.eff} \cdot \beta_{ult}$ $\qquad L_e := 0.7 \cdot 4000\ mm = 2.8\ m$

$\alpha_0 = \sqrt{\dfrac{A_{ceff}}{b_0 . t_f}} = 1 \qquad \alpha_0 := 1$ $\qquad$ From single plate buckling no reduction occured and $\rho = 1$

Inside stiffener $\qquad b_0 := \dfrac{450\ mm}{2} = 225\ mm \qquad \kappa := \dfrac{\alpha_0 \cdot b_0}{L_e} = 0.08 \qquad \beta_{ult} := \dfrac{1}{1 + 6.4 \cdot \kappa^2} = 0.96$

$b_{eff} := \beta_{ult} \cdot b_0 = 216.071\ mm$

North bridge plate flange $\qquad b_0 := \dfrac{440\ mm}{2} = 220\ mm \qquad \kappa := \dfrac{\alpha_0 \cdot b_0}{L_e} = 0.079 \qquad \beta_{ult} := \dfrac{1}{1 + 6.4 \cdot \kappa^2} = 0.962$

$b_{eff} := \beta_{ult} \cdot b_0 = 211.638\ mm$

Top flange $\qquad b_0 := \dfrac{250\ mm}{2} = 125\ mm \qquad \kappa := \dfrac{\alpha_0 \cdot b_0}{L_e} = 0.045 \qquad \beta_{ult} := \dfrac{1}{1 + 6.4 \cdot \kappa^2} = 0.987$

$b_{eff} := 2 \cdot \beta_{ult} \cdot b_0 = 246.851\ mm \qquad b_{eff} := 250\ mm$

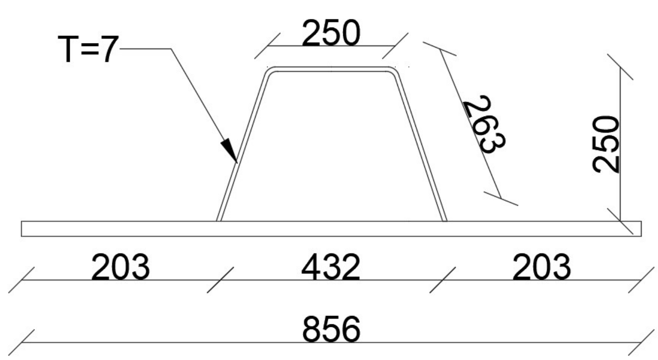

Considering Northern side only

$b_{eff} := 856\ mm$ $f_y := 460\ MPa$ $t_p := 30\ mm$ $t_s := 7\ mm$ $E := 200\ GPa$

Cross section class for the plate:

$$\varepsilon := \sqrt{\frac{235\ MPa \cdot E}{f_y \cdot 210\ GPa}} = 0.698$$

$$\frac{440\ mm}{t_p} = 14.667 \qquad 30.7 \cdot \varepsilon = 21.414 \qquad \text{Class 3}$$

Cross section class for the stiffener:

Inclined web:

$$B := \frac{263\ mm - 5\ mm - 20\ mm}{8\ mm} = 29.75 \qquad 30.7 \cdot \varepsilon = 21.414 \qquad \text{Class 4}$$

Reduction is needed. According to the upper calculation for stiffeners noreduction is needed up to $\sigma_{Rd} := 364\ MPa$

Section properties:
Stiffener only:

$t_p := 30\ mm$ $l_p := 856\ mm$ $S_w := 263\ mm$ $Z_s := 250\ mm$
$S_t := 250\ mm$ $t_s := 7\ mm$

$$A_{st.0} := 2 \cdot S_w \cdot t_s + S_t \cdot t_s = \left(5.432 \cdot 10^3\right)\ mm^2$$

$$Z_0 := \frac{2 \cdot S_w \cdot t_s \cdot \dfrac{Z_s}{2} + S_t \cdot t_s \cdot \left(Z_s - \dfrac{t_s}{2}\right)}{A_{st.0}} = 164.143\ mm$$

$$I_{st.0} := S_t \cdot t_s \left(Z_s - \frac{t_s}{2} - Z_0\right)^2 + S_w \cdot 2 \cdot t_s \cdot \left(\frac{Z_s}{2} - Z_0\right)^2 + 2 \cdot \frac{t_s \cdot \left(Z_s\right)^3}{12} = \left(3.574 \cdot 10^7\right)\ mm^4$$

$$I_{st.0} = \left(3.574 \cdot 10^7\right)\ mm^4$$

Stiffener with the plate:

$$A_{st.1} := l_p \cdot t_p + 2 \cdot S_w \cdot t_s + S_t \cdot t_s = \left(3.111 \cdot 10^4\right)\ mm^2$$

$$Z_0 := \frac{l_p \cdot t_p \cdot \dfrac{t_p}{2} + 2 \cdot S_w \cdot t_s \cdot \left(\dfrac{t_s}{2} + t_p\right) + S_t \cdot t_s \cdot \left(Z_s - \dfrac{t_s}{2} + t_p\right)}{A_{st.1}} = 31.898\ mm$$

$$I_{st.1} := S_t \cdot t_s \cdot \left(Z_s + t_p - \frac{t_s}{2} - Z_0\right)^2 + 2 \cdot S_w \cdot t_s \cdot \left(\frac{Z_s}{2} + t_p - Z_0\right)^2 + l_p \cdot t_p \cdot \left(Z_0 - \frac{t_p}{2}\right)^2 + 2 \cdot \frac{t_s \cdot (Z_s)^3}{12} + \frac{l_p \cdot t_p{}^3}{12}$$

$$I_{st.1} = \left(1.88 \cdot 10^8\right)\ mm^4$$

Plate type buckling

$t := 3\ cm$ $\quad b := 400\ cm$ $\quad a := 400\ cm$ $\quad \psi := 1$ $\quad E := 200\ GPa$

$\beta := 1$ No local plate buckling is allowed

$$\sigma_E := 190000\ MPa \cdot \left(\frac{t}{b}\right)^2 = 10.688\ MPa \qquad \delta := \frac{4 \cdot A_{st.0}}{b \cdot t} = 0.181$$

$$\alpha := \frac{a}{b} = 1 \qquad I_p := \frac{b \cdot t^3}{10.92} = \left(9.89 \cdot 10^{-6}\right)\ m^4 \qquad \gamma := \frac{3 \cdot I_{st.1}}{I_p} = 57.023$$

$$\sqrt[4]{\gamma} = 2.748 \qquad \alpha < \sqrt[4]{\gamma}$$

$$K_{\sigma.p} := \frac{2 \cdot \left(\left(1 + \alpha^2\right)^2 + \gamma - 1\right)}{\alpha^2\ (\psi + 1)\ (1 + \delta)} = 50.821 \qquad \sigma_{cr.p} := K_{\sigma.p} \cdot \sigma_E = 543.149\ MPa$$

$$\lambda_P := \sqrt{\frac{\beta \cdot f_y}{\sigma_{cr.p}}} = 0.92$$

Reduction using EN 1993-1-4, 5.2.3 $\qquad \rho := \frac{0.772}{\lambda_P} - \frac{0.125}{\lambda_P{}^2} = 0.691$

Column type buckling

$$\sigma_{cr.c} := \frac{(3.14)^2 \cdot E \cdot I_{st.1}}{A_{st.1} \cdot a^2} = 744.682\ MPa$$

$$\lambda_c := \sqrt{\frac{f_y}{\sigma_{cr.c}}} = 0.786$$

Reduction using EN 1993-1-4, 5.4.2

EN 1993-1-4 table 5.3: A1.17.2017 Table 6.1

$$\alpha := 0.49 \qquad \lambda_0 := 0.2 \qquad \phi := 0.5 \cdot \left(1 + \alpha \cdot \left(\lambda_c - \lambda_0\right) + \lambda_c{}^2\right) = 0.952$$

$$\chi_c := \frac{1}{\phi + \left(\phi^2 - \lambda_c{}^2\right)^{0.5}} = 0.671$$

$$\xi := \frac{\sigma_{cr.p}}{\sigma_{cr.c}} - 1 = -0.271$$

smaller than one, this means that the column type buckling is govering

$$\rho_c := \chi_c = 0.671 \qquad \sigma_{Rd} := \rho_c \cdot \frac{f_y}{1} = 308.652\ MPa$$

North Side Bottom flange with stiffeners t=8 mm

a mm	B mm	tmm	fyk	∑ Asl mm^2	Ist (mm^4)	Zstiff(m	Ast.1	Xc	Isl	Ap	Ip	δ	γ	(γ)^0.25	α	Kσ	σE	σcr,p	λp	ρp	σcr,c	λc	λ0	α	ϕ	χ	ξ	ρc	λM1	σRd, Global	σRd, local	σRd, min
4000	4000	12	460	24832	40680000	164	31890	21	194373176	48000	632967.03	0.5	921	6	1	609	2	1042	0.7	0.88	751	0.8	0.2	0.5	0.9	0.7	0.4	0.8	1	369	317	317
4000	4000	14	460	24832	40680000	164	31890	22	196542580	56000	1005128.2	0.4	587	5	1	408	2	951	0.7	0.85	760	0.8	0.2	0.5	0.9	0.7	0.3	0.8	1	346	356	346
4000	4000	15	460	24832	40680000	164	31890	22	197571747	60000	1236263.7	0.4	479	5	1	341	3	912	0.7	0.84	764	0.8	0.2	0.5	0.9	0.7	0.2	0.7	1	338	375	338
4000	4000	16	460	24832	40680000	164	31890	23	198566314	64000	1500366.3	0.4	397	4	1	288	3	876	0.7	0.83	767	0.8	0.2	0.5	0.9	0.7	0.1	0.7	1	330	392	330
4000	4000	18	460	24832	40680000	164	31890	24	200459731	72000	2136263.7	0.3	282	4	1	212	4	814	0.8	0.81	775	0.8	0.2	0.5	0.9	0.7	0.1	0.7	1	319	425	319
4000	4000	20	460	24832	40680000	164	31890	26	202240653	80000	2930402.9	0.3	207	4	1	160	5	761	0.8	0.79	782	0.8	0.2	0.5	0.9	0.7	0.0	0.7	1	314	453	314
4000	4000	21	461	24832	40680000	164	31890	27	203095319	84000	3392307.7	0.3	180	4	1	141	5	738	0.8	0.78	785	0.8	0.2	0.5	0.9	0.7	-0.1	0.7	1	315	460	315
4000	4000	22	460	24832	40680000	164	31890	27	203929967	88000	3900366.3	0.3	157	4	1	125	6	717	0.8	0.77	788	0.8	0.2	0.5	0.9	0.7	-0.1	0.7	1	315	460	315
4000	4000	23	460	24832	40680000	164	31890	28	204747783	92000	4456776.6	0.3	138	3	1	111	6	697	0.8	0.76	791	0.8	0.2	0.5	0.9	0.7	-0.1	0.7	1	315	460	315
4000	4000	24	460	24832	40680000	164	31890	29	205552218	96000	5063736.3	0.3	122	3	1	99	7	678	0.8	0.75	794	0.8	0.2	0.5	0.9	0.7	-0.1	0.7	1	316	460	316
4000	4000	25	460	24832	40680000	164	31890	30	206347010	100000	5723443.2	0.2	108	3	1	89	7	661	0.8	0.75	797	0.8	0.2	0.5	0.9	0.7	-0.2	0.7	1	316	460	316
4000	4000	26	460	24832	40680000	164	31890	31	207136197	104000	6438095.2	0.2	97	3	1	80	8	645	0.8	0.74	801	0.8	0.2	0.5	0.9	0.7	-0.2	0.7	1	317	460	317
4000	4000	28	460	24832	40680000	164	31890	32	208715538	112000	8041025.6	0.2	78	3	1	66	9	616	0.9	0.73	807	0.8	0.2	0.5	0.9	0.7	-0.2	0.7	1	318	460	318
4000	4000	30	460	24832	40680000	164	31890	34	210329304	120000	9890109.9	0.2	64	3	1	55	11	592	0.9	0.71	813	0.8	0.2	0.5	0.9	0.7	-0.3	0.7	1	318	460	318
4000	4000	31	461	24832	40680000	164	31890	35	211162936	124000	10912454	0.2	58	3	1	51	11	580	0.9	0.71	816	0.8	0.2	0.5	0.9	0.7	-0.3	0.7	1	319	460	319
4000	4000	32	460	24832	40680000	164	31890	36	212022585	128000	12002930	0.2	53	3	1	47	12	570	0.9	0.70	819	0.7	0.2	0.5	0.9	0.7	-0.3	0.7	1	319	460	319
4000	4000	33	461	24832	40680000	164	31890	38	212914928	132000	13163736	0.2	49	3	1	43	13	561	0.9	0.70	823	0.7	0.2	0.5	0.9	0.7	-0.3	0.7	1	320	460	320
4000	4000	35	460	24832	40680000	164	31890	40	214826661	140000	15705128	0.2	41	3	1	37	15	544	0.9	0.69	830	0.7	0.2	0.5	0.9	0.7	-0.3	0.7	1	321	460	321
4000	4000	36	461	24832	40680000	164	31890	41	215861728	144000	17090110	0.2	38	2	1	35	15	537	0.9	0.69	834	0.7	0.2	0.5	0.9	0.7	-0.4	0.7	1	322	460	322
4000	4000	38	460	24832	40680000	164	31890	43	218133221	152000	20099634	0.2	33	2	1	31	17	524	0.9	0.68	843	0.7	0.2	0.5	0.9	0.7	-0.4	0.7	1	322	460	322
4000	4000	40	460	24832	40680000	164	31890	46	220736674	160000	23443223	0.2	28	2	1	27	19	514	0.9	0.68	853	0.7	0.2	0.5	0.9	0.7	-0.4	0.7	1	324	460	324
4000	4000	41	460	24832	40680000	164	31890	47	222188799	164000	25245788	0.2	26	2	1	26	20	510	0.9	0.67	859	0.7	0.2	0.5	0.9	0.7	-0.4	0.7	1	324	460	324
4000	4000	42	460	24832	40680000	164	31890	48	223756183	168000	27138462	0.1	25	2	1	24	21	506	1.0	0.67	865	0.7	0.2	0.5	0.9	0.7	-0.4	0.7	1	325	460	325
4000	4000	43	460	24832	40680000	164	31890	50	225450840	172000	29123443	0.1	23	2	1	23	22	503	1.0	0.67	871	0.7	0.2	0.5	0.9	0.7	-0.4	0.7	1	326	460	326
4000	4000	45	460	24832	40680000	164	31890	52	229273219	180000	33379121	0.1	21	2	1	21	24	499	1.0	0.67	886	0.7	0.2	0.5	0.9	0.7	-0.4	0.7	1	327	460	327
4000	4000	48	460	24832	40680000	164	31890	57	236299187	192000	40509890	0.1	17	2	1	18	27	497	1.0	0.67	913	0.7	0.2	0.5	0.9	0.7	-0.5	0.7	1	331	460	331
4000	4000	50	460	24832	40680000	164	31890	60	242024277	200000	45787546	0.1	16	2	1	17	30	498	1.0	0.67	935	0.7	0.2	0.5	0.9	0.7	-0.5	0.7	1	333	433	333
4000	4000	55	460	24832	40680000	164	31890	68	261009757	220000	60943223	0.1	13	2	1	14	36	512	0.9	0.68	1009	0.7	0.2	0.5	0.8	0.7	-0.5	0.7	1	340	348	340
4000	4000	60	460	24832	40680000	164	31890	77	288739314	240000	79120879	0.1	11	2	1	13	43	540	0.9	0.69	1116	0.6	0.2	0.5	0.8	0.8	-0.5	0.8	1	350	240	240
4000	4000	63	460	24832	40680000	164	31890	82	310821499	252000	91592308	0.1	10	2	1	12	47	566	0.9	0.70	1201	0.6	0.2	0.5	0.8	0.8	-0.5	0.8	1	356	164	164
4000	4000	65	460	24832	40680000	164	31890	86	328270170	260000	100595238	0.1	10	2	1	12	50	586	0.9	0.71	1269	0.6	0.2	0.5	0.8	0.8	-0.5	0.8	1	361	109	109
4000	4000	70	460	24832	40680000	164	31890	96	383264936	280000	125641026	0.1	9	2	1	11	58	649	0.8	0.74	1481	0.6	0.2	0.5	0.7	0.8	-0.6	0.8	1	373	-46	-46
4000	4000	80	460	24832	40680000	164	31890	118	557670510	320000	187545788	0.1	9	2	1	11	76	841	0.7	0.82	2155	0.5	0.2	0.5	0.7	0.9	-0.6	0.9	1	397	-426	-426

By introducing the same geometry and maintaining the same plate thicknesses we get the following:

Bottom plate ULSB Long stresses

Coordinates (m)	Plates thickness	Box #	Box position						S355							1.4462 new Geometry						
			NÖ		NM		NV		yield strength		uckling strength Plat		Stiffeners strength		Min σ	yield strength		uckling strength Plat		Stiffeners strength		Min σ
			Tension	Compress	Tension	Compress	Tension	Compress			Local	Global	8 mm	10 mm				Local	Global	T2, 7 mm	T2, 8 mm	
1100	45&25	7&6	-25	-245	-25	-270	-33	-268	335	-335	-335	-281	-325		-281	460	-460	-460	-316	-329		-316
1105	25	6	48	-179	30	-197	31	-179	345	-345	-299	-281	-325		-281	460	-460	-460	-316	-329		-316
1108	25&16	6	114	-169	106	-158	94	-150	355	-355	-299	-299	-325		-299	460	-460	-392	-316	-329		-316
1121	16	6	161	-67	150	-52	151	-43	355	-355	-299	-299	-325		-299	460	-460	-392	-330	-329		-329
1130	16	5	213	-43	200	-27	201	-21	355	-355	-299	-299	-325		-299	460	-460	-392	-330	-329		-329
1134	16	5	166	-65	166	-43	145	-39	355	-355	-299	-299	-325		-299	460	-460	-392	-330	-329		-329
1140	16&20	5	153	-117	149	-105	143	-109	345	-345	-299	-299	-325		-299	460	-460	-392	-314	-329		-314
1148	20&40	5	28	-201	33	-223	23	-228	345	-345	-333	-261	-325		-261	460	-460	-453	-314	-329		-314
1156	40&20	5&4	39	-201	39	-190	43	-205	345	-345	-333	-261		-355	-261	460	-460	-453	-314		-364	-314
1162	20	4	79	-106	70	-105	65	-112	345	-345	-333	-289	-325		-289	460	-460	-453	-314	-329		-314
1166	20&16	4	128	-87	126	-65	121	-74	345	-345	-299	-289	-325		-289	460	-460	-392	-314	-329		-314
1170	16	4	157	-64	145	-59	148	-69	355	-355	-299	-299	-325		-299	460	-460	-392	-330	-329		-329
1176	16	4	162	-56	156	-52	154	-61	355	-355	-299	-299	-325		-299	460	-460	-392	-330	-329		-329
1180	16	4&3	163	-51	157	-45	154	-53	355	-355	-299	-299	-325		-299	460	-460	-392	-330	-329		-329
1186	16	3	109	-65	109	-56	93	-65	355	-355	-299	-299	-325		-299	460	-460	-392	-330	-329		-329
1190	16	3	74	-82	74	-91	81	-78	355	-355	-299	-299	-325		-299	460	-460	-392	-330	-329		-329
1196	16&35	3	41	-174	45	-209	35	-183	345	-345	-299	-267	-325		-267	460	-460	-392	-330	-329		-329
1204	35&16	3&2	54	-169	57	-175	48	-175	345	-345	-299	-267		-355	-267	460	-460	-392	-321		-364	-321
1210	16	2	116	-98	109	-97	108	-94	355	-355	-299	-299	-325		-299	460	-460	-392	-330	-329		-329
1212	16	2	77	-34	69	-39	77	-28	355	-355	-299	-299	-325		-299	460	-460	-392	-330	-329		-329
1220	16	2	136	-4	137	-3	139	-5	355	-355	-299	-299	-325		-299	460	-460	-392	-330	-329		-329
1226	16	1	201	15	196	19	190	20	355	-355	-299	-299	-325		-299	460	-460	-392	-330	-329		-329
1232	16&25	1	173	34	173	34	165	38	345	-345	-299	-281	-325		-281	460	-460	-392	-316	-329		-316

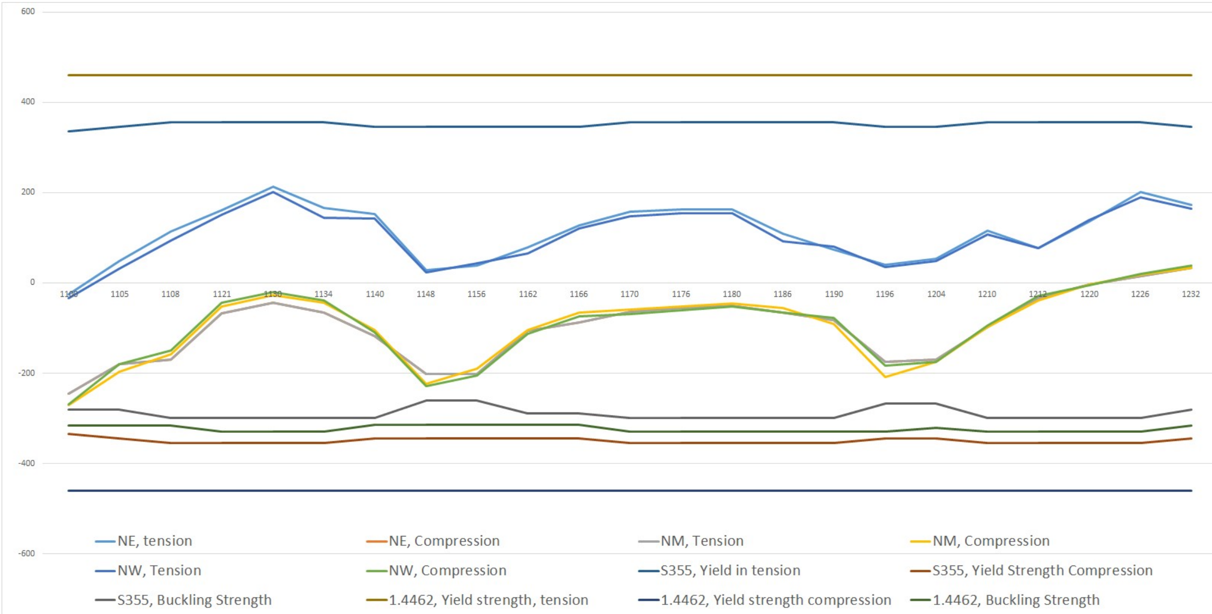

From plott we see that changing the geometry of bottom flange increased the gap between the lines representing S355 buckling strength and 1.4462 buckling strength. Now we can introduce new plate thicknesses:

By reducing bottom plate thickness by 2mm every where, we get the following results:

1.4462 plate- 2mm								
Coordinates	Plates thickness	yield strength		Buckling strength Plate		Stiffeners strength		Min σ
				Local	Global	T2, 7 mm	T2, 8 mm	
1100	43+23	460	-460	-460	-315	-329		-315
1105	23	460	-460	-460	-315	-329		-315
1108	23+14	460	-460	-356	-315	-329		-315
1121	14	460	-460	-356	-346	-329		-329
1130	14	460	-460	-356	-346	-329		-329
1134	14	460	-460	-356	-346	-329		-329
1140	14+18	460	-460	-356	-319	-329		-319
1148	18+38	460	-460	-425	-319	-329		-319
1156	18+38	460	-460	-425	-319		-364	-319
1162	18	460	-460	-425	-319	-329		-319
1166	18+14	460	-460	-356	-319	-329		-319
1170	14	460	-460	-356	-346	-329		-329
1176	14	460	-460	-356	-346	-329		-329
1180	14	460	-460	-356	-346	-329		-329
1186	14	460	-460	-356	-346	-329		-329
1190	14	460	-460	-356	-346	-329		-329
1196	14+33	460	-460	-356	-320	-329		-320
1204	33+14	460	-460	-356	-320		-364	-320
1210	14	460	-460	-356	-346	-329		-329
1212	14	460	-460	-356	-346	-329		-329
1220	14	460	-460	-356	-346	-329		-329
1226	14	460	-460	-356	-346	-329		-329
1232	14+23	460	-460	-356	-315	-329		-315

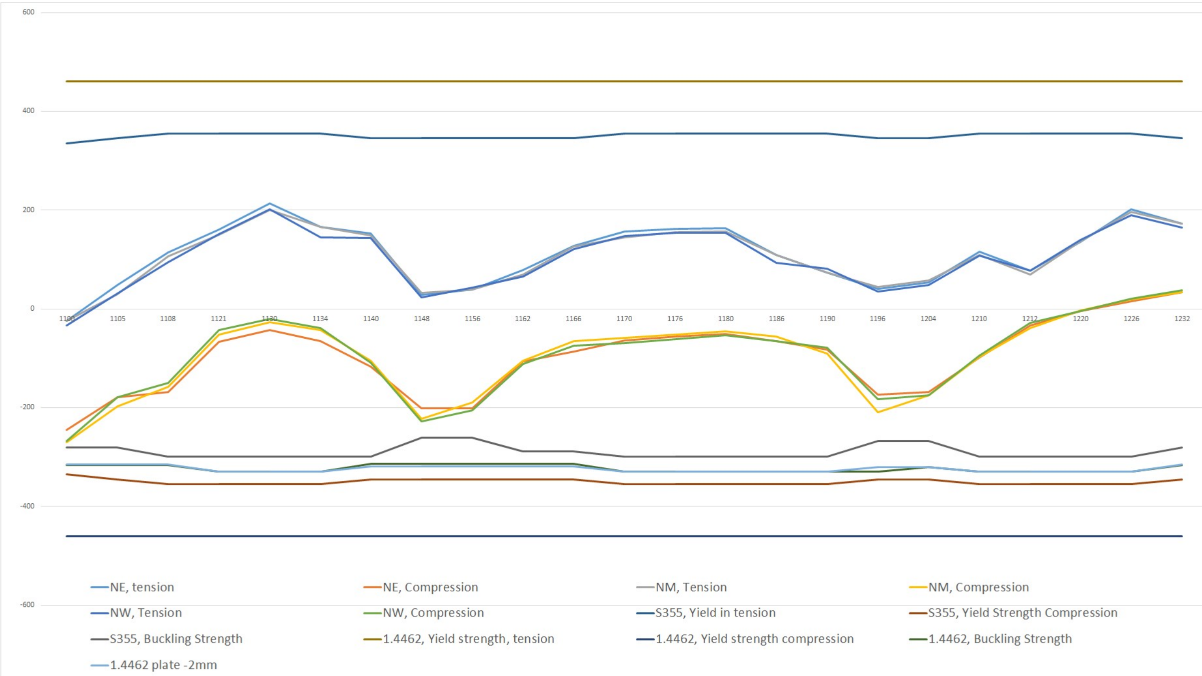

It can be noticed that reducing the plate thickness with 2mm did not affect the capacity of the bottom flang, it means that we can reduce the thickness with another 2mm

1.4462 plate- 4mm								
Coordinates	ates thickne	yield strength		Buckling strength Plate		Stiffeners strength		Min σ
				Local	Global	T2, 7 mm	T2, 8 mm	
1100	41+21	460	-460	-460	-315	-329		-315
1105	21	460	-460	-460	-315	-329		-315
1108	21+12	460	-460	-317	-315	-329		-315
1121	12	460	-460	-317	-369	-329		-317
1130	12	460	-460	-317	-369	-329		-317
1134	12	460	-460	-317	-369	-329		-317
1140	12+16	460	-460	-317	-330	-329		-317
1148	16+36	460	-460	-392	-322	-329		-322
1156	16+36	460	-460	-392	-322		-364	-322
1162	16	460	-460	-392	-330	-329		-329
1166	16+12	460	-460	-317	-330	-329		-317
1170	12	460	-460	-317	-369	-329		-317
1176	12	460	-460	-317	-369	-329		-317
1180	12	460	-460	-317	-369	-329		-317
1186	12	460	-460	-317	-369	-329		-317
1190	12	460	-460	-317	-369	-329		-317
1196	12+31	460	-460	-317	-369	-329		-317
1204	31+12	460	-460	-317	-369		-364	-317
1210	12	460	-460	-317	-369	-329		-317
1212	12	460	-460	-317	-369	-329		-317
1220	12	460	-460	-317	-369	-329		-317
1226	12	460	-460	-317	-369	-329		-317
1232	12+21	460	-460	-317	-315	-329		-315

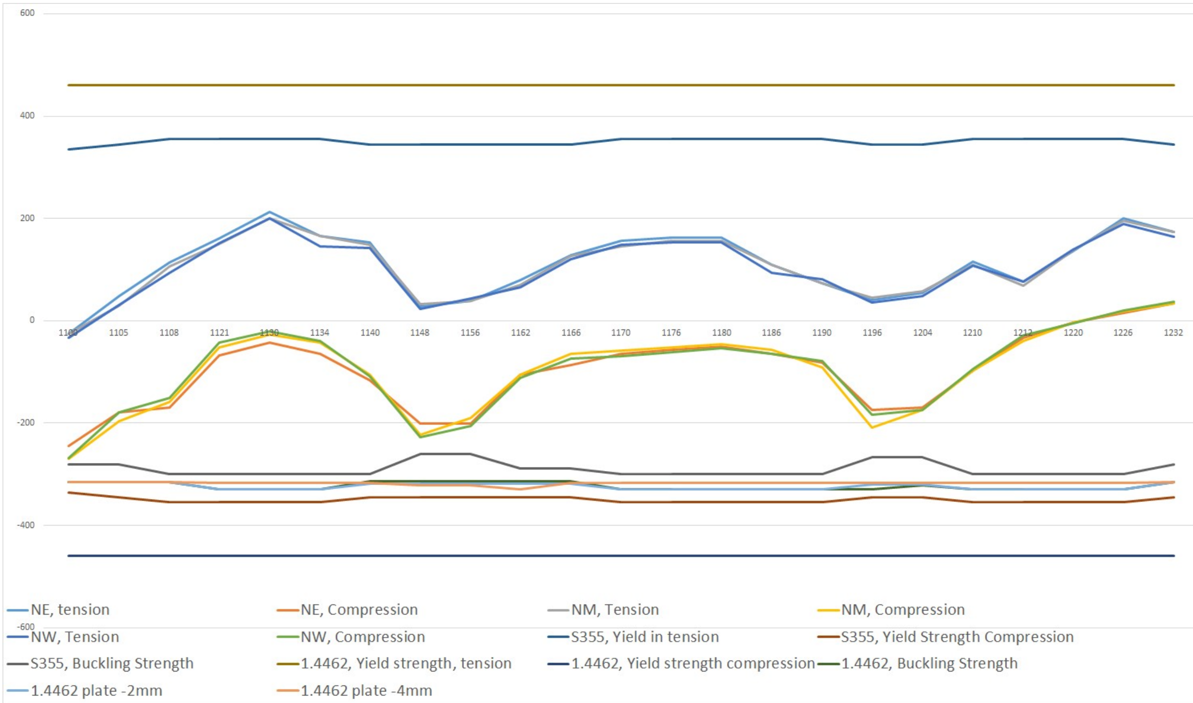

It is visible now that buckling strength is moved upwards (the orange line) when reducing the plate thickness by 4mm.

Summary:

Changes in stiffeners:

the original design has three stiffeners type T3 with 8 mm thickness, these stiffeners has the following cross sectional area:

$$A_{t3.8} := (2 \cdot 316\ mm \cdot 8\ mm + 250\ mm \cdot 8\ mm) \cdot 3 = 211.68\ cm^2$$

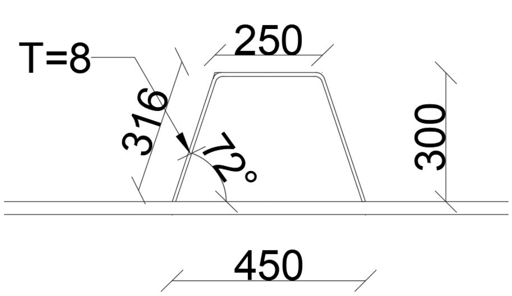

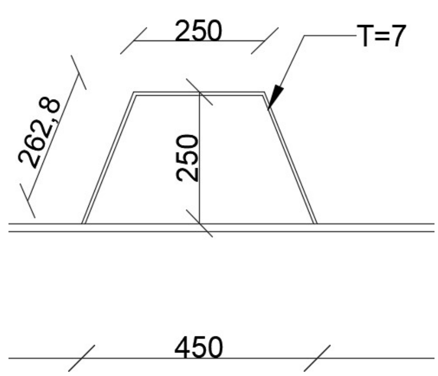

In the new suggestion we used 4*T2 stiffeners with 7mm thickness, the area of this stiffeners beacme:

$$A_{t2.7} := (2 \cdot 263\ mm \cdot 7\ mm + 250\ mm \cdot 7\ mm) \cdot 4 = 217.28\ cm^2$$

The cross section of stiffeners increased with the following value:

$$A_t := A_{t2.7} - A_{t3.8} = 5.6\ cm^2$$

the plate thickness has decreased by 4mm in all sections, thus we have the follwing reduction every where in the plate:

$$A_p := 4\ mm \cdot 4000\ mm = 160\ cm^2$$

As a result the cross section every where along the bridge has decreased by the following value:

$$A_{reduced} := A_p - A_t = 154.4\ cm^2$$

This means that along the bridge between coordinate 1100 to 1232 and without changing supports cross sectional area, volume of the bridge has reduced by the following value:

$$V_{red} := A_{reduced} \cdot 115.8\ m = 1.788\ m^3 \qquad g := V_{red} \cdot 77000\ \frac{kg}{m^3} = 151.758\ ton$$

At the same time the surface area is increased with the following value:

$$A_{ineer.surface} := 115.8\ m \cdot (4 \cdot (263\ mm \cdot 2 + 250\ mm) + 480\ mm \cdot 5 - 3 \cdot (316\ mm \cdot 2 + 250\ mm) - 663\ mm \cdot 4) =$$

$$A_{ineer.surface} = 23.855\ m^2$$

C

Webs Buckling capacity using Duplex stainless steel 1.4462

C- Webs Buckling capacity using Duplex stainless steel 1.4462

Local Single panel buckling:

Transverse stress:

Webs will be checked in a simillar way to the bottom flange with some differences. In webs shear stresses are higher than those in the bottom flange. web's top plate will be exposed to transversal stresses σ y,ed. Longitudinal stresses are varying throught the height of the web.
In chapter D5.2.8, all of the transversal stresses above above -40 MPa are registered and it was that found that the maximum value of theses stresses is -40 MPa with some higher localized values at cross frame which will are treated in the cross frame part of the study.

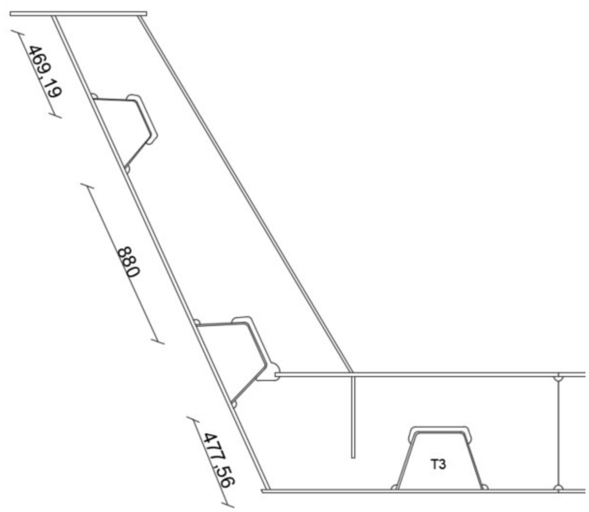

Transverse stresses will be checked according to A1. 17, 2017, 6.4.4:

A single panel of the web will have height of 880 mm between t1 and t2. This values will be checked for transverse stresses coming from the vehicle weels above the slab of the box girder.

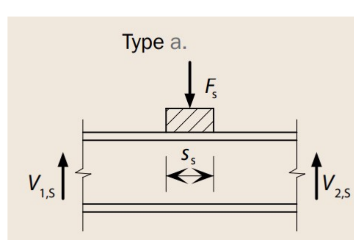

We have type A buckling:

$\alpha := 4000\ mm$ Distance between two cross frames

$h_w := 880\ mm$ $t_w := 16\ mm$ $E := 200\ GPa$

$$\kappa_{F.y} := 6 + 2\left(\frac{h_w}{\alpha}\right)^2 = 6.097 \qquad f_y := 460\ MPa$$

$$F_{cr} := 0.9 \cdot \kappa_{F.y} \cdot E \cdot \frac{t_w^{\ 3}}{h_w} = \left(5.108 \cdot 10^3\right)\ kN \qquad \lambda_F := \sqrt{\frac{\left(\alpha \cdot t_w \cdot f_y\right)}{F_{cr}}} = 2.401$$

$\gamma_{m1} := 1$ 18 kap. SS-EN 1993-1-4 – Rostfritt stål

$\chi_f := \dfrac{0.5}{\lambda_F} = 0.208$ $L_{eff} := \chi_f \cdot \alpha = 0.833\ m$ $F_{Rd} := f_y \cdot L_{eff} \cdot \dfrac{t_w}{\gamma_{m1}} = \left(6.131 \cdot 10^3\right)\ kN$

$\sigma_{Rd} := \dfrac{F_{Rd}}{\alpha \cdot t_w} = 95.804\ MPa$

From ULS stresses $\sigma_{yEd} := 40\ MPa$ $\eta_2 := \dfrac{\sigma_{yEd}}{\sigma_{Rd}} = 0.418$

Using interaction rule Eq 7.2 from 1993-1-5 and assuming that the panel is fully used in (longitudina stresses) σxED

$\eta_1 := 1$ $\eta_2 + \eta_1 \cdot 0.8 = 1.218$

$$\begin{Vmatrix} \text{if } \eta_2 + \eta_1 \cdot 0.8 \le 1.4 \\ \quad \Vert \text{“Ok”} \\ \text{else if } \eta_2 + \eta_1 \cdot 0.8 > 1.4 \\ \quad \Vert \text{“Problem”} \end{Vmatrix} = \text{“Ok”}$$

Single Panel Check for each subpart of the web

$\alpha := 4000\ mm$ $t_w := 16\ mm$ $B_{tot} := 2685\ mm$

Top Edge subpanel:

$B_{brutto} := 700\ mm$ $\quad B_{s1} := 400\ mm$ $\quad B_{panel} := B_{brutto} - \frac{B_{s1}}{2} = 500\ mm$

$a := \frac{\alpha}{B_{panel}} = 8$ $\quad h_w := B_{panel}$

Assuming that we have pure compression σxtop=σxbottom

$\sigma_{x.top} := 1$ $\quad \sigma_{x.bottom} := \sigma_{x.top}$ $\quad f_{y.plate} := 460\ MPa$ $\quad t_w := \begin{bmatrix} 16 \\ 20 \\ 25 \end{bmatrix} mm$

$\psi := \frac{\sigma_{x.top}}{\sigma_{x.bottom}}$ $\quad \varepsilon := \sqrt{\frac{235\ MPa}{f_{y.plate}} \cdot \frac{E}{210\ GPa}} = 0.698$ $\quad \kappa_\sigma := 4$ $\quad i := 0..2$

$\lambda_{p.x} := \left(\frac{B_{panel}}{t_w \cdot 28.4 \cdot \varepsilon \cdot \sqrt{\kappa_\sigma}}\right) = \begin{bmatrix} 0.789 \\ 0.631 \\ 0.505 \end{bmatrix}$ $\quad \rho_i := \frac{0.772}{\lambda_{p.x_i}} - \frac{0.079}{\left(\lambda_{p.x}{}^2\right)_i} = \begin{bmatrix} 0.852 \\ 1.025 \\ 1.219 \end{bmatrix}$ $\quad \rho := \begin{bmatrix} 0.852 \\ 1 \\ 1 \end{bmatrix}$

$\gamma_{m0} := 1$ 18 kap. SS-EN 1993-1-4 – Rostfritt stål

$\sigma_{Rd.local.top} := \frac{\rho \cdot f_{y.plate}}{\gamma_{m0}} = \begin{bmatrix} 391.92 \\ 460 \\ 460 \end{bmatrix} MPa$

Shear buckling resistance 6.4.3 A1.17,2017

$\eta := 1.2$ $\quad \frac{h_w}{t_w} = \begin{bmatrix} 31.25 \\ 25 \\ 20 \end{bmatrix}$ $\quad \frac{56.2 \cdot \varepsilon}{\eta} = 32.667$

$\kappa_\tau := 5.34 + 4 \left(\frac{B_{panel}}{\alpha}\right)^2 = 5.403$ $\quad \lambda_w := \frac{h_w}{37.4 \cdot t_w \cdot \varepsilon \cdot (\kappa_\tau)^{0.5}} = \begin{bmatrix} 0.515 \\ 0.412 \\ 0.33 \end{bmatrix}$ (6.25 A1)

$$\chi_{w_i} := \begin{cases} \eta & \text{if } \lambda_{w_i} \le \frac{0.65}{\eta} \\ \frac{0.65}{\lambda_{w_i}} & \text{else if } \frac{0.65}{\eta} < \lambda_{w_i} < 0.65 \\ \frac{1.56}{0.91 + \lambda_{w_i}} & \text{else} \end{cases} = \begin{bmatrix} 1.2 \\ 1.2 \\ 1.2 \end{bmatrix}$$

$$\tau_{Rd_i} := \chi_{w_i} \cdot \frac{f_{y.plate}}{\sqrt{3} \cdot \gamma_{m1}} = \begin{bmatrix} 318.697 \\ 318.697 \\ 318.697 \end{bmatrix} MPa$$

$\eta_3 = \frac{\tau_{Ed}}{\tau_{Rd}}$ According to A1 no interaction will be checked for : $\tau_{Ed} \le 0.5 \cdot \tau_{Rd}$

So, it is assumed that $\tau_{Ed} = 0.5 \cdot \tau_{Rd}$

$$\tau_{Ed} := 0.5 \cdot \tau_{Rd} = \begin{bmatrix} 159.349 \\ 159.349 \\ 159.349 \end{bmatrix} \; MPa$$

Mid Subpanel

$B_{brutto} := 700 \; mm$ $B_{s1} := 400 \; mm$ $B_{s2} := 450 \; mm$ $B_{tot} = 2.685 \; m$

$B_{panel.mid} := B_{tot} - 2 \cdot B_{brutto} - \frac{B_{s1}}{2} - \frac{B_{s2}}{2} = 860 \; mm$ $t_w := 16 \; mm$

$a := \frac{\alpha}{B_{panel.mid}} = 4.651$ $h_w := B_{panel.mid}$

Assuming that we have pure compression σxtop=σxbottom, and another time assuming that we have compression at the top and tension at the bottom i.e:

$\sigma_{x.top} := \begin{bmatrix} 1 \\ -1 \end{bmatrix}$ $\sigma_{x.bottom} := \begin{bmatrix} 1 \\ 1 \end{bmatrix}$ $f_{y.plate} := 460 \; MPa$

$\psi := \frac{\sigma_{x.top}}{\sigma_{x.bottom}} = \begin{bmatrix} 1 \\ -1 \end{bmatrix}$ $\varepsilon := \sqrt{\frac{235 \; MPa}{f_{y.plate}} \cdot \frac{E}{210 \; GPa}} = 0.698$

$\kappa_\sigma := \begin{bmatrix} 4 \\ 23.9 \end{bmatrix}$ $\lambda_{p.x} := \left(\frac{B_{panel.mid}}{t_w \cdot 28.4 \cdot \varepsilon \cdot \sqrt{\kappa_\sigma}} \right) = \begin{bmatrix} 1.357 \\ 0.555 \end{bmatrix}$ $\gamma_{m0} := 1$

$\rho := \frac{0.772}{\lambda_{p.x}} - \frac{0.079}{{\lambda_{p.x}}^2} = \begin{bmatrix} 0.526 \\ 1.135 \end{bmatrix}$ $\rho := \begin{bmatrix} 0.526 \\ 1 \end{bmatrix}$

$\sigma_{Rd.local.mid} := \frac{\rho \cdot f_{y.plate}}{\gamma_{m0}} = \begin{bmatrix} 241.96 \\ 460 \end{bmatrix} \; MPa$ $\kappa_\tau := 5.34 + 4 \left(\frac{B_{panel.mid}}{\alpha} \right)^2 = 5.525$

$$\lambda_w := \frac{B_{panel.mid}}{37.4 \cdot t_w \cdot \varepsilon \cdot (\kappa_\tau)^{0.5}} = 0.877$$

$$\chi_w := \begin{cases} \eta & \text{if } \lambda_w \le \dfrac{0.65}{\eta} \\ \dfrac{0.65}{\lambda_w} & \text{else if } \dfrac{0.65}{\eta} < \lambda_w < 0.65 \\ \dfrac{1.56}{0.91+\lambda_w} & \text{else} \end{cases} = 0.873 \qquad \tau_{Rd} := \chi_w \cdot \frac{f_{y.plate}}{\sqrt{3} \cdot \gamma_{m1}} = 231.901 \text{ MPa}$$

$\eta_3 := \dfrac{\tau_{Ed}}{\tau_{Rd}}$ According to 93-1-5 no interaction will be checked for : $\tau_{Ed} \le 0.5 \cdot \tau_{Rd}$

So, it is assumed that $\tau_{Ed} = 0.5 \cdot \tau_{Rd}$

$$\tau_{Ed} := 0.5 \cdot \tau_{Rd} = 115.951 \text{ MPa}$$

$B_{brutto} := 700 \text{ mm}$ $B_{s1} := 400 \text{ mm}$ $B_{s2} := 450 \text{ mm}$ $B_{tot} = 2.685 \text{ m}$

$B_{panel.mid} := B_{tot} - 2 \cdot B_{brutto} - \dfrac{B_{s1}}{2} - \dfrac{B_{s2}}{2} = 860 \text{ mm}$ $t_w := 20 \text{ mm}$

$a := \dfrac{\alpha}{B_{panel.mid}} = 4.651$ $h_w := B_{panel.mid}$

Assuming that we have pure compression σxtop=σxbottom, and another time assuming that we have compression at the top and tension at the bottom i.e:

$\sigma_{x.top} := \begin{bmatrix} 1 \\ -1 \end{bmatrix}$ $\sigma_{x.bottom} := \begin{bmatrix} 1 \\ 1 \end{bmatrix}$ $f_{y.plate} := 460 \text{ MPa}$

$\psi := \dfrac{\sigma_{x.top}}{\sigma_{x.bottom}} = \begin{bmatrix} 1 \\ -1 \end{bmatrix}$ $\varepsilon := \sqrt{\dfrac{235 \text{ MPa}}{f_{y.plate}} \cdot \dfrac{E}{210 \text{ GPa}}} = 0.698$

$\kappa_\sigma := \begin{bmatrix} 4 \\ 23.9 \end{bmatrix}$ $\lambda_{p.x} := \left(\dfrac{B_{panel.mid}}{t_w \cdot 28.4 \cdot \varepsilon \cdot \sqrt{\kappa_\sigma}} \right) = \begin{bmatrix} 1.085 \\ 0.444 \end{bmatrix}$ $\gamma_{m0} := 1$

$$\rho := \frac{0.772}{\lambda_{p.x}} - \frac{0.079}{{\lambda_{p.x}}^2} = \begin{bmatrix} 0.644 \\ 1.338 \end{bmatrix} \qquad \rho := \begin{bmatrix} 0.644 \\ 1 \end{bmatrix}$$

$$\sigma_{Rd.local.mid} := \frac{\rho \cdot f_{y.plate}}{\gamma_{m0}} = \begin{bmatrix} 296.24 \\ 460 \end{bmatrix} \mathbf{MPa} \qquad \kappa_\tau := 5.34 + 4 \left(\frac{B_{panel.mid}}{\alpha}\right)^2 = 5.525$$

$$\lambda_w := \frac{B_{panel.mid}}{37.4 \cdot t_w \cdot \varepsilon \cdot \left(\kappa_\tau\right)^{0.5}} = 0.701$$

$$\chi_w := \begin{cases} \eta & \text{if } \lambda_w \le \dfrac{0.65}{\eta} \\ \dfrac{0.65}{\lambda_w} & \text{else if } \dfrac{0.65}{\eta} < \lambda_w < 0.65 \\ \dfrac{1.56}{0.91 + \lambda_w} & \text{else} \end{cases} = 0.968 \qquad \tau_{Rd} := \chi_w \cdot \frac{f_{y.plate}}{\sqrt{3} \cdot \gamma_{m1}} = 257.133 \ \mathbf{MPa}$$

$\eta_3 := \dfrac{\tau_{Ed}}{\tau_{Rd}}$ According to 93-1-5 no interaction will be checked for : $\tau_{Ed} \le 0.5 \cdot \tau_{Rd}$

So, it is assumed that $\tau_{Ed} = 0.5 \cdot \tau_{Rd}$

$\tau_{Ed} := 0.5 \cdot \tau_{Rd} = 128.567 \ \mathbf{MPa}$

$B_{brutto} := 700\ mm \qquad B_{s1} := 400\ mm \qquad B_{s2} := 450\ mm \qquad B_{tot} = 2.685\ m$

$$B_{panel.mid} := B_{tot} - 2 \cdot B_{brutto} - \frac{B_{s1}}{2} - \frac{B_{s2}}{2} = 860\ mm \qquad t_w := 25\ mm$$

$$a := \frac{\alpha}{B_{panel.mid}} = 4.651 \qquad h_w := B_{panel.mid}$$

Assuming that we have pure compression σxtop=σxbottom, and another time assuming that we have compression at the top and tension at the bottom i.e:

$$\sigma_{x.top} := \begin{bmatrix} 1 \\ -1 \end{bmatrix} \quad \sigma_{x.bottom} := \begin{bmatrix} 1 \\ 1 \end{bmatrix} \qquad f_{y.plate} := 460\ MPa$$

$$\psi := \frac{\sigma_{x.top}}{\sigma_{x.bottom}} = \begin{bmatrix} 1 \\ -1 \end{bmatrix} \qquad \varepsilon := \sqrt{\frac{235\ MPa}{f_{y.plate}} \cdot \frac{E}{210\ GPa}} = 0.698$$

$$\kappa_\sigma := \begin{bmatrix} 4 \\ 23.9 \end{bmatrix} \qquad \lambda_{p.x} := \left(\frac{B_{panel.mid}}{t_w \cdot 28.4 \cdot \varepsilon \cdot \sqrt{\kappa_\sigma}} \right) = \begin{bmatrix} 0.868 \\ 0.355 \end{bmatrix} \qquad \gamma_{m0} := 1$$

$$\rho := \frac{0.772}{\lambda_{p.x}} - \frac{0.079}{{\lambda_{p.x}}^2} = \begin{bmatrix} 0.784 \\ 1.547 \end{bmatrix} \qquad \rho := \begin{bmatrix} 0.784 \\ 1 \end{bmatrix}$$

$$\sigma_{Rd.local.mid} := \frac{\rho \cdot f_{y.plate}}{\gamma_{m0}} = \begin{bmatrix} 360.64 \\ 460 \end{bmatrix} MPa \qquad \kappa_\tau := 5.34 + 4 \left(\frac{B_{panel.mid}}{\alpha} \right)^2 = 5.525$$

$$\lambda_w := \frac{B_{panel.mid}}{37.4 \cdot t_w \cdot \varepsilon \cdot (\kappa_\tau)^{0.5}} = 0.561$$

$$\chi_w := \begin{cases} \eta & \text{if } \lambda_w \le \frac{0.65}{\eta} \\ \frac{0.65}{\lambda_w} & \text{else if } \frac{0.65}{\eta} < \lambda_w < 0.65 \\ \frac{1.56}{0.91 + \lambda_w} & \text{else} \end{cases} = 1.159 \qquad \tau_{Rd} := \chi_w \cdot \frac{f_{y.plate}}{\sqrt{3} \cdot \gamma_{m1}} = 307.713\ MPa$$

$\eta_3 := \frac{\tau_{Ed}}{\tau_{Rd}}$ According to 93-1-5 no interaction will be checked for : $\tau_{Ed} \le 0.5 \cdot \tau_{Rd}$

So, it is assumed that $\tau_{Ed} = 0.5 \cdot \tau_{Rd}$

$\tau_{Ed} := 0.5 \cdot \tau_{Rd} = 153.857\ MPa$

Global buckling check of the web:

The global buckling check of the web is done using EBPlate for the northern side of the bridge with the following dimensions and input data:

In order to avoid stress interaction we got a maximum value for transverse stresses in a single panel buckling $\sigma_{y.RD} := 40\ MPa$ and maximum shear stress is less than $\tau_{ED} := 159.35\ MPa$, regardless the plate thickness.
the stiffeners will not buckle upp to 291MPa, according to the buckling checks.

We will check now using EBplate the maximum shear stress resistance for the plate with three different dimensions 16, 20, 25 mm. and to insure that all of these resistances are larger than 318 to avoid interaction.

$fyw := 460\ MPa \quad h_w := 2685\ mm \qquad \varepsilon = 0.698 \qquad i := 0..2 \qquad t_w := \begin{bmatrix} 16 \\ 20 \\ 25 \end{bmatrix} mm$

$$\tau_{cr} := \begin{bmatrix} 442 \\ 572 \\ 721 \end{bmatrix} MPa \qquad \lambda_w := 0.76 \cdot \sqrt{\frac{fyw}{\tau_{cr}}} = \begin{bmatrix} 0.775 \\ 0.682 \\ 0.607 \end{bmatrix}$$

$$\chi_i := \begin{cases} \eta & \text{if } \lambda_{w_i} \le \dfrac{0.65}{\eta} \\ \dfrac{0.65}{\lambda_{w_i}} & \text{else if } \dfrac{0.65}{\eta} < \lambda_{w_i} < 0.65 \\ \dfrac{1.56}{0.91 + \lambda_{w_i}} & \text{else} \end{cases} = \begin{bmatrix} 0.926 \\ 0.98 \\ 1.071 \end{bmatrix}$$

$$\tau_{Rd} := \chi \cdot \frac{f_{y.plate}}{\sqrt{3} \cdot \gamma_{m1}} = \begin{bmatrix} 245.832 \\ 260.317 \\ 284.371 \end{bmatrix} MPa$$

All of the upper values are smaller than 318 for single panel buckling, but at the same time equal or larger than the critical shear stress value calculated in the original design (246MPa), this mean that interaction is not needed in this situation too as all of shear stresses did not exceed 123MPa

Hence only the stability for longitudinal stess need to be verified. From single panel beckling tha maximum allowed stress on the middle panel is 242 MPa. thus we choose the following stress distributon as the most critical case for web buckling.
in most cases web will have compression at one side and tension at another, and in critical case web will have compression stress at one side and zero stress at the other side. This compression stress at one side is chosen to be 300 MPa in order not to exceed the maximum allowed stress in a single panel.

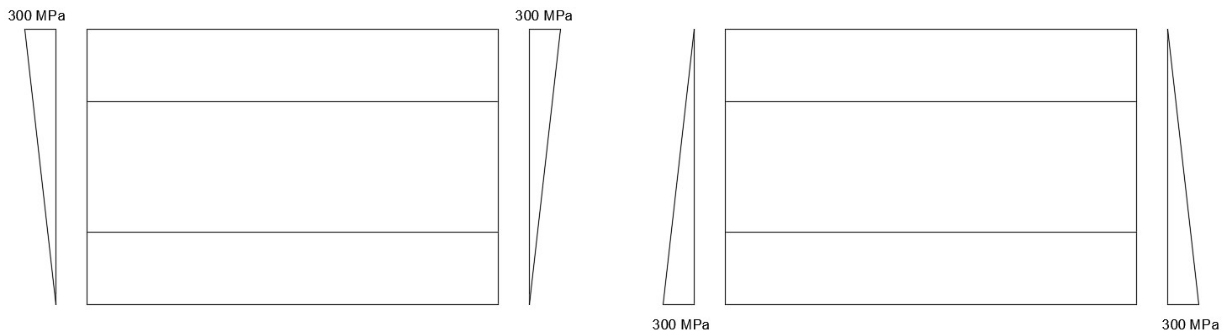

These checks are done using EBplate. When checking for plate type buckling the single panel buckling mode is switched of in EBplate. We get the following results when compression at the top:

Plate type buckling: 16, 20, 25:

Maximum stress at the top:

EBplate: $\phi_t := \begin{bmatrix} 2.508 \\ 2.706 \\ 3.01 \end{bmatrix}$ $\sigma_{cr.top} := 300\ MPa \cdot \phi_t = \begin{bmatrix} 752.4 \\ 811.8 \\ 903 \end{bmatrix} MPa$ $fyw = 460\ MPa$

$$\lambda_p := \sqrt{\frac{fyw}{\sigma_{cr.top}}} = \begin{bmatrix} 0.782 \\ 0.753 \\ 0.714 \end{bmatrix} \qquad \rho_{p.t} := \frac{0.772}{\lambda_p} - \frac{0.125}{\lambda_p^{\ 2}} = \begin{bmatrix} 0.783 \\ 0.805 \\ 0.836 \end{bmatrix}$$

Maximum stress at the bottom:

EBplate: $\phi_b := \begin{bmatrix} 3.77 \\ 3.86 \\ 3.98 \end{bmatrix}$ $\sigma_{cr.bot} := 300\ MPa \cdot \phi_b = \begin{bmatrix} 1.131 \cdot 10^3 \\ 1.158 \cdot 10^3 \\ 1.194 \cdot 10^3 \end{bmatrix} MPa$

$$\lambda_p := \sqrt{\frac{fyw}{\sigma_{cr.bot}}} = \begin{bmatrix} 0.638 \\ 0.63 \\ 0.621 \end{bmatrix} \qquad \rho_{p.b} := \frac{0.772}{\lambda_p} - \frac{0.125}{\lambda_p^{\ 2}} = \begin{bmatrix} 0.903 \\ 0.91 \\ 0.919 \end{bmatrix}$$

Column type buckling:

Compression at the top: Stiffener T1

$t := 16\ mm \qquad a := 4000\ mm \qquad E := 200\ GPa$

Stiffener T1 effective cross section due to shear lag as the stresses will not exceed local buckling stresses:

$\alpha_0 := 1 \qquad L_e := 4000\ mm = 4\ m$

Hogging:

Inside stiffener $\quad b_0 := \dfrac{400}{2}\ mm \qquad \kappa := \dfrac{\alpha_0 \cdot b_0}{L_e} = 0.05$

$$\beta_{ult} := \frac{1}{1 + 6 \cdot \left(\kappa - \dfrac{1}{2500 \cdot \kappa}\right) + 1.6 \cdot \kappa^2} = 0.796 \qquad b_{eff.1} := \beta_{ult} \cdot b_0 = 159.236\ mm$$

Upper plate: $\quad b_0 := 500\ mm \qquad \kappa := \dfrac{\alpha_0 \cdot b_0}{L_e} = 0.125$

$$\beta_{ult} := \frac{1}{1 + 6 \cdot \left(\kappa - \dfrac{1}{2500 \cdot \kappa}\right) + 1.6 \cdot \kappa^2} = 0.57 \qquad b_{eff.2} := \beta_{ult} \cdot b_0 = 284.77\ mm$$

Middle plate $\quad b_0 := 860\ mm \qquad \kappa := \dfrac{\alpha_0 \cdot b_0}{L_e} = 0.215$

$$\beta_{ult} := \frac{1}{1 + 6 \cdot \left(\kappa - \dfrac{1}{2500 \cdot \kappa}\right) + 1.6 \cdot \kappa^2} = 0.425 \qquad b_{eff.3} := \beta_{ult} \cdot b_0 = 365.522\ mm$$

$$b_{eff.bot} := 2 \cdot b_{eff.1} + b_{eff.2} + b_{eff.3} = 968.764\ mm$$

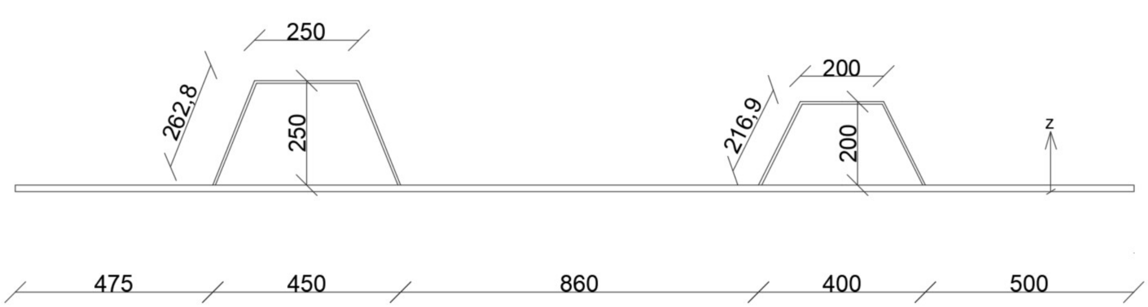

$A_{topflange} := 20\ cm \cdot 6\ mm = 12\ cm^2$

$Z_{top} := 197\ mm + t = 213\ mm$

$A_{topflange} \cdot Z_{top} = 255.6\ cm^3$

$A_{topflange} \cdot Z_{top}^{\ 2} = \left(5.444 \cdot 10^3\right)\ cm^4$

$I_{topflange} := 0$

$A_{web} := 2 \cdot 21.6\ cm \cdot 6\ mm = 25.92\ cm^2$

$Z_{web} := 116\ mm$

$A_{web} \cdot Z_{web} = 300.672\ cm^3$

$A_{web} \cdot Z_{web}^{\ 2} = \left(3.488 \cdot 10^3\right)\ cm^4$

$I_{web} := 814\ cm^4$

$A_{bottomflange} := b_{eff.bot} \cdot t = 155.002\ cm^2$

$Z_{bot.flange} := \dfrac{t}{2} = 8\ mm$

$A_{bottomflange} \cdot Z_{bot.flange} = 124.002\ cm^3$

$A_{bottomflange} \cdot Z_{bot.flange}^{\ 2} = 99.201\ cm^4$

$$I_{bot} := \frac{b_{eff.bot} \cdot t^3}{12} = 33.067\ cm^4$$

$A_{tot} := A_{topflange} + A_{web} + A_{bottomflange} = 192.922\ cm^2$

$AZ_{tot} := A_{topflange} \cdot Z_{top} + A_{web} \cdot Z_{web} + A_{bottomflange} \cdot Z_{bot.flange} = 680.274\ cm^3$

$$Cg := \frac{AZ_{tot}}{A_{tot}} = 3.526\ cm$$

$$I_{tot} := I_{topflange} + A_{topflange} \cdot \left(Z_{top} - Cg\right)^2 + I_{web} + A_{web} \cdot \left(Z_{web} - Cg\right)^2 + I_{bot} + A_{bottomflange} \cdot \left(Z_{bot.flange} - Cg\right)^2$$

$I_{sl} := I_{tot} = \left(7.48 \cdot 10^{-5}\right)\ m^4$

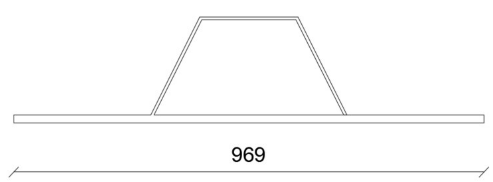

$$\sigma_{cr.sl} := \frac{(3.14)^2 \cdot E \cdot I_{sl}}{A_{tot} \cdot a^2} = 477.821\ MPa$$

Linear interpolation:

$\sigma_{cr.c} := 645\ MPa$ $\qquad f_{yk} := 460\ MPa$

$$\lambda_c := \sqrt{\frac{f_{yk}}{\sigma_{cr.c}}} = 0.844$$

EN 1993-1-4 table 5.3: A1.17.2017 Table 6.1

$\alpha := 0.49$ $\lambda_0 := 0.2$ $\phi := 0.5 \cdot \left(1 + \alpha \cdot \left(\lambda_c - \lambda_0\right) + {\lambda_c}^2\right) = 1.014$

$\chi_c := \dfrac{1}{\phi + \left(\phi^2 - {\lambda_c}^2\right)^{0.5}} = 0.634$ $\sigma_{cr.p} := \sigma_{cr.top_0} = 752.4\ MPa$

$\xi := \dfrac{\sigma_{cr.p}}{\sigma_{cr.c}} - 1 = 0.167$

$\rho_c := \left(\rho_{p.t_0} - \chi_c\right) \cdot \xi \cdot (2 - \xi) + \chi_c = 0.68$ $\sigma_{Rd} := \rho_c \cdot \dfrac{f_{yk}}{1} = 312.63\ MPa$

$t := 20\ mm$

$A_{topflange} := 20\ cm \cdot 6\ mm = 12\ cm^2$ $Z_{top} := 197\ mm + t = 217\ mm$

$A_{topflange} \cdot Z_{top} = 260.4\ cm^3$ $A_{topflange} \cdot {Z_{top}}^2 = \left(5.651 \cdot 10^3\right)\ cm^4$

$I_{topflange} := 0$

$A_{web} := 2 \cdot 21.6\ cm \cdot 6\ mm = 25.92\ cm^2$ $Z_{web} := 100\ mm + t = 120\ mm$

$A_{web} \cdot Z_{web} = 311.04\ cm^3$ $A_{web} \cdot {Z_{web}}^2 = \left(3.732 \cdot 10^3\right)\ cm^4$

$I_{web} := 814\ cm^4$

$A_{bottomflange} := b_{eff.bot} \cdot t = 193.753\ cm^2$ $Z_{bot.flange} := \dfrac{t}{2} = 10\ mm$

$A_{bottomflange} \cdot Z_{bot.flange} = 193.753\ cm^3$ $A_{bottomflange} \cdot {Z_{bot.flange}}^2 = 193.753\ cm^4$

$I_{bot} := \dfrac{b_{eff.bot} \cdot t^3}{12} = 64.584\ cm^4$

$A_{tot} := A_{topflange} + A_{web} + A_{bottomflange} = 231.673\ cm^2$

$AZ_{tot} := A_{topflange} \cdot Z_{top} + A_{web} \cdot Z_{web} + A_{bottomflange} \cdot Z_{bot.flange} = 765.193\ cm^3$

$Cg := \dfrac{AZ_{tot}}{A_{tot}} = 3.303\ cm$

$I_{tot} := I_{topflange} + A_{topflange} \cdot \left(Z_{top} - Cg\right)^2 + I_{web} + A_{web} \cdot \left(Z_{web} - Cg\right)^2 + I_{bot} + A_{bottomflange} \cdot \left(Z_{bot.flange} - Cg\right)^2$

$I_{sl} := I_{tot} = \left(7.928 \cdot 10^{-5}\right)\ m^4$

$$\sigma_{cr.sl} := \frac{(3.14)^2 \cdot E \cdot I_{sl}}{A_{tot} \cdot a^2} = 421.76\ MPa$$

Linear interpolation:

$\sigma_{cr.c} := 570\ MPa$ $\quad f_{yk} := 460\ MPa$ $\quad \lambda_c := \sqrt{\frac{f_{yk}}{\sigma_{cr.c}}} = 0.898$

EN 1993-1-4 table 5.3: A1.17.2017 Table 6.1

$\alpha := 0.49$ $\quad \lambda_0 := 0.2$ $\quad \phi := 0.5 \cdot \left(1 + \alpha \cdot \left(\lambda_c - \lambda_0\right) + {\lambda_c}^2\right) = 1.075$

$\chi_c := \frac{1}{\phi + \left(\phi^2 - {\lambda_c}^2\right)^{0.5}} = 0.601$ $\quad \sigma_{cr.p} := \sigma_{cr.top_1} = 811.8\ MPa$

$\xi := \frac{\sigma_{cr.p}}{\sigma_{cr.c}} - 1 = 0.424$

$\rho_c := \left(\rho_{p.t_1} - \chi_c\right) \cdot \xi \cdot (2 - \xi) + \chi_c = 0.737$ $\quad \sigma_{Rd} := \rho_c \cdot \frac{f_{yk}}{1} = 339.156\ MPa$

$t := 25\ mm$

$A_{topflange} := 20\ cm \cdot 6\ mm = 12\ cm^2$ $\quad Z_{top} := 197\ mm + t = 222\ mm$

$A_{topflange} \cdot Z_{top} = 266.4\ cm^3$ $\quad A_{topflange} \cdot {Z_{top}}^2 = \left(5.914 \cdot 10^3\right)\ cm^4$

$I_{topflange} := 0$

$A_{web} := 2 \cdot 21.6\ cm \cdot 6\ mm = 25.92\ cm^2$ $\quad Z_{web} := 100\ mm + t = 125\ mm$

$A_{web} \cdot Z_{web} = 324\ cm^3$ $\quad A_{web} \cdot {Z_{web}}^2 = \left(4.05 \cdot 10^3\right)\ cm^4$

$I_{web} := 814\ cm^4$

$A_{bottomflange} := b_{eff.bot} \cdot t = 242.191\ cm^2$ $\quad Z_{bot.flange} := \frac{t}{2} = 12.5\ mm$

$A_{bottomflange} \cdot Z_{bot.flange} = 302.739\ cm^3$ $\quad A_{bottomflange} \cdot {Z_{bot.flange}}^2 = 378.424\ cm^4$

$I_{bot} := \frac{b_{eff.bot} \cdot t^3}{12} = 126.141\ cm^4$

$A_{tot} := A_{topflange} + A_{web} + A_{bottomflange} = 280.111\ cm^2$

$$AZ_{tot} := A_{topflange} \cdot Z_{top} + A_{web} \cdot Z_{web} + A_{bottomflange} \cdot Z_{bot.flange} = 893.139 \; cm^3$$

$$Cg := \frac{AZ_{tot}}{A_{tot}} = 3.189 \; cm$$

$$I_{tot} := I_{topflange} + A_{topflange} \cdot \left(Z_{top} - Cg\right)^2 + I_{web} + A_{web} \cdot \left(Z_{web} - Cg\right)^2 + I_{bot} + A_{bottomflange} \cdot \left(Z_{bot.flange} - Cg\right)^2$$

$$I_{sl} := I_{tot} = \left(8.435 \cdot 10^{-5}\right) \; m^4$$

$$\sigma_{cr.sl} := \frac{(3.14)^2 \cdot E \cdot I_{sl}}{A_{tot} \cdot a^2} = 371.122 \; MPa$$

Linear interpolation:

$$\sigma_{cr.c} := 501 \; MPa \qquad f_{yk} := 460 \; MPa \qquad \lambda_c := \sqrt{\frac{f_{yk}}{\sigma_{cr.c}}} = 0.958$$

EN 1993-1-4 table 5.3: A1.17.2017 Table 6.1

$$\alpha := 0.49 \qquad \lambda_0 := 0.2 \qquad \phi := 0.5 \cdot \left(1 + \alpha \cdot \left(\lambda_c - \lambda_0\right) + {\lambda_c}^2\right) = 1.145$$

$$\chi_c := \frac{1}{\phi + \left(\phi^2 - {\lambda_c}^2\right)^{0.5}} = 0.565 \qquad \sigma_{cr.p} := \sigma_{cr.top_2} = 903 \; MPa$$

$$\xi := \frac{\sigma_{cr.p}}{\sigma_{cr.c}} - 1 = 0.802$$

$$\rho_c := \left(\rho_{p.t_2} - \chi_c\right) \cdot \xi \cdot (2 - \xi) + \chi_c = 0.826 \qquad \sigma_{Rd} := \rho_c \cdot \frac{f_{yk}}{1} = 379.798 \; MPa$$

Compression at the bottom: Stiffener T2

$t := 16\ mm$ $a := 4000\ mm$ $E := 200\ GPa$

Stiffener T1 effective cross section due to shear lag as the stresses will not exceed local buckling stresses:

$\alpha_0 := 1$ $L_e := 4000\ mm = 4\ m$

Hogging:

Inside stiffener $b_0 := \frac{450}{2}\ mm$ $\kappa := \frac{\alpha_0 \cdot b_0}{L_e} = 0.056$

$$\beta_{ult} := \frac{1}{1 + 6 \cdot \left(\kappa - \frac{1}{2500 \cdot \kappa}\right) + 1.6 \cdot \kappa^2} = 0.769 \qquad b_{eff.1} := \beta_{ult} \cdot b_0 = 173.091\ mm$$

Middl plate: $b_0 := 860\ mm$ $\kappa := \frac{\alpha_0 \cdot b_0}{L_e} = 0.215$

$$\beta_{ult} := \frac{1}{1 + 6 \cdot \left(\kappa - \frac{1}{2500 \cdot \kappa}\right) + 1.6 \cdot \kappa^2} = 0.425 \qquad b_{eff.2} := \beta_{ult} \cdot b_0 = 365.522\ mm$$

Lower plate $b_0 := 475\ mm$ $\kappa := \frac{\alpha_0 \cdot b_0}{L_e} = 0.119$

$$\beta_{ult} := \frac{1}{1 + 6 \cdot \left(\kappa - \frac{1}{2500 \cdot \kappa}\right) + 1.6 \cdot \kappa^2} = 0.583 \qquad b_{eff.3} := \beta_{ult} \cdot b_0 = 276.992\ mm$$

$b_{eff.bot} := 2 \cdot b_{eff.1} + b_{eff.2} + b_{eff.3} = 988.696\ mm$

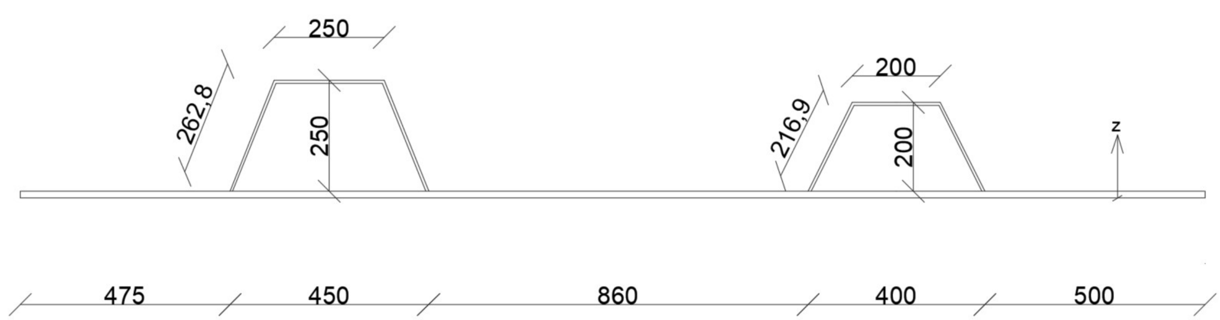

$A_{topflange} := 25\ cm \cdot 6\ mm = 15\ cm^2$

$Z_{top} := 247\ mm + t = 263\ mm$

$A_{topflange} \cdot Z_{top} = 394.5\ cm^3$

$A_{topflange} \cdot Z_{top}^{\ 2} = \left(1.038 \cdot 10^4\right)\ cm^4$

$I_{topflange} := 0$

$A_{web} := 2 \cdot 26.3\ cm \cdot 6\ mm = 31.56\ cm^2$

$Z_{web} := \dfrac{250\ mm}{2} + t = 141\ mm$

$A_{web} \cdot Z_{web} = 444.996\ cm^3$

$A_{web} \cdot Z_{web}^{\ 2} = \left(6.274 \cdot 10^3\right)\ cm^4$

$I_{web} := 1562.5\ cm^4$

$A_{bottomflange} := b_{eff.bot} \cdot t = 158.191\ cm^2$

$Z_{bot.flange} := \dfrac{t}{2} = 8\ mm$

$A_{bottomflange} \cdot Z_{bot.flange} = 126.553\ cm^3$

$A_{bottomflange} \cdot Z_{bot.flange}^{\ 2} = 101.242\ cm^4$

$$I_{bot} := \frac{b_{eff.bot} \cdot t^3}{12} = 33.747\ cm^4$$

$$A_{tot} := A_{topflange} + A_{web} + A_{bottomflange} = 204.751\ cm^2$$

$$AZ_{tot} := A_{topflange} \cdot Z_{top} + A_{web} \cdot Z_{web} + A_{bottomflange} \cdot Z_{bot.flange} = 966.049\ cm^3$$

$$Cg := \frac{AZ_{tot}}{A_{tot}} = 4.718\ cm$$

$$I_{tot} := I_{topflange} + A_{topflange} \cdot \left(Z_{top} - Cg\right)^2 + I_{web} + A_{web} \cdot \left(Z_{web} - Cg\right)^2 + I_{bot} + A_{bottomflange} \cdot \left(Z_{bot.flange} - Cg\right)^2$$

$$I_{sl} := I_{tot} = \left(1.379 \cdot 10^{-4}\right)\ m^4$$

$$\sigma_{cr.sl} := \frac{(3.14)^2 \cdot E \cdot I_{sl}}{A_{tot} \cdot a^2} = 830.014\ MPa$$

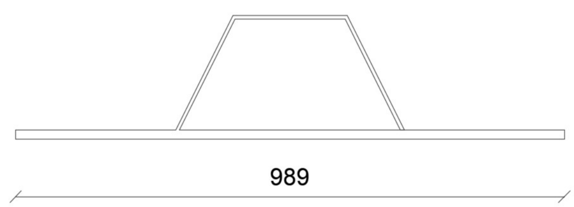

Linear interpolation:

$\sigma_{cr.c} := 1125.4\ MPa \qquad f_{yk} := 460\ MPa$

$$\lambda_c := \sqrt{\frac{f_{yk}}{\sigma_{cr.c}}} = 0.639$$

EN 1993-1-4 table 5.3: A1.17.2017 Table 6.1

$\alpha := 0.49$ $\quad \lambda_0 := 0.2$ $\quad \phi := 0.5 \cdot \left(1 + \alpha \cdot \left(\lambda_c - \lambda_0\right) + {\lambda_c}^2\right) = 0.812$

$\chi_c := \dfrac{1}{\phi + \left(\phi^2 - {\lambda_c}^2\right)^{0.5}} = 0.762$ $\quad \sigma_{cr.p} := \sigma_{cr.bot_0} = \left(1.131 \cdot 10^3\right)\ MPa$

$\xi := \dfrac{\sigma_{cr.p}}{\sigma_{cr.c}} - 1 = 0.005$

$\rho_c := \left(\rho_{p.b_0} - \chi_c\right) \cdot \xi \cdot \left(2 - \xi\right) + \chi_c = 0.763$ $\quad \sigma_{Rd} := \rho_c \cdot \dfrac{f_{yk}}{1} = 351.089\ MPa$

$t := 20\ mm$

$A_{topflange} := 25\ cm \cdot 6\ mm = 15\ cm^2$ $\quad Z_{top} := 247\ mm + t = 267\ mm$

$A_{topflange} \cdot Z_{top} = 400.5\ cm^3$ $\quad A_{topflange} \cdot {Z_{top}}^2 = \left(1.069 \cdot 10^4\right)\ cm^4$

$I_{topflange} := 0$

$A_{web} := 2 \cdot 26.3\ cm \cdot 6\ mm = 31.56\ cm^2$ $\quad Z_{web} := \dfrac{250\ mm}{2} + t = 145\ mm$

$A_{web} \cdot Z_{web} = 457.62\ cm^3$ $\quad A_{web} \cdot {Z_{web}}^2 = \left(6.635 \cdot 10^3\right)\ cm^4$

$I_{web} := 1562.5\ cm^4$

$A_{bottomflange} := b_{eff.bot} \cdot t = 197.739\ cm^2$ $\quad Z_{bot.flange} := \dfrac{t}{2} = 10\ mm$

$A_{bottomflange} \cdot Z_{bot.flange} = 197.739\ cm^3$ $\quad A_{bottomflange} \cdot {Z_{bot.flange}}^2 = 197.739\ cm^4$

$I_{bot} := \dfrac{b_{eff.bot} \cdot t^3}{12} = 65.913\ cm^4$

$A_{tot} := A_{topflange} + A_{web} + A_{bottomflange} = 244.299\ cm^2$

$AZ_{tot} := A_{topflange} \cdot Z_{top} + A_{web} \cdot Z_{web} + A_{bottomflange} \cdot Z_{bot.flange} = \left(1.056 \cdot 10^3\right)\ cm^3$

$Cg := \dfrac{AZ_{tot}}{A_{tot}} = 4.322\ cm$

$I_{tot} := I_{topflange} + A_{topflange} \cdot \left(Z_{top} - Cg\right)^2 + I_{web} + A_{web} \cdot \left(Z_{web} - Cg\right)^2 + I_{bot} + A_{bottomflange} \cdot \left(Z_{bot.flange} - Cg\right)^2$

$I_{sl} := I_{tot} = \left(1.459 \cdot 10^{-4}\right)\ m^4$

$$\sigma_{cr.sl} := \frac{(3.14)^2 \cdot E \cdot I_{sl}}{A_{tot} \cdot a^2} = 736.122 \; MPa$$

Linear interpolation:

$\sigma_{cr.c} := 998 \; MPa$ $\qquad f_{yk} := 460 \; MPa$

$$\lambda_c := \sqrt{\frac{f_{yk}}{\sigma_{cr.c}}} = 0.679$$

EN 1993-1-4 table 5.3: A1.17.2017 Table 6.1

$\alpha := 0.49$ $\qquad \lambda_0 := 0.2$ $\qquad \phi := 0.5 \cdot \left(1 + \alpha \cdot \left(\lambda_c - \lambda_0\right) + {\lambda_c}^2\right) = 0.848$

$$\chi_c := \frac{1}{\phi + \left(\phi^2 - {\lambda_c}^2\right)^{0.5}} = 0.738 \qquad \sigma_{cr.p} := \sigma_{cr.bot_1} = \left(1.158 \cdot 10^3\right) \; MPa$$

$$\xi := \frac{\sigma_{cr.p}}{\sigma_{cr.c}} - 1 = 0.16$$

$$\rho_c := \left(\rho_{p.b_1} - \chi_c\right) \cdot \xi \cdot (2 - \xi) + \chi_c = 0.789 \qquad \sigma_{Rd} := \rho_c \cdot \frac{f_{yk}}{1} = 362.745 \; MPa$$

$t := 25 \; mm$

$A_{topflange} := 25 \; cm \cdot 6 \; mm = 15 \; cm^2$ $\qquad Z_{top} := 247 \; mm + t = 272 \; mm$

$A_{topflange} \cdot Z_{top} = 408 \; cm^3$ $\qquad A_{topflange} \cdot {Z_{top}}^2 = \left(1.11 \cdot 10^4\right) \; cm^4$

$I_{topflange} := 0$

$A_{web} := 2 \cdot 26.3 \; cm \cdot 6 \; mm = 31.56 \; cm^2$ $\qquad Z_{web} := \frac{250 \; mm}{2} + t = 150 \; mm$

$A_{web} \cdot Z_{web} = 473.4 \; cm^3$ $\qquad A_{web} \cdot {Z_{web}}^2 = \left(7.101 \cdot 10^3\right) \; cm^4$

$I_{web} := 1562.5 \; cm^4$

$A_{bottomflange} := b_{eff.bot} \cdot t = 247.174 \; cm^2$ $\qquad Z_{bot.flange} := \frac{t}{2} = 12.5 \; mm$

$A_{bottomflange} \cdot Z_{bot.flange} = 308.967 \; cm^3$ $\qquad A_{bottomflange} \cdot {Z_{bot.flange}}^2 = 386.209 \; cm^4$

$$I_{bot} := \frac{b_{eff.bot} \cdot t^3}{12} = 128.736 \; cm^4$$

$$A_{tot} := A_{topflange} + A_{web} + A_{bottomflange} = 293.734 \; cm^2$$

$$AZ_{tot} := A_{topflange} \cdot Z_{top} + A_{web} \cdot Z_{web} + A_{bottomflange} \cdot Z_{bot.flange} = \left(1.19 \cdot 10^{3}\right)\ cm^{3}$$

$$Cg := \frac{AZ_{tot}}{A_{tot}} = 4.053\ cm$$

$$I_{tot} := I_{topflange} + A_{topflange} \cdot \left(Z_{top} - Cg\right)^{2} + I_{web} + A_{web} \cdot \left(Z_{web} - Cg\right)^{2} + I_{bot} + A_{bottomflange} \cdot \left(Z_{bot.flange} - Cg\right)^{2}$$

$$I_{sl} := I_{tot} = \left(1.545 \cdot 10^{-4}\right)\ m^{4}$$

$$\sigma_{cr.sl} := \frac{(3.14)^{2} \cdot E \cdot I_{sl}}{A_{tot} \cdot a^{2}} = 648.337\ MPa$$

Linear interpolation:

$\sigma_{cr.c} := 878.6\ MPa$ $\qquad f_{yk} := 460\ MPa$

$$\lambda_{c} := \sqrt{\frac{f_{yk}}{\sigma_{cr.c}}} = 0.724$$

EN 1993-1-4 table 5.3: A1.17.2017 Table 6.1

$\alpha := 0.49$ $\qquad \lambda_{0} := 0.2$ $\qquad \phi := 0.5 \cdot \left(1 + \alpha \cdot \left(\lambda_{c} - \lambda_{0}\right) + \lambda_{c}^{2}\right) = 0.89$

$$\chi_{c} := \frac{1}{\phi + \left(\phi^{2} - \lambda_{c}^{2}\right)^{0.5}} = 0.71 \qquad \sigma_{cr.p} := \sigma_{cr.bot_{2}} = \left(1.194 \cdot 10^{3}\right)\ MPa$$

$$\xi := \frac{\sigma_{cr.p}}{\sigma_{cr.c}} - 1 = 0.359$$

$$\rho_{c} := \left(\rho_{p.b_{2}} - \chi_{c}\right) \cdot \xi \cdot \left(2 - \xi\right) + \chi_{c} = 0.833 \qquad \sigma_{Rd} := \rho_{c} \cdot \frac{f_{yk}}{1} = 383.329\ MPa$$

$$\begin{bmatrix} t & \sigma_{Rd.top} & \sigma_{Rd.bot} \\ 16 & -313 & 0 \\ 20 & -339 & 0 \\ 25 & -380 & 0 \\ 16 & 0 & -351 \\ 20 & 0 & -363 \\ 25 & 0 & -383 \end{bmatrix}$$

tweb [mm]	σRd,top [MPa]	σRd,bott [MPa]
16	-285	0
20	-310	0
25	-341	0
16	0	-291
20	0	-296
25	0	-312

Comparison between S355 and 1.4462 strength capacity, we have the follwoing:
For bottom field:

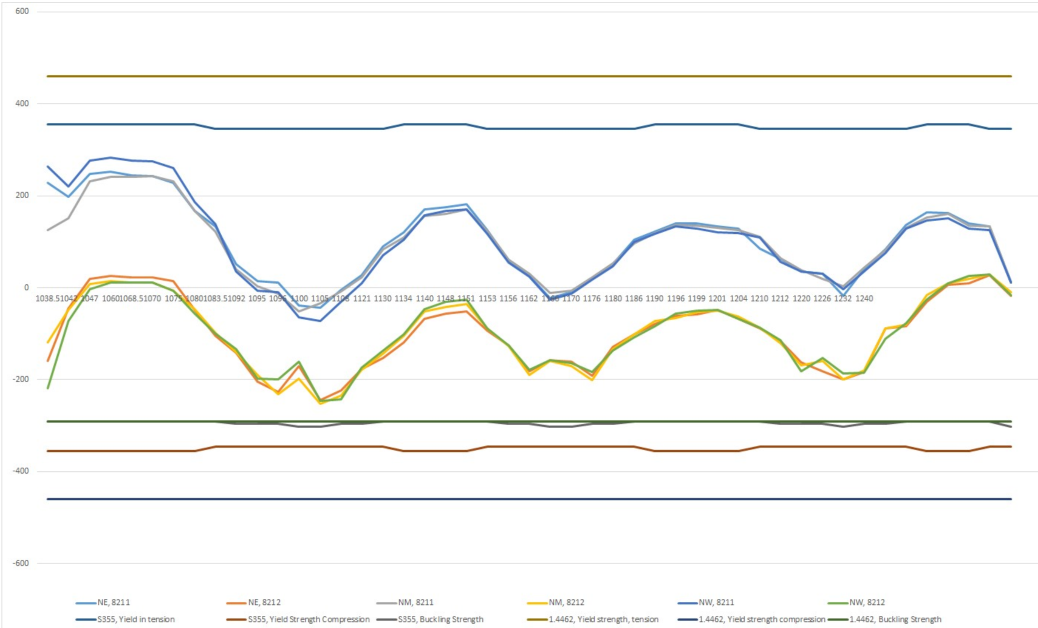

Top Field:

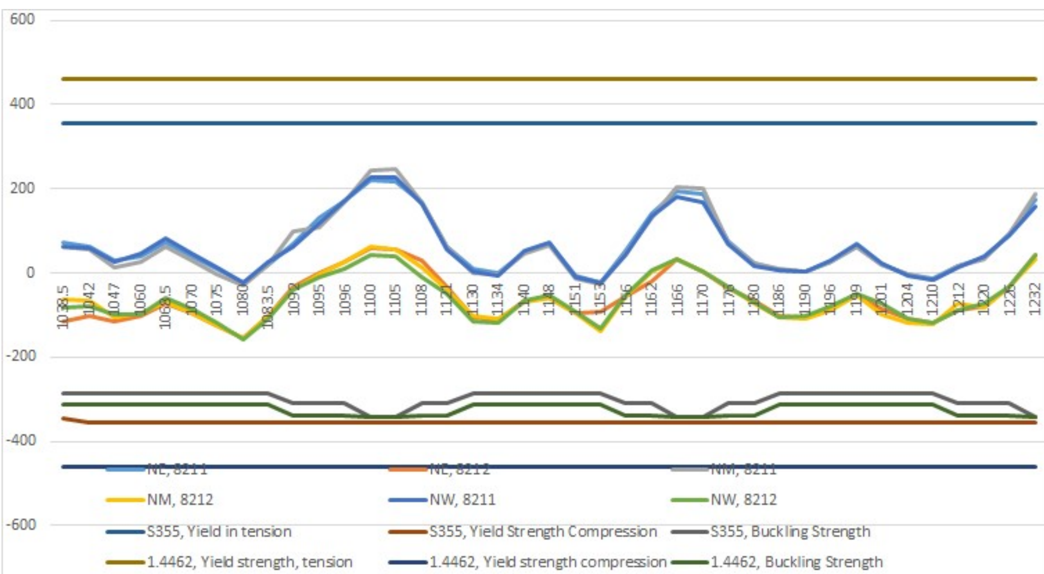

From the previous charts we see that buckling capacity for bottom field is not adequte to reduce the section thickness and this is due to the stiffener cpacity T2. we will try to increase T2 thickness in order to be able to acheive higher capacity and to reduce the web thickness

We repeat all of the previouse calculation exactly with the same geometry and by increasing only T2 thickness to 7mm. we have the following geometry:

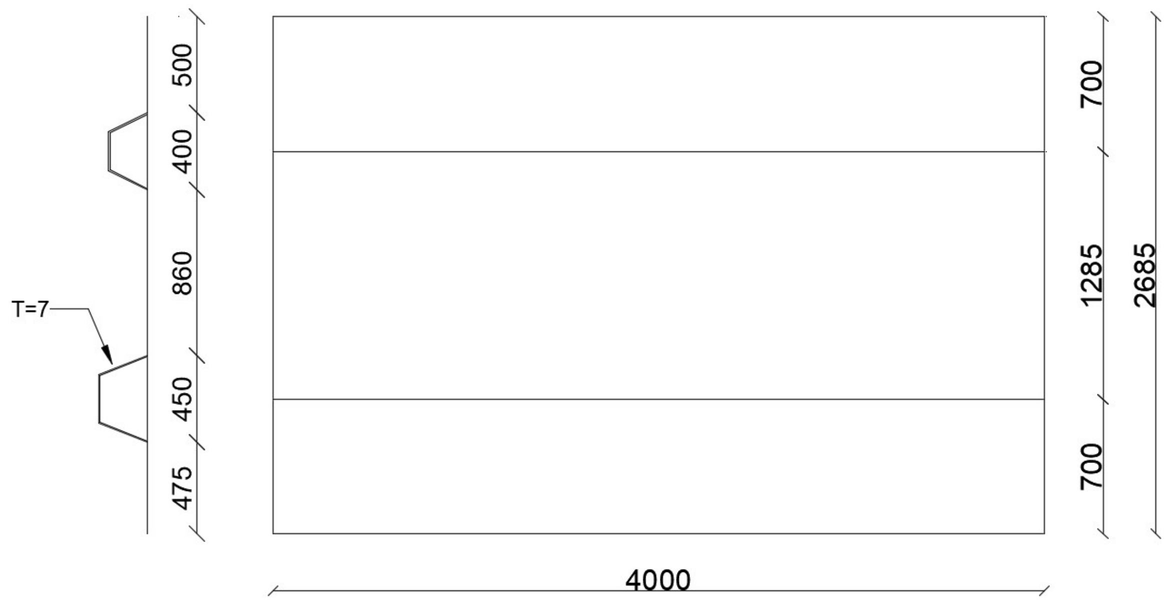

As we did not change the overall geometry there is no need to re-do shear stress check, transversal stress checks, and single panel buckling checks and we will redo the global buckling check for longitudinal stress

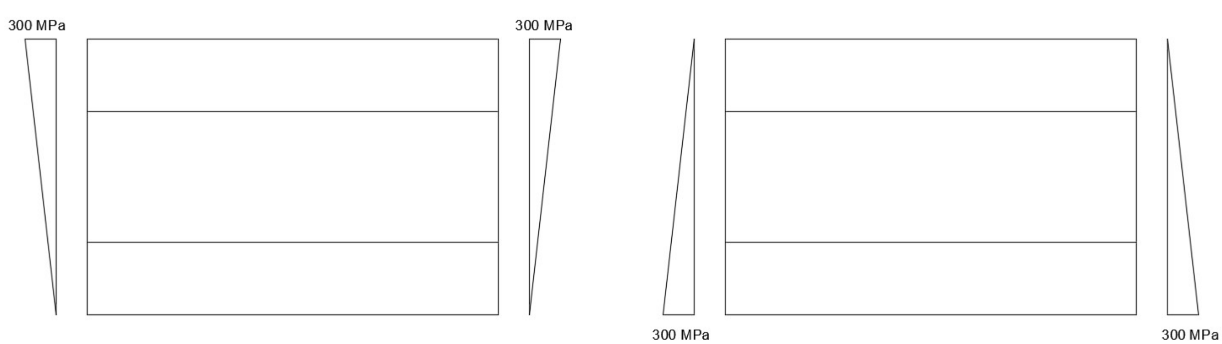

Using EBplate when compression at the top with 16, 20, 25mm we have the following results:

Plate type buckling: 16, 20, 25:

Maximum stress at the top:

EBplate: $\phi_t := \begin{bmatrix} 2.5118 \\ 2.7149 \\ 3.0397 \end{bmatrix}$ $\sigma_{cr.top} := 300\ MPa \cdot \phi_t = \begin{bmatrix} 753.54 \\ 814.47 \\ 911.91 \end{bmatrix} MPa$ $fyw = 460\ MPa$

$$\lambda_p := \sqrt{\frac{fyw}{\sigma_{cr.top}}} = \begin{bmatrix} 0.781 \\ 0.752 \\ 0.71 \end{bmatrix} \qquad \rho_{p.t} := \frac{0.772}{\lambda_p} - \frac{0.125}{\lambda_p^{\ 2}} = \begin{bmatrix} 0.783 \\ 0.806 \\ 0.839 \end{bmatrix}$$

Maximum stress at the bottom:

EBplate: $\phi_b := \begin{bmatrix} 4.0145 \\ 4.1217 \\ 4.2417 \end{bmatrix}$ $\sigma_{cr.bot} := 300\ MPa \cdot \phi_b = \begin{bmatrix} 1.204 \cdot 10^3 \\ 1.237 \cdot 10^3 \\ 1.273 \cdot 10^3 \end{bmatrix} MPa$

$$\lambda_p := \sqrt{\frac{fyw}{\sigma_{cr.bot}}} = \begin{bmatrix} 0.618 \\ 0.61 \\ 0.601 \end{bmatrix} \qquad \rho_{p.b} := \frac{0.772}{\lambda_p} - \frac{0.125}{\lambda_p^{\ 2}} = \begin{bmatrix} 0.922 \\ 0.93 \\ 0.938 \end{bmatrix}$$

Column type buckling:

Compression at the top: Stiffener T1

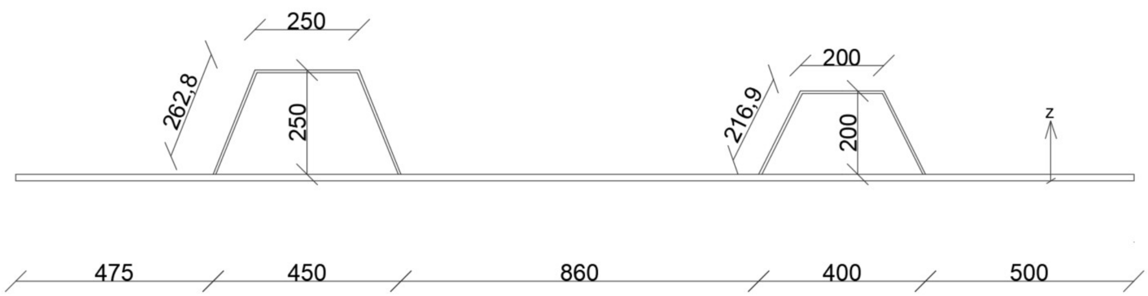

These values will not change and it remains simillar to the above calculations as there is no change in T1 thickness. only the interaction is repeated as the EBplate results for top field has also changes by changing the T2 thickness

$i := 0..2$ $\qquad \lambda_c := \begin{bmatrix} 0.844 \\ 0.898 \\ 0.958 \end{bmatrix}$ $\qquad \sigma_{cr.c} := \begin{bmatrix} 645 \\ 570 \\ 501 \end{bmatrix} MPa$

EN 1993-1-4 table 5.3: A1.17.2017 Table 6.1

$\alpha := 0.49$ $\qquad \lambda_0 := 0.2$ $\qquad \phi_i := 0.5 \cdot \left(1 + \alpha \cdot \left(\lambda_{c_i} - \lambda_0\right) + {\lambda_{c_i}}^2\right) = \begin{bmatrix} 1.014 \\ 1.074 \\ 1.145 \end{bmatrix}$

$\chi_{c_i} := \dfrac{1}{\phi_i + \left({\phi_i}^2 - {\lambda_{c_i}}^2\right)^{0.5}} = \begin{bmatrix} 0.635 \\ 0.601 \\ 0.565 \end{bmatrix}$ $\qquad \sigma_{cr.p} := \sigma_{cr.top} = \begin{bmatrix} 753.54 \\ 814.47 \\ 911.91 \end{bmatrix} MPa$

$\xi := \dfrac{\sigma_{cr.p}}{\sigma_{cr.c}} - 1 = \begin{bmatrix} 0.168 \\ 0.429 \\ 0.82 \end{bmatrix}$

$\rho_{c_i} := \left(\rho_{p.t_i} - \chi_{c_i}\right) \cdot \xi_i \cdot \left(2 - \xi_i\right) + \chi_{c_i} = \begin{bmatrix} 0.68 \\ 0.739 \\ 0.83 \end{bmatrix}$ $\qquad \sigma_{Rd} := \rho_c \cdot \dfrac{f_{yk}}{1} = \begin{bmatrix} 312.993 \\ 339.989 \\ 381.931 \end{bmatrix} MPa$

Compression at the bottom: Stiffener T2

$t := 16\ mm$ $\quad a := 4000\ mm$ $\quad E := 200\ GPa$

Stiffener T2 effective cross section due to shear lag as the stresses will not exceed local buckling stresses:

$\alpha_0 := 1$ $\quad L_e := 4000\ mm = 4\ m$

Hogging:

Inside stiffener $\quad b_0 := \frac{450}{2}\ mm$ $\quad \kappa := \frac{\alpha_0 \cdot b_0}{L_e} = 0.056$

$$\beta_{ult} := \frac{1}{1 + 6 \cdot \left(\kappa - \frac{1}{2500 \cdot \kappa}\right) + 1.6 \cdot \kappa^2} = 0.769 \qquad b_{eff.1} := \beta_{ult} \cdot b_0 = 173.091\ mm$$

Middl plate: $\quad b_0 := 860\ mm$ $\quad \kappa := \frac{\alpha_0 \cdot b_0}{L_e} = 0.215$

$$\beta_{ult} := \frac{1}{1 + 6 \cdot \left(\kappa - \frac{1}{2500 \cdot \kappa}\right) + 1.6 \cdot \kappa^2} = 0.425 \qquad b_{eff.2} := \beta_{ult} \cdot b_0 = 365.522\ mm$$

Lower plate $\quad b_0 := 475\ mm$ $\quad \kappa := \frac{\alpha_0 \cdot b_0}{L_e} = 0.119$

$$\beta_{ult} := \frac{1}{1 + 6 \cdot \left(\kappa - \frac{1}{2500 \cdot \kappa}\right) + 1.6 \cdot \kappa^2} = 0.583 \qquad b_{eff.3} := \beta_{ult} \cdot b_0 = 276.992\ mm$$

$$b_{eff.bot} := 2 \cdot b_{eff.1} + b_{eff.2} + b_{eff.3} = 988.696\ mm$$

$A_{topflange} := 25\ cm \cdot 7\ mm = 17.5\ cm^2$ $\qquad Z_{top} := 247\ mm + t = 263\ mm$

$A_{topflange} \cdot Z_{top} = 460.25\ cm^3$ $\qquad A_{topflange} \cdot Z_{top}^2 = \left(1.21 \cdot 10^4\right)\ cm^4$

$I_{topflange} := 0$

$A_{web} := 2 \cdot 26.3\ cm \cdot 7\ mm = 36.82\ cm^2$ $\qquad Z_{web} := \frac{250\ mm}{2} + t = 141\ mm$

$A_{web} \cdot Z_{web} = 519.162\ cm^3$ $\qquad A_{web} \cdot Z_{web}^2 = \left(7.32 \cdot 10^3\right)\ cm^4$

$I_{web} := 1562.5\ cm^4$

$A_{bottomflange} := b_{eff.bot} \cdot t = 158.191\ cm^2$

$Z_{bot.flange} := \frac{t}{2} = 8\ mm$

$A_{bottomflange} \cdot Z_{bot.flange} = 126.553\ cm^3$

$A_{bottomflange} \cdot Z_{bot.flange}^{\ 2} = 101.242\ cm^4$

$$I_{bot} := \frac{b_{eff.bot} \cdot t^3}{12} = 33.747\ cm^4$$

$$A_{tot} := A_{topflange} + A_{web} + A_{bottomflange} = 212.511\ cm^2$$

$$AZ_{tot} := A_{topflange} \cdot Z_{top} + A_{web} \cdot Z_{web} + A_{bottomflange} \cdot Z_{bot.flange} = \left(1.106 \cdot 10^3\right)\ cm^3$$

$$Cg := \frac{AZ_{tot}}{A_{tot}} = 5.204\ cm$$

$$I_{tot} := I_{topflange} + A_{topflange} \cdot \left(Z_{top} - Cg\right)^2 + I_{web} + A_{web} \cdot \left(Z_{web} - Cg\right)^2 + I_{bot} + A_{bottomflange} \cdot \left(Z_{bot.flange} - Cg\right)^2$$

$$I_{sl} := I_{tot} = \left(1.537 \cdot 10^{-4}\right)\ m^4$$

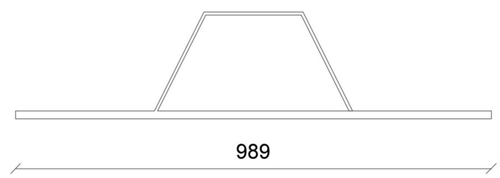

$$\sigma_{cr.sl} := \frac{(3.14)^2 \cdot E \cdot I_{sl}}{A_{tot} \cdot a^2} = 891.174\ MPa$$

Linear interpolation:

$\sigma_{cr.c} := 1205\ MPa$ $\qquad f_{yk} := 460\ MPa$

$$\lambda_c := \sqrt{\frac{f_{yk}}{\sigma_{cr.c}}} = 0.618$$

EN 1993-1-4 table 5.3: A1.17.2017 Table 6.1

$\alpha := 0.49$ $\qquad \lambda_0 := 0.2$ $\qquad \phi := 0.5 \cdot \left(1 + \alpha \cdot \left(\lambda_c - \lambda_0\right) + \lambda_c^{\ 2}\right) = 0.793$

$$\chi_c := \frac{1}{\phi + \left(\phi^2 - \lambda_c^{\ 2}\right)^{0.5}} = 0.775$$

$$\sigma_{cr.p} := \sigma_{cr.bot_0} = \left(1.204 \cdot 10^3\right)\ MPa$$

$$\xi := \frac{\sigma_{cr.p}}{\sigma_{cr.c}} - 1 = -5.394 \cdot 10^{-4}$$

$$\rho_c := \left(\rho_{p.b_0} - \chi_c\right) \cdot \xi \cdot \left(2 - \xi\right) + \chi_c = 0.775$$

$$\sigma_{Rd.b.16} := \rho_c \cdot \frac{f_{yk}}{1} = 356.313\ MPa$$

$t := 20\ mm$

$A_{topflange} := 25\ cm \cdot 7\ mm = 17.5\ cm^2$

$Z_{top} := 247\ mm + t = 267\ mm$

$A_{topflange} \cdot Z_{top} = 467.25\ cm^3$

$A_{topflange} \cdot Z_{top}{}^2 = \left(1.248 \cdot 10^4\right)\ cm^4$

$I_{topflange} := 0$

$A_{web} := 2 \cdot 26.3\ cm \cdot 7\ mm = 36.82\ cm^2$

$Z_{web} := \dfrac{250\ mm}{2} + t = 145\ mm$

$A_{web} \cdot Z_{web} = 533.89\ cm^3$

$A_{web} \cdot Z_{web}{}^2 = \left(7.741 \cdot 10^3\right)\ cm^4$

$I_{web} := 1562.5\ cm^4$

$A_{bottomflange} := b_{eff.bot} \cdot t = 197.739\ cm^2$

$Z_{bot.flange} := \dfrac{t}{2} = 10\ mm$

$A_{bottomflange} \cdot Z_{bot.flange} = 197.739\ cm^3$

$A_{bottomflange} \cdot Z_{bot.flange}{}^2 = 197.739\ cm^4$

$$I_{bot} := \frac{b_{eff.bot} \cdot t^3}{12} = 65.913\ cm^4$$

$A_{tot} := A_{topflange} + A_{web} + A_{bottomflange} = 252.059\ cm^2$

$AZ_{tot} := A_{topflange} \cdot Z_{top} + A_{web} \cdot Z_{web} + A_{bottomflange} \cdot Z_{bot.flange} = \left(1.199 \cdot 10^3\right)\ cm^3$

$$Cg := \frac{AZ_{tot}}{A_{tot}} = 4.756\ cm$$

$$I_{tot} := I_{topflange} + A_{topflange} \cdot \left(Z_{top} - Cg\right)^2 + I_{web} + A_{web} \cdot \left(Z_{web} - Cg\right)^2 + I_{bot} + A_{bottomflange} \cdot \left(Z_{bot.flange} - Cg\right)^2$$

$I_{sl} := I_{tot} = \left(1.634 \cdot 10^{-4}\right)\ m^4$

$$\sigma_{cr.sl} := \frac{(3.14)^2 \cdot E \cdot I_{sl}}{A_{tot} \cdot a^2} = 798.99\ MPa$$

Linear interpolation:

$\sigma_{cr.c} := 1079\ MPa$ $\quad f_{yk} := 460\ MPa$

$$\lambda_c := \sqrt{\frac{f_{yk}}{\sigma_{cr.c}}} = 0.653$$

EN 1993-1-4 table 5.3: A1.17.2017 Table 6.1

$\alpha := 0.49 \qquad \lambda_0 := 0.2 \qquad \phi := 0.5 \cdot \left(1 + \alpha \cdot \left(\lambda_c - \lambda_0\right) + {\lambda_c}^2\right) = 0.824$

$\chi_c := \dfrac{1}{\phi + \left(\phi^2 - {\lambda_c}^2\right)^{0.5}} = 0.754 \qquad \sigma_{cr.p} := \sigma_{cr.bot_1} = \left(1.237 \cdot 10^3\right)\ MPa$

$\xi := \dfrac{\sigma_{cr.p}}{\sigma_{cr.c}} - 1 = 0.146$

$\rho_c := \left(\rho_{p.b_1} - \chi_c\right) \cdot \xi \cdot \left(2 - \xi\right) + \chi_c = 0.801 \qquad \sigma_{Rd.b.20} := \rho_c \cdot \dfrac{f_{yk}}{1} = 368.577\ MPa$

$t := 25\ mm$

$A_{topflange} := 25\ cm \cdot 7\ mm = 17.5\ cm^2 \qquad Z_{top} := 247\ mm + t = 272\ mm$

$A_{topflange} \cdot Z_{top} = 476\ cm^3 \qquad A_{topflange} \cdot {Z_{top}}^2 = \left(1.295 \cdot 10^4\right)\ cm^4$

$I_{topflange} := 0$

$A_{web} := 2 \cdot 26.3\ cm \cdot 7\ mm = 36.82\ cm^2 \qquad Z_{web} := \dfrac{250\ mm}{2} + t = 150\ mm$

$A_{web} \cdot Z_{web} = 552.3\ cm^3 \qquad A_{web} \cdot {Z_{web}}^2 = \left(8.285 \cdot 10^3\right)\ cm^4$

$I_{web} := 1562.5\ cm^4$

$A_{bottomflange} := b_{eff.bot} \cdot t = 247.174\ cm^2 \qquad Z_{bot.flange} := \dfrac{t}{2} = 12.5\ mm$

$A_{bottomflange} \cdot Z_{bot.flange} = 308.967\ cm^3 \qquad A_{bottomflange} \cdot {Z_{bot.flange}}^2 = 386.209\ cm^4$

$I_{bot} := \dfrac{b_{eff.bot} \cdot t^3}{12} = 128.736\ cm^4$

$A_{tot} := A_{topflange} + A_{web} + A_{bottomflange} = 301.494\ cm^2$

$AZ_{tot} := A_{topflange} \cdot Z_{top} + A_{web} \cdot Z_{web} + A_{bottomflange} \cdot Z_{bot.flange} = \left(1.337 \cdot 10^3\right)\ cm^3$

$Cg := \dfrac{AZ_{tot}}{A_{tot}} = 4.435\ cm$

$I_{tot} := I_{topflange} + A_{topflange} \cdot \left(Z_{top} - Cg\right)^2 + I_{web} + A_{web} \cdot \left(Z_{web} - Cg\right)^2 + I_{bot} + A_{bottomflange} \cdot \left(Z_{bot.flange} - Cg\right)^2$

$I_{sl} := I_{tot} = \left(1.738 \cdot 10^{-4}\right)\ m^4$

$$\sigma_{cr.sl} := \frac{(3.14)^2 \cdot E \cdot I_{sl}}{A_{tot} \cdot a^2} = 710.369\ MPa$$

Linear interpolation: $\sigma_{cr.c} := 960\ MPa$ $f_{yk} := 460\ MPa$

$$\lambda_c := \sqrt{\frac{f_{yk}}{\sigma_{cr.c}}} = 0.692$$

EN 1993-1-4 table 5.3: A1.17.2017 Table 6.1

$\alpha := 0.49$ $\lambda_0 := 0.2$ $\phi := 0.5 \cdot \left(1 + \alpha \cdot \left(\lambda_c - \lambda_0\right) + {\lambda_c}^2\right) = 0.86$

$$\chi_c := \frac{1}{\phi + \left(\phi^2 - {\lambda_c}^2\right)^{0.5}} = 0.73$$

$$\sigma_{cr.p} := \sigma_{cr.bot_2} = \left(1.273 \cdot 10^3\right)\ MPa$$

$$\xi := \frac{\sigma_{cr.p}}{\sigma_{cr.c}} - 1 = 0.326$$

$$\rho_c := \left(\rho_{p.b_2} - \chi_c\right) \cdot \xi \cdot \left(2 - \xi\right) + \chi_c = 0.843$$

$$\sigma_{Rd.b.25} := \rho_c \cdot \frac{f_{yk}}{1} = 387.905\ MPa$$

$$\begin{bmatrix} t & \sigma_{Rd.top} & \sigma_{Rd.bot} \\ 16 & -313 & 0 \\ 20 & -339 & 0 \\ 25 & -380 & 0 \\ 16 & 0 & -356 \\ 20 & 0 & -368 \\ 25 & 0 & -388 \end{bmatrix}$$

Comparison:
For the top field the change in buckling strength is negligable, while for bottom field we have the following results

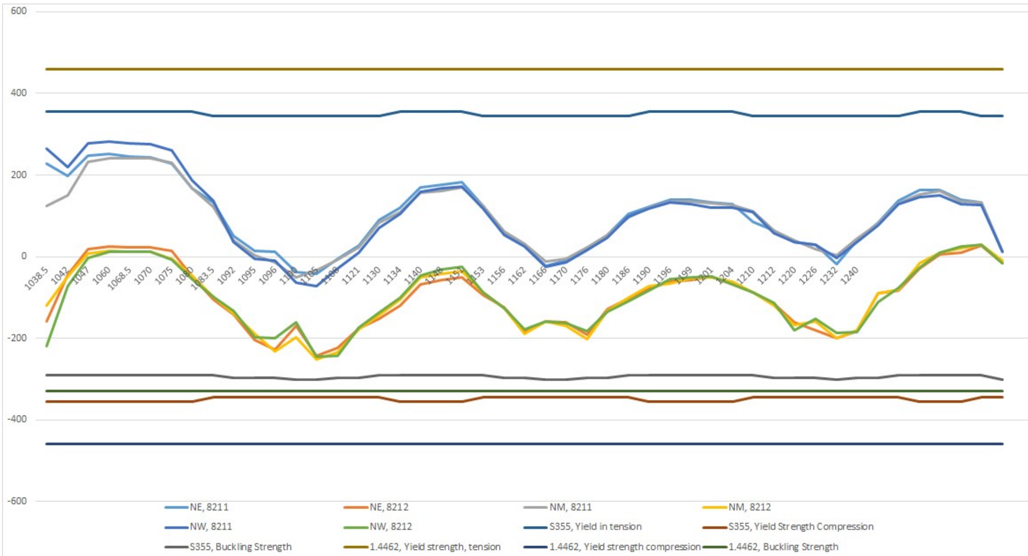

It is obvious that increasing T2 thickness to 7mm increased the capacity in the bottom field significantly and now we are able to reduce a new web thicknesses.

New suggestion (-2, -3 mm)

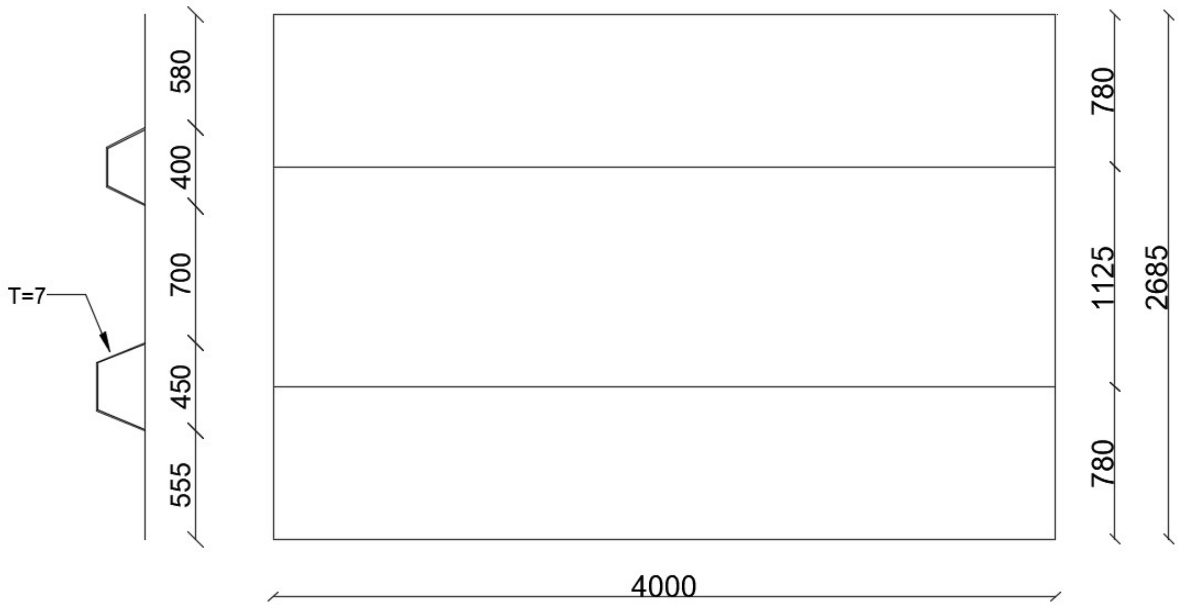

Local Single panel buckling:

Transverse stress: 40 MPa

Transverse stresses will be checked according to A1. 17, 2017, 6.4.4:

A single panel of the web will have height of 880 mm between t1 and t2. This values will be checked for transverse stresses coming from the vehicle weels above the slab of the box girder.

We have type A buckling:

$\alpha := 4000\ mm$ Distance between two cross frames

$h_w := 700\ mm$ $E := 200\ GPa$ $i := 0..5$

$$t_w := \begin{bmatrix} 13 \\ 14 \\ 17 \\ 18 \\ 22 \\ 23 \end{bmatrix} mm$$

$\kappa_{F.y} := 6 + 2\left(\frac{h_w}{\alpha}\right)^2 = 6.061$ $f_y := 460\ MPa$ $\gamma_{m1} := 1$ 18 kap. SS-EN 1993-1-4 – Rostfritt stål

$$F_{cr_i} := 0.9 \cdot \kappa_{F.y} \cdot E \cdot \frac{{t_{w_i}}^3}{h_w} \qquad \lambda_F := \sqrt{\frac{\left(\alpha \cdot t_w \cdot f_y\right)}{F_{cr}}} \qquad \chi_{f_i} := \frac{0.5}{\lambda_{F_i}} \qquad L_{eff_i} := \chi_{f_i} \cdot \alpha$$

$$F_{Rd_i} := f_y \cdot L_{eff_i} \cdot \frac{t_{w_i}}{\gamma_{m1}}$$

$$\sigma_{Rd_i} := \frac{F_{Rd_i}}{\alpha \cdot t_{w_i}} = \begin{bmatrix} 87.022 \\ 93.716 \\ 113.798 \\ 120.492 \\ 147.269 \\ 153.963 \end{bmatrix} MPa$$

From ULS stresses

$\sigma_{yEd} := 40\ MPa$ $\quad \eta_2 := \frac{\sigma_{yEd}}{\sigma_{Rd}}$ $\quad \eta_1 := 1$

Using interaction rule Eq 7.2 from 1993-1-5 and assuming that the panel is fully used in (longitudina stresses) σxED

$$\left\| \begin{array}{l} \text{if } \eta_{2_i} + \eta_1 \cdot 0.8 \le 1.4 \\ \quad \| \text{"Ok"} \\ \text{else if } \eta_{2_i} + \eta_1 \cdot 0.8 > 1.4 \\ \quad \| \text{"Problem"} \end{array} \right\| = \begin{bmatrix} \text{"Ok"} \\ \text{"Ok"} \\ \text{"Ok"} \\ \text{"Ok"} \\ \text{"Ok"} \\ \text{"Ok"} \end{bmatrix}$$

Single Panel Check for each subpart of the web

Top Edge subpanel:

$\alpha := 4000\ mm$ $\quad B_{tot} := 2685\ mm$ $\quad B_{brutto} := 780\ mm$ $\quad B_{s1} := 400\ mm$

$B_{panel} := B_{brutto} - \frac{B_{s1}}{2} = 580\ mm$ $\quad a := \frac{\alpha}{B_{panel}} = 6.897$ $\quad h_w := B_{panel}$

Assuming that we have pure compression σxtop=σxbottom

$\sigma_{x.top} := 1$ $\quad \sigma_{x.bottom} := \sigma_{x.top}$ $\quad f_{y.plate} := 460\ MPa$ $\quad \psi := \frac{\sigma_{x.top}}{\sigma_{x.bottom}}$ $\quad \kappa_\sigma := 4$

$\varepsilon := \sqrt{\frac{235\ MPa}{f_{y.plate}} \cdot \frac{E}{210\ GPa}} = 0.698$ $\quad \lambda_{p.x_i} := \left(\frac{B_{panel}}{t_{w_i} \cdot 28.4 \cdot \varepsilon \cdot \sqrt{\kappa_\sigma}} \right)$ $\quad \rho_i := \frac{0.772}{\lambda_{p.x_i}} - \frac{0.079}{{\lambda_{p.x_i}}^2}$

18 kap. SS-EN 1993-1-4 – Rostfritt stål $\quad \gamma_{m0} := 1$

$$\rho_i := \text{if } \rho_i \le 1 \;\; \| \; \rho_i \;\; \text{else} \;\; \| \; 1$$

$$\sigma_{Rd.local.top_i} := \frac{\rho_i \cdot f_{y.plate}}{\gamma_{m0}} = \begin{bmatrix} 286.697 \\ 306.377 \\ 363.381 \\ 381.705 \\ 451.606 \\ 460 \end{bmatrix} \textit{MPa}$$

Shear buckling resistance 6.4.3 A1.17,2017

$$\eta := 1.2 \qquad \frac{h_w}{t_{w_i}} = \begin{bmatrix} 44.615 \\ 41.429 \\ 34.118 \\ 32.222 \\ 26.364 \\ 25.217 \end{bmatrix} \qquad \frac{56.2 \cdot \varepsilon}{\eta} = 32.667 \qquad \frac{h_w}{t_w} > \frac{56.2 \cdot \varepsilon}{\eta}$$

$$\kappa_\tau := 5.34 + 4 \left(\frac{B_{panel}}{\alpha} \right)^2 = 5.424 \qquad \lambda_w := \frac{h_w}{37.4 \cdot t_w \cdot \varepsilon \cdot (\kappa_\tau)^{0.5}} \qquad \text{(6.25 A1)}$$

$$\chi_{w_i} := \begin{array}{l} \text{if } \lambda_{w_i} \le \dfrac{0.65}{\eta} \\ \quad \| \; \eta \\ \text{else if } \dfrac{0.65}{\eta} < \lambda_{w_i} < 0.65 \\ \quad \| \; \dfrac{0.65}{\lambda_{w_i}} \\ \text{else} \\ \quad \| \; \dfrac{1.56}{0.91 + \lambda_{w_i}} \end{array}$$

$$\tau_{Rd} := \chi_w \cdot \frac{f_{y.plate}}{\sqrt{3} \cdot \gamma_{m1}} = \begin{bmatrix} 251.961 \\ 260.263 \\ 307.417 \\ 318.697 \\ 318.697 \\ 318.697 \end{bmatrix} \textit{MPa}$$

$\eta_3 := \dfrac{\tau_{Ed}}{\tau_{Rd}}$ According to A1 no interaction will be checked for : $\tau_{Ed} \le 0.5 \cdot \tau_{Rd}$

So, it is assumed that $\tau_{Ed} = 0.5 \cdot \tau_{Rd}$

$$\tau_{Ed} := 0.5 \cdot \tau_{Rd} = \begin{bmatrix} 125.981 \\ 130.132 \\ 153.708 \\ 159.349 \\ 159.349 \\ 159.349 \end{bmatrix} \textit{MPa}$$

Mid Subpanel

$B_{brutto} := 780\ mm \qquad B_{s1} := 400\ mm \qquad B_{s2} := 450\ mm \qquad B_{tot} := 2685\ mm$

$B_{panel.mid} := B_{tot} - 2 \cdot B_{brutto} - \frac{B_{s1}}{2} - \frac{B_{s2}}{2} = 700\ mm \qquad \varepsilon = 0.698$

$a := \frac{\alpha}{B_{panel.mid}} = 5.714 \qquad h_w := B_{panel.mid} = 0.7\ m$

Assuming that we have pure compression σxtop=σxbottom, and another time assuming that we have compression at the top and tension at the bottom i.e:

$\sigma_{x.top} := \begin{bmatrix} 1 \\ -1 \end{bmatrix} \quad \sigma_{x.bottom} := \begin{bmatrix} 1 \\ 1 \end{bmatrix} \qquad f_{y.plate} := 460\ MPa \qquad \psi := \frac{\sigma_{x.top}}{\sigma_{x.bottom}} = \begin{bmatrix} 1 \\ -1 \end{bmatrix} \qquad \gamma_{m0} := 1$

$\kappa_\sigma := 4 \qquad \lambda_{p.x} := \left(\frac{B_{panel.mid}}{t_w \cdot 28.4 \cdot \varepsilon \cdot \sqrt{\kappa_\sigma}} \right)$

$\rho := \frac{0.772}{\lambda_{p.x}} - \frac{0.079}{\lambda_{p.x}^{\ 2}} \qquad \rho_i := \begin{cases} \text{if } \rho_i \le 1 \\ \quad \rho_i \\ \text{else} \\ \quad 1 \end{cases}$

$t_w = \begin{bmatrix} 13 \\ 14 \\ 17 \\ 18 \\ 22 \\ 23 \end{bmatrix} mm \qquad \sigma_{Rd.local.mid} := \frac{\rho \cdot f_{y.plate}}{\gamma_{m0}} = \begin{bmatrix} 241.62 \\ 258.576 \\ 308.048 \\ 324.073 \\ 385.845 \\ 400.706 \end{bmatrix} MPa$

$\kappa_\tau := 5.34 + 4 \left(\frac{B_{panel.mid}}{\alpha} \right)^2 = 5.463 \qquad \lambda_w := \frac{B_{panel.mid}}{37.4 \cdot t_w \cdot \varepsilon \cdot \left(\kappa_\tau\right)^{0.5}}$

$\chi_{w_i} := \begin{cases} \text{if } \lambda_{w_i} \le \frac{0.65}{\eta} \\ \quad \eta \\ \text{else if } \frac{0.65}{\eta} < \lambda_{w_i} < 0.65 \\ \quad \frac{0.65}{\lambda_{w_i}} \\ \text{else} \\ \quad \frac{1.56}{0.91 + \lambda_{w_i}} \end{cases}$

$\tau_{Rd} := \chi_w \cdot \frac{f_{y.plate}}{\sqrt{3} \cdot \gamma_{m1}} = \begin{bmatrix} 231.052 \\ 239.476 \\ 261.336 \\ 270.653 \\ 318.697 \\ 318.697 \end{bmatrix} MPa$

$\eta_3 := \frac{\tau_{Ed}}{\tau_{Rd}}$ According to A1 no interaction will be checked for : $\tau_{Ed} \le 0.5 \cdot \tau_{Rd}$

So, it is assumed that $\tau_{Ed} = 0.5 \cdot \tau_{Rd}$

$$\tau_{Ed} := 0.5 \cdot \tau_{Rd} = \begin{bmatrix} 115.526 \\ 119.738 \\ 130.668 \\ 135.326 \\ 159.349 \\ 159.349 \end{bmatrix} MPa$$

$\kappa_\sigma := 23.9$

$$\lambda_{p.x} := \left(\frac{B_{panel.mid}}{t_w \cdot 28.4 \cdot \varepsilon \cdot \sqrt{\kappa_\sigma}} \right)$$

$\gamma_{m0} := 1$

$$\rho := \frac{0.772}{\lambda_{p.x}} - \frac{0.079}{\lambda_{p.x}^{\ 2}}$$

$$\rho_i := \text{if } \rho_i \le 1 \; \| \; \rho_i \; \text{else} \; \| \; 1$$

$$\sigma_{Rd.local.mid} := \frac{\rho \cdot f_{y.plate}}{\gamma_{m0}} = \begin{bmatrix} 460 \\ 460 \\ 460 \\ 460 \\ 460 \\ 460 \end{bmatrix} MPa$$

$$\kappa_\tau := 5.34 + 4 \left(\frac{B_{panel.mid}}{\alpha} \right)^2 = 5.463$$

$$\lambda_w := \frac{B_{panel.mid}}{37.4 \cdot t_w \cdot \varepsilon \cdot (\kappa_\tau)^{0.5}}$$

$$\chi_{w_i} := \begin{cases} \eta & \text{if } \lambda_{w_i} \le \frac{0.65}{\eta} \\ \frac{0.65}{\lambda_{w_i}} & \text{else if } \frac{0.65}{\eta} < \lambda_{w_i} < 0.65 \\ \frac{1.56}{0.91 + \lambda_{w_i}} & \text{else} \end{cases}$$

$$\tau_{Rd} := \chi_w \cdot \frac{f_{y.plate}}{\sqrt{3} \cdot \gamma_{m1}} = \begin{bmatrix} 231.052 \\ 239.476 \\ 261.336 \\ 270.653 \\ 318.697 \\ 318.697 \end{bmatrix} MPa$$

$\tau_{Ed} \le 0.5 \cdot \tau_{Rd}$

$$\tau_{Ed} := 0.5 \cdot \tau_{Rd} = \begin{bmatrix} 115.526 \\ 119.738 \\ 130.668 \\ 135.326 \\ 159.349 \\ 159.349 \end{bmatrix} MPa$$

Global buckling check of the web:

The global buckling check of the web is done using EBPlate for the northern side of the bridge.

In order to avoid stress interaction we got a maximum value for transverse stresses in a single panel buckling $\sigma_{y.RD} := 40\ MPa$ and maximum shear stress is less than $\tau_{ED} := 133\ MPa$, regardless the plate thickness.
the stiffeners will not buckle upp to 329MPa, according to the buckling checks of hollow stiffeners.

We will check now using EBplate the maximum shear stress resistance for the plate with three different dimensions 12, 14, 16, 18, 21, 23 mm. and to insure that all of these resistances are larger than 266 to avoid interaction.

$fyw := 460\ MPa$ $\qquad h_w := 2685\ mm$ $\qquad \varepsilon = 0.698$ $\qquad \tau_{cr} := \begin{bmatrix} 464 \\ 506 \\ 624 \\ 661 \\ 790 \\ 831 \end{bmatrix} MPa$

$$\lambda_{w_i} := 0.76 \cdot \sqrt{\frac{fyw}{\tau_{cr_i}}}$$

$$\chi_i := \begin{cases} \eta & \text{if } \lambda_{w_i} \le \dfrac{0.65}{\eta} \\ \dfrac{0.65}{\lambda_{w_i}} & \text{else if } \dfrac{0.65}{\eta} < \lambda_{w_i} < 0.65 \\ \dfrac{1.56}{0.91 + \lambda_{w_i}} & \text{else} \end{cases}$$

$$\tau_{Rd} := \chi \cdot \frac{f_{y.plate}}{\sqrt{3} \cdot \gamma_{m1}} = \begin{bmatrix} 248.576 \\ 253.456 \\ 265.151 \\ 272.282 \\ 297.668 \\ 305.294 \end{bmatrix} MPa$$

All of shear stresses in D file have values less than 123. To avoid interaction between shear and compression stresses, shear resistance need to be larger than 246MPa. this assumption is achieved from the upper calculations (singel panel buckling "Top panel=266MPa" and "Global shear buckling=247MPa")

Hence only the stability for longitudinal stess need to be verified. From single panel beckling tha maximum allowed stress on the middle panel is 245 MPa. thus we choose the following stress distributon as the most critical case for web buckling.
in most cases web will have compression at one side and tension at another, and in critical case web will have compression stress at one side and zero stress at the other side. This compression stress at one side is chosen to be 300 MPa in order not to exceed the maximum allowed stress in a single panel.

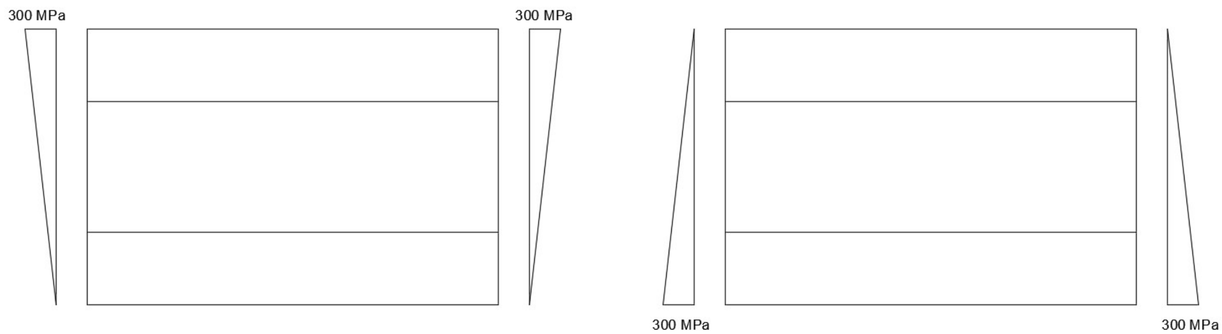

These checks are done using EBplate. When checking for plate type buckling the single panel buckling mode is switched of in EBplate. We get the following results when compression at the top:

Plate type buckling: Maximum stress at the top:

EBplate: $\phi_t := \begin{bmatrix} 2.5589 \\ 2.6002 \\ 2.7342 \\ 2.7841 \\ 2.9974 \\ 3.0564 \end{bmatrix}$ $\sigma_{cr.top} := 300\ MPa \cdot \phi_t$ $\lambda_p := \sqrt{\dfrac{fyw}{\sigma_{cr.top}}}$ $\rho_{p.t} := \dfrac{0.772}{\lambda_p} - \dfrac{0.125}{{\lambda_p}^2}$

Maximum stress at the bottom:

EBplate: $\phi_b := \begin{bmatrix} 4.1072 \\ 4.1376 \\ 4.1879 \\ 4.1970 \\ 4.2213 \\ 4.2195 \end{bmatrix}$ $\sigma_{cr.bot} := 300\ MPa \cdot \phi_b$ $\lambda_p := \sqrt{\dfrac{fyw}{\sigma_{cr.bot}}}$ $\rho_{p.b} := \dfrac{0.772}{\lambda_p} - \dfrac{0.125}{{\lambda_p}^2}$

Column type buckling:

Compression at the top: Stiffener T1

$t := t_w$ $\quad a := 4000\ mm$ $\quad E := 200\ GPa$

Stiffener T1 effective cross section due to shear lag as the stresses will not exceed local buckling stresses:

$\alpha_0 := 1$ $\quad L_e := 4000\ mm = 4\ m$

Hogging:

Inside stiffener $\quad b_0 := \dfrac{400}{2}\ mm$ $\quad \kappa := \dfrac{\alpha_0 \cdot b_0}{L_e} = 0.05$

$$\beta_{ult} := \frac{1}{1 + 6 \cdot \left(\kappa - \dfrac{1}{2500 \cdot \kappa}\right) + 1.6 \cdot \kappa^2} = 0.796 \qquad b_{eff.1} := \beta_{ult} \cdot b_0 = 159.236\ mm$$

Upper plate: $\quad b_0 := 580\ mm$ $\quad \kappa := \dfrac{\alpha_0 \cdot b_0}{L_e} = 0.145$

$$\beta_{ult} := \frac{1}{1 + 6 \cdot \left(\kappa - \dfrac{1}{2500 \cdot \kappa}\right) + 1.6 \cdot \kappa^2} = 0.53 \qquad b_{eff.2} := \beta_{ult} \cdot b_0 = 307.352\ mm$$

Middle plate $\quad b_0 := 700\ mm$ $\quad \kappa := \dfrac{\alpha_0 \cdot b_0}{L_e} = 0.175$

$$\beta_{ult} := \frac{1}{1 + 6 \cdot \left(\kappa - \dfrac{1}{2500 \cdot \kappa}\right) + 1.6 \cdot \kappa^2} = 0.48 \qquad b_{eff.3} := \beta_{ult} \cdot b_0 = 335.685\ mm$$

$$b_{eff.bot} := 2 \cdot b_{eff.1} + b_{eff.2} + b_{eff.3} = 961.509\ mm$$

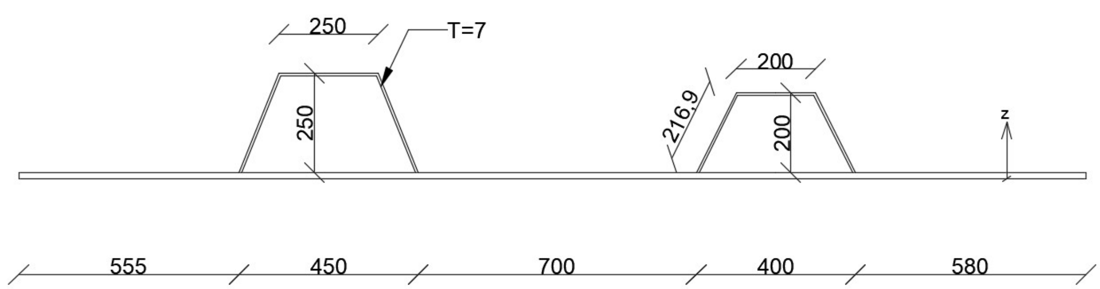

$A_{topflange} := 20\ cm \cdot 6\ mm = 12\ cm^2$ $Z_{top_i} := 197\ mm + t_i$ $I_{topflange} := 0$

$A_{web} := 2 \cdot 21.6\ cm \cdot 6\ mm = 25.92\ cm^2$ $Z_{web_i} := 100\ mm + t_i$ $I_{web} := 814\ cm^4$

$A_{bottomflange_i} := b_{eff.bot} \cdot t_i$ $Z_{bot.flange_i} := \dfrac{t_i}{2}$ $I_{bot_i} := \dfrac{b_{eff.bot} \cdot t_i^{\,3}}{12}$

$A_{tot_i} := A_{topflange} + A_{web} + A_{bottomflange_i}$

$AZ_{tot_i} := A_{topflange} \cdot Z_{top_i} + A_{web} \cdot Z_{web_i} + A_{bottomflange_i} \cdot Z_{bot.flange_i}$ $Cg_i := \dfrac{AZ_{tot_i}}{A_{tot_i}}$

$$I_{tot_i} := I_{topflange} + A_{topflange} \cdot \left(Z_{top_i} - Cg_i\right)^2 + I_{web} + A_{web} \cdot \left(Z_{web_i} - Cg_i\right)^2 + I_{bot_i} + A_{bottomflange_i} \cdot \left(Z_{bot.flange_i} - Cg_i\right)^2$$

$I_{sl} := I_{tot}$

$$\sigma_{cr.sl_i} := \frac{(3.14)^2 \cdot E \cdot I_{sl_i}}{A_{tot_i} \cdot a^2} = \begin{bmatrix} 535.571 \\ 515.556 \\ 464.448 \\ 449.929 \\ 401.537 \\ 391.443 \end{bmatrix} MPa$$

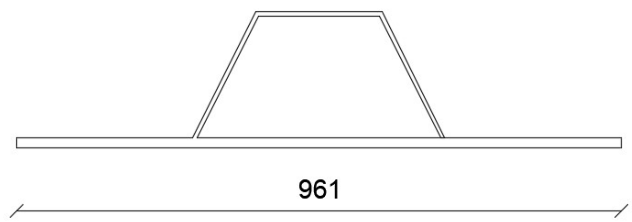

Linear interpolation:

$$\sigma_{cr.c} := \begin{bmatrix} 755 \\ 727 \\ 654 \\ 633 \\ 565 \\ 551 \end{bmatrix} MPa \qquad f_{yk} := 460\ MPa$$

$$\lambda_c := \sqrt{\frac{f_{yk}}{\sigma_{cr.c}}}$$

EN 1993-1-4 table 5.3: A1.17.2017 Table 6.1

$\alpha := 0.49$ $\lambda_0 := 0.2$ $\phi := 0.5 \cdot \left(1 + \alpha \cdot \left(\lambda_c - \lambda_0\right) + \lambda_c^{\,2}\right)$ $\chi_c := \dfrac{1}{\phi + \left(\phi^2 - \lambda_c^{\,2}\right)^{0.5}}$

$\sigma_{cr.p} := \sigma_{cr.top}$ $\xi_i := \dfrac{\sigma_{cr.p_i}}{\sigma_{cr.c_i}} - 1$ $\rho_{c_i} := \left(\rho_{p.t_i} - \chi_{c_i}\right) \cdot \xi_i \cdot \left(2 - \xi_i\right) + \chi_{c_i}$

$$\sigma_{Rd.top} := \rho_c \cdot \frac{f_{yk}}{1} = \begin{bmatrix} 311.959 \\ 314.209 \\ 328.161 \\ 334.916 \\ 365.95 \\ 373.818 \end{bmatrix} \; MPa$$

Compression at the bottom: Stiffener T2

$a := 4000 \; mm \qquad E := 200 \; GPa$

Stiffener T2 effective cross section due to shear lag as the stresses will not exceed local buckling stresses:

$\alpha_0 := 1 \qquad L_e := 4000 \; mm = 4 \; m$

Hogging:

Inside stiffener $\quad b_0 := \frac{450}{2} \; mm \qquad \kappa := \frac{\alpha_0 \cdot b_0}{L_e} = 0.056$

$$\beta_{ult} := \frac{1}{1 + 6 \cdot \left(\kappa - \frac{1}{2500 \cdot \kappa}\right) + 1.6 \cdot \kappa^2} = 0.769 \qquad b_{eff.1} := \beta_{ult} \cdot b_0 = 173.091 \; mm$$

Middl plate: $\quad b_0 := 700 \; mm \qquad \kappa := \frac{\alpha_0 \cdot b_0}{L_e} = 0.175$

$$\beta_{ult} := \frac{1}{1 + 6 \cdot \left(\kappa - \frac{1}{2500 \cdot \kappa}\right) + 1.6 \cdot \kappa^2} = 0.48 \qquad b_{eff.2} := \beta_{ult} \cdot b_0 = 335.685 \; mm$$

Lower plate $\quad b_0 := 555 \; mm \qquad \kappa := \frac{\alpha_0 \cdot b_0}{L_e} = 0.139$

$$\beta_{ult} := \frac{1}{1 + 6 \cdot \left(\kappa - \frac{1}{2500 \cdot \kappa}\right) + 1.6 \cdot \kappa^2} = 0.542 \qquad b_{eff.3} := \beta_{ult} \cdot b_0 = 300.649 \; mm$$

$b_{eff.bot} := 2 \cdot b_{eff.1} + b_{eff.2} + b_{eff.3} = 982.516 \; mm$

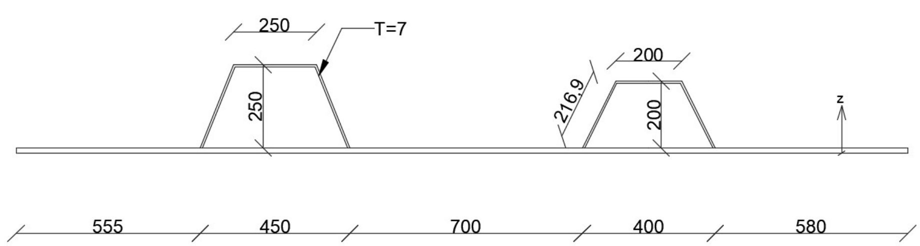

$A_{topflange} := 25\ cm \cdot 7\ mm = 17.5\ cm^2$ $\quad Z_{top_i} := 247\ mm + t_i$ $\quad I_{topflange} := 0$

$A_{web} := 2 \cdot 26.3\ cm \cdot 7\ mm = 36.82\ cm^2$ $\quad Z_{web_i} := \frac{250\ mm}{2} + t_i$ $\quad Z_{bot.flange_i} := \frac{t_i}{2}$

$I_{web} := 2 \cdot \frac{7\ mm \cdot 250\ mm^3}{12} = \left(2.917 \cdot 10^{-10}\right)\ m^4$ $\quad A_{bottomflange_i} := b_{eff.bot} \cdot t_i$

$I_{bot_i} := \frac{b_{eff.bot} \cdot t_i^{\ 3}}{12}$ $\quad A_{tot_i} := A_{topflange} + A_{web} + A_{bottomflange_i}$

$AZ_{tot_i} := A_{topflange} \cdot Z_{top_i} + A_{web} \cdot Z_{web_i} + A_{bottomflange_i} \cdot Z_{bot.flange_i}$ $\quad Cg_i := \frac{AZ_{tot_i}}{A_{tot_i}}$

$$I_{tot_i} := I_{topflange} + A_{topflange} \cdot \left(Z_{top_i} - Cg_i\right)^2 + I_{web} + A_{web} \cdot \left(Z_{web_i} - Cg_i\right)^2 + I_{bot_i} + A_{bottomflange_i} \cdot \left(Z_{bot.flange_i} - Cg_i\right)^2$$

$I_{sl} := I_{tot}$

$$\sigma_{cr.sl_i} := \frac{(3.14)^2 \cdot E \cdot I_{sl_i}}{A_{tot_i} \cdot a^2} = \begin{bmatrix} 873.481 \\ 848.872 \\ 782.062 \\ 762.078 \\ 692.315 \\ 677.142 \end{bmatrix} MPa$$

Linear interpolation:

$$\sigma_{cr.c} := \begin{bmatrix} 1230 \\ 1196 \\ 1102 \\ 1074 \\ 975 \\ 954 \end{bmatrix} MPa$$

$$\lambda_c := \sqrt{\frac{f_{yk}}{\sigma_{cr.c}}}$$

EN 1993-1-4 table 5.3: A1.17.2017 Table 6.1

$\alpha := 0.49$ $\quad \lambda_0 := 0.2$ $\quad \phi_i := 0.5 \cdot \left(1 + \alpha \cdot \left(\lambda_{c_i} - \lambda_0\right) + \lambda_{c_i}^{\ 2}\right)$ $\quad \chi_{c_i} := \frac{1}{\phi_i + \left(\phi_i^{\ 2} - \lambda_{c_i}^{\ 2}\right)^{0.5}}$

$\sigma_{cr.p} := \sigma_{cr.bot}$ $\quad \xi_i := \frac{\sigma_{cr.p_i}}{\sigma_{cr.c_i}} - 1$ $\quad \rho_{c_i} := \left(\rho_{p.b_i} - \chi_{c_i}\right) \cdot \xi_i \cdot \left(2 - \xi_i\right) + \chi_{c_i}$

$$\sigma_{Rd.bot_i} := \rho_{c_i} \cdot \frac{f_{yk}}{1} = \begin{bmatrix} 358.363 \\ 361.129 \\ 369.74 \\ 372.656 \\ 384.795 \\ 387.41 \end{bmatrix} MPa$$

$$\sigma_{Rd.} := \begin{bmatrix} -\sigma_{Rd.top_0} & 0 \\ -\sigma_{Rd.top_1} & 0 \\ -\sigma_{Rd.top_2} & 0 \\ -\sigma_{Rd.top_3} & 0 \\ -\sigma_{Rd.top_4} & 0 \\ -\sigma_{Rd.top_5} & 0 \\ 0 & -\sigma_{Rd.bot_0} \\ 0 & -\sigma_{Rd.bot_1} \\ 0 & -\sigma_{Rd.bot_2} \\ 0 & -\sigma_{Rd.bot_3} \\ 0 & -\sigma_{Rd.bot_4} \\ 0 & -\sigma_{Rd.bot_5} \end{bmatrix} = \begin{bmatrix} -311.959 & 0 \\ -314.209 & 0 \\ -328.161 & 0 \\ -334.916 & 0 \\ -365.95 & 0 \\ -373.818 & 0 \\ 0 & -358.363 \\ 0 & -361.129 \\ 0 & -369.74 \\ 0 & -372.656 \\ 0 & -384.795 \\ 0 & -387.41 \end{bmatrix} MPa$$

t (mm)	$\sigma_{Rd.top}$ (MPa)	$\sigma_{Rd.bot}$ (MPa)
13	−312	0
17	−328	0
22	−366	0
13	0	−358
17	0	−370
22	0	−385

t (mm)	$\sigma_{Rd.top}$ (MPa)	$\sigma_{Rd.bot}$ (MPa)
14	−314	0
18	−335	0
23	−374	0
14	0	−361
18	0	−373
23	0	−387

Results:

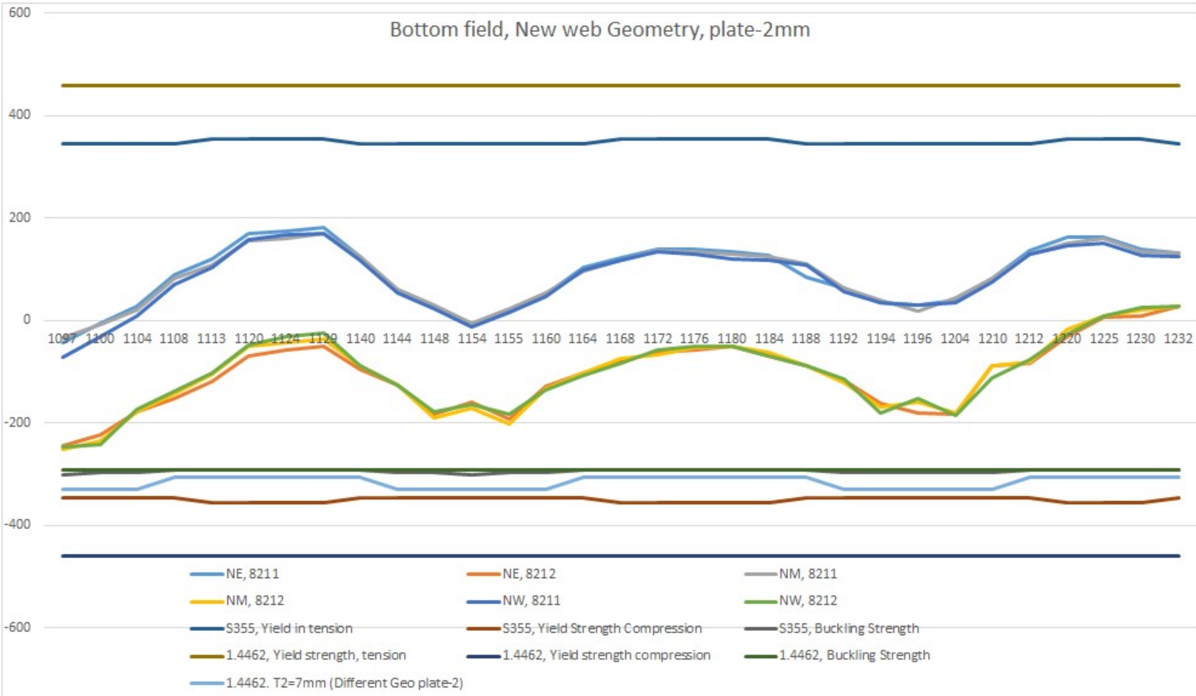
Bottom field, New web Geometry, plate-2mm
600
400
200
0
-200
-400
-600
1097 1100 1104 1108 1113 1120 1124 1129 1140 1144 1148 1154 1155 1160 1164 1168 1172 1176 1180 1184 1188 1192 1194 1196 1204 1210 1212 1220 1225 1230 1232
NE, 8211
NE, 8212
NM, 8211
NM, 8212
NW, 8211
NW, 8212
S355, Yield in tension
S355, Yield Strength Compression
S355, Buckling Strength
1.4462, Yield strength, tension
1.4462, Yield strength compression
1.4462, Buckling Strength
1.4462. T2=7mm (Different Geo plate-2)

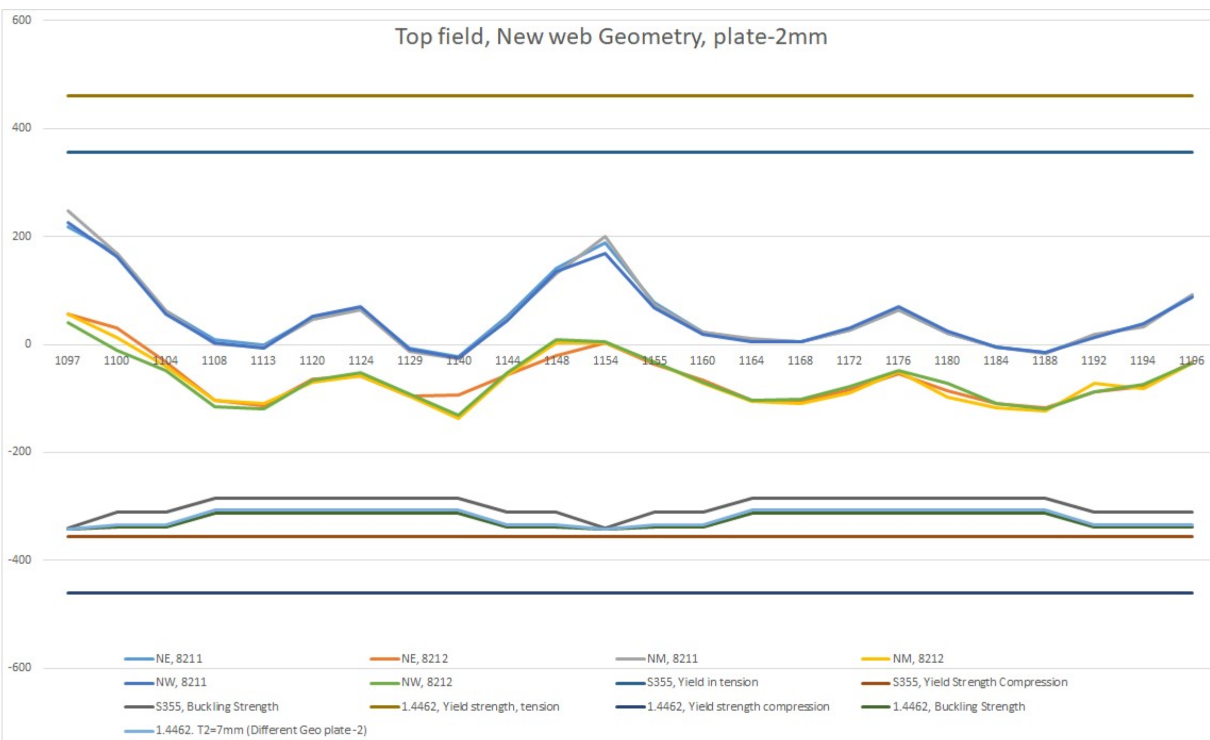
Top field, New web Geometry, plate-2mm
600
400
200
0
-200
-400
-600
1097 1100 1104 1108 1113 1120 1124 1129 1140 1144 1148 1154 1155 1160 1164 1168 1172 1176 1180 1184 1188 1192 1194 1196
NE, 8211
NE, 8212
NM, 8211
NM, 8212
NW, 8211
NW, 8212
S355, Yield in tension
S355, Yield Strength Compression
S355, Buckling Strength
1.4462, Yield strength, tension
1.4462, Yield strength compression
1.4462, Buckling Strength
1.4462. T2=7mm (Different Geo plate-2)

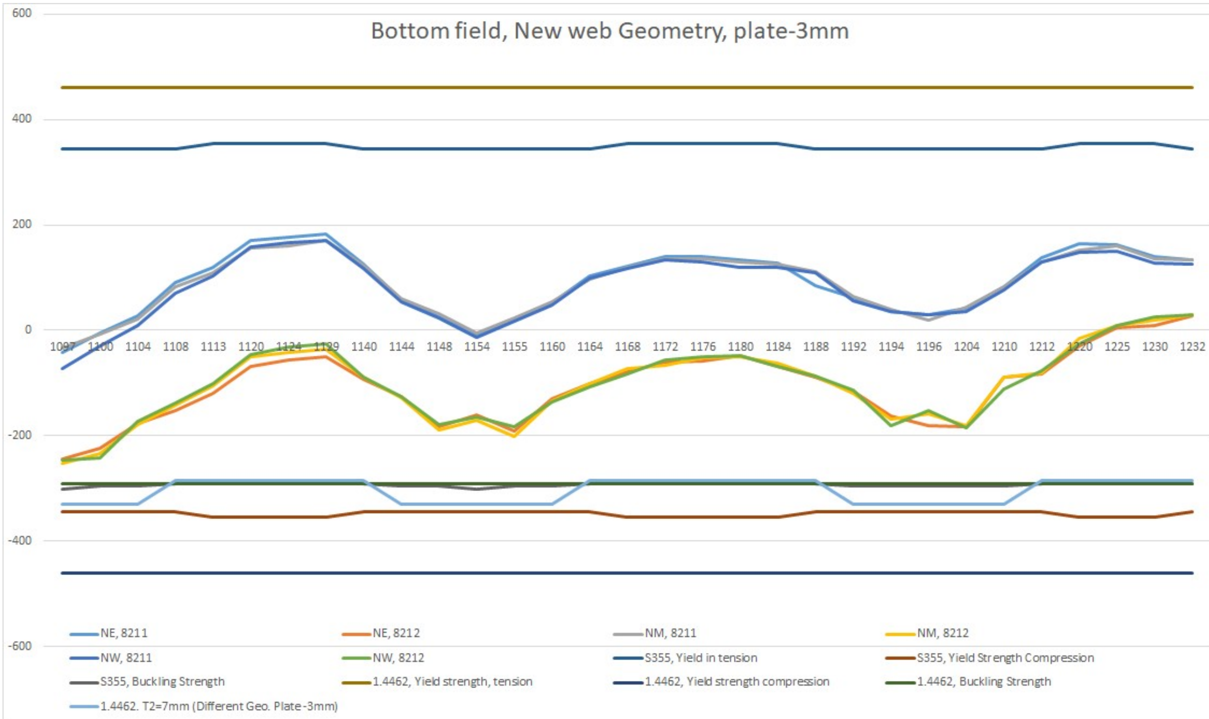

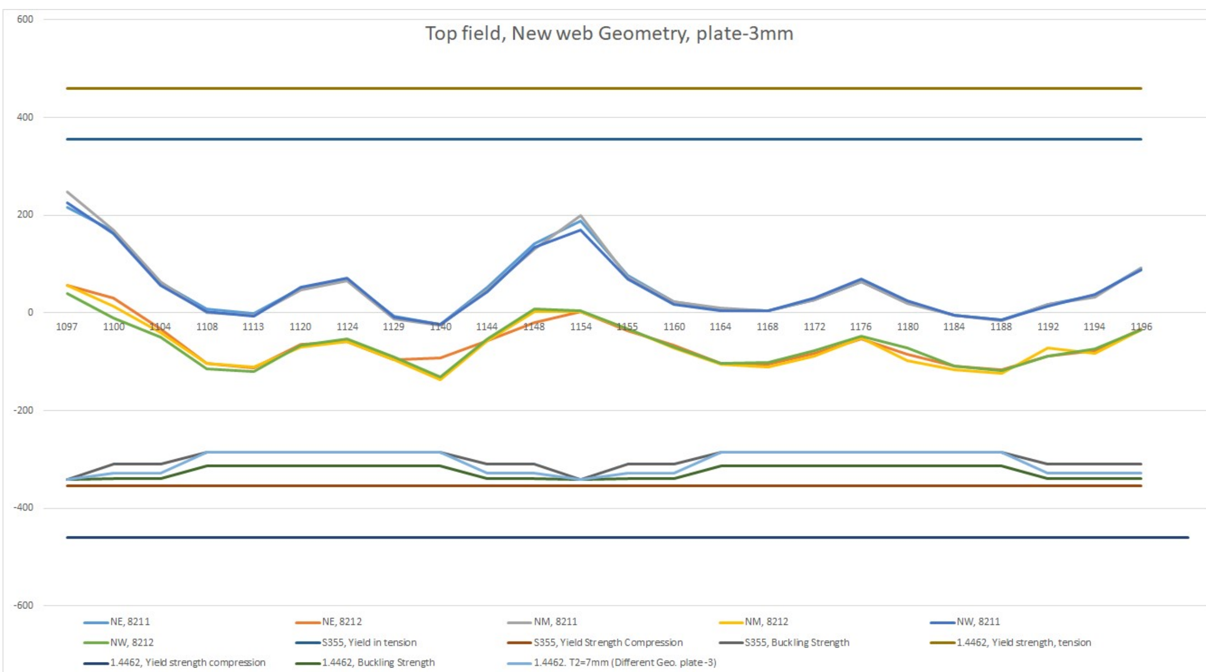

Cross section reduction:

$$Ared := 3\ mm \cdot 2685\ mm - 1\ mm \cdot (270\ mm \cdot 2 + 250\ mm) = 72.65\ cm^2$$

$$154.4 + 72.65 = 227.05$$

Department of Architecture and Civil Engineering
CHALMERS UNIVERSITY OF TECHNOLOGY
Gothenburg, Sweden
www.chalmers.se